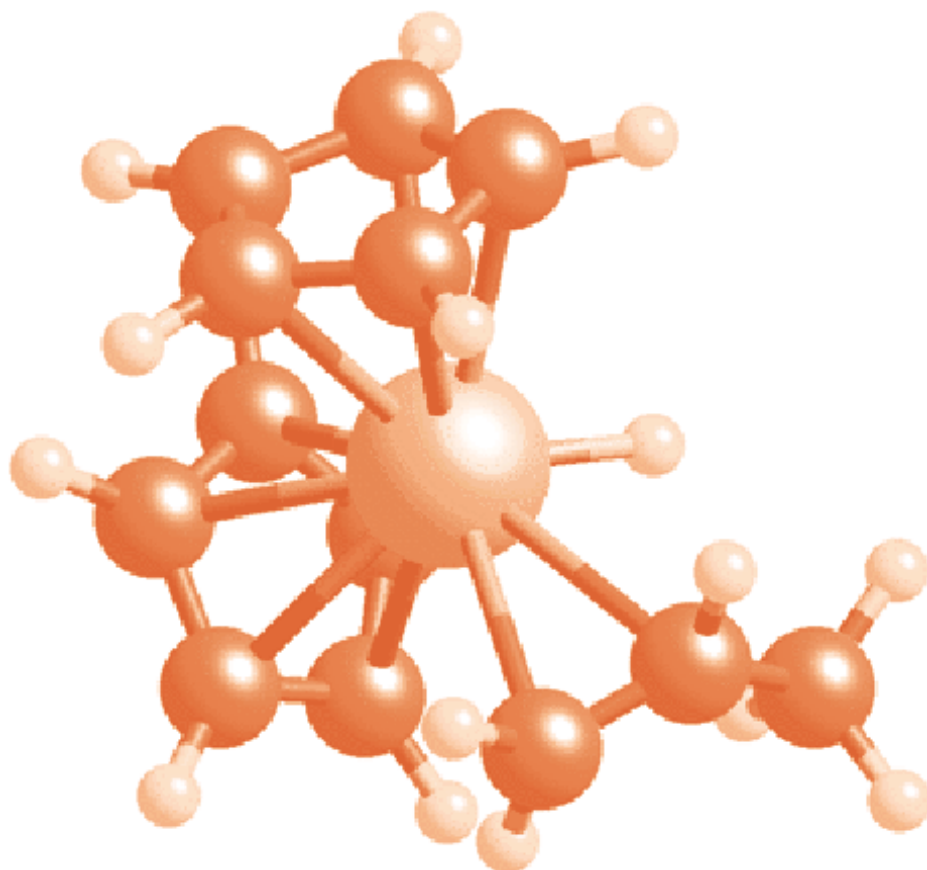




STUDIA UNIVERSITATIS
BABEŞ-BOLYAI



CHEMIA

4/2007

S T U D I A
UNIVERSITATIS BABEȘ-BOLYAI
CHEMIA

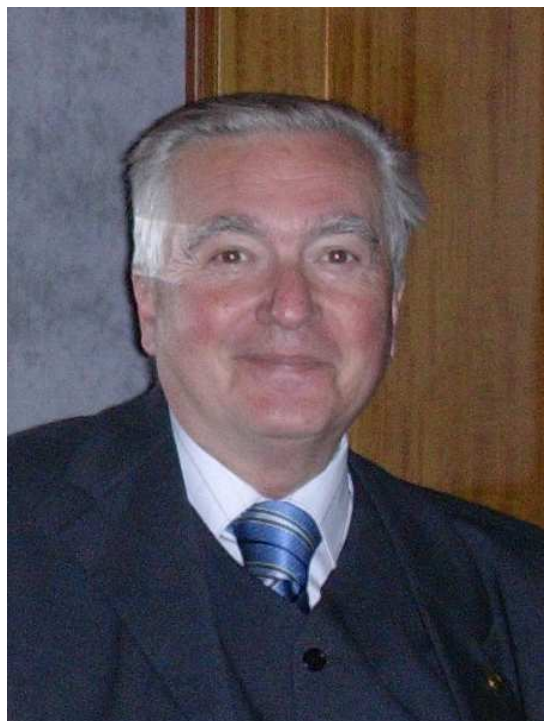
4

Desktop Editing Office: 51ST B.P. Hasdeu Street, Cluj-Napoca, Romania, Phone + 40 264-405352

CUPRINS – CONTENT – SOMMAIRE – INHALT

<i>In memoriam prof. dr. Ioan A. Silberg</i>	3
<i>PUBLICATIONS</i>	7
C. CRISTEA, G. CORMOS, L. GĂINĂ, L. SILAGHI-DUMITRESCU, D. GLIGOR, L. MURESAN, I. CĂTĂLIN POPESCU, <i>Microwave-Assisted Synthesis and Electrochemical Behaviour of Phenothiazine-Formaldehyde Polymer Derivative</i>	21
T. LOVÁSZ, G. OLTEAN, A.-M. TOMA, L. GĂINĂ, L. SILAGHI-DUMITRESCU, M. JITARU, C. CRISTEA, P. SOHÁR, A. CSÁMPAI, <i>Electronic Properties Of Chalcones Containing Phenothiazine Units</i>	31
D. PORUMB, I. SILAGHI-DUMITRESCU, L. GAINA, L. SILAGHI-DUMITRESCU, C. CRISTEA, G. CORMOS, <i>The Formylation of Bis-(N-Alkyl-Phenothiazinyl)-Methane; A Theoretical Approach</i>	39
L. N. POPA, M. PUTALA, <i>Photoactive Binaphthyl Phenothiazine Derivatives</i>	43
I. OPREAN, V. FĂRCĂȘAN, I. BÂTIU, <i>Mass Spectra of the New Hydrazido- Hydrazones Obtained by the Condensation of the Isonicotinic Acid Hydrazide (Hin) with Citral, (+)-Carvone and β-Ionone</i>	51

S. TOTOS, I. OPREAN, F. PIRON, <i>Pd(0)-Catalyzed Cross-Coupling Reactions in the Synthesis of (7E,9Z)-7,9-Dodecadienyl Acetate, the Sex Pheromone of the Leaf Roller Moth (Lobesia Botrana)</i>	61
A. SAPONAR, I. SILAGHI-DUMITRESCU, E.-J. POPOVICI, N. POPOVICI, <i>Calix[n] Arene Derivatives with Binding Properties Toward Eu³⁺</i>	67
C. BĂTIU, I. PANEA, M. PELEA, A. MARCU, L. DAVID, <i>Synthesis and Spectroscopic Investigation of Metal Complexes with an Azo-Dye as Ligand</i>	75
G. NEMEȘ, R. ȘEPTLEAN, P. M. PETRAR, L. SILAGHI-DUMITRESCU, I. SILAGHI-DUMITRESCU, <i>Towards New Double-Bonded Organophosphorus Derivative of C=P=C=P Type</i>	89
M. – L. SORAN, M. CURTUI, D. GHERMAN, <i>Tlc Separation of Th(IV) and Lanthanides(III) on Various Stationary Phases Using HDEHDP as Complexing Agent</i>	95
M. M. VENTER, V. ZAHARIA, <i>Spectral Investigation of 3-Mercapto-1,2,4-Triazole Ligands</i>	103
B. MIHÁLY, E. FORIZS, I. SILAGHI-DUMITRESCU, <i>Synthesis and Characterization of Some Mixed Ligand Zinc(II) Complexes of Theophylline</i>	111
O. BABAN, D. RUSU, A. PATRUT, C. CRACIUN, M. RUSU, <i>Synthesis and Characterization of a New Bismutho(III)Polyoxometalate with Mixed Addenda</i>	117
R. SILAGHI-DUMITRESCU, <i>An Alternative Mechanism for Catalase Activity</i>	127
I. KACSO, I. BRATU, A. FARCAS, M. BOJITA, <i>Spectrophotometric Studies of Diazepam - β-Cyclodextrin Complex Formation</i>	131
G. TOMOAI, V.-D. POP-TOADER, A. MOCANU, O. HOROVITZ, D.-L. BOBOS, M. TOMOAI-COTISEL, <i>Supramolecular Organization and Nano Structuration of Collagen and Anti Cancer Drugs</i>	137
M.-C. TERTIS, M. JITARU, <i>Removal of Nitroderivates from Synthetic Wastewaters by Electrochemical Reduction</i>	153
S. DRĂGAN, A. GHIRIȘAN, <i>Kinetic Study of Calcination for Precipitate Calcium Carbonate</i>	165
O. NEMEȘ, <i>Adhesive Influence Modeling on Double-Lap Joints Assemblies</i>	175



Professor Ioan A. Silberg, corresponding member of the Roumanian Academy, was born in Cluj on November the 6th 1937. He graduated with honors the Faculty of Chemistry at the University of Cluj in 1959, specialty organic chemistry. He received his doctoral degree in 1970 from the Institute of Chemistry Cluj-Napoca, where he worked under the scientific supervision of prof. C. Bodea corresponding member of the Roumanian Academy, on free radicals and charge transfer complexes in the polihalophenothiazine series. After periods of research activity at the Institute of Chemistry, Cluj (1960-1980) and Institute of Chemical and Biochemical Energetics, "Babeș-Bolyai" University Electrochemical Energetics Research Group (1980-1990), since 1990 he became professor of Organic Chemistry at "Babeș-Bolyai" University, Faculty of Chemistry and Chemical Engineering. During 1992-2003 he was the **head of Organic Chemistry Department**. Since 2000 he became also the **director of the Institute of Chemistry Raluca Ripan Cluj-Napoca**.

The research interests were related to the chemistry of aromatic heterocycles, free radicals and charge-transfer complexes, organic semiconductors, structural organic analysis, organic electrosynthesis and electron-transfer phenomena involving organic compounds. As results of his scientific activity, 4 books, 6 chapters included in multi-author books, 118 papers in peer-reviewed journals in Romania and abroad and 17 patented inventions were published. As recognition, he received The "Nicolae Teclu" award of the Romanian Academy in 1985 for fundamental research concerning the adiponitrile electrosynthesis, prizes of the Scientific Research Council of "Babeş-Bolyai" University for the books: "*Teoria reactivității compușilor organici*", M. Vlăssă and I. A. Silberg, vol. I și II (1998) and "*Chimia organică a produșilor naturali*", Castelia Cristea, Ionel Hopârtean și I. A. Silberg (2003). In 1996 he was elected **Corresponding member of the Romanian Academy**.

Prof. Silberg engaged many academic appointments with high professionalism: Member of the Editorial Boards of "*Revue Roumaine de Chimie*" (since 1997), "*Proceedings of the Romanian Academy, Ser. B, Chemistry, Life Sciences and Geosciences*" (since 1999), and "*Studia Univ. Babeş-Bolyai Ser. Chemia*" (since 1995); Member of the National Council of Validation of University Titles and Diplomas, since 1992, Member of the National Council of the Society of Romanian Chemists; Volunteer abstractor for "Chemical Abstracts", 1969-1990 and evaluator for *INTAS* European Program European since 2002.

As he mastered the foreign languages with high proficiency: English (fluently), French (fluently), Russian (fluently), German (well), and Italian (well), he was able to establish many scientific contacts with the international scientific community. He participated at many international scientific meetings and became an ambassador of the Romanian school of chemistry on the occasion of stages abroad in: *Germany* (Institute of Chemistry of the German - East - Academy, Berlin-Adlershof, Halle, Institut für Biochemie, visiting scientist, 1962; University of Heidelberg, visiting scientist, DAAD grant, 1993), *USA* (University of California Medical Center, San Francisco, Prof. Cymermann-Craig, and Palo Alto, California, Biochemical Laboratory of the Veterans Administration Hospital, visiting exchange scientist, 1968; University of Florida, Gainesville, 1994-95), *United Kingdom* (University of East Anglia, Norwich, TEMPUS grant, 1992), *France* (Université de la Méditerranée, Marseille, Prof. J. Barbe, visiting professor, 1995 and 1997) and *Sweden* (University of Lund, Electrochemical Biosensors Group, Dr Elisabeth Csöregi, visiting scientist, 1998).

Biographical notes are included in: *“Marquis Who’s Who in Science and Engineering”* 6th Edition, **2002-2003**; 7th Edition, **2003-2004**; *“Marquis Who’s Who in the World”* 21st Edition, **2004**; *“International Who’s Who of Intellectuals”* **2001**; *“International Dictionary of Distinguished Leadership”* **2002**; *“Who’s Who in Romania”* **2002**; *“The Contemporary Who’s Who”* 1st Edition, **2003**; *“2000 Outstanding Intellectuals of the 21st Century”***2004**.

As a man of encyclopedic spirit, he was able to inter-relate knowledge from different scientific areas, literature, philosophy and arts. He was an excellent speaker and his discourses were always extremely pleasant for everybody in the audience (from students to academic staff). I. A. Silberg was an outstanding professor with passion for science and a man of great honor who remains in our souls as a model of academic devotion.

Editor-in-Chief
Luminita Silaghi-Dumitrescu

PROF. DR. IOAN A. SILBERG*

PUBLICATIONS

I. Books and Monographs

1. C. Bodea and **I. A. Silberg** "*Recent Advances in the Chemistry of Phenothiazines*" in "*Advances in Heterocyclic Chemistry*", (Eds. A. R. Katritzky and A. J. Boulton), Academic Press Inc. New-York and London, **1968**, 9, p. 325-475.
2. **I. A. Silberg**, "*Metode magnetice de analiza (Magnetic methods of analysis)*" in "*Physico-Chemistry analysis methods*", (Eds. Ministry of Chemical Industry), Documentation Center, Bucharest, VI, **1970**.
3. **I. A. Silberg** and C. Marian, "*Chimie Organica-ghidul elevului (Organic Chemistry – student handbook)*", Dacia, Cluj, **1973**.
4. **I. A. Silberg** "*Kohlenstoff-Brom Verbindungen*" in "*Methodicum Chimicum*" (ed. F. Korte), Georg Thieme Verlag, Stuttgart and Academic Press, New-York, **1976**, VII, p.239-253; engl., **1977**, 7/A, p. 238-253.
5. **I. A. Silberg**, "*Kohlenstoff-Chlor Verbindungen*" in "*Methodicum Chimicum*" (ed. F. Korte), Georg Thieme Verlag, Stuttgart and Academic Press, New-York, **1976**, VII, p. 254-282; engl., 7/A, **1977**, p. 254-283.
6. **I. A. Silberg**, "*Spectrometria RMN a compușilor organici (NMR Spectrometry of Organic Compounds)*", Dacia, Cluj-Napoca, **1978**.
7. **I. A. Silberg**, "*Enciclopedia de chimie (Chemistry Encyclopedia)*", vol. 5 (E) and vol. 6 (F-G), Ed. Stiintifica si Enciclopedica, Bucharest, **1989** and **1996**.
8. M. Vlăsa and **I. A. Silberg** "*Teoria reactivității compușilor organici (Reactivity of Organic Compounds, Theoretical Approach)*", Conphys., Rm. Vâlcea, **1997**; I, ISBN 973-9334-03-2, *Idem*, **1998**; II, ISBN 973-9334-02-4.
9. C. Cristea, I. Hopârtean and **I. A. Silberg** "*Chimia organica a produsilor naturali (Organic Chemistry of Natural Products)*", RISOPRINT, Cluj-Napoca, **2002**; ISBN 973-656-273-5.
10. **I. A. Silberg**, G. Cormoș, and D. C. Oniciu, "*Retrosynthetic Approach to the Synthesis of Phenothiazines*" in *Advances in Heterocyclic Chemistry*, **2006**, 90, 205-237.

* "Babeș-Bolyai" University Cluj-Napoca, Faculty of Chemistry and Chemical Engineering, Organic Chemistry Department

PUBLICATIONS

II. Scientific Papers

A. IN INTERNATIONAL PEER-REVUES

1. C. Bodea and **I. A. Silberg**, "Octachlorophenothiazinyl, a Very Stable Nitrogen Radical", *Nature (London)*, **1963**, 198, 883.
2. C. Bodea, M. Terdic und **I. A. Silberg** „Über Phenthiazone. IX. Hochhalogenierte Phenthiazine and Phenthiazone", *Liebigs Ann. Chem.*, **1964**, 673, 113.
3. I. S. Forrest, S. D. Rose, L. G. Brooks, B. Halpern, V. A. Bacon and **I. A. Silberg** "Fluorescent Labeling of Psychoactive Drugs", *Agressologie*, **1970**, 11, 127.
4. **I. A. Silberg**, and M. Bartha "1H-Phenothiazin-1-ones, a New Class of Heterocyclic *ortho*-Quinone-imines", *Tetrahedron Letters*, **1974**, 3801-3804.
5. **I. A. Silberg**, R. Macarovici and N. Palibroda "Photolysis of 2-*ortho*-Nitrophenyl-5-aryloxazoles, a New Route to 2-Aroyl-1H-4-Quinazolinones", *Tetrahedron Letters*, **1976**, 1321.
6. **I. A. Silberg**, V. Fărcășan and M. V. Diudea "Free Radicals of Phenothiazines and Related Compounds. III. Selective Chlorination of Phenothiazines with Copper (II) Chloride", *J. prakt. Chem.*, **1976**, 318, 353.
7. C. Liteanu, E. Hopârtean and **I. A. Silberg** "Redox-Sensitive Membrane-Electrode Based on the Organic Free Radical Octachlorophenothiazinyl", *Talanta*, **1977**, 24, 589.
8. M. V. Diudea and **I. A. Silberg** "Free Radicals of Phenothiazine and Related Compounds. IV. Phenothiazinyl- and Diphenothiazine-Copper Complexes as Intermediates and Products in the Interaction of Phenothiazines with Cooper (II) Halides", *J. prakt. Chem.*, **1982**, 324, 769.
9. L. Oniciu, D. A. Löwy, **I. A. Silberg** and D. F. Anghel, "Potentiometric Determination of Cationic Surfactants Used in Adiponitrile Electrosynthesis", *Analisis*, **1986**, 14, 456.
10. L. Oniciu, D. A. Löwy, **I. A. Silberg**, and C. E. Florea "A New Multi-Purpose Reference Electrode", *Analisis*, **1987**, 15, 197.
11. M. Vlassa, **I. A. Silberg**, and C. Afloroaei "A New Rearrangement of Heterocyclic Isothiocyanates", *Heterocyclic Communications*, **1994**, 1, 55-58.
12. M. Vlassa, **I. A. Silberg**, R. Custelcean, and M. Culea "Reactions of π -Deficient Aromatic Heterocycles with Ammonium Polyhalides. I. Halogenation of Acridone and Acridine Derivatives Using Benzyltrimethylammonium Polyhalides", *Synthetic Communications*, **1995**, 25, 3493-3501.
13. **I.A.Silberg**, and C. Cristea, "Free Radicals of Phenothiazine and Related Compounds. VI. Radicals and Charge Transfer Complexes of Some Oligophenothiazines", *Heterocyclic Communication*, **1995**, 2, 117-124.

PUBLICATIONS

14. S. Filip, E. Surducan, M. Vlassa, **I. A. Silberg**, and G. Jucan, "Microwave-Assisted Acridones Preparation Using an Inorganic Acidic Solid Support" *Heterocyclic Communications*, **1996**, 3, 431-434.
15. D. A. Löwy, M. Jitaru, B. C. Toma, **I. A. Silberg**, and L. Oniciu "Technological Use of Propionitrile Electrosynthesis", *Indian Journal of Chemical Technology*, **1997**, 4, 18-24.
16. **I. A. Silberg**, S. Silberg, and A. Ghirişan "Aromaticity of Thiazole. III. The Transmission of Substituent Effects and the Polarizability of the Electronic System of Thiazole", *Heterocyclic Communications*, **1997**, 3, 35-39.
17. R. Custelceanu, M. Vlassa, **I. A. Silberg**, M. Szöke, S. I. Fărcaş and M. Culea "Reaction of π -Deficient Aromatic Heterocycles with Ammonium Polyhalides. II. Halogenation of Phenothiazine with Benzyltriethyl-ammonium Polyhalides" *Heterocyclic Communications*, **1997**, 3, 317-322.
18. R. Custelceanu, M. Vlassa and **I. A. Silberg** "Reaction of π -Deficient Aromatic Heterocycles with Ammonium Polyhalides. III. Halogenation of Phenothiazine-5-oxide with Benzyl-triethylammonium Polyhalides", *Monatshefte für Chemie*, **1997**, 128, 919-925.
19. M. Vlassa, **I. A. Silberg**, and L. I. Găină "Application of Phase Transfer Catalysis (PTC) without Solvent in Organic Synthesis. IV. Selective O-Alkylation of Hydroxyphenothiazine and Hydroxy-diphenylamine Derivatives", *J. prakt. Chem./Chemiker Zeitung*, **1998**, 340, 576-577.
20. S. V. Filip, **I. A. Silberg**, E. Surducan, M. Vlassa and E. Surducan, "Microwave-assisted Phenothiazines Preparations by Thionation of Diphenylamines", *Synthetic Communications*, **1998**, 28, 337-345.
21. **I. A. Silberg**, I. Silaghi-Dumitrescu, C. Cristea, P. Tordo, and D. Gîgmes "Molecular Orbital Calculations and Physical Properties of 1,4-Benzothiazino[2,3-*b*] phenothiazine and its Substituted Derivatives", *Heterocyclic Communications*, **1999**, 5, 147-150.
22. N. Palibroda, C. Cristea, **I. A. Silberg**, and Il. Chirtoc, "Mass Spectrometry Discrimination of Isomeric N,N'-Diarylphenylenediamine Derivatives", *Rapid Communications in Mass Spectrometry*, **1999**, 13, 2227.
23. E. Glodeanu, **I. A. Silberg**, M. Pleniceanu and C. Spînu, "New Phenothiazine Compounds with Dyeing Properties" *J. Indian Chem. Soc.*, **1999**, 76, 411-412.
24. I. Silaghi-Dumitrescu, **I. A. Silberg**, S. Filip, M. Vlassa, L. Silaghi-Dumitrescu and S. Hernandez-Ortega "The Crystal and Molecular Structure of the 2,4,6,8-tetra-*t*-Bu-Phenothiazine-0.5 Benzene Adduct", *Journal of Molecular Structure*, **2000**, 526, 279-286.

PUBLICATIONS

25. D. Dicu, L. Mureşan, I. C. Popescu, C. Cristea, **I. A. Silberg**, and P. Brouant "Modified Electrodes with New Phenothiazine Derivatives for Electrocatalytic Oxidation of NADH", *Electrochimica Acta*, **2000**, *45*, 3951-3957.
26. M. Dărăbanţu, G. Plé, I. Silaghi-Dumitrescu, C. Măiereanu, I. Turos, **I. A. Silberg**, and S. Mager, "Synthesis and Stereochemistry of Some 1,3-Oxazolidine Systems Based on TRIS (α, α, α -Trimethylaminomethane) and Related Aminopolyols Skeleton. Part I: (Di)spiro-1,3-oxazolidines", *Tetrahedron*, **2000**, *56*, 3785-3798.
27. M. Toşa, Cs. Paizs, C. Majdik, L. Poppe, P. Kolonits, **I. A. Silberg**, L. Novák, and F.-D. Irimie, "Selective Oxidation Methods for Preparation of N-Alkylphenothiazine Sulfoxides and Sulfones" *Heterocyclic Communications*, **2001**, *7*, 277-282.
28. V. Roşca, L. Mureşan, I. C. Popescu, C. Cristea and **I. A. Silberg**, "Gold Electrodes Modified with 16H,18H-Dibenzo[c,l]-7,9-Dithia-16,18-Diazapentacene for Electrocatalytic Oxidation of NADH" *Electrochem. Commun.*, **2001**, *3*, 439-445.
29. L. Găină, T. Lovasz, **I. A. Silberg**, C. Cristea, and S. Udrea, "New Schiff Bases Derived from 3-Formyl-10-alkyl-phenothiazine. I. NMR and UV-VIS Structural Assignments", *Heterocyclic Communications*, **2001**, *7*, 549-554.
30. I. Panea, A. Ghirişan, I. Cristea, R. Gropeanu, and **I. A. Silberg**, "Azocoupling Products. II. Synthesis and Structural Study of Azocoupling Products of 1-(5,6-Dimethyl-4-X-pyrimidin-2-yl)-3-methyl-pyrazolin-5-ones with Diazonium Salts", *Heterocyclic Communications*, **2001**, *7*, 563-570.
31. L. Ghizdavu, C. Cristea, **I. A. Silberg**, C. Bălan, and L. David, "Coordination Compounds of Copper(II) with New 1,4-Benzothiazino-[2,3-b] phenothiazine Derivatives" *Synth. React. Inorg. Met-Org. Chem.*, **2002**, *32*, 1-7.
32. I. Ciocan Tarţa, **I. A. Silberg**, M. Vlassa and I. Oprean, "Synthesis of Aldehydes and Ketones by the Dehydrogenation of Alcohols in the Presence of a Raney Nickel/Aluminium Isopropoxide/Alumina Catalyst" *Central Eur. J. Chem.*, (www.cesj.com) **2004**, *2*, 214-219.
33. C. Moldovan, C. Cristea, **I. A. Silberg**, A. Mahamoud, C. Deleanu, and J. Barbe, "A Convenient Route to 1,4-Dihydro-3-cyano-10-methyl-pyrido[3,2-g]-quinoline Derivatives as Key-Intermediates for the Synthesis of Novel MDR Reversal Agents", *Heterocyclic Communications*, **2004**, *10*, 19-24.
35. L. Gaina, C. Cristea, C. Moldovan, D. Porumb, E. Surducun, C. Deleanu, A. Mahamoud, J. Barbe and **I. A. Silberg**, "Microwave-assisted synthesis of phenothiazine and quinoline derivatives", *Int. J. Mol. Sci.*, **2007**, *8*, 70-80.

B. PROCEEDINGS OF INTERNATIONAL SCIENTIFIC MEETINGS (in extenso)

1. L. Oniciu, **I. A. Silberg**, I. Bâldea, and F. Ciomoş, "Kinetics of Competing Reactions of Acrylonitrile Electroreduction to Adiponitrile and Propionitrile" *36th Meeting of the International Society of Electrochemistry*, Salamanca, Spain, 23-28 sept. **1985**, Extended Abstracts, 13010-13012.

PUBLICATIONS

2. L. Oniciu, **I. A. Silberg**, V. Danciu, M. Olea, and S. Bran, "Kinetics and Mechanism of *p,p'*-Diaminodibenzyl Electrosynthesis" *36th Meeting of the International Society of Electrochemistry*, Salamanca, Spain, 23-28 sept. **1985**, Extended Abstracts p. 13020-13021.
3. **I. A. Silberg** and S. Silberg, "Heterolytic Fragmentation of Thiazolyl-phenothiazines and its Implications on the Degradation Mechanism of Phenothiazine Drugs", in "*Thiazines and Structurally Related Compounds*"; - Proceedings of the *6th International Conference on Phenothiazines and Related Psychotropic Drugs*, Pasadena, California, USA, 11-14 sept. 1990 (ed H.Keyzer), R.E.Krieger Publ. Co., Malabar, Florida, SUA, **1992**, 163-170.
4. C. Cristea, and **I. A. Silberg**, "Radical Salts of 1,4-Benzothiazino[2,3-b]phenothiazine", *7-th Blue Danube Symposium on Heterocyclic Chemistry* Eger, Ungaria, **1998** *Proceedings*, CD-ROM ISBN 963 03 5095 5, pag. 48-54.
5. **I. A. Silberg**, and I. Druțu, "The Synthesis of Some Highly Chlorinated Oligophenothiazines", *7-th Blue Danube Symposium on Heterocyclic Chemistry* Eger, Ungaria, **1998**, *Proceedings*, CD-ROM ISBN 963 03 5095 5, pag. 55-62.
6. J. Sabău, **I. A. Silberg**, and P. Vaillancourt, "The Impact of Oil Decay on Gassing and Reliability of Aging Power Transformers", *2002 Annual Report of the CEIDP (IEEE Dielectrics and Insulation Society, ed.)* **2002**, pag. 408-411.

C. ROUMANIAN JOURNALS

1. C. Bodea, M. Răileanu and **I. A. Silberg** "Despre fenotiazine. VIII. Adiția de hidracizi la nucleul chinoniminic al fenotiazonelor", *Analele Științ. Univ. "Al.I.Cuza" (Iași)*, **1960**, 6, 1023.
2. C. Bodea and **I. A. Silberg** „Zur Struktur des Phenothiazons-3“, *Revue de Chimie Acad. RPR*, **1962**, (apărut 1964), 7, 683.
3. C. Bodea and **I. A. Silberg** "Prepararea fenotiazin-5-oxizilor cu ajutorul alchilhidroperoxizilor", *Studii Cercet. Chimie (Cluj)*, **1963**, 14, 317.
4. C. Bodea and **I. A. Silberg** "Phenothiazones. X. Derivatives of 1,2-Dihydro-3H-phenothiazine; Undecachloro-1,2-dihydro-3H-phenothiazine", *Rev. Roumaine Chim.*, **1964**, 9, 425.
5. C. Bodea and **I. A. Silberg** "Free Radicals of Phenothiazines and Related Compounds I. The Thermal Decomposition of Undecachloro-1,2-dihydro-3H-phenothiazine and the Free Radical Octachlorophenothiazinyl", *Rev. Roumaine Chim.*, **1964**, 9, 505.
6. C. Bodea and **I. A. Silberg** "Free Radicals of Phenothiazines and Related Compounds II. The Influence of Substituents on the Magnetochemical Properties of Some Chloro- and Bromophenothiazinyls", *Rev. Roumaine Chim.*, **1965**, 10, 887.

PUBLICATIONS

7. **I. A. Silberg** and M. V. Diudea, "Phenazathionium Cations. I. The Dual Mechanistic Behaviour of Phenazathionium Cations and its Implications in the Reaction of NaNO_2 with Halophenothiazines" *Rev. Roumaine Chim.*, **1980**, 25, 1229.
8. **I. A. Silberg** and M. V. Diudea "Phenazathionium Cations. II. Accessibility of Positions 1(9) in Nucleophilic Substitutions Involving Phenazathionium Cations" *Rev. Roum. Chim.*, **1980**, 25, 1239.
9. **I. A. Silberg** and S. Silberg, "Derivatives of 4-Aminomethyl-thiazole. II. New Thiazole Derivatives of Urea and Thiourea", *Rev. Roumaine Chim.*, **1983**, 28, 719.
10. **I. A. Silberg** and S. Silberg "Derivatives of 4-Aminomethyl-thiazole. III. Oxidative Cyclizations and Dethionations in the Series of 1-Phenyl-3-(2-aryl-4-thiazolylmethyl)-thioureas", *Rev. Roumaine Chim.*, **1983**, 28, 139.
11. S. Silberg, **I. A. Silberg** and C. Bodea, „Derivatives of 4-Aminomethyl-thiazole. IV. Thiazole Derivatives of Phenothiazine”, *Rev. Roumaine Chim.*, **1983**, 28, 243.
12. D. A. Löwy, **I. A. Silberg**, and L. Oniciu "1,1'-Oxi-bis-(2,3,3,-tetracloropropan)-ul agent sinergetic pentru pesticide", *Rev. Chim.*, **1985**, 36, 33.
13. V. Danciu, **I. A. Silberg** and L. Oniciu, "Metodă spectrofotometrică de determinare a gradului de reducere electrochimică a acidului *p*-nitrobenzoic", *Rev. Chim.*, **1985**, 36, 243-246.
14. D. A. Löwy, **I. A. Silberg**, and L. Oniciu, "Metode gaz-cromatografice de separare a produşilor de electroreducere a acrilonitrilului", *Rev. Chim.*, **1985**, 36, 354-358.
15. L. Oniciu, **I. A. Silberg** and F. Ciomoş, "Electrosinteza adiponitrilului. I. Căi de obţinere a adiponitrilului; mecanismul reacţiei de electrohidrodimerizare a acrilonitrilului la adiponitril", *Rev. Chim.*, **1985**, 36, 406-410.
16. L. Oniciu, **I. A. Silberg** and F. Ciomoş "Electrosinteza adiponitrilului. II. Influenţa condiţiilor experimentale asupra selectivităţii electrosintezei adiponitrilului", *Rev. Chim.*, **1985**, 36, 503- 508.
17. L. Oniciu, **I. A. Silberg** and F. Ciomoş, "Electrosinteza adiponitrilului. III. Aspecte tehnologice", *Rev. Chim.*, **1985**, 36, 628-634.
18. E. Glodeanu şi **I. A. Silberg**, "Reacţii de alchilare şi arilare a fenotiazinei în scopul obţinerii de noi coloranţi", *Analele Univ. Craiova, Secţ. Mat. Fiz. Chim.*, **1985**, 14, 87.
19. L. Oniciu, **I. A. Silberg**, D. A. Löwy, M. Jitaru and F. Ciomoş "Electrosynthesis of Propionitrile. I. Preliminary Experiments", *Studia Univ. Babeş-Bolyai, Ser. Chemia*, **1986**, 31, 80.

PUBLICATIONS

20. L. Oniciu, D. A. Löwy, M. Jitaru, **I. A. Silberg**, and B. C. Toma, "Electrosynthesis of Propionitrile. II. Phase Equilibria in the Acrylonitrile-Propionitrile-Water System in the Presence of Cationic Surfactants and Electrolytes" *Rev. Roumaine Chim.*, **1987**, *32*, 701.
21. **I. A. Silberg**, and I. Marian, "Structural Considerations and Their Correlation with Possible Conduction Mechanism in Organic Free Radicals of the Highly Halogenated Phenothiazines Series", *Studia Univ. Babeş-Bolyai, Ser. Chemia*, **1988**, *33*, 91.
22. L. Oniciu, D. A. Löwy, M. Jitaru, **I. A. Silberg**, B. C. Toma and I. Bâldea "Electrosinteza propionitrilului. III. Aspecte cinetice ale reducerii electrochimice nedimerizante a acrilonitrilului la propionitril", *Rev. Chim.*, **1988**, *39*, 219.
23. L. Oniciu, M. Jitaru and **I. A. Silberg**, "Mediated Electrocatalysis. I. General Aspects" *Rev. Roumaine Chim.*, **1989**, *34*, 537-549.
24. M. Brie and **I. A. Silberg** "Derivatives of Pyrazoles. I. Synthesis and IR-Spectra of Some New 3-Methyl-5-aryl-pyrazoles", *Rev. Roumaine Chim.*, **1989**, *34*, 733.
25. M. Brie, **I. A. Silberg** and N. Palibroda "Derivatives of Pyrazoles. II. The Influence of Alkaline Media on the Reaction of 1,3-Dicarbonyl Compounds with Hydrazine", *Rev. Roumaine Chim.*, **1989**, *34*, 945.
26. M. Brie, N. Palibroda and **I. A. Silberg** "Derivatives of Pyrazoles. III. Mass Spectra of 3-Methyl-5-*o*-substituted-phenyl-pyrazoles", *Rev. Roumaine Chim.*, **1989**, *34*, 2067.
27. L. Oniciu, **I. A. Silberg**, D. A. Löwy, M. Jitaru, F. Ciomoş, O. H. Oprea, B. C. Toma and M. Toma, "Effect of Surfactants on the Electroreduction of Acrylonitrile" *Rev. Roumaine Chim.*, **1990**, *35*, 859-866.
28. M. Brie and **I. A. Silberg** "Derivatives of Pyrazoles. IV. Bromination of 3-Methyl-5-Aryl-Pyrazoles", *Rev. Roumaine Chim.*, **1992**, *37*, 1279-1283.
29. **I. A. Silberg**, M. Bossany and C. Molnariu, "Free Radicals of Phenothiazines and Related Compounds. V. Light-Assisted, One-Electron Reduction of Highly Halogenated Phenazathionium Cations", *Rev. Roumaine Chim.*, **1993**, *38*, 1215-1222.
30. T. Budiu, R. Văţulescu and **I. A. Silberg** "Complecşi ai Cu(II) şi Ni(II) cu sulfatiazolul", *Rev. Chim.*, **1993**, *44*, 435-440.
31. R. Văţulescu, T. Budiu and **I. A. Silberg**, "Complecşi ai Co(III) cu sulfametinel şi sulfatiazolul", *Rev. Chim.*, **1993**, *44*, 712-718.
32. M. Vlassa, C. Molnariu and **I. A. Silberg** "Applications of Phase-Transfer Catalysis in Acridine Series. VI. Preparation of Some 9-Vinylacridine Derivatives", *Rev. Roumaine Chim.*, **1994**, *39*, 315-317.

PUBLICATIONS

33. I. Bâldea, **I. A. Silberg** and A. Ghirişan, "Cinetica cuplării pirimidinil-pirazolonelor cu săruri de diazoniu", *Analele Univ. Craiova, Ser. Chimie*, **1995**, *1*, 95-98.
34. E. Glodeanu and **I.A. Silberg** «Sinteza unor compuși 10-substituiți ai fenotiazinei», *Analele Univ. Craiova, Ser. Chimie*, **1995**, *1*, 151-154.
35. S. Silberg, **I. A. Silberg**, and A. Ghirişan "Aromaticity of Thiazole. I. Transmission of Substituent Effects Through the 2,5-Thiazolylene Bridge", *Studia Univ. "Babeş-Bolyai" Ser. Chem*, **1996**, *41*, 19-26.
36. **I. A. Silberg**, A. Ghirişan, and S. Silberg "Aromaticity of Thiazole. II. Transmission of Substituent Effects Through the 2,4-Thiazolylene Bridge", *Studia Univ. "Babeş-Bolyai" Ser. Chem.*, **1996**, *41*, 27-34.
37. C. Cristea and **I. A. Silberg**, "Sulfur Oxidation of 16H, 18H - Dibenzo-[c,l]-7,9-dithia-16,18-diazapentacene", *Studia Univ. "Babeş-Bolyai" Ser. Chem.*, **1996**, *41*, 51-54.
38. C. Cristea and **I. A. Silberg**, "Cation Radical Salts of 1,4-Benzothiazino-[2,3 b]-phenothiazine", *Studia Univ. "Babeş-Bolyai" Ser. Chem.*, **1996**, *41*, 77-80.
39. **I. A. Silberg**, L. Oniciu, L.D. Boboş, I. Silaghi-Dumitrescu, S. Avram and C. Cuibus, "Ion-Molecule Interactions in Organic Electrochemical Systems. I. NMR Investigations of Electrolyte Solutions Used in Lithium Anode Batteries", *Rev. Roumaine Chim.* **1997**, *42*, 535-540.
40. P. Şteţiu, **I. A. Silberg**, Gh. Borodi, I. Bobailă and L. Ilieş, "Crystal Growth and Crystalline Structure of Octachlorophenothiazine", *Studia Univ. "Babeş-Bolyai" Ser. Chem.*, **1997**, *42*, 89-93.
41. I. Bâldea, A. Ghirişan, **I. A. Silberg**, and I. Cristea, "Tautomerism, Acid Dissociation Equilibria and Azo-Coupling Reaction Rates of 1-Pyrimidinyl -3-Methylpyrazolon - 5 ones.", *Rev. Roumaine Chim.* **1997**, *42*, 865-872.
42. M. Simihăian, and **I. A. Silberg**, "The Effect of Temperature and pH on Kinetic Properties of Soil Urease.", *Studia Univ. "Babeş-Bolyai" Ser. Biologia*, **1998**, *43*, 143-149.
43. I. Ciocan-Tarţa, M. Vlassa, **I. A. Silberg**, and I. Oprean, "Synthesis of Ketones by Oppenauer Oxidation.", *Rev. Roumaine Chim.* **1999**, *44*, 45-49.
44. P. Ioniţă, T. Constantinescu, H. Căldăraru, C. Luca, M. T. Căproiu, F. Dumitraşcu, **I. A. Silberg**, and A. T. Balaban, "The Reaction Between the DPPH Free Radical and KCN in the Presence of Crown Ether 18-C-6 – a Correction.", *Rev. Roumaine Chim.* **1999**, *44*, 393-396.

PUBLICATIONS

45. M. Jitaru, C. Cristea and **I. A. Silberg**, "Voltammetric Behaviour of 1,4-Benzothiazino-[2,3-b]-phenothiazine and Some of its Derivatives. I.", *Rev. Roumaine Chim.* **1999**, *44*, 865-868.
46. **I. A. Silberg** and A. Ghirişan "The Transmission of Substituent Effects in Organic Compounds. I. The Inductive Effect.", *Roumanian Chemical Quarterly Reviews*, **2000**, *8*, 45-54.
47. **I. A. Silberg** and A. Ghirişan "The Transmission of Substituent Effects in Organic Compounds. II. The Separation of Inductive and Resonance Effects.", *Roumanian Chemical Quarterly Reviews*, **2000**, *8*, 145-155.
48. C. Cristea, C. Filip, I. Silaghi-Dumitrescu and **I. A. Silberg** "Voltammetric Behaviour of 1,4-Benzothiazino-[2,3-b]-phenothiazine and Some of its Derivatives. II. The Influence of N-Substitution and S-Oxidation." *Rev. Roumaine Chim.* **2000**, *45*, 639-642.
49. I. Ciocan-Tarţa, I. Oprean, A.-R. Tomşa, S. Puiu, S. Fărcaş and **I. A. Silberg**, "One-Step Synthesis of Lavandulol by Homogeneous Catalysis in the Presence of Water-Soluble Pd(0) Catalyst.", *Proc. Rom. Acad. Series B*, **2000**, *2*, 133-134.
50. Fl. Ciomoş and **I. A. Silberg** "The Co-ordinative Chemistry of Acrylonitrile", *Roumanian Chemical Quarterly Reviews*, **2000**, *8*, 225-232.
51. F. D. Irimie, M. Toşa, Cs. Paizs, C. Majdik, P. Moldovan, and **I. A. Silberg** "Biocatalytic Synthesis of Some Novel (10-Alkyl-10H-phenothiazine-3-yl)methyl Acetates Mediated by Lipase B from *Candida antarctica*.", *Roum. Biotechnol. Lett.*, **2000**, *5*, 55-62.
52. M. Jitaru, C. Moinet, **I. A. Silberg**, C. Filip and A. Katona, "Electrochemical Reduction of Some Nitrophenothiazines", *Rev. Roumaine Chim.* **2001**, *46*, 51-56.
53. A. Katona, J. Stroka, M. Jitaru, **I. A. Silberg**, and G. Petrica, "New Aspects of the Electrochemical Behaviour of Phenothiazine Derivatives", *Scientific Bulletin of University POLITEHNICA of Bucharest (Series B: Chemistry & Materials Science)*, **2001**, *63*, 399-404.
54. L. Găină, C. Cristea, **I. A. Silberg**, T. Lovász, C. Deleanu, and S. Udrea, "Solvent Effects in ¹H-NMR Spectrum of 3-Formyl-10-methyl-phenothiazine", *Studia Univ. "Babeş-Bolyai" Ser. Chem.*, **2002**, *47*, 41-44
55. D. Porumb, C. Cristea, and **I. A. Silberg**, "The Synthesis of New Phenothiazine Compounds by the Thiation of Diphenylamine Derivatives", *Studia Univ. "Babeş-Bolyai" Ser. Chem.*, **2002**, *47*, 45-50.
56. M. Jitaru, G. Petrica, L. Găină, C. Cristea, T. Lovász, and **I. A. Silberg** "Electrochemical Investigations of Electron-Transfer Phenomena in the Series of Phenothiazines and of Related Compounds I. Comparative Study of N-Alkyl-3-formyl-phenothiazines and of a Phenothiazine Schiff Base", *Rev. Roumaine Chim.* **2002**, *47*, 249-255.

PUBLICATIONS

57. M. Brie, C. Prejmerean, M. Moldovan, R. Grecu, G. Furtos and **I. A. Silberg** "Obtaining and Characterizing Some Composites Based on Polyelectrolytic Systems Modified with Compatible Monomers and Superficially Active Glasses", *Rev. Roumaine Chim.* **2002**, *47*, 559-569.
58. D. Gligor, L. Mureşan, I. C. Popescu and **I. A. Silberg**, "Chlorinated Phenothiazine Derivatives as Mediators for NADH Oxidation. I. Undecachloro-1,2-dihydro-phenothiazine Graphite Modified Electrode", *Rev. Roumaine Chim.* **2002**, *47*, 953-961.
59. L. Găină, C. Cristea, T. Lovász, **I. A. Silberg**, and S. Udrea, "Aryl-Substituted Phenothiazinyl-Enones I. Synthesis and Structural NMR Assignments", *Rev. Roumaine Chim.* **2002**, *47*, 983-988.
60. C. Cristea, C. Orac, D. Fodoca, D. Porumb and **I. A. Silberg**, "Aromatic Secondary Amines, Molecular Structure and Chemical Reactivity in Thiation Reactions.", *Annals of West University of Timisoara, Series Chemistry*, **2003**, *12*, 11-16.
61. D. Gligor, L. Mureşan, I. C. Popescu and **I. A. Silberg**, "Chlorinated Phenothiazine Derivatives as Mediators for NADH Oxidation. II. Comparative Study of Octachloro-phenothiazinyl and Heptachloro-hydroxy-phenothiazine Modified Graphite Electrodes" *Rev. Roumaine Chim.* **2003**, *48*, 463-470.
62. L. Găină, T. Lovász, C. Cristea, **I. A. Silberg**, and C. Deleanu, "Synthesis and Structural Assignments of New Long-Chain Alkyldioxy-bis-Diphenylamines and Phenothiazines", *Rev. Roumaine Chim.* **2003**, *48*, 549-554.
63. L. Ferencz, V. Fărcăşan, and **I. A. Silberg**, "Synthesis in Mixture of Some New Sulphonamides with Acridinic Nucleus" *Analele Ştiinţ. Univ. "Al.I.Cuza" (Iaşi), Ser. Chimie*, **2003**, *11*, 139-146.
64. L. Ferencz, V. Fărcăşan, and **I. A. Silberg**, "New Sulphonamides with Acridinic Nucleus", *Rev. Roumaine Chim.* **2003**, *48*, 801-811.
65. I. Panea, A. Ghirişan, F. Iura, R. Gropeanu and **I. A. Silberg**, "Azocoupling Products. III. Spectroscopic Investigation and Synthesis of Some Azocoupling Products between 1-(4-Hydroxy-6-methyl-pyrimidin-2-yl)-3-methyl-pyrazolin-5-one and Aromatic Diazonium Salts", *Studia Univ. "Babeş-Bolyai" Ser. Chem.*, **2003**, *48*, 55-65.
66. I. Panea, A. Ghirişan, I. Baldea, I. Silaghi-Dumitrescu, L. Crăciun, and **I. A. Silberg**, "Azocoupling Products. IV. The Structure of Dyes Obtained by Azo-Coupling Reaction of 1-(4-Hydroxy-6-methyl-pyrimidin-2-yl)-3-methyl-pyrazolin-5-one with Aromatic Diazonium Salts", *Studia Univ. "Babeş-Bolyai" Ser. Chem.*, **2003**, *48*, 67-83.

PUBLICATIONS

67. S. Lozovanu, L. Silaghi-Dumitrescu, and **I. A. Silberg**, "Applications of Calix[4]pyrroles", *Studia Univ. "Babeş-Bolyai" Ser. Chem.*, **2004**, 49, (1) 125-148.
68. Cl. Moldovan, C. Cristea, **I. A. Silberg**, A. Mahamoud, C. Deleanu, and J. Barbe, "Reactions of the 3-Cyano-10-methyl-pyrido[3,2-g]quinolin-4-one", *Studia Univ. "Babeş-Bolyai" Ser. Chem.*, **2004**, 49, (2) 117-122.
69. D. Gligor, M. Socol, I. C. Popescu, C. Cristea and **I. A. Silberg**, "Graphite Electrode Modified by Charge Transfer Complex between Tetracyanoquinodimethane and 16H,18H-Dibenzo[c,1]-7,9-dithia-16,18-diazapentacene Used for NADH Electro-Oxidation", *Studia Univ. "Babeş-Bolyai" Ser. Chem.*, **2004**, 49, (2) 123-130.
70. Cl. Moldovan, C. Cristea, **I. A. Silberg**, A. Mahamoud, S. Udrea and J. Barbe, "Reactions of the 3-cyano-10-methyl-Pyrido[3,2-g]quinolin-4-one. II", *Studia Univ. "Babeş-Bolyai" Chemia LI*, 1, **2006**, 21-26.
71. G. Cormos, C. Cristea, I. Filip, **I. A. Silberg**, "Bis-phenothiazinyl-phenyl-methane derivatives", *Studia Univ. "Babeş-Bolyai" Chemia*, LI, 2, **2006** pag155-157.

D. OTHER NATIONAL PUBLICATIONS

1. H. Bednar, I. Sabău and **I. A. Silberg**, "Puritatea uleiurilor electroizolante", *Energetica*, **1978**, 26, 291.
2. L. Oniciu, D. A. Löwy, O. H. Oprea, **I. A. Silberg** and Z. Csipor-Fazakas, "Studiul comportamentului unor sorturi de elastomeri la acțiunea acrilonitrilului", *Materiale Plastice*, **1984**, 21, 146-148.
3. D. A. Löwy, **I. A. Silberg**, L. Oniciu and O. H. Oprea, "Modificarea chimică a polietilenei. I. Studiul polimerului funcționalizat prin spectrometrie IR", *Materiale Plastice*, **1985**, 22, 111-114.
4. D. A. Lowy, **I. A. Silberg**, L. Oniciu, O. H. Oprea and A. Horvath, "Modificarea chimică a polietilenei. II. Studiul produșilor de condensare a polimerului funcționalizat prin spectrometria IR", *Materiale Plastice*, **1987**, 24, 8-11.
5. L. Oniciu, D. A. Löwy, O. H. Oprea, and **I. A. Silberg**, "Studii structurale asupra membranelor schimbătoare de ioni obținute prin funcționalizarea unor folii de polimer", *Materiale Plastice*, **1988**, 25, 177-180.
6. M. Simihăian and **I. A. Silberg**, "Efectul cryseanului și benzoil-cryseanului asupra activității ureazei din sol", *Analele Univ. Oradea*, fasc. Biologie, **1996**, 3, 149-156.

PUBLICATIONS

PATENTS

1. C. Bodea and **I. A. Silberg**, "Procedeu de eliminare a peroxizilor din eteri (Process for removing peroxides from ethers)" RPR Patent 42266 (**1962**); secondary Patents: Belg. 625714; Brit. 1032633; Ger. 1216279; Ger. (East). 31929; Ital. 679229; Fr. 1341116.
2. C. Liteanu, E. Hopârtean and **I. A. Silberg**, "Electrod-membrană redox-sensibil (Redox-senzitive membrane electrode)", RSR Patent 59.022 (**1974**).
3. **I. A. Silberg** and M. Bartha, "Procedeu de preparare a acizilor N-aril-antranilici (Process for preparing N-arylantranilic acids)", RSR Patent 64.163 (**1977**).
4. **I. A. Silberg**, "Procedeu de preparare a 1,2,3,4,6,7,8,9-octaclorofenotiazinilului (Process for preparing 1,2,3,4,6,7,8,9-octachlorophenothiazinyl)", RSR Patent 68.246 (**1977**).
5. C. Anghel and **I. A. Silberg**, "Procedeu de preparare a 2,4-difenil-6-clor-chinazolinei (Process for preparing 2,4-diphenyl-6-chloro-quinazoline)", RSR Patent 70.108 (**1977**).
6. M. V. Diudea and **I. A. Silberg**, "Derivați de fenotiazină și procedeu de preparare a lor (Phenothiazine derivatives and preparation process) RSR Patent 79.933 (**1982**).
7. L. Oniciu, O. H. Oprea, D. A. Löwy and **I. A. Silberg**, "Procedeu de obținere a unor membrane schimbătoare de ioni (Process for obtaining some ion exchange membranes)", RSR Patent 87.994 (**1985**).
8. L. Oniciu, D. A. Löwy, O. H. Oprea, **I. A. Silberg** and A. Horvath, "Procedeu pentru îmbunătățirea permselectivității membranelor cationice polietilensulfonice (Process for enhancement of permselectivity of cationic polyethylenesulfonic membranes)" RSR Patent 88088 (**1985**).
9. L. Oniciu, **I. A. Silberg**, F. Ciomoș, M. Jitaru, P. Popescu, D. A. Löwy and O. H. Oprea, "Procedeu de preparare a adiponitrilului (Process for preparation of adiponitrile)" RSR Patent 88.417 (**1985**).
10. L. Oniciu, **I. A. Silberg**, V. Toc, F. Ciomoș, O. H. Oprea, D. A. Löwy and M. Jitaru, "Reactor electrochimic pentru sinteza adiponitrilului (Electrochemical reactor for the synthesis of adiponitrile)", RSR Patent 91.208 (**1986**).
11. L. Oniciu, **I. A. Silberg**, F. Ciomoș, D. A. Löwy, M. Jitaru and O. H. Oprea, "Procedeu de obținere a anozilor de dioxid de plumb pentru electrosinteza adiponitrilului (Process for obtaining lead dioxide anodes for the electrosynthesis of adiponitrile)", RSR Patent 91.210 (**1986**).

PUBLICATIONS

12. **I. A. Silberg**, V. A. Topan, P. S. Agachi, I. Bâldea, M. Vezensyi, M. Brie, F. Eftimie and L. Oniciu, "Procedeu și reactor pentru prepararea cloraminei (Process and reactor for the preparation of chloramine)" RSR Patent 93.338 (1987).

13. L. Oniciu, **I. A. Silberg**, V. A. Topan, F. Eftimie, P. S. Agachi, M. Vezensyi, M. Brie and I. Bâldea, "Procedeu de preparare a hidratului de hidrazină (Process for preparation of Hydrazine hydrate)", RSR patent 93.339 (1987).

14. I. Bâldea, **I. A. Silberg**, V. A. Topan, F. Eftimie, P. S. Agachi, M. Vezensyi, M. Brie and L. Oniciu, "Procedeu de preparare a 3,3-dialchil diaziridinelor și dialchil cetazinelor (Process for preparation of 3,3-dialkylaziridines and dialkylcetazines) RSR Patent, 93.340 (1987).

15. V. A. Topan, **I. A. Silberg**, P. S. Agachi, F. Eftimie, M. Vezensyi, M. Brie, I. Bâldea and L. Oniciu, "Procedeu de obținere a sulfatului de hidrazină (Process for preparation of hydrazine sulphate)", RSR Patent 93.341 (1987).

16. V. Danciu, **I. A. Silberg**, O. H. Oprea and L. Oniciu, "Procedeu de obținere pe cale electrochimică a *p,p'*-diaminodibenzilului (Process for the electrochemical preparation of *p,p'*-diaminodibenzyl)", RSR Patent 94.517 (1987).

17. A. Gergely, A. Bodor, **I. A. Silberg**, R. Schwartz, A. Schwartz, V. Cadiș, D. Breazu and A. Șerbănescu, "Procedeu de scindare a ciclului epoxidic 6,19 din seria steranilor androstanici (Process for epoxide cycle 6,19 cleavage in the series of steran androstanes), Roumanian Patent 104.492 (1991).

In memoriam prof. dr. Ioan A. Silberg

**MICROWAVE-ASSISTED SYNTHESIS AND ELECTROCHEMICAL
BEHAVIOUR OF PHENOTHIAZINE-FORMALDEHYDE
POLYMER DERIVATIVE**

**CASTELIA CRISTEA^a, GABRIELA CORMOS^b, LUIZA GĂINĂ^a,
LUMINIȚA SILAGHI-DUMITRESCU^a, DELIA GLIGOR^a,
LIANA MURESAN^a, IONEL CĂTĂLIN POPESCU^a**

ABSTRACT. Phenothiazine-formaldehyde polymer was obtained by condensation reaction of 10*H*-phenothiazine with formaldehyde in the presence of acid catalysts. The synthesis was performed both under classical heating and microwave assisted heating conditions. Two different microwave installations were employed for optimizing the reaction conditions. Modified electrodes were prepared by adsorption of this polymer material on spectrographic graphite and the electrochemical parameters were estimated.

Keywords: phenothiazine, MAOS, modified electrodes, cyclic voltammetry

INTRODUCTION

During the last decade, the microwave heating became a popular alternative to conventional conductive heating not only for domestic food processing, but also for chemical synthesis purposes. The increasing number of scientific reports dedicated to the microwave-assisted organic synthesis (MAOS) shows that this technique is very convenient for the processing of organic matter. A survey of literature data shows that MAOS was applied to almost all of previously conventionally heated reactions [1-4]. Due to certain advantages, particularly shorter reaction times, which offer the possibility of rapid optimization of chemical reactions, MAOS became an experimental technique applied for the syntheses of a large number of organic fine chemicals. MAOS also joins some of the major principles of the *green chemistry* such as: *the increase of energy efficiency* by effective *in situ* conversion of the electromagnetic energy into heat which avoids energy loss, and *the use of safer solvents and reaction conditions* by avoiding the use of toxic solvents in solvent-free reactions, or the use of water and other solvents under supercritical conditions (reaction pressures of 2-3 Mpa which

^a "Babeș-Bolyai" University, Faculty of Chemistry and Chemical Engineering, Cluj-Napoca-Ro

^b "L. Blaga" University, Faculty of Medicine, Sibiu

would facilitate temperatures in the order of 200 °C for common solvents such as methanol, ethanol, acetone, all which boil below 85 °C at atmospheric pressure).

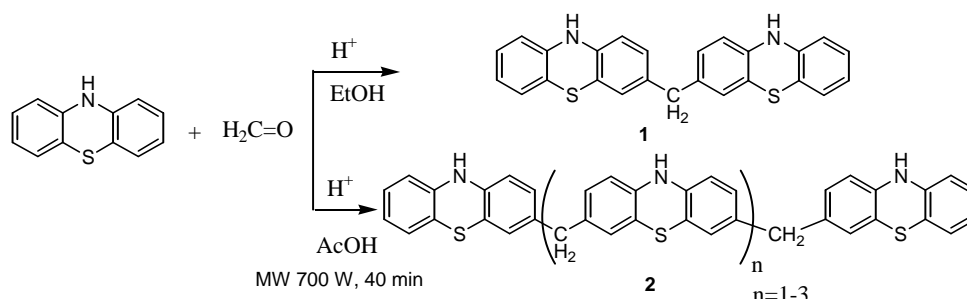
The synthesis and electrochemical characterization of several phenothiazine derivatives was a constant interest for our research group during last years [5-8]. In this paper, we present the microwave assisted synthesis and the electrochemical characterization of a phenothiazine-formaldehyde polymer derivative based on *bis*-(phenothiazin-3-yl)-methane moiety. A comparison between classical synthesis and the microwave assisted syntheses performed using two different experimental techniques was attempted. The electrochemical behaviour was studied by simple adsorption on graphite electrode surface, using cyclic voltammetric (CV) measurements and an explanation of the electrochemical parameters was attempted. An electrochemical study can be performed using two methods: (i) the investigated compound dissolved in solution [9-16] or (ii) the investigated compound adsorbed on an electrode surface [17-19]. We choosed the second method because the investigation of the adsorbed systems requires small quantities of organic compounds, so that modified electrodes can be easily obtained at laboratory scale and the observed properties may recommend them as electrocatalysts for the obtaining of sensors / biosensors, etc.

RESULTS AND DISCUSSION

Synthesis

Phenothiazine dimer or higher oligomer obtaining by the condensation reaction of phenothiazine with aldehydes such as formaldehyde, acetaldehyde or benzaldehyde, was already reported [20-21]. The condensation of phenothiazine with formaldehyde in solution, in the presence of an acid catalyst leads to *bis*-(10*H*-phenothiazin-3-yl)-methane **1** accompanied by oligomers **2** (Scheme 1). The catalytic activity of hydrochloric acid, methanesulfonic acid and respectively trifluoroacetic acid were compared. Best results were obtained in the presence of hydrochloric acid.

The reaction conditions can be optimized in order to change the relative ratios of the reaction products. Thus, when acetic acid was employed as solvent, *bis*-(10*H*-phenothiazin-3-yl)-methane **1** was obtained in lower amounts and oligomers **2** appeared as major reaction products. The condensation products **1**, **2** precipitated from the reaction mixture and were easily separated by filtration. The conversion of the phenothiazine was about 90%. **1** was removed by dissolution in THF. The mixture of oligomers **2** is a dark powder highly insoluble in organic solvents such as ethanol, acetone, ether, toluene.



The structure assignment of **1** is supported by spectroscopic data. EI mass spectrum shows the molecular peak situated at 410 m/e. The substitution in position 3 of the phenothiazine units was unambiguously assigned by $^1\text{H-NMR}$ spectroscopy; thus, in the 2D $^1\text{H-}^1\text{H}$ homocorrelation COSY-45 spectrum, the cross peaks of the signals situated in the 6.6-6.9 ppm range reveals the aromatic protons coupling patterns. For the methylene bridge, $^{13}\text{C-NMR}$ spectrum shows one signal situated at 40 ppm.

For the polymer structure **2**, FT-IR spectroscopy indicate the stretching vibration of N-H bonds by the absorption band situated at 3230 cm^{-1} . 300 MHz $^1\text{H-NMR}$ spectrum shows a singlet signal situated at 3.5 ppm for the equivalent methylene protons and a singlet signal situated at 8.5 ppm assigned to the protons in the NH groups of the equivalent phenothiazine units. Unfortunately, the signals of the protons attached to the heteroaromatic ring give an overlapping multiplet in the 6.6-7 ppm range. The analogy with the well resolved spectrum of parent compound **1** enables us to suggest the same substitution pattern for oligomer **2**.

Microwave assisted synthesis of phenothiazine-formaldehyde polymer derivative 2

The experimental techniques applied for the microwave-assisted syntheses of phenothiazine-formaldehyde polymer derivatives described below, are based on two different microwave installations:

a) dynamic microwave power system designed by INCDTIM Cluj-Napoca [22], as a mono-mode cavity reactor for open vessel operating conditions. The advantage of the single-mode cavity is the uniform heating pattern, higher field strengths and reproducible conditions in small reactors. The disadvantage is due to small sample volumes and to the fact that only one reaction vessel can be irradiated at the time.

b) microwave installation *Synthos 3000* designed by Parr instrument company as a multimode cavity reactor for high pressure operating conditions. Reproducible operating conditions are ensured in the reactor equipped with temperature and pressure sensors, built-in magnetic stirrer, cooling mechanisms, power control and software operation. The advantage relies on the fact that parallel syntheses can be performed in several reaction vessels which can be irradiated simultaneously in multivessel rotors.

Two different reaction techniques were employed:

a) “Dry media” procedure, which involved solventless conditions and the reagents were preadsorbed onto a more or less microwave transparent inorganic support (silica gel, alumina or clay). This solvent free approach is appropriate for MAOS in open vessel conditions.

b) Pressurized systems procedure, where the reaction was carried out in standard organic solvents under sealed vessel conditions.

Table 1 presents a comparison between the experimental conditions employed and the results obtained in the microwave-assisted synthesis of **2**. Classical heating by thermal convection and microwave heating of the reaction mixture in acetic acid solvent affords similar reaction yields of **2**, but significantly shorter reaction times are requested by MAOS. Dry media procedure generated lower yields due to the immobilization of the highly insoluble reaction product on the solid support.

Table 1.

Experimental conditions for the synthesis of phenothiazine-formaldehyde polymer derivative **2**

Procedure	Heating type	Solvent/ Support	Temp. [°C]	Time [min]	Yield [%]
Classical	Thermal convection	AcOH	60	120	78
Dry media	Single-mode MW cavity	Al ₂ O ₃	60	15	38
Pressurized systems	Multi-mode MW cavity	AcOH	60	40	75

Electrochemical behaviour of phenothiazine-formaldehyde polymer derivative **2**

The electrochemical behavior of **2** was studied by simple adsorption on a graphite electrode surface, using cyclic voltammetric (CV) measurements. The modified graphite electrodes were obtained by spreading onto the electrode surface a solution 1 mM of **2** in dimethylsulfoxide and leaving them to dry at room temperature. Before immersion in the test solution the modified electrodes were carefully washed with water. For each electrode, the surface coverage (Γ , mol cm⁻²) was estimated from the under peak areas, recorded during the CV measurements at low scan rate (< 10 mV s⁻¹), and considering as 1 the surface redox valency [23]. The presented results are the average of three identically prepared electrodes.

Figure 1 shows the voltammetric response corresponding to compound **2** adsorbed on the surface of a graphite electrode in a phosphate buffer solution (pH 7) and the stability of the modified electrode expressed by the time dependence of the surface coverage for the obtained modified electrode.

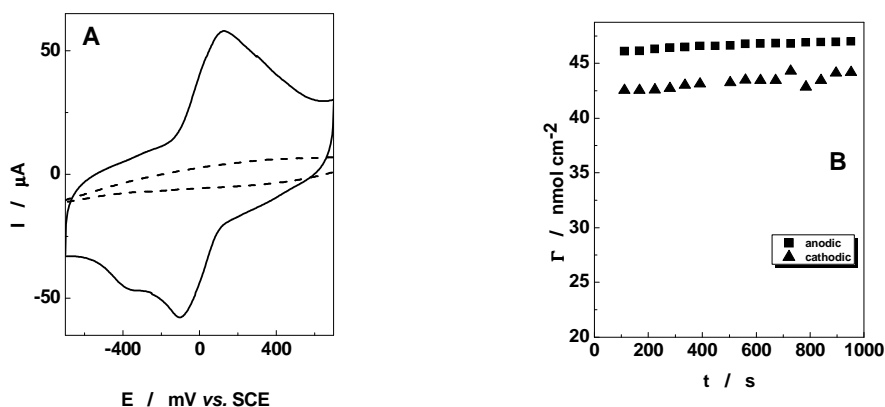
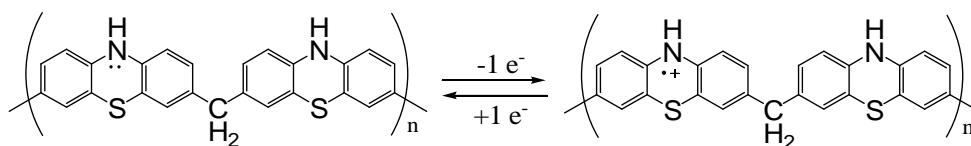


Figure 1. (A) Cyclic voltammograms of graphite electrode (---) and of compound **2** adsorbed on graphite (—). (B) Time dependence of surface coverage for compound **2** adsorbed on graphite.

Experimental conditions: starting potential -0.700 V/SCE; potential scan rate 50 mV s⁻¹; supporting electrolyte, 0.1M phosphate buffer, pH 7.

The voltammogram of compound **2** (fig. 1A) shows an oxidation wave ($E_{pa}^{0/+1} = 74$ mV vs. SCE), which can be assigned to the formation of stable radical cations generated by the phenothiazine structural units present in the molecular structure (scheme 2).



Scheme 2

The width at half peak height (E_{FWHM} values given in table 2) was different to the one corresponding to the ideal case ($E_{FWHM} = 90.6/n$ mV, where n is the number of electrons). The observed discrepancies might prove the existence of

repulsive interactions between the adsorbed redox species (radical cations generated in the anodic process) [23,25]. Compound **2** exhibits the relative current ratio I_{pa}/I_{pc} close to one, specific to adsorbed conditions [23]. The electrochemical stability was studied by cycling the electrode potential in phosphate buffer solution during 20 cycles. It was observed that the shape of the voltammogram remained unchanged (results not shown) and the peak parameters were not affected by the surface coverage. The modified electrode presents a good electrochemical stability as shown in figure 1B, due to good adsorption properties of the polymer derivative.

Table 2
Electrochemical parameters of the voltametric response for graphite electrode modified with **2**. Experimental conditions as in Fig1.

Cpd *	E_{pa} [mV] vsSCE	E_{pc} [mV] vsSCE	E^0 [mV] vsSCE	ΔE_{peak} [mV]	E_{FWHM} [mV]		$\frac{I_{pa}}{I_{pc}}$	Γ 10^8 mol cm^{-2}
					anodic	cathodic		
2	74	-70	2	144	272	235	1.24	5.4

*Compound **2**

CONCLUSIONS:

The two microwave installations employed in the microwave-assisted synthesis of **2** offered an efficient heating of the reaction mixture and comparison with the conventional synthetic methods demonstrates advantages related to shorter reaction times. In this particular case, *dry media* procedure presented the disadvantage of lower yields, due to the immobilization of the highly insoluble reaction product on the solid support.

The electrochemical behavior of a graphite electrode modified with phenothiazine-formaldehyde polymer derivative **2**, shows redox activity and good adsorption properties of this compound.

EXPERIMENTAL PART

The reactions were performed using:

- dynamic microwave power system designed by INCDTIM Cluj-Napoca
 - microwave installation *Synthos 3000* designed by Parr instruments
- Reagents from Merck were used.

TLC was used to monitor the reaction progress (Merck silica gel F 254 plates). NMR spectra were recorded using a 300 MHz Bruker NMR spectrometer. FT-IR spectra were recorded using a Bruker Vector 22 FT-IR spectrometer.

Phenothiazine-formaldehyde polymer 2

a) Phenothiazine 0,5 g (2,5 mmol) was solved in acetic acid (50 mL), conc. hydrochloric acid (0.5 mL) was added and then formaldehyde (4mmol, 0.32 mL aqueous solution 36%) was added drop wise under vigorous stirring at room temperature. After 30 minutes, a dark precipitate start to accumulate and the reaction is perfected for 2 hours at 60 °C. The dark grey precipitate was filtered and washed several times with warm methanol; the precipitate was suspended in THF and then filtered. 0.4 g dark powder was obtained, yield 78%.

b) Phenothiazine (0,5 g 2,5 mmol) was solved in acetone (30 mL) and aluminium oxide (0.5 g) was added to the clear solution. The solvent was then removed under vacuum by rotary evaporator. Formaldehyde (4 mmol, 0.32 mL aqueous solution 36%) and conc. hydrochloric acid (0.1 mL) were added to the phenothiazine adsorbed on the solid support. The mixture was subjected to microwave irradiation in the resonance cavity of the dynamic microwave power system designed by INCDTIM, with prescribed power level 700 W and temperature monitoring. TLC was used to monitor the reaction progress. After 15 minutes total time of irradiation the solid material was extracted 3 times with DMF (10 mL). The product precipitated when water was added to the reunited DMF solutions. 0.2 g dark powder precipitate was obtained by filtration, yield 38%.

c) Phenothiazine 0,5 g (2,5 mmol), formaldehyde (4 mmol) aqueous solution 36% 0.32 mL, conc. hydrochloric acid 0.5 mL and acetic acid 20 mL were introduced in a quartz reaction vessel which was then sealed and subjected to microwave irradiation in the resonance cavity of the microwave *Synthos 3000* instrument with controlled heating at 60 °C and after 40 minutes generated a dark grey precipitate which was filtered from the reaction mixture and then washed several times with warm methanol; the precipitate was solubilized in THF and filtered. 0.38 g dark powder was obtained, yield 75%.

¹H-NMR (300MHz, DMSO-d₆): δ=3.57 ppm (s, 2H), 6.61-7 ppm (m, 12H), 8.5 ppm (s, 2H).

IR (cm⁻¹): 3328, 1595, 1487, 1314, 798, 743.

Electrode preparation

A spectrographic graphite rod (Ringsdorff-Werke, GmbH, Bonn-Bad Godesberg, Germany), of ~ 3 mm diameter, was wet polished on fine (grit 400 and 600) emery paper (Buehler, Lake Bluff, Ill., USA). Then, a graphite piece of suitable length was carefully washed with deionized water, dried, and finally press-fitted into a PTFE holder in order to obtain a graphite electrode having, in contact with the solution, a flat circular surface of ~ 0.071 cm².

The modified graphite electrode was obtained by spreading onto the electrode surface 2 μ l of 1 mM derivative **2** solution in dimethylsulfoxide, and leaving them for one day at room temperature to evaporate the solvent. Before immersion in the test solution the modified electrodes were carefully washed with deionized water.

Electrochemical measurements

CV measurements were carried out in a conventional three-electrode electrochemical cell. A saturated calomel electrode (SCE) and a coiled Pt wire served as reference and counter electrode, respectively. The cell was connected to a computer-controlled voltammetric analyzer (Autolab-PGSTAT10, Eco Chemie, Utrecht, Netherlands). The supporting electrolyte was a 0.1 M phosphate buffer, pH 7 prepared using $K_2HPO_4 \cdot 2H_2O$ and $KH_2PO_4 \cdot H_2O$ from Merck (Darmstadt, Germany).

ACKNOWLEDGEMENT

Financial support from Romanian Ministry of Education and Research, grants ID_564 and ID_512 is greatly acknowledged.

REFERENCES

1. P. Lindstrom, J. Tierney, B. Wathey, J. Westman, *Tetrahedron*, **2001**, 57, 9225.
2. A. Loupy, "Microwaves in organic synthesis" Wiley-VCH Verlag GmbH & Co. KGaA, Weinheim, **2002**.
3. C. O. Kappe, *Angew. Chem. Int. Ed.*, **2004**, 43, 6250.
4. D. Dallinger, C. O. Kappe, *Chem. Rev.* **2007**, 107(6), 2563.
5. I. A. Silberg, C. Cristea, *Het. Commun.*, **1996**, 2, 117.
6. D. Dicu, L. Muresan, I. C. Popescu, C. Cristea, I.A. Silberg, P. Brouant, *Electrochimica Acta*, **2000**, 45, 3951.
7. M. Jitaru, G. Petrică, L. I. Găină, C. Cristea, T. Lovász, I. A. Silberg, *Rev. Roum.* **2002**, 47 (3-4), 249.
8. D. Gligor, M. Socol, I. C. Popescu, C. Cristea, I. A. Silberg, *Studia Univ. "Babes-Bolyai" Chemia*, XLIX, 2, **2004**, 123.
9. N. Zimova, I. Nemeč, J. Zima, *Talanta*, **1986**, 33, 467.
10. N. Sulcova, I. Nemeč, K. Waisser, H. L. Kies, *Microchem. J.*, **1980**, 25, 551.
11. M. Jitaru, C. Cristea, I. A. Silberg, *Rev. Roumaine Chim.*, **1999**, 44 (9), 865.

12. T.-Y. Wu, Y. Chen, *J. Polym. Sci., Part A: Polym. Chem.*, **2002**, *40*, 4452.
13. X. Kong, A. P. Kulkarni, S. A. Jenekhe, *Macromolecules*, **2003**, *36*, 8992.
14. C. Buhrmester, L. Moshurchak, R. L. Wang, J. R. Dahn, *J. Electrochem. Soc.*, **2006**, *153*, A288.
15. D. Gligor, L. Muresan, I. C. Popescu, I. A. Silberg, *Rev. Roumaine Chim.*; **2002**, *47*, 953.
16. D. Gligor, L. Muresan, I. C. Popescu, I. A. Silberg, *Rev. Roumaine Chim.*, **2003**, *48*, 463.
17. F. Fungo, S. A. Jenekhe, A. J. Bard, *Chem. Mater.*, **2003**, *15*, 1264.
18. Q. Gao, W. Wang, Y. Ma, X. Yang, *Talanta*, **2004**, *62*, 477.
19. S. Abraham John, R. Ramaraj, *J. Electroanal. Chem.*, 2004, *561*, 119.
20. Watarai *US Pat.*, 4,229,510, Oct, **1980**.
21. G. Cormos, C. Cristea, I. Filip, I. A. Silberg, *Studia Univ. "Babes-Bolyai" Chemia*, **2006**, *LI*, 2, 155.
22. E. Surducun, V. Surducun, G. Nagy, S. V. Filip, RO Pat., 00116514, **2001**.
23. R. W., Murray, "Techniques of Chemistry", Wiley, XXII, **1992**.
24. N. Sulcova, I. Nemec, M. Ehlova, K. Waisser, *Collect. Czech. Chem. Commun.*, **1990**, *55*, 63.
25. E. Laviron, L. Roulier, *J. Electroanal. Chem.*, **1979**, *101*, 19.

In memoriam prof. dr. Ioan A. Silberg

ELECTRONIC PROPERTIES OF CHALCONES CONTAINING PHENOTHIAZINE UNITS

TAMÁS LOVÁSZ^a, GABRIEL OLTEAN^a, ANA-MARIA TOMA^a, LUIZA GĂINĂ^a, LUMINIȚA SILAGHI-DUMITRESCU^a, MARIA JITARU^a, CASTELIA CRISTEA^a, PÁL SOHÁR^b, ANTAL CSÁMPAI^b

ABSTRACT. Phenothiazinyl substituted enones were synthesized by the condensation of N-methyl-3-oxo-phenothiazine derivatives with several acetyl-ferrocene and benzaldehyde derivatives respectively, in alkaline conditions. The structures of new chalcones and *bis*chalcones thus obtained were assigned by high resolution NMR. Comparative electrochemical behaviour and UV-Vis spectra of chalcones containing phenothiazine and ferrocene or phenyl units are described.

INTRODUCTION

This paper is a continuation of previous contributions showing a constant interest on the synthesis and structural investigation of phenothiazine derivatives containing conjugated unsaturated chains, in our research group [1-4]. Due to the low oxidation potential and the pronounced propensity to form stable radical cations, properly substituted phenothiazine derivatives may find applications in material science investigations and sensors studies. The target of this work was to synthesize some chalcones with cross conjugated structure, containing phenothiazine and ferrocene or other aromatic units as well as to characterize their electronic properties by UV-Vis spectroscopy and cyclic voltammetry. These structures might develop interesting unconventional physical properties due to the combination of the electron donor effects of phenothiazine [5], ferrocene or phenyl units, with those of an extended π conjugated system.

The UV-Vis spectra of phenothiazine derivatives were recorded long time ago for analytical purposes (characterization, identification and dosage) due to the large extent of derivatives with practical applications (drugs, dyes, antioxidants). The correlation between UV spectra and the structure of phenothiazine derivatives was thoroughly investigated and important

^a "Babes-Bolyai" University Cluj-Napoca, Faculty of Chemistry and Chemical Engineering

^b Eotvos Lorand University, Research group for Structural Chemistry and Spectroscopy, H-1518 Budapest 112, Hungary.

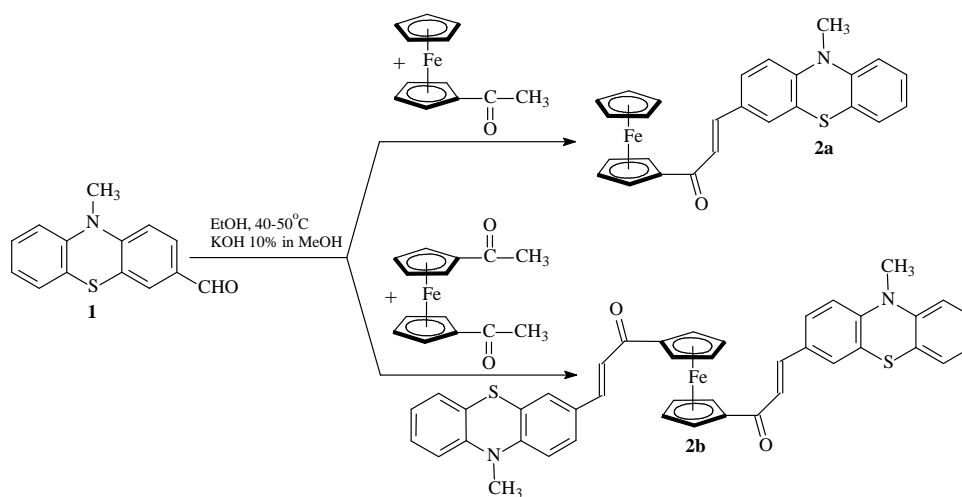
differences between 2- and 3-substituted derivatives were noticed, while the presence of a alkyl substituent in position 10 affects very little the spectrum. Greater influence was observed to be exerted by electron withdrawing groups such as $-\text{NO}_2$, $-\text{SO}_2$, $-\text{S-CO-R}$ [6-8].

The electron donor properties of the phenothiazine nucleus were also clearly demonstrated by different methods including chemical [9] and electrochemical generation of the oxidized forms. The first systematic investigation of the anodic oxidation of phenothiazine at a platinum electrode [10] indicated a first step at + 270 mV vs Ag/Ag^+ 10^{-2}M electrode and a second step situated at about +750 mV. Further, different electrochemical methods were also employed: polarography [11-13], cyclic voltammetry [14-19], chronoamperometry [8,20], especially in the range of positive potentials. However, much remains to be done in order to establish the influence exerted by functional groups on the redox behaviour of phenothiazine nucleus. We decided to use the cyclic voltammetric measurements for the investigation of the redox processes implied by the presence of different redox active groups and their reciprocal influences in the structure of phenothiazine containing chalcones.

RESULTS AND DISCUSSIONS

Synthesis

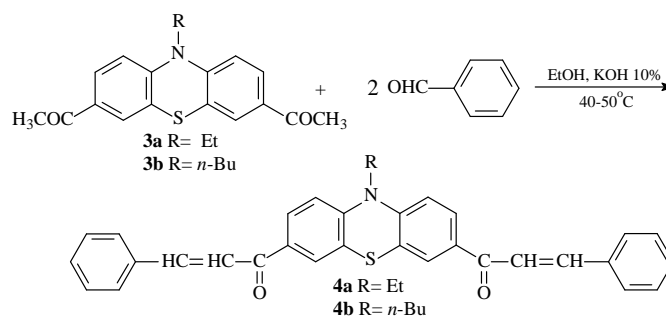
Chalcones containing phenothiazine and ferrocene units, **2a** and **2b** were previously synthesized by the condensation of N-methyl-formyl-phenothiazine with acetylferrocene and 1,1'-diacetylferrocene respectively (Scheme1). The reactions were performed in the presence of catalytic amounts of KOH, and afforded high yields of chalcones (>70%).



Scheme 1

An explanation of structure-reactivity relationship related to the nucleophilicity of the enolate anion generated by the acetylferrocene in the aldol condensation reaction was formulated based on density functional (DFT) calculations [21].

Bis-chalcones containing a 3,7-disubstituted phenothiazine unit were obtained in high yields by the condensation of 3,7-diacetyl-10-alkylphenothiazines with benzaldehyde in alkaline media (compounds **4a** and **4b** in Scheme 2).



Scheme 2

High resolution NMR (500 MHz $^1\text{H-NMR}$) and FT-IR spectra were used in order to completely assign the structures of the synthesized compounds **4a,b**. FT-IR spectroscopy indicates the stretching vibration of the carbonyl bond by the absorption band situated at 1654 cm^{-1} for **4a** and 1659 cm^{-1} for **4b** respectively; these low values are consistent with the vibration of an α,β unsaturated ketone and are accompanied by the absorption band situated at 1594 cm^{-1} due to the vibration of the C=C bond. The formation of *E* diastereoisomers of **4a** and **4b** can be clearly identified by $^1\text{H-NMR}$ spectra: two *doublet* signals situated at 7.4 and 7.8 ppm in the spectrum of **4a** were assigned to the vinyl protons and the coupling constant of 15.5 Hz is consistent with a *trans* geometry around the double bond. Similar chemical shifts and coupling pattern were observed in the spectrum of **4b**.

UV-Vis spectra

For the unsubstituted phenothiazine, literature indicates two characteristic UV absorption maxima situated at 253 and 320 nm. Shifts and intensity variations of these maxima were observed and are due to substitution pattern of phenothiazine derivatives [5]. The UV spectrum for ferrocene shows maxima situated at 330 nm and 440 nm [22].

The UV-Vis spectra of compounds **2a**, **2b** and **4a**, were recorded in DMF solution and are presented in figure 1. Compounds **2a** and **2b** contain the same chromophor unit: 1-ferrocenyl-3-phenothiazinyl-propenone; a very small bathochromic shift can be observed in the position of the absorption maxima of **2b** accompanied by an important increase in absorbance value due to additive effect of the identical two chromophor units in the molecular structure.

Compounds **4a** and **4b** contain as a chromophore the 3-phenyl-1-phenothiazinyl-propenone unit which produces in the UV-Vis spectrum an absorption band showing an important bathochromic shift as compared to compounds **2** (Figure 1), a fact that suggests a longer π conjugated system which implies smaller energy amounts required for the $n \rightarrow \pi^*$ transition between the molecular orbitals.

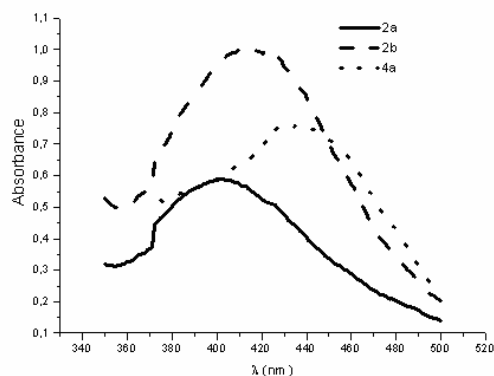


Figure 1. UV-Vis spectra of chalcones **2a**, **2b** and **4a** solution 10^{-5} M in DMF.

Electrochemical measurements

Cyclic voltammetric (CV) measurements were carried out in order to compare the electrochemical behaviours of chalcone derivatives **2**, **4** with those of parent aromatic units: N-alkyl-phenothiazine and ferrocene respectively. The oxidation potentials determined by the presence of different redox active groups and their reciprocal influences can be observed in Figure 2.

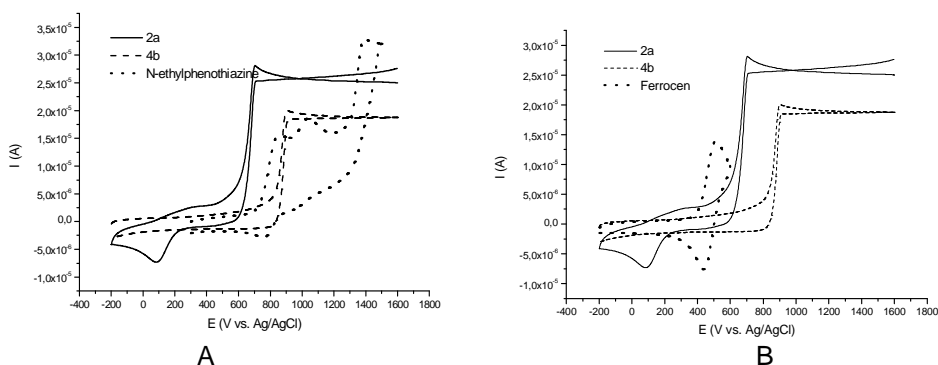


Figure 2. Cyclic Voltammograms of: A) **2a**, **4b**, N-ethylphenothiazine; B) **2a**, **4b**, ferrocene. Experimental conditions: solvent DMF, supporting electrolyte 0.1M LiClO_4 , GC electrode, scan rate $v=100 \text{ mVsec}^{-1}$

A shape of strong oxidation can be observed for **2a** and **4b** adsorbed on GC electrode; this process is continuing slowly, along a large potential range (800-1600 mV). This oxidation peak appears shifted towards lower positive values for **2a** as compared to **4b** ($\Delta E_{4b-2a} = 200$ mv).

The presence of extended π conjugated system in chalcones **2**, **4** strongly affects the redox behaviour of phenothiazine nucleus as it can be observed in Figure 2A where CVs of N-ethylphenothiazine, **2a** and **4b** are plotted together. The characteristic redox behaviour of the phenothiazine unit (which can be clearly seen in the CV pattern of N-ethyl-phenothiazine), is suppressed in the CVs of chalcone derivatives **2a**, **4b**.

Figure 2B shows the CVs of ferrocene, **2a** and **4b** plotted together. In the CV of chalcone **2a**, the intense oxidation peak is accompanied by the answer of ferrocene/ferrocynium system which appears strongly affected. This peak couple became almost irreversible and shifted towards lower positive potential values, as compared to that of the normal reversible answer of ferrocene/ferrocynium redox couple.

EXPERIMENTAL PART

Melting points (uncorrected) were obtained with an Electrothermal IA 9200 digital melting point apparatus. IR spectra were recorded in KBr pellets with a BRUKER IFS 55FT-pectrometer. ^1H - and ^{13}C -NMR were recorded in CDCl_3 solution in 5mm tubes at RT, on a Bruker DRX 500 at 500MHz, using TMS as internal reference with deuterium signal of the solvent as the lock. UV-VIS spectra were recorded on a Spectrometer UV-VIS UNICAM Helios β in DMF solution 10^{-5} M.

The electrochemical measurements were performed using a potentiostatic set-up in a classical cell having three electrodes. All the samples were deaerated 20-30 minutes before each test. Because of low solubility of the complex in the protic medium, the non aqueous medium of DMF was chosen.

Cyclic voltammograms were recorded in a cell purged with argon. DMF used as solvent was purified according to standard procedures [9]. LiClO_4 dried in an oil pump vacuum at 100°C was added as supporting electrolyte at a concentration of 0.1 M. Compounds under investigation were added at 10 mM concentration. The working electrode (GC) and platinum wire counter-electrode were used. An Ag/AgCl electrode, in a separate compartment served as reference electrode. CVs were recorded in positive-going direction at the starting potentials, at different scan rate using a BAS potentiostat equipped with BAS100W soft. All experiments were run at room temperature (22°C).

Phenothiazine oxo-derivatives, 1,1'-diacetyl-ferrocen and ferrocenyl-enones **2a** and **2b** were prepared according to described procedures [23,24,7]. Spectral data and melting points of compounds **2a** and **2b** are according to the literature [21].

General procedure for the preparation of phenothiazinyl chalcones 4a,b

To a stirred solution of the appropriate 3,7-diacetyl-10-alkyl-phenothiazine (0.01 mol) and benzaldehyde (2.12g, 0.02 mol) in ethanol (20 cm³), 10% methanol solution of KOH (1 cm³) was added drop wise over 3 min at 25°C. The mixture was stirred for 8h at 50°C. The product precipitated on cooling was filtered and washed with cold ethanol (5 cm³) then purified by column chromatography on silica using dichloromethane as eluent.

3,7-bis[(E)-3-phenylprop-2-en-1-on]-10-ethyl-10H-phenothiazine (4a)

Orange-red powder; yield 4.29g (88%); m.p. 153-154°C

IR (KBr) ν [cm⁻¹]: 1654, 1596, 1574, 1474, 1367, 1331, 1284, 1244, 1208, 763
500MHz, ¹H-NMR (CHCl₃-d₁): δ_{H} : 1.49ppm (t, 3H, ³J= 7Hz, H_b), 4.02ppm (q, 2H, ³J= 7Hz, H_a), 6.94ppm (d, 2H, ³J= 8.5Hz, H_{1,9}), 7.86ppm (dd, 2H, ⁴J= 2Hz, ³J= 8.5Hz H_{2,8}), 7.78ppm (d, 2H, ⁴J=2Hz, H_{4,6}), 7.65ppm (m, 4H, H_{2',6'}), 7.42ppm (m, 4H, H_{3',5'}), 7.42ppm (m, 2H, H₄), 7.49ppm (d, 2H, ³J_{trans}= 15.5Hz, H _{α}), 7.80ppm (d, 2H, ³J_{trans}= 15.5Hz, H _{β}). 100MHz ¹³C-NMR (CHCl₃-d₁): δ_{C} : 13.1ppm (CH₃, C_b), 43.2ppm (CH₂, C_a); 115.0ppm (CH, C_{1,9}), 121.8ppm (CH, C _{α}), 123.6ppm (Cq, C_{4a,5a}), 128.1ppm (CH, C_{4,6}), 128.9ppm (CH, C_{2',6'}), 129.2ppm (CH, C_{2,8}), 129.4ppm (CH, C_{4'}), 130.9ppm (CH, C_{3',5'}), 133.5 (Cq, C₃), 135.4 (Cq, C_{1'}), 144.8ppm (CH, C _{β}), 147.7ppm (Cq, C_{9a,10a}), 188.1ppm (CO)

3,7-bis[(E)-3-phenylprop-2-en-1-on]-10-butyl-10H-phenothiazine (4b)

Red powder; yield 3.66g (71%); m.p. 166°C

IR (KBr) ν [cm⁻¹]: 1657, 1595, 1575, 1476, 1367, 1328, 1281, 1252, 1204, 760
500MHz, ¹H-NMR (CHCl₃-d₁): δ_{H} : 0.95ppm (t, 3H, ³J= 7.5Hz, H_d), 1.50ppm (m, 2H, H_c), 1.83ppm (m, 2H, H_b), 3.95ppm (t, 2H, ³J= 7.5Hz, H_a), 6.92ppm (d, 2H, ³J= 8.5Hz, H_{1,9}), 7.87ppm (dd, 2H, ⁴J= 2Hz, ³J= 8.5Hz H_{2,8}), 7.79ppm (s, 2H, H_{4,6}), 7.65ppm (m, 4H, H_{2',6'}), 7.43ppm (m, 4H, H_{3',5'}), 7.41ppm (m, 2H, H₄), 7.49ppm (d, 2H, ³J_{trans}= 20Hz, H _{α}), 7.80ppm (d, 2H, ³J_{trans}= 20Hz, H _{β}). 100MHz ¹³C-NMR (CHCl₃-d₁) δ_{C} : 14.1ppm (CH₃, C_d), 20.4ppm (CH₂, C_c), 29.1ppm (CH₂, C_b), 48.3ppm (CH₂, C_a), 115.5ppm (CH, C_{1,9}), 121.9ppm (CH, C _{α}), 124.3ppm (Cq, C_{4a,5a}), 128.2ppm (CH, C_{4,6}), 128.9ppm (CH, C_{2',6'}), 129.2ppm (CH, C_{2,8}), 129.4ppm (CH, C_{4'}), 130.9ppm (CH, C_{3',5'}), 133.6 (Cq, C₃), 135.4 (Cq, C_{1'}), 144.8ppm (CH, C _{β}), 148.2ppm (Cq, C_{9a}), 188.2ppm (CO)

CONCLUSIONS

Chalcones containing phenothiazine and ferrocen units were synthesized and their electronic properties were analyzed by UV-Vis spectroscopy and cyclic voltammetry. Their conjugated structure determined a bathochromic shift of the UV absorption maxima when compared to parent aromatic units. The electrochemical measurements of chalcones adsorbed on GC electrode show strong irreversible oxidation processes. It will be of interest to study their electrosorption process depending on the electrode nature.

REFERENCES

1. L. Gaina, T. Lovasz, I. A. Silberg, C. Cristea, S. Udrea, *Heterocyclic Communications*, **2001**, 7 (6), 549.
2. L. Gaina, Castelia Cristea, I. A. Silberg, T. Lovasz, S. Udrea, *Rev. Roum. Chim.*, **2002**, 47 (10-11), 983.
3. M. Jitaru, G. Petrică, L. I. Găină, C. Cristea, T. Lovász, I. A. Silberg. *Rev. Roum. Chim.*, **2002**, 47 (3-4), 249.
4. L. Gaina, T. Lovasz, C. Cristea, I. A. Silberg, C. Deleanu, *Rev. Roum. Chim.*, **2003**, 48 (7), 549.
5. C. Bodea, I. A. Silberg in A. R. Katritzky, A. J. Boulton (Eds) „*Advances in Heterocyclic Chemistry*” vol 9, academic Press Inc., New York, **1968**, 341.
6. J. Cymerman-Craig, W. K. Warburton, *Australian J. Chem.*, **1956**, 9, 294.
7. C. Bodea, V. Fărcășan, I. Oprean, *Rev. Roum. Chim.* **1965**, 10, 1103.
8. G. Cauquil, A. Casadeval, *Bull. Soc. Chim. France*, **1955**, 1061.
9. H. J. Shine, E. E. Mach, *J. Org. Chem.*, **1965**, 30, 2130.
10. J. P. Billon, *Bull. Soc. Chim. France*, 1960, 1784.
11. A. P. Poltorakov, F. N. Pirnazarova, P. G. But, L. A. Piruzyan, V. M. Chibrikin, Yu. I. Vikhlyayev, O. V. Ul'yanova, *Russian Chem. Bull.*, **1973**, 22(9), 2050.
12. S. V. Zhuravlev, *Dokl. Akad. Nauk. SSSR*, **1971**, 200, 348.
13. T. K. Pashkevich, V. A. Shapovalov, V. D. Bezuglyi, G. B. Afanas'eva, I. Ya. Postovskii, *Zh. Obshch. Kim.* **1977**, 47, 910.
14. I. Nemeč, N. Sulcova, K. Waisser, *Cesk. Farm.*, **1979**, 28, 59.
15. B. Paduszek, M. K. Kalinowski, *Electrochim. Acta*, **1983**, 28, 639.
16. J. P. Billo, *Bull. Soc. Chim. Fr.*, **1961**, 1932.
17. M. Neptune, R. L. McCreery, *J. Org. Chem.*, **1978**, 43, 5006.
18. H. Y. Cheng, P. H. Sackett, R. L. McCreery, *J. Am. Chem. Soc.*, **1978**, 100, 962.
19. L. A. Tinke, A. J. Bard, *J. Am. Chem. Soc.*, **1979**, 101, 2316.
20. P. H. Sackett, R. L. McCreery, *J. Med. Chem.*, **1979**, 22, 1447.
21. T. Lovász, Gy. Túrós, L. Găină, A. Csámpai, D. Frigyes, B. Fábíán, I. A. Silberg, P. Sohár, *J. of Mol. Structure*, **2005**, 751, 100.
22. W. L. Jolly, *The Synthesis and Characterization of Inorganic Compounds*, Prentice-Hall: New Jersey, **1970**.
23. M. Sato, M. Koga, I. Motoyama, K. Hata, *Bull. Chem. Soc. Jpn.*, **1970**, 43, 1142.
24. R. E. Bozak, *J. Chem. Educ.*, **1966**, 43, 73.

In memoriam prof. I. A. Silberg

THE FORMYLATION OF *BIS*-(N-ALKYL-PHENOTHIAZINYL)-METHANE; A THEORETICAL APPROACH

DAN PORUMB^a, IOAN SILAGHI-DUMITRESCU^a, LUIZA GAINA^a,
LUMINITA SILAGHI-DUMITRESCU^a, CASTELIA CRISTEA^a,
GABRIELA CORMOS^b

ABSTRACT. Duff formylation of *bis*-(10-methylphenothiazin-3-yl)-methane obtained by the condensation of phenothiazine with formaldehyde was attempted. Theoretical data based on Density Functional Theory were used in order to explain the reduced reactivity of this substrate, as compared to parent 10-methylphenothiazine. Structural assignments were based on NMR spectroscopy.

INTRODUCTION

Numerous N- or C-substituted phenothiazine derivatives were prepared taking into account the enhanced chemical reactivity of phenothiazine nucleus towards electrophiles. The highest electron density is located at the heterocyclic nitrogen atom (due to its relatively high electronegativity) and consequently many electrophile reagents preferentially attack in position 10 of the phenothiazine nucleus. As a consequence of the transmission of heteroatoms electronic effects, C-substitution of the phenothiazine nucleus occurs readily in positions 3,7 (activated by electronic effects of nitrogen in position *para*, as shown in figure 1), followed by positions 1,9 (*orto* to nitrogen) and then by positions 2,8 and 4,6 respectively (activated by the electronic effects of heterocyclic sulfur atom) [1].

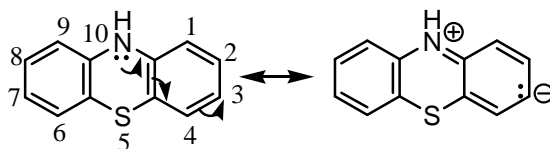


Figure 1. Phenothiazine: IUPAC numbering and resonance structures.

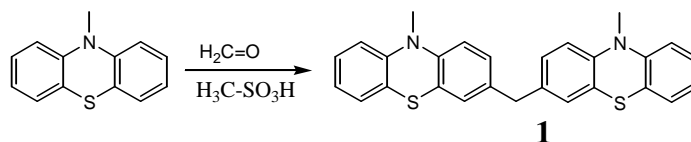
^a "Babeș-Bolyai" University, Faculty of Chemistry and Chemical Engineering, Organic Chemistry Department, Cluj-Napoca, RO- 400028, Romania

^b "L. Blaga" University, Faculty of Medicine, Sibiu

This paper presents the condensation reaction of 10-methylphenothiazine with formaldehyde and the attempts to subsequent formylation of *bis*-(10-methylphenothiazin-3-yl)-methane **1** thus obtained. Theoretical data, based on DFT calculations, were used in order to explain the reduced reactivity of substrate **1**.

RESULTS AND DISCUSSIONS

Similarly to the condensation reaction of phenothiazine with formaldehyde, which leads to *bis*-(10*H*-phenothiazin-3-yl)-methane, the condensation of 10-methylphenothiazine with formaldehyde solution in the presence of an acid catalyst generates *bis*-(10-methylphenothiazin-3-yl)-methane **1** (Scheme 1) in good yields.

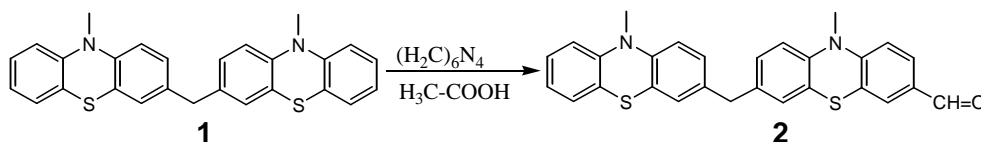


Scheme 1

¹H-NMR spectroscopy was used in order to completely assign the structure of **1**. Thus, due to the symmetry of the molecule the two methyl groups appear as a singlet signal situated at 3.1 ppm, while a singlet signal situated at 3.8 ppm is assigned to the bridging methylene protons. The protons attached to the two equivalent phenothiazine units generate six multiplet signals which appear in the 6.7-7.2 ppm range.

Duff formylation of 10-methylphenothiazine with urotropine in acidic media generated 3-formyl-10-methylphenothiazine in moderate yields. The electrophilic substitution occurs in position 3, characterized by the highest electron density of the substrate [1]. The reduced reactivity of 10-methylphenothiazine (as compared to 10*H*-phenothiazine), combined with the low reactivity of the electrophile generated by the urotropine in acidic media [2-6], explain the moderate yields.

The same formylation reaction was attempted by using **1** as a substrate. The expected (10-methylphenothiazin-3-yl)-(7-formyl-10-methylphenothiazin-3-yl)-methane **2** (Scheme 2) was obtained in extremely low yields.



Scheme 2

A theoretical explanation for this difference of reactivity between the two similar substrates: 10-methylphenothiazine and *bis*-(10-methylphenothiazin-3-yl)-methane **1**, has been attempted. Based on DFT calculations, Figure 2 shows the electrostatic potential surfaces generated on the lowest energy conformer of 10-methylphenothiazine and **1**, using Spartan software [7].

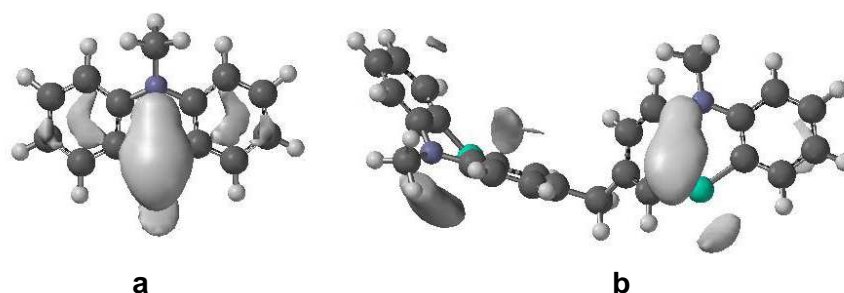


Figure 2. Electrostatic potential surfaces generated for: a) 10-methylphenothiazine and b) *bis*-(10-methylphenothiazin-3-yl)-methane **1**

The mild electrophile $\text{H}_2\text{C}=\text{N}^+ \leftrightarrow \text{H}_2\text{C}^+-\text{N}^-$ [2] generated by the urotropine during the Duff formylation reaction may selectively be attached in position 3 of the 10-methylphenothiazine substrate, but it is not capable to interact with the carbon atom in position 7 of **1** substrate, as it can be observed from the electrostatic potential surface in figure 2a (there is no electrostatic potential surface covering carbon atom in position 7).

Stronger electrophiles may be required in order to perform the same substitution reaction of **1**, so Vilsmeier [8,9], Reimer-Tiemann [10-12] or Gattermann [13-15] formylation procedures are to be tested.

CONCLUSIONS

As a consequence of the moderate reactivity of 10-methylphenothiazine substrate, reaction with electrophiles generated by formaldehyde or urotropine in acidic media proceeds selectively in position 3 (*para* to heterocyclic nitrogen atom). Further electrophilic substitution reactions occur only in the presence of stronger electrophiles, so that the formylation of *bis*-(10-methylphenothiazin-3-yl)-methane was not observed under the present conditions. Comparison between generated electrostatic potential surfaces using Spartan software, for *bis*-(10-methylphenothiazin-3-yl)-methane and 10-methylphenothiazine suggest that the mild electrophile generated by the urotropine in the Duff formylation reaction is not able to interact with the heterocycle carbon atoms.

EXPERIMENTAL PART

The chemical reagents and the solvents were purchased from Merck (for synthesis purity)

The H-NMR spectra were recorded on a Bruker Avance 300 MHz spectrometer.

***Bis*-(10-methylphenothiazin-3-yl)-methane 1**

10-methylphenothiazine 0,5g (2,5mmol) was solved in acetic acid (50 mL), methanesulfonic acid (0.5 mL) was added and then formaldehyde (4mmol, 0.32 mL aqueous solution 36%) was added drop wise under vigorous stirring at room temperature. After refluxing for 1 hour, a white-pink precipitate started to accumulate and the reaction was perfected for 3 hours. The precipitate was filtered and washed several times with warm methanol; 0.4g white-pink powder was obtained, yield 65%, m.p. = 248 °C.

¹H-NMR (300MHz, DMSO-d₆): δ=3.10 ppm (s, 6H), 3.80 ppm (s, 2H), 6.70 ppm (d, 2H), 6.75 ppm (d, 2H), 6.8 ppm (t, 2H), 6.85 ppm (s, 2H), 6.90 ppm (d, 2H), 7.02 ppm (d, 2H), 7.12 ppm (t, 2H).

REFERENCES

1. I. A. Silberg, C. Bodea, "Advances in Heterocyclic Chemistry" **1968**, 9, 430.
2. J. C. Duff, E. J. Bills, *J. Chem. Soc.* **1932**, 1987.
3. J. C. Duff, E. J. Bills, *J. Chem. Soc.* **1934**, 1305.
4. J. C. Duff, E. J. Bills, *J. Chem. Soc.* **1941**, 547.
5. J. C. Duff, E. J. Bills, *Rev.* **1946**, 38, 227.
6. Y. Ogata, F. Sugiura, *Tetrahedron* **1968**, 24, 5001.
7. *Spartan'04* Wavefunction, Inc. Irvine, CA
8. A. Vilsmeier, A. Haack, *Ber.* **1927**, 60, 119.
9. O. Meth-Cohn, S. P. Stanforth, *Comp. Org. Syn.* **1991**, 2, 777
10. K. Reimer. F. Tiemann, *Ber.* **1876**, 9, 824 & 1268 & 1285.
11. H. Wynberg, E. Meijer, *W. Org. React.* **1982**, 28, 2.
12. H. Wynberg, *Comp. Org. Syn.* **1991**, 2, 769.
13. L. Gattermann, *Ber.* **1898**, 31, 1149; *Ann.* **1907**, 357, 313.
14. P. Karrer, *Helvetica Chim. Acta*, **1919**, 2, 89.
15. R. Adams, E. Montgomery, *J. Am. Chem. Soc.*, **1924**, 46 1518.

In memoriam prof. dr. Ioan A. Silberg

PHOTOACTIVE BINAPHTHYL PHENOTHIAZINE DERIVATIVES

LARISA NATALIA POPA^a, MARTIN PUTALA^b

ABSTRACT. The preparation of new *bis*-(10-alkyl-phenothiazin-3yl)-1,1'-binaphthalene derivatives 10,13, following a rational synthetic approach based on Suzuki or Negishi arylation of suitable precursors, is discussed. Positive results were obtained by Suzuki arylation of the (*RS*)-6,6'-dibromo-[1,1'-binaphthalene]-2,2'-dicyanitrile (11) with 10-hexyl-3-(4,4,5,5-tetramethyl-1,3,2-dioxaborolan-2-yl)-phenothiazine (5) and Negishi arylation of the (*RS*)-2,2'-diiodo-[1,1'-binaphthalene] with 3-bromo-10-hexyl-phenothiazine. These compounds are candidates for new molecular materials with potentially efficient photoinduced electron transfer properties due to the axial chirality of the binaphthyl moiety combined with the low-oxidation potential and high tendency to form stable radical cations of the phenothiazine units.

INTRODUCTION

Axially chiral binaphthyl derivatives represent one of the most important groups of the artificial chiral-pool compounds [1]. Their widespread applications lay stress upon their facile accessibility in enantiomerically pure state, as well as possibility of easy structural modifications. Unique stereochemical properties of axially chiral C₂-symmetric binaphthyl moiety (symmetrically substituted at the both naphthalene rings) are the reason for enhanced interest in the synthesis, study, and application of binaphthyl derivatives.

Synthetic approaches to binaphthyl derivatives

Main synthetic approach for the synthesis of enantiomerically pure axially chiral C₂-symmetric binaphthyl derivatives consist in stereoselective formation of C-C bond connecting two naphthyl units and transformations of the groups on the binaphthalene scaffold without any configurational scrambling. Chemical transformations of the binaphthyl derivatives, except for replacing the atoms bonded directly to the binaphthyl moiety at the 2,2'-positions, do not impair the enantiomeric purity and are routinely used.

^a "Babes-Bolyai" University Cluj Napoca, Faculty of Chemistry and Chemical Engineering, Department of Organic Chemistry

^b "Comenius" University in Bratislava, Faculty of Natural Sciences, Department of Organic Chemistry

Chiral C_2 -symmetric 1,1'-binaphthyl-2,2'-disubstituted derivatives can be easily functionalized in the 3,3'-positions [2] (*via* orthometallation directed by substituents at the positions 2,2', $Y = OR, NR_2$) or 6,6' (by electrophilic aromatic substitution as reported for $Y = OH$) [3]. Substituents at the other positions (more often 4,4' and 7,7') have to be incorporated before the coupling of naphthyl units [4].

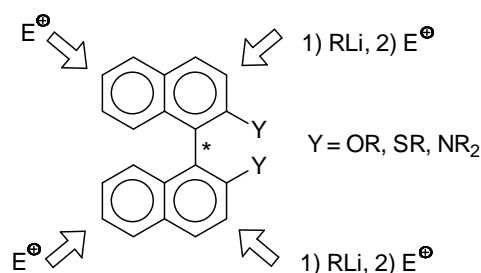


Figure 1

It is of great interest to investigate new photoactive and electroactive binaphthyl derivatives as molecular materials for potential application in optoelectronics as information storage media and logic gates (processing data). Phenothiazines derivatives as electron-rich tricyclic nitrogen-sulfur heterocycles with a low-oxidation potential and a high tendency to form stable radical cations are candidates for groups, which should bring interesting properties to binaphthyl derivatives. Besides above mentioned properties of phenothiazine derivatives, thanks to their physiological activities, pronounced biological and pharmacological activity, they were applied in a broad range as anthelmintics, antipsychotics, antiepileptics, antituberculosics and antitumor agents [5], more recently, due to their low oxidation potential and reversible oxidations, deep colored radical cation absorptions, phenothiazines have become very interesting spectroscopic probes in molecular and supramolecular arrangements for photoinduced electron transfer (PET) studies [6].

As a consequence the integration of phenothiazinyl units into conjugated chains in the sense of a “push-pull” substitution is an intriguing objective both from the synthetic and the physical properties points of view. As shown by the work of Lambert for expanded benzidines and triarylaminines [7], for bridged and unbridged oligophenothiazines there is also a strong dependence of the electronic communication between aromatic units on the distance of electrophores and the nature of the bridge [8,9].

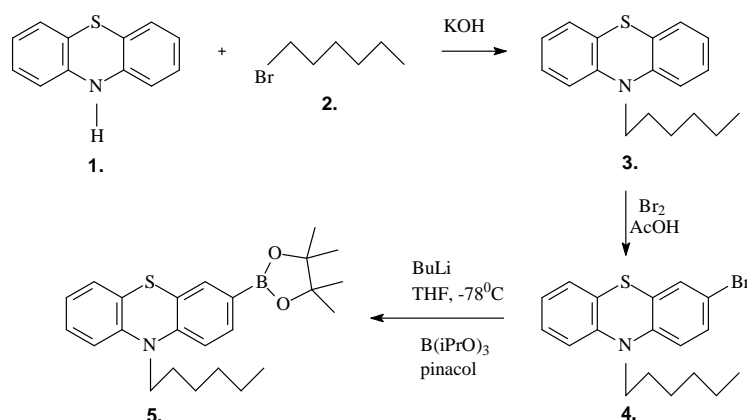
We aimed to prepare a series of binaphthyl derivatives bearing phenothiazine groups at positions 2,2' and/or 6,6'. Investigation of the photochemical and electrochemical properties of such derivatives should give

us valuable information about electronic communication among these groups *via* binaphthyl spacer as a background for construction of optoelectronic devices. In order to obtain the desired compounds **10** and **11** we proposed a rational synthetic approach based on Suzuki or Negishi arylation fo suitable binaphthyl precursors.

RESULTS AND DISCUSSIONS

For Suzuki cross-coupling approach [10] the boronic acid derivative of phenothiazine **5** was coupled with the dibromobinaphthyl derivative **10** (Scheme 3). Compounds **5** and **10** were synthesized according to the procedures described below.

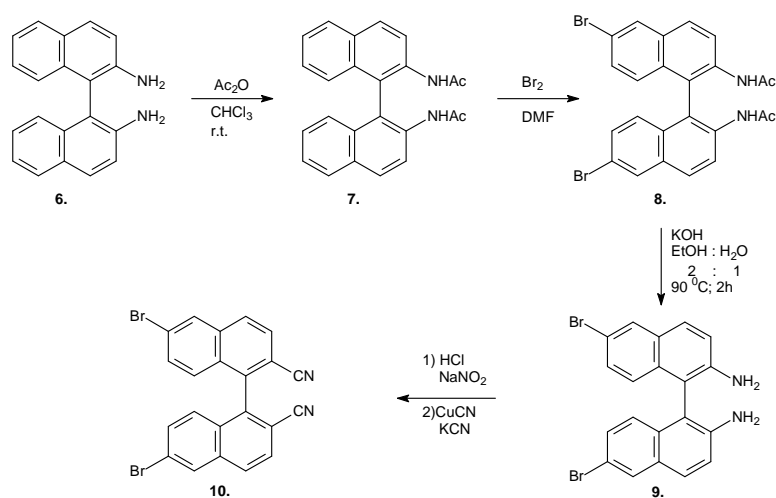
The boronic acid derivative of phenothiazine **5** was readily synthesized from alkylbromophenothiazine **4** by bromine-lithium exchange followed by quenching with trialkyl borate. The derivative **4** was previously synthesized from the *N*-hexylphenothiazine **10** by bromination reaction with bromine in acetic acid. (Scheme 1)



Scheme 1

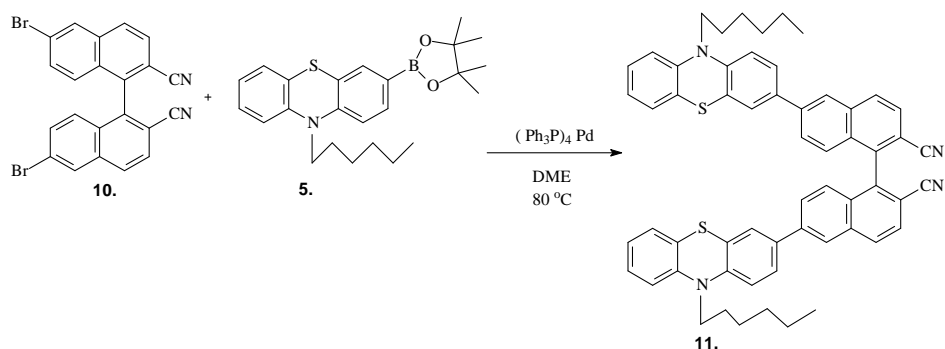
The synthesis of dibromo-dicyanobinaphthyl **10** started with 2,2'-diaminobinaphthyl **6** which was acetylated with acetic anhydride and the protected compound **7** was brominated to give the 6,6'-dibromobinaphthyl derivative **8**. This intermediate was deprotected and then converted into the corresponding dicyanodibromobinaphthyl derivative **10** by diazotization followed by Sandmeyer substitution reaction with KCN and CuCN (Scheme 2). The hydrolysis of the cyano groups in presence of NaOH in diethylene glycol was attempted, but unfortunately it was not successful.

Suzuki coupling of phenothiazine-boronic acid **5** with dibromobinaphthyl **10** under standard conditions in DME / water at 80 °C with Pd(PPh₃)₄ for 3 days gave the target compound **11** as a brown precipitate in good yield (Scheme 3). The structure of compound **11** was assigned by ¹H-NMR and ¹³C-NMR.



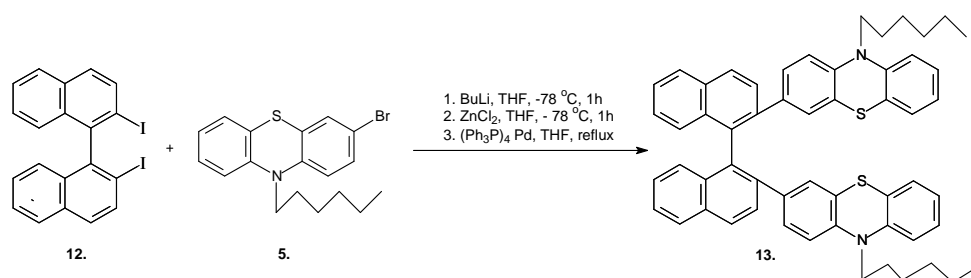
Scheme 2

The hydrolysis of the nitrile functional groups of **11** and the reduction of the intermediate carboxylic acid to hydroxymethyl derivatives were attempted, but unsatisfactory results were obtained, most probably because of steric reasons.



Scheme 3

Negishi arylation also offer a broadly applicable methodology for biaryl synthesis with a relatively high functional group tolerance. The target compound **13** was obtained by Negishi reaction of 2,2'-diiodo-binaphthyl **12** with phenothiazinylzinc halides (Scheme 4). The purification of compounds by column chromatography was very difficult because of very close R_f values of **13** and 10-hexyl phenothiazine dimer formed as side product of this homocoupling reaction.



Scheme 4

CONCLUSIONS

New *bis*-(10-alkyl-phenothiazin-3-yl)-1,1'-binaphthalene derivatives **10**, **13** were synthesized by Suzuki or Negishi coupling reactions of properly substituted phenothiazine and binaphthyl derivatives. Strategies for the syntheses of starting compounds were also developed.

EXPERIMENTAL PART

All reaction were carried out in flame-dried Schlenk flasks under nitrogen by using septum and syringe techniques. Reagents, catalysts, ligands and solvents were purchased reagent grade and used without further purification. Solvents were dried and distilled. Column chromatography: silica gel 30–60 μm and thin-layer chromatography (TLC) on Silufol UV 254 foils: silica gel plates. Melting points were measured on a Koffler block and are uncorrected values. ¹H and ¹³C NMR spectra were measured on a Varian Gemini 300 (300 MHz) instrument in CDCl₃ and DMSO with tetramethylsilane as internal standard.

10-hexylphenothiazine (**3**)

3 was prepared according to [11] by a modified procedure.

A mixture of phenothiazine (2 g, 0.01 mol) and powdered KOH (1.03 g, 0.02 mol) in dry DMF (10 mL) was stirred under N₂ for 30 min. The 1-bromohexane (5.8 mL) was introduced and the mixture was stirred 48 h at r.t. The mixture was poured into water (50 mL) and extracted with hexane. After the removal of the solvent 2.46g of the pure product ($\eta = 86\%$) remained. Spectral analyses were in good agreement with [11].

3-Bromo-10-hexylphenothiazine (4) [12]

Sodium hydroxide (0.62g, 0.0155 mol) was dissolved in 38 mL acetic acid under N₂. 10-hexylphenothiazine (1.5g, 0.0053 mol) solution in CHCl₃ (10 mL) was added. The solution was cooled to 0-5 °C on ice-bath. Bromine (0.3 mL, 0.005 mol) dissolved in acetic acid (5 mL) was added drop wise. The suspension was stirred at r.t. for 1 h. Acetic acid was removed under reduced pressure, giving a purple solid residue. The residue was dissolved in a mixture of saturated aqueous sodium bicarbonate solution (100 mL) and CH₂Cl₂ (100 mL). The aqueous phase was separated from the organic phase and extracted with CH₂Cl₂ (100 mL). The combined organic layer were dried over Na₂SO₄ and filtered chromatography on silica gel with hexane as eluent. 1,5 g of product was obtained. (η = 90%). Spectral analyses were in good agreement with [12]

10-Hexyl-3-(4,4,5,5-tetramethyl-1,3,2-dioxaborolan-2-yl)-10H-phenothiazine (5) [13]

To a solution of **4** in anhydrous THF (40 mL) under N₂ were added drop wise at –78 °C a 2.5 M solution of BuLi in hexane (9 mL). This yellow viscous mixture was stirred at –78 °C for 15 min. Before triisopropyl borate was added drop wise and stirring was continued for another 30 min at –78 °C. Then, the cooling bath was removed and the mixture was allowed to warm up to r.t. and the stirring was continued for another 1 h. To the yellow reaction mixture was added a solution of dry pinacol (1.7g, 0.015 mol) in anhydrous THF (10 mL) and the stirring was continued for 48 h to give an orange mixture. After the addition of AcOH (0.5 mL, 0.007 mol) the mixture turns light orange and highly viscous. After stirring for 16 h, aq. sat. Na₂SO₃ solution (100 mL) was added to the mixture and the aqueous layer was extracted with Et₂O (4 x 100 mL). The combined organic phases were dried (MgSO₄) and the solvents were removed in vacuum. The residue was purified by column chromatography on silica gel (hexanes) to furnish 0.76 g (30 %) as orange colored oil.

¹H NMR (CDCl₃, 300 MHz): δ = 0.87ppm (t, 3H), 1.30 ppm (m, 16 H), 1.43 ppm (m, 2H), 1.79 ppm (m, 2H), 3.84 ppm (t, 2H), 6.88 ppm (m, 3H), 7.11 ppm (m, 2H), 7.58-7.61 ppm (m, 2H).

(RS)-N,N'-(1,1'-binaphthalene-2,2'-diyl)-diacetamide (7)

Mixture of 2,2'-diamino-binaphthyl (5 g, 18 mmol) and acetic anhydride (6.7, 71 mmol) was stirred at room temperature for 2h to give pure compound (**7**) (η = 100 %).

(RS)-N,N'-(6,6'-dibromo-1,1'-binaphthalene-2,2'-diyl)-diacetamide (8)

The flask containing compound **7** (0.73 g, 2 mmol), bromine (0.52 mL, 0.01 mmol) and anhydrous DMF (15 mL) was flushed with N₂ atmosphere. The reaction mixture was stirred and heated on the oil bath at 90 °C for 11 h. The resulting mixture was washed with water, 10 % aqueous NaOH (10 mL) and was extracted with 50 mL CHCl₃, dried over anhydrous Na₂SO₄. Solvent was evaporated and the product made complex with DMF. The mixture was dissolved in minimum amount of CH₂Cl₂ and hexanes, after the precipitate was filtered. (η = 95 %). Crude product was used in following reaction step.

(RS)-6,6'-Dibromo-1,1'-binaphthalene-2,2'-diamine (9)

The flask containing compound **8** (1.043 g, 2 mmol), KOH (4.44 g, 79 mmol) and solution of EtOH : H₂O = 2 : 1 (40 mL) was stirred and heated on the oil bath at 90 °C under N₂ for 2 h. The reaction mixture was quenched with 50 mL CHCl₃ and was washed with NH₄Cl. The crude product 0.69 g. (η = 80 %) was used in following reaction step without further purification.

(R,S)6,6'-Dibromo-1,1'-binaphthalene-2,2'-dicarbonitrile (10)

A solution of diamine **9** (0.69 g, 1.5 mmol) in 27 % HCl (10 mL) was diazotized by addition of solid NaNO₂ (0.45 g, 6.5 mmol) at 0 °C. The mixture was stirred and the temperature was maintained at 0–5 °C for 2 h. The filtered diazo-solution was added to the mixture of KCN and CuCN (0.23 g CuCN in 5.6 mL of 5 % KCN solution). The reaction mixture was warmed on the water-bath at 80 °C for 15 min. and the solid filtered off and washed with dilute HCl (10 mL) and water (100 mL). After drying, the product was obtained in 95 % yield.

¹H NMR (DMSO, 300 MHz) ppm: δ = 6.99 ppm (d, 2H), 7.54 ppm (d, 2H), 7.86 ppm (d, 2H), 8.18 ppm (d, 2H), 8.43 ppm (s, 2H)

¹³C NMR (DMSO, 300 MHz): δ ppm = 119.9 (CN), 126.4 (CH), 128.3 (CH), 129.9 (CH), 130.5(CH), 130.5 (CH), 130.9 (CH), 130.9 (CH), 131.7 (CH), 131.9 (CH), 131.6 (CH), 131.8(CH)

(R,S)6,6'-Bis-(N-hexylphenothiazin-3-yl)-1,1'-binaphthalene-2,2'-dicarbonitrile (11)

To the mixture of **10** (0.5g, 0.001 mol) and **5** in degassed 1,2-dimethoxyethane (60 mL) were added K₂CO₃ (0.1 g, 0.0008 mol) dissolved in a minimum amount of water, and (Ph₃P)₄Pd (0.0008 g, 16 μmol). The reaction mixture was heated to reflux for 3 days under N₂. After the cooling to r.t. H₂O (300 mL) was added and the precipitate was collected by suction filtration and dried in vacuum. The residue was purified by column chromatography on silica gel (CHCl₃) to give 0.1 g (72 %) after recrystallization from methanol.

¹H NMR (DMSO, 300 MHz) ppm: δ = 0.87 ppm (t, 6H), 1.29 ppm (m, 12 H), 1.67 ppm (m, 4H), 3.80 ppm (t, 4H), 6.80-7.22 ppm (m, 12H), 7.60 ppm (m, 6H), 7.84 ppm (d, 2H), 8.17 ppm (dd, 3H), 8.42 ppm (dd, 3H)

¹³C NMR (DMSO, 300 MHz): δ ppm = 13.8 (CH₃), 21.9 (CH₂), 25.9 (CH₂), 30.8 (CH₂), 199.9 (CN), 126.9 (CH), 128.3 (CH), 128.8 (CH), 129.94 (CH), 130.5 (CH), 130.9 (CH), 131.1 (CH), 131.4 (CH), 131.5 (CH), 131.7 (CH), 131.9 (CH), 133.1 (CH)

(R,S) 2,2' -Bis (N-hexylphenothiazin-3-yl) 1,1'-binaphthalene (13)

To a solution of **4** (468 mg, 1.34 mmol) in dry THF (10 mL) under N₂ were added drop wise at –78 °C a 2.5 M sol BuLi (6 mL). This yellow viscous mixture was stirred at –78 °C for 1h before zinc chloride (222 mg, 1.6 mmol) and THF (2 mL) was added drop wise and stirring was continued for another 1h at –78 °C. Then the cooling bath was removed and the mixture was allowed to warm up to r.t. The mixture of **12** (116 mg, 0.2 mmol), (Ph₃P)₄Pd (0.0006 g, 11 μmol) in dry THF (6 mL) was added drop-wise to the yellow reaction mixture and the mixture was refluxed for 1 h to give a brown mixture. After 1 hour, the reaction mixture was cooled down to r.t and diluted HCl (10 mL) was added; the aqueous layer was extracted with Et₂O (4 x 100mL). The combined organic phases were dried (MgSO₄) and the solvents were removed in vacuum. The residue was recrystallized in methanol to furnish 50 mg (27 %) as white precipitate.

¹H NMR (DMSO, 300 MHz): δ = 0.87 ppm (t, 6H), 1.29 ppm (m, 12 H), 1.67 ppm (m, 4H), 3.80 ppm (t, 4H), 6.80-7.25 ppm (m, 17H), 7.45 ppm (t, 2H), 7.50 ppm (dd, 3H), 7.70 ppm (t, 2H), 8.05 ppm (dd, 3H).

REFERENCES

1. M. Putala, *Enantiomer*, **1999**, *4*, 243.
2. D. Fabbri, G. Delogu, O. De Lucchi, *J. Org. Chem.*, **1995**, *60*, 6599.
3. a) H.-J. Deussen, E. Hendrickx, C. Boutton, D. Krog, K. Clays, K. Bechgaard, A. Persoons, T. Bjørnholm, *J. Am. Chem. Soc.*, **1996**, *118*, 6841; b) J.J.G.S. van Es, H.A.M. Biemans, E.W. Meijer, *Tetrahedron Asymmetry*, **1997**, *8*, 1825.
4. a) H.-F. Chow, M.-K. Ng, *Tetrahedron Asymmetry*, **1996**, *7*, 2251; b) P.-A. Jaffrés, N. Bar, D. Villemin, *J. Chem. Soc., Perkin Trans. 1*, **1998**, 2083; c) B.H. Lipshutz, B. James, S. Vance, I. Carrico, *Tetrahedron Lett.*, **1997**, *38*, 753; d) M. Sridhar, S.K. Vadivel, U.T. Bhalerao, *Tetrahedron Lett.*, **1997**, *38*, 5695.
5. a) C. Bodea, I. A. Silberg, *Adv. Heterocycl. Chem.* **1968**, *9*, 321; b) H. Mc L. Gordon, M. J. Lipson, *Conn. Sci. Ind. Res. (S.A.)* **1940**, *13*, 173; c) N. Griffon, C. Pilon, F. Santel, J. C. Schwartz, P. Sokoloff, *J. Neural. Transm.* **1996**, *103(10)*, 1163; *Chem. Abstr.* **1997**, *126*, 54678v; d) G. M. Gilad, V. H. I. Gilad, **US 5,677,349**; *Chem. Abstr.* **1997**, *127*, 341809k; e) Z. Eckstein, T. Urbanski, *Adv. Heterocycl. Chem.* **1978**, *23*, 1; f) M. Ionescu, H. Mantsch, *Adv. Heterocycl. Chem.* **1967**, *8*, 83.
5. a) R. Duesing, G. Tapolski, T. J. Meyer, *J. Am. Chem. Soc.* **1990**, *112*, 5378; b) W. E. Jones Jr, P. Chen, T. J. Meyer, *J. Am. Chem. Soc.* **1992**, *114*, 387; c) J. Daub, R. Engl, J. Kurzawa, S. E. Miller, S. Schneider, A. Stockmann, M. R. Wasielewski, *J. Phys. Chem. A* **2001**, *105*, 5655.
6. C. Lambert, G. Nöll, *J. Am. Chem. Soc.*, **1999**, *121*, 8434.
7. C. S. Krämer, K. Zeitler, T. J. J. Müller, *Tetrahedron Lett.*, **2001**, *42*, 8619
8. For synthetic studies on phenothiazine oligomers and functionalized derivatives, see also a) M. Sailer, R.-A. Gropeanu, T. J. J. Müller, *J. Org. Chem.*, **2003**, *68*, 7509. b) C. S. Krämer, T. J. J. Müller, *Eur. J. Org. Chem.*, **2003**, 3534. c) C. S. Krämer, T. J. Zimmermann, M. Sailer, T. J. J. Müller, *Synthesis*, **2002**, 1163.
9. (a) Miyaura, N; Suzuki, A; *Chem.Rev.* **1995**, *95*, 2457; (b) Suzuki, A, *In Metal Catalyzed Cross Coupling Reactiona*; Stang, P.J, Diederich, F, Eds.; Wiley-VCH: Weinheim, **1998**, 49-97; Stanforth, S.P., *Tetrahedron*, **1998**, *54*, 263, (d) Suzuki, A., *J.Organomet. Chem.*, **1999**, *576*, 147.
10. G. Mehta, T. Sambaiah, B.G. Maiya, M. Sirish, *J.Chem.Soc. Perkin Trans I*, **1995**, 295.
11. R.Y. Lai, X.Kong, S.A. Jenekhe, A.J. Bard, *J. Am. Chem. Soc.*, **2003**, *125*, 12631.
12. C.S.Kramer, T.J.Zimmermann, T.J.J. Muller, *Synthesis*, **2002**, *9*, 1163.

In memoriam prof. dr. Ioan A. Silberg

**MASS SPECTRA OF THE NEW HYDRAZIDO- HYDRAZONES
OBTAINED BY THE CONDENSATION OF THE IZONICOTINIC
ACID HYDRAZIDE (HIN) WITH CITRAL, (+)-CARVONE
AND β -IONONE**

IOAN OPREAN^a, VALER FĂRCĂȘAN^a, IOAN BĂTIU^a

ABSTRACT. Mass spectra of some new hydrazido-hydrazones of the izonicotinic acid hydrazide (HIN) with citral, (+)-carvone and β -ionone were recorded and discussed by comparison with the mass spectra of the starting compounds.

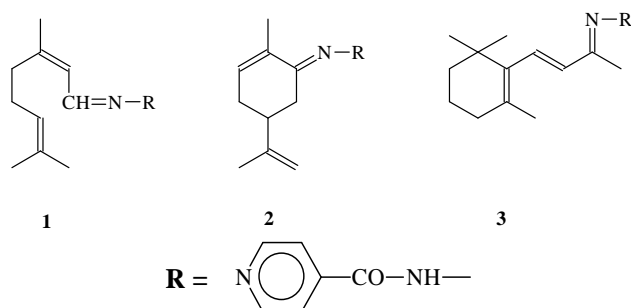
INTRODUCTION

In a previous contributions to the chemistry of the terpenoids we described the synthesis of new hydrazido-hydrazones and hydrazones based on the condensation of some hydrazides and pyrimidyl hydrazines with terpenoid carbonyl compounds (aldehydes and ketones) from the terpenoid class and related compounds [1]. Our new hydrazido-hydrazones and hydrazones were assigned based on IR and UV-VIS spectra [1] and TLC [2]. In addition, we already reported the effect of gamma irradiation using electron spin resonance (ESR) and UV radiation of some terpenoid hydrazones and hydrazido-hydrazones [3,4]. In the field of terpenoids, new 1,3-dioxanic derivatives thereof we previously described [5]. The biological activity of the new compounds was tested [6].

The aim of the present work is the investigation of the mass spectra of new hydrazido-hydrazones **1**, **2** and **3 (Scheme 1)** available by the condensation of the izonicotinic acid hydrazide with citral, (+)-carvone and β -ionone, respectively.

^a "Babes-Bolyai" University of Cluj-Napoca, Faculty of Chemistry and Chemical Engineering, Str. Arany Janos 11, 400028 Cluj-Napoca, Romania

IOAN OPREAN, VALER FĂRCĂȘAN, IOAN BĂTIU



Scheme 1

RESULTS AND DISCUSSIONS

Mass spectra of the hydrazido-hydrazone **1**, **2** and **3** are presented in the Figures 1, 2 and 3.

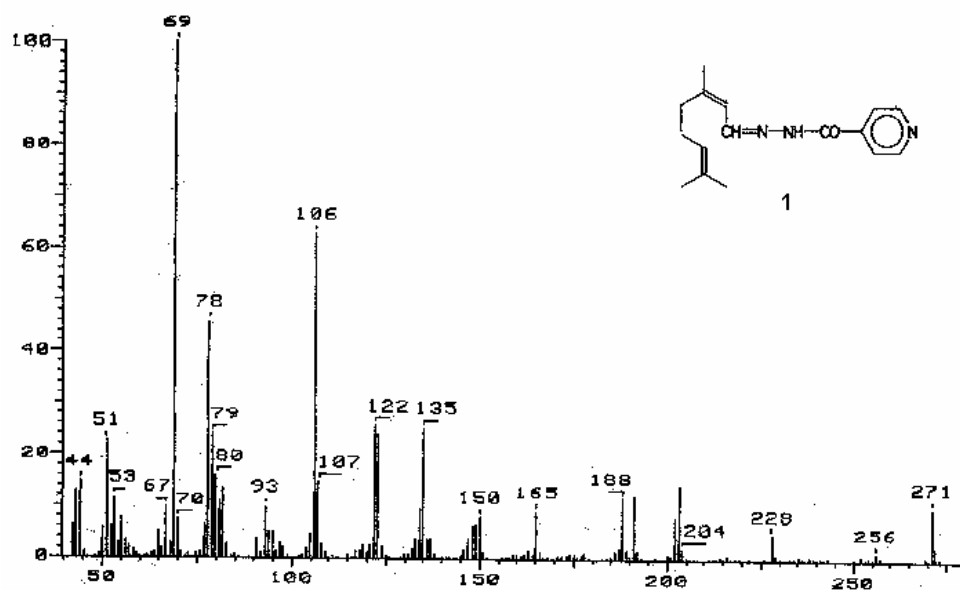


Figure 1. Mass spectrum of the hydrazido-hydrazone **1**

Table 1 lists the m/z values of the first eight main fragments, their abundances, base peaks and molecular ions of the starting materials: HIN, citral, (+) carvone and β -ionone available from the literature [7].

Table 2 lists the m/z values of the first eight main fragments, their abundances, base peaks and molecular ions of the hydrazido-hydrazones 1, 2 and 3.

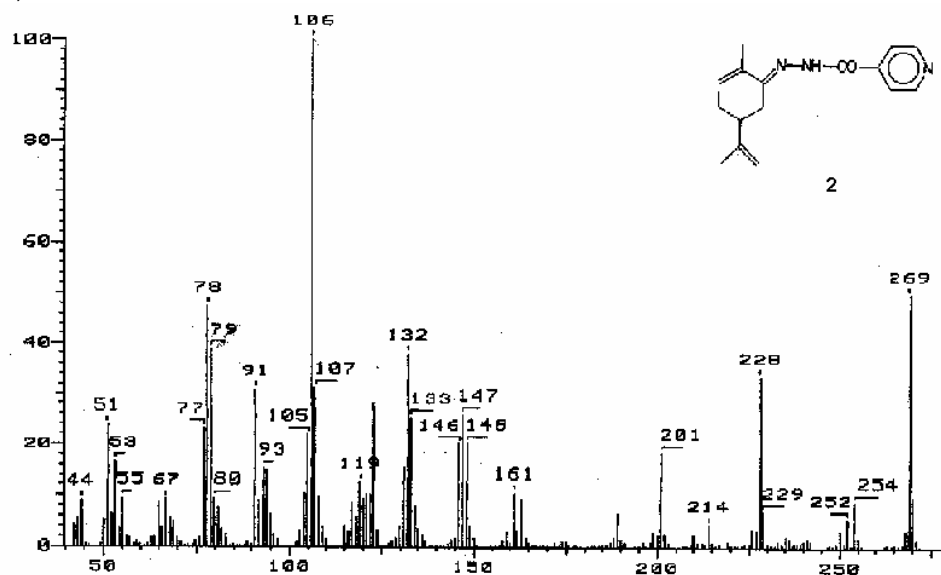


Figure 2. Mass spectrum of the hydrazido-hydrazone 2

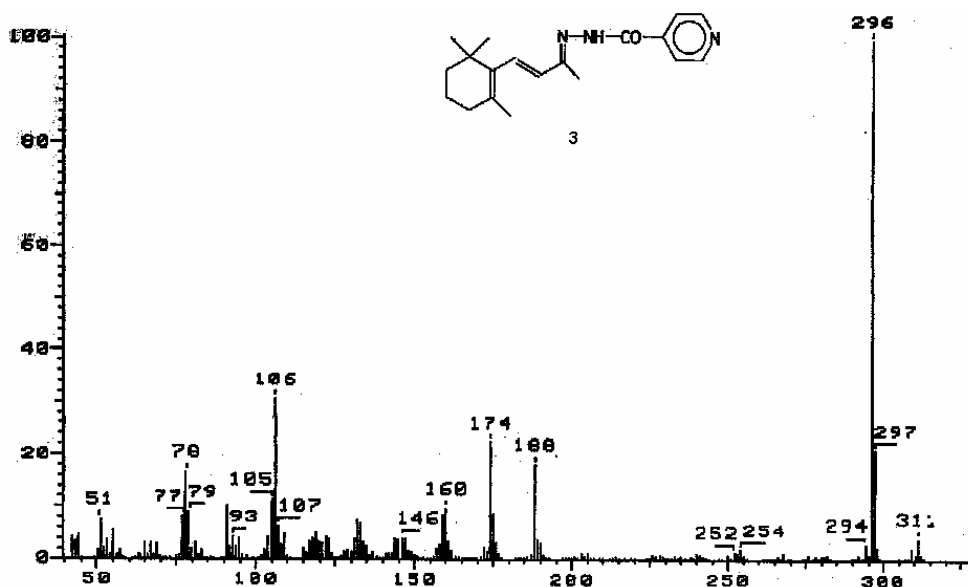


Figure 3. Mass spectrum of the hydrazido-hydrazone 3

Table 1.

The m/z values of the first eight main fragments, their abundances (%), base peaks and molecular ions of HIN, citral, (+) carvone and β -ionone [7].

Compounds	Mol. ions	Base peaks	m/z fragments (%)						
			106	137	51	50	79	31	107
HIN	137 (54)	78 (100)	(99)	(54)	(53)	(16)	(15)	(13)	(11)
Citral	152 (8,3)	69 (100)	(69)	(30)	(19)	(16)	(13)	(10)	(10)
Carvone	150 (7,2)	82 (100)	(65)	(50)	(35)	(35)	(30)	(28)	(22)
β -ionone	192 (6,8)	177 (100)	(74)	(22)	(18)	(16)	(15)	(14)	(14)

Table 2.

The values, m/z of the first eight main fragments, their abundances (%), base peaks and molecular ions of the hydrazido-hydrazones **1**, **2** and **3**.

Compounds	Mol. ions	Base peaks	m/z fragments (%)						
			106	78	122	135	79	123	51
1	271 (10)	69 (100)	(63)	(45,7)	(25,7)	(25,4)	(24,6)	(24,3)	(23)
2	269 (49,3)	106 (100)	(49,3)	(47)	39,3)	(38,6)	(33,6)	(31,8)	(30,7)
3	311 (4,3)	296 (100)	(31)	(22,7)	(21,2)	(18)	(16,5)	(11,5)	(10)

Considering the mass spectra of the hydrazido-hydrazones **1**, **2** and **3** the followings can be observe and discuss.

Hydrazido-hydrazone 1

The molecular ion, m/z 271 (10 %) presents a relative low stability close to that of the molecular ion of the citral, m/z 152 (8.3%) and lower than that of the molecular ion of the HIN, m/z 137 (54%).

The base peak, m/z 69 is the same as in citral, while for the HIN is the fragment, m/z 78. The base peak, m/z 69 results from the molecular ion by an allylic cleavage able to afford two fragments stabilized by an allylic type resonance. Such fragmentation is supported by the presence in the mass spectrum of the corresponding ion, m/z 202 (Figure 1) This type of fragmentation is confirmed by the metastable transition, m/z 271 \rightarrow m/z 202 (Scheme 2). The high resolution measurements confirm the presence of the $C_{11}H_{12}N_3O^+$ fragments, m/z 202 (Table 3).

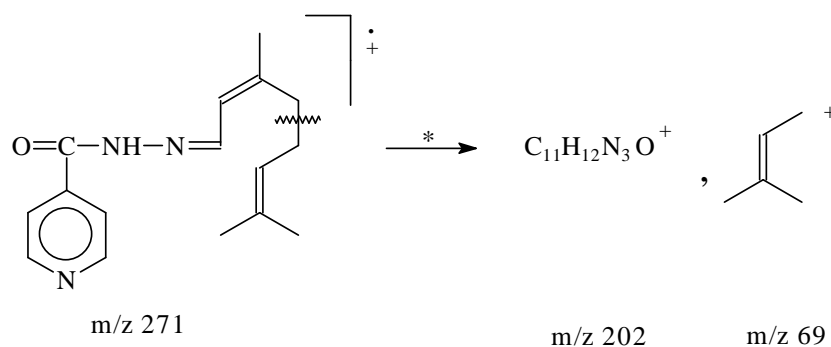
In fact, the same fragmentation takes place in the mass spectrum of the citral, supported by the presence in the mass spectrum of the fragment m/z 83 (10%) (Table 1).

In the mass spectrum of the HIN the base peak (pyridilium ion), m/z 78 results from the acylium ion, m/z 106 (99%) by a decarbonylation process (Scheme 3). The abundances of the two fragments are very close.

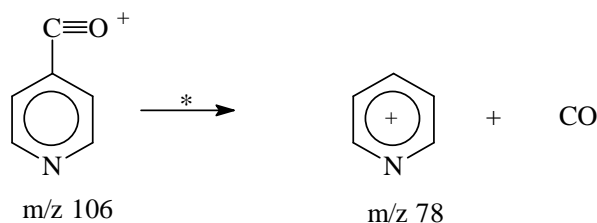
Table 3.

High resolution measurements of some fragments, m/z of the hydrazido-hydrazone **1**, **2** and **3**.

Fragments, m/z	High resolution	
	measurements	calculated
m/z 78 - C ₅ H ₄ N ⁺ - C ₅ H ₂ O ⁺	78.035 78.035	78.035172 78.0105633
m/z 108 - C ₈ H ₁₂ ⁺	108.097	108.098952
m/z 161 - C ₈ H ₇ N ₃ O ⁺	161.059	161.0589077
m/z 163 - C ₁₀ H ₁₅ N ₂ ⁺	163.124	163.1235166
m/z 202 - C ₁₁ H ₁₂ N ₃ O ⁺	202.097	202.0980307
m/z 296 - C ₁₈ H ₂₂ N ₃ O ⁺	296.175	296.1762767



Scheme 2



Scheme 3

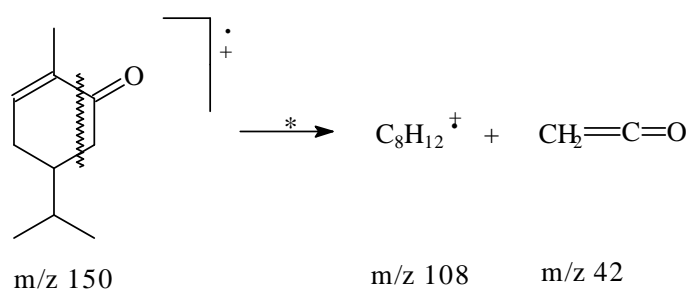
The presence of fragment, m/z 78 can also be obtained by elimination of hydrogen cyanide and hydrogen from m/z 106, generating the $\text{C}_5\text{H}_2\text{O}^+$ ion. The high resolution measurements confirm the presence of the $\text{C}_5\text{H}_4\text{N}^+$ fragments, m/z 78 (Table 3).

We note that in the mass spectrum of the hydrazido-hydrazone **1** there are present the same m/z 106 and m/z 78 fragments, respectively like as in the mass spectrum of HIN. Their decreased abundance is m/z 106 > m/z 78.

Hydrazido-hydrazone 2

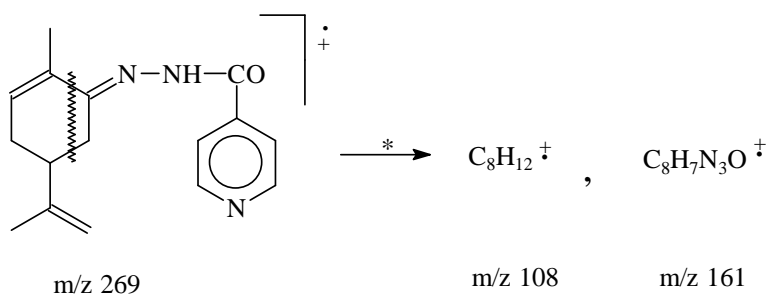
The molecular ion, m/z 269 (49,3%) presents higher stability in comparison with the molecular ion of the (+)- carvone, m/z 150 (7,2%), closed to the molecular ion of the HIN, m/z 137 (54%).

This stability allow us to suppose that blocking of the carbonyl group by the condensation with the izonicotinic acid hydrazide (HIN) disadvantages the braking up of the linkage in which it is directly involved. Taking into account the characteristic fragmentation of the α , β -unsaturated ketones [8], in the mass spectrum of the (+) carvone, the $\text{C}_8\text{H}_{12}^+$ m/z 108 fragment (35%) is present (Table 1) (Scheme 4).

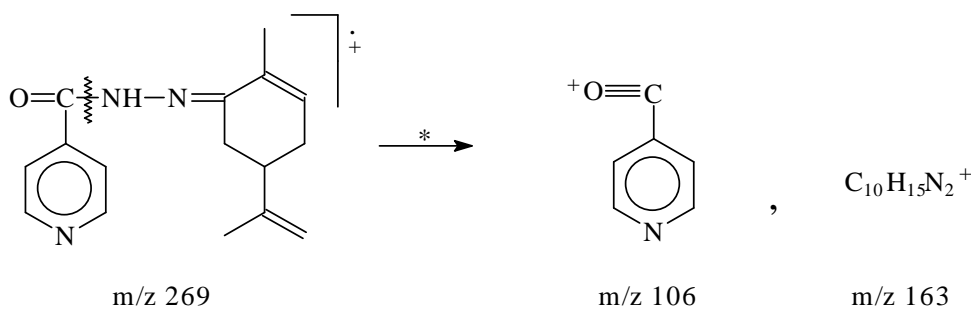


Scheme 4

If a similar cleavage takes place in the mass spectrum of the hydrazido-hydrazone **2** it is expected to find the $C_8H_{12}^+$ m/z 108 fragment, and the $C_8H_7N_3O^+$ m/z 161 fragment, respectively (Scheme 5). The high resolution measurements confirm the presence in the mass spectrum of the hydrazido-hydrazone **2** of the $C_8H_{12}^+$ m/z 108 fragment and of the $C_8H_7N_3O^+$ m/z 161 fragment, respectively (Table 3), but their abundance is small (Figure 2). The differences between the abundance of the m/z 108 fragment, in (+)-carvone (35%) and in the hydrazido-hydrazone **2** (10%) confirm such a supposition.


Scheme 5

The base peak, m/z 106 (acylium ion) results from the molecular ion, m/z 269 by the fragmentation presented in Scheme 6.


Scheme 6

Such fragmentation is supported by the presence in the mass spectrum of the corresponding ion, m/z 163 (Figure 2). The high resolution measurements confirm the presence of the $C_{10}H_{15}N_2^+$ m/z 163 fragment, (Table 3).

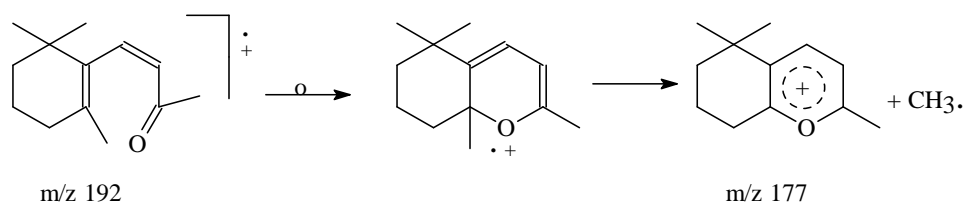
We note that in the mass spectrum of the hydrazido-hydrazone **2** there are present the same fragments, m/z 106 and m/z 78, respectively as observed in the mass spectrum of the hydrazido-hydrazone **1** and in the mass spectrum of the HIN. Their abundance decreased as m/z 106 > m/z 78.

Hydrazido-hydrazone **3**

The molecular ion, m/z 311 presents a low abundance (4,3%) even lower than that of the corresponding ion of the β -ionone, m/z 192 (6,8%) and much lower than that of the molecular ion of the HIN, m/z 137 (54%).

The base peak, m/z 296 results from molecular ion, m/z 311 by a demethylation process (M-CH₃).

A systematic previous reported study focus on the mass spectra of the doubly unsaturated carbonyl compounds A. F. Thomas *et al.* [9] shows the main characteristic feature of the mass spectrum of the β -ionone, namely the presence of the fragment M-15. It results from the molecular ion by loss of a methyl group linked to the double bond of the cycle, as proved by the behaviour of the properly deuterated compound. By this kind of fragmentation the base peak, m/z 177 stabilized by resonance (aromatization) (Scheme 7) results.



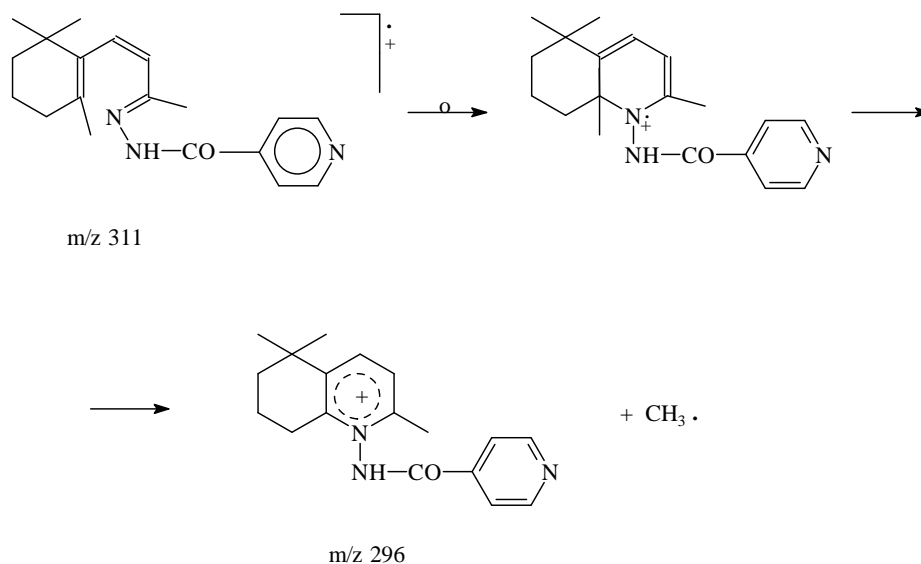
Scheme 7

Taking into account the literature data [9] we consider that in the mass spectrum of the hydrazido-hydrazone **3** a similar demethylation process takes place, yielding the cyclic aromatic system which has, in this case, the nitrogen as heteroatom (Scheme 8). The high resolution measurements confirm the presence of the C₁₈H₂₂N₃O⁺ fragment, m/z 296 (Table 3).

We note the relative high abundance of the acylium ion, m/z 106 (31%) like as in the mass spectra of the hydrazido-hydrazones **1** and **2**.

We also note that in the mass spectrum of the hydrazido-hydrazone **3** there are present the same fragments, m/z 106 and m/z 78, respectively as observed in the mass spectra of the hydrazido-hydrazones **1** and **2** and in the mass spectrum of the HIN. Their abundance decreased in the same order, m/z 106 > m/z 78, in reversed than that order observed in the mass spectrum of HIN.

MASS SPECTRA OF THE NEW HYDRAZIDO- HYDRAZONES OBTAINED BY THE CONDENSATION ...



Scheme 8

CONCLUSIONS

We have presented and discussed the mass spectra of three new hydrazido-hydrazones issued from the condensation of the izonicotinic acid hydrazide (HIN) with citral, (+)-carvone and β -ionone, respectively. The molecular ions of the hydrazido-hydrazones exhibit low stability close to that of the starting terpenoids and much lower than that of the HIN's molecular ion, except the hydrazido-hydrazone **2**. The base peaks contain pyridine nucleus except hydrazido-hydrazone **1**. In the mass spectrum of the hydrazido-hydrazone **3** a very stable ion is observed as a result of a demethylation (M-15) and cyclization processes involving the nitrogen atom.

EXPERIMENTAL PART

The synthesis of the hydrazido-hydrazones **1**, **2** and **3** we described in a previous paper [1]. Their purity was checked by TLC.

The mass spectra were recorded by using a high resolution Varian-MAT 312 mass spectrometer with double focalization equipped with an ionization source of 70 eV.

REFERENCES

1. I. Bătiu, I. Cristea, V. Fărcășan *Studia Universitatis Babeș-Bolyai.Chemia*, **1993**, XXXVIII (1-2), 125.
2. S. Gocan, L. Damian, I. Bătiu, *Revue Roumaine de Chimie*, **1996**, 41 (5-6), 453.
3. I. Barbur, I. Bătiu, V. Simon, *Journal of Radioanalytical and Nuclear Chemistry*, **1995**, 196 (I), 153.
4. I. Barbur, V. Chiș, I. Bătiu, *Studia Universitatis Babeș-Bolyai Physica*, **2000**, XLV, 2, 91.
5. I. Grosu, S. Mager, I. Bătiu, *Revue Roumaine de Chimie* **1995**, 40 (11-12) 1175.
6. I. Bătiu Ph.D. Thesis *Contributions to the separation process and high added value of the essential oils (Contribuții la tehnologia de separare și valorificare superioară a uleiurilor volatile)* Cluj-Napoca, **1995**.
7. "Eight Peak Index of Mass Spectrometry data Center", The Royal Society of Chemistry. The University Nothinghane, Third Edition, vol.I, part I, **1983**, reprinted **1986**, 170, 247, 235, 445.
8. I. Oprean, "*Spectrometria de masă a compușilor organici*", Editura Dacia Cluj-Napoca, **1974**, 173.
9. A. F. Thomas, B. Willhalm R. Müller, *Organic Mass Spectrometry*, **1969**, 2, 223.

In memoriam prof. dr. Ioan A. Silberg

**Pd(0)-CATALYZED CROSS-COUPPLING REACTIONS IN THE
SYNTHESIS OF (7E,9Z)-7,9-DODECADIENYL ACETATE,
THE SEX PHEROMONE OF THE LEAF ROLLER MOTH
(*Lobesia Botrana*)**

STEFANIA TOTOS^a, IOAN OPREAN^a, FLAVIA PIRON^b

ABSTRACT. A short step synthesis of (7E,9Z)-7,9-dodecadien-1-yl acetate is reported. The route features the cross-coupling reactions to assemble an enyne, which is then reduced to the desired (E,Z)-diene.

INTRODUCTION

Lobesia botrana is the key pest of vineyard, it presents two to five generations per year which cause a direct damage to grapes by perforating berries and an indirect damage by favoring the installation of rot fungi like *Botrytis cinerea*. The major sex pheromone of the female grape vine moth has been identified as (7E,9Z)-7,9-dodecadien-1-yl acetate **7** by Roelofs [1]. The compound can be used as an attractant for monitoring, through selective trapping, the population of *Lobesia botrana* in a given area. Population counts thus obtained are used in determining the frequency and quantity of spray of insecticide or other insect control agent.

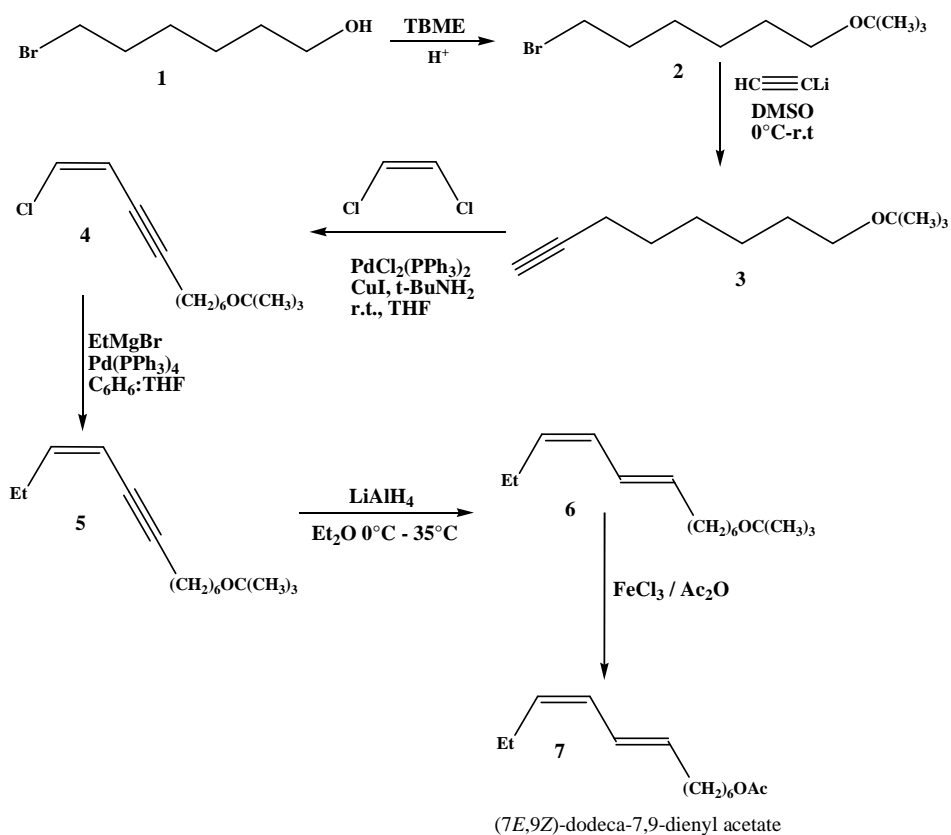
During the last years, various strategies have been developed for the stereoselective construction of the conjugated diene moiety in **7** [2-7]. Among them, the Wittig-type reaction [2] and its many modifications, represents one of the most classical approach to the synthesis of **7**. An alternative to this reaction is the transition metal catalyzed C(sp)-C(sp²) and C(sp²)-C(sp³) cross-coupling reactions of alk-1-yne **3** or organometallic derivatives with vinyl halogenides. This "vinyl" cross-coupling approach offers high isomeric purity of products and reasonable yields in comparison with other synthetic paths.

^a "Babes-Bolyai" University, "Raluca Ripan" Institute for Research in Chemistry, 30 Fantanele str., 400294, Cluj-Napoca, Romania

^b "Babes-Bolyai" University, Organic Chemistry Department and CCOCCAN, 11 Arany Janos str., 400028, Cluj-Napoca, Romania

RESULTS AND DISCUSSIONS

In this paper we described a short-step synthesis of (7*E*,9*Z*)-7,9-dodecadien-1-yl acetate **7**, using **3**, that can be easily prepared from **2** with lithium acetylide, as key step [8]. As shown in (Scheme 1), the cross-coupling reaction of **3** with *cis*-1,2-dichloroethylene in the presence of PdCl₂(PPh₃)₂, CuI and *t*-BuNH₂ afforded **4** in high yield and isomeric purity [9].



Scheme 1

The *Z*-chloroenynene **4** was transformed into the corresponding *Z*-enyne **5** by reaction with ethyl magnesium bromide in the presence of Pd(PPh₃)₄ in C₆H₆: THF at reflux [10]. The reduction of **5** with LiAlH₄ afforded **6** in good yield and isomeric purity [11]. The structural analysis of the synthesized compounds was carried out using GC-MS and NMR investigations.

CONCLUSIONS

A new method for the construction of the required carbon chain with a conjugated diene moiety in **7** is described, based on the Pd catalyzed cross-coupling reactions. Stereoisomeric purity of **7** was higher than 95% (GC). Overall yield was 19% based on the starting 6-bromohexan-1-ol.

EXPERIMENTAL PART

¹H-NMR (300 MHz) spectra were recorded at *rt* in C₆D₆ on a Bruker 300 MHz spectrometer, using the solvent line as reference. Electron impact (70 eV) mass spectra were obtained on Hewlett-Packard MD 5972 GC-MS instrument. GC analyses were performed on a Hewlett-Packard HP 5890 gaz chromatograph. A HP-5MS capillary column (30 m x 0.25 mm x 0.33 μm) and helium gas were used for separations.

All chemical reactions were run in dried glassware under nitrogen atmosphere. THF and DMSO were used as purchased. Pd catalysts were prepared as described in the literature¹⁰.

1-Bromo-6-(*tert*-butoxy)hexane **2**

The compound **2** was prepared by a standard manner from 6-bromohexan-1-ol (40.0 g, 0.22 mol) in the presence of catalytic amount of H₂SO₄ in *t*-butyl-methyl-ether as solvent. Yield 90%, (47 g). C₁₀H₂₁BrO. Mol. Wt.: 237.18. ¹H-NMR (300 MHz, C₆D₆, δ ppm): 3.19-3.15 (2H, t, J = 6.3 Hz, -CH₂-Br), 2.95-2.91 (2H, t, J = 6.7 Hz, -CH₂-OtBu), 1.5-1.17 (m, 8 H), 1.17 (9H, s).

8-(*tert*-Butoxy)oct-1-yne **3**

To a stirred and cooled (0 °C) suspension of lithium acetylide-ethylenediamine complex (2.52 g, 0.042 mol) in anhydrous dimethyl sulfoxide (25 mL) was slowly added compound **2** (5 g, 0.021 mol). The reaction mixture was stirred at room temperature for 6 h, then it was poured into ice water and extracted with hexane (4 x 25 mL). The combined hexane extracts were washed with water (3 x 25 mL), brine (2 x 25 mL) and dried over anhydrous MgSO₄. The solvent was evaporated, and the oily residue was used further without purification. Yield 91%, (3.5 g). C₁₂H₂₂O. Mol. Wt.: 182.3. ¹H-NMR (300 MHz, C₆D₆, δ ppm): 3.21-3.17 (2H, t, J = 6.3 Hz, -CH₂-OtBu), 1.95-1.93 m (2H, m, -CH₂-C≡), 1.78-1.76 (1H, t, J = 2.7 Hz, -C≡H), 1.48-1.23 (8H, m), 1.10 (9H, s).

(*Z*)-10-*tert*-Butoxy-1-chlorodec-1-en-3-yne **4**

A mixture of PdCl₂(PPh₃)₂ (0.3 g, 0.5 mmol, 0.05 % eq.), (*Z*)-1,2-dichloroethene (3.34 g, 0.034 mol), terminal alkyne **3** (2.1 g, 0.0115 mol) and *t*-butylamine (1.68 g, 0.023 mol) in absolute THF was stirred for 15 min. at room temperature under nitrogen atmosphere, and CuI (0.2 g, 1.15 mmol) was then added.

The stirring was continued until TLC analysis indicated complete consumption of the alkyne. The reaction mixture was treated with a saturated solution of NaHCO_3 and extracted with diethyl ether. The organic layer was dried over MgSO_4 and the solvent was removed in vacuo. The crude product was purified by column chromatography, using CH_2Cl_2 : petroleum ether = 1 : 1 as eluent, to yield the desired chloroenyne. Yield 72%, (2.0 g). $\text{C}_{14}\text{H}_{23}\text{ClO}$. Mol. Wt.: 242.78. $^1\text{H-NMR}$ (300 MHz, C_6D_6 , δ ppm): 5.73-5.71 (1H, d, $J = 7.3$ Hz, Cl-CH=), 5.48-5.45 (1H, m, Cl-CH=CH-), 3.22-3.17 (2H, t, $J = 6.3$ Hz, $-\text{CH}_2\text{OtBu}$), 2.11-2.09 (2H, m, $-\text{CH}_2-\text{CH=}$), 1.55-1.11 (8H, m), 1.11 (9H, s).

(Z)-1-tert-Butoxydodec-9-en-7-yne 5

To a mixture of $\text{Pd}(\text{PPh}_3)_4$ (0.23 g, 0.2 mmol) and chloroenyne **4** (1.0 g, 4.12 mmol) in benzene : THF = 1 : 1 under nitrogen atmosphere was added dropwise a solution 1M in THF of EtMgBr (6.2 mL) at 0 °C. The resulting dark brown reaction mixture was then refluxed for 8 h. The reaction mixture was diluted with diethyl ether (50 mL) and quenched with 2N HCl. The layers were separated and the aqueous layer was extracted with diethyl ether; the combined organic layers were washed with saturated brine and dried over anhydrous MgSO_4 . The solvent was removed in vacuo and the product was purified by column chromatography using CH_2Cl_2 : petroleum ether = 1 : 1 as eluent to afford **5**. Yield: 41 % (0.4 g). $\text{C}_{16}\text{H}_{28}\text{O}$. Mol. Wt.: 236.39. $^1\text{H-NMR}$ (300 MHz, C_6D_6 , δ ppm): 5.67-5.59 (1H, m, $-\text{CH}_2-\text{CH=}$), 5.56-5.49 (1H, m, $-\text{CH=CH-}$), 3.22-3.18 (2H, t, $J = 6.7$ Hz, $-\text{CH}_2-\text{CH}_3$), 2.19-2.11 (2H, m), 1.32-1.29 (6H, m), 1.10 (m, 2H), 1.10 (9H, s), 0.93-0.88 (3H, t, $J = 7.5$ Hz, $-\text{CH}_2-\text{CH}_3$).

(7E,9Z)-1-tert-Butoxydodeca-7,9-diene 6

To a suspension of lithium aluminum hydride (32 mg, 0.83 mmol) in diethyl ether (10 mL) at -5 °C under nitrogen atmosphere was added a solution of **5** (0.4 g, 1.7 mmol) in diethyl ether (10 mL) dropwise over a period of 15 min. The reaction mixture was stirred for 2 h at 35 °C and then cooled to 0 °C.

The reaction mixture was diluted with diethyl ether (20mL) and quenched with 2N HCl. The layers were separated and the aqueous layer was extracted with ether; the combined organic layers were washed with saturated brine and dried over anhydrous MgSO_4 . The solvent was removed in vacuo. The product was purified by column chromatography using CH_2Cl_2 : petroleum ether = 1 : 1 to afford **6**. Yield: 70% (0.28 g). $\text{C}_{16}\text{H}_{30}\text{O}$. Mol. Wt.: 238.41. $^1\text{H-NMR}$ (300 MHz, C_6D_6 , δ ppm): 6.39-6.34 (1H, m), 6.05-5.95 (1H, m), 5.63-5.54 (1H, m), 5.30-5.28 (1H, m), 3.94-3.90 (2H, t, $J = 7.5$ Hz, $-\text{CH}_2-\text{CH=}$), 2.12-2.06 (2H, m, $-\text{CH}_2-\text{CH}_3$), 1.30-1.26 (6H, m), 1.09 (11H, m, s), 0.92-0.87 (3H, t, $J = 7.5$ Hz, $-\text{CH}_2-\text{CH}_3$).

(7E,9Z)-7,9-Dodecadien-1-yl acetate 7⁸

To a solution of protected alcohol **6** (0.28 g, 1.18 mmol) in diethyl ether was added acetic anhydride (1 mL), and then anhydrous FeCl₃ (18 mg, 0.11 mmol). The dark brown solution was stirred for 20 h at room temperature. A saturated aqueous solution of Na₂PO₄ (10 mL) was added, and the mixture was stirred for 2 h. The solid FePO₄ was filtered off, and the aqueous layer was extracted with diethyl ether (3 x 10 mL). The collected organic phases were dried over anhydrous MgSO₄ and then concentrated. The red oily residue was further purified on column chromatography to afford **7** using CH₂Cl₂ : petroleum ether = 1 : 1. Yield 80% (0.2 g). C₁₄H₂₄O₂. Mol. Wt.: 224.34. ¹H-NMR (300 MHz, C₆D₆, δ ppm): 6.41-6.36 (1H, m), 6.09-6.01 (1H, m), 5.62-5.54 (1H, m), 5.33-5.29 (1H, m), 3.96-3.92 (2H, t, J = 6.7 Hz, -CH₂-CH=), 2.14-2.09 (2H, m, -CH₂-CH₃), 1.99-1.97 (2H, m), 1.68 (5H, m), 1.68 (5H, m+s), 1.38-1.10 (6H, m), 0.93-0.88 (3H, t, J = 7.6 Hz, -CH₂-CH₃).

REFERENCES

1. W. L. Roelofs, J. Kochansky, R. Carde, H. Arn, S. Rauscher, *Bull. Soc. Entomol. Suisse*, **1973b**, 46, 71.
2. A. Yamamoto, T. Fukumoto, *Agric. Biol. Chem.*, **1989**, 53, 2521.
3. O. S. Kukovinets, V. G. Kasradze, E. V. Chernukha, V. N. Odinkov, B. Z. Galin, M. I. Abdulin, P. I. Fedorov, G. A. Tolsikov, *Russ. Journal of Organic Chemistry*, **2000**, 36, 211.
4. Z. G. Chrelashvili, M. V. Mavrov, B. I. Ugrak, A. A. Kutin, E. P. Serebryakov, *Russ. Chem. Bull.*, **1993**, 42, 1593.
5. L. Daradics, I. Oprean, F. Hodosan, *Journal f. prakt. Chem.*, **1987**, 329, 277.
6. V. Ratavelomanana, G. Linstumelle, *Tetrahedron Lett.*, **1981**, 22, 315.
7. D.G. Diego, R.L.O.R. Cunha, J.V. Comasseto, *Tetrahedron Lett.*, **2006**, 47, 7147.
8. M. Hoskovec, D. Saman, A. Svatos, *Collect. Czech. Chem. Commun.*, **2000**, 65, 5 11.
9. M. Alami, J. F. Peyrat, J. D. Brion, *Synthesis*, **2000**, 11, 1499.
10. L. Brandsma, S. F. Vasilevsky, H. D. Verkruijse, *Application of Transition Metal Catalysts in Organic Synthesis*, Springer-Verlag Berlin, **1999**.
11. J. S. Yadav, E. J. Reddy, T. Ramalingam, *New J. Chem.*, **2001**, 25, 223.

In memoriam prof. dr. Ioan A. Silberg

CALIX[n]ARENE DERIVATIVES WITH BINDING PROPERTIES TOWARD Eu^{3+}

ALINA SAPONAR^{a, b}, IOAN SILAGHI-DUMITRESCU^b,
ELISABETH-JEANNE POPOVICI^a, NICOLAE POPOVICI^a

ABSTRACT. Narrow rim functionalized calix[6]arene with 2-Butenyl, ethylacetate and N,N-diethylacetamide were synthesized and investigated by Elemental Analysis (EA) and various spectroscopic methods such as: UV-VIS, FT-IR and ^1H and ^{13}C NMR. These derivatives were tested for the extraction of Eu^{3+} ions from the aqueous phase.

Keywords: *synthesis, calix[n]arene, functionalisation, Eu extraction;*

INTRODUCTION

The coordination as well as extraction properties of calix[n]arenes is very well known for a long time [1]. Calixarene derivatives incorporating ionophoric functional such as amine, amide, organophosphoric and ester or acid groups at the "narrow rim" exhibit selective extraction/complexation properties [2, 3].

The high ability of these calixarenes to form coordination compounds offers large utilization possibilities in the manufacture of sensitive membrane for electrical and optical sensors [4-6], elaboration of extraction methods for various cations [7], utilization in modern recovery procedures [8] and for the environmental protection [9].

Many preparation procedures have been developed for specific synthesis of calix[n]arene derivatives with oxygen or/and nitrogen and oxygen or/and organo-phosphorous functional groups because of their extraction / coordination properties toward metallic ions. Calixarene derivatives with ester, acid, amide and organo-phosphorous moieties are effective for extraction/complexation of alkaline[10], alkaline earth[11], as well as lanthanide [12, 13] and transition metals [14].

^a "Raluca Ripan" Institute for Research in Chemistry, "Babes-Bolyai" University, 30 Fantanele Str., 400294 Cluj-Napoca, Romania

^b Faculty of Chemistry and Chemical Engineering, "Babes-Bolyai" University, 1 Kogalniceanu Str., 400084 Cluj-Napoca, Romania; saponar_alina@yahoo.com

Our earlier work on extraction of precious metallic ions revealed that acylated calix[6] and calix[4]arene derivatives show a good extraction ability toward platinum(II) and palladium(II) ions but not for rhodium(III)ion [15]. This results encouraged us to extend our works on the synthesis of other calix[n]arene derivatives (n = 4, 6, 8) with possible extraction abilities [16-19].

The aim of this study is to present our works referring to synthesis of calix[n]arene derivatives with alkenyl, ester and/or amide groups and to test their extraction properties.

RESULTS AND DISCUSSIONS

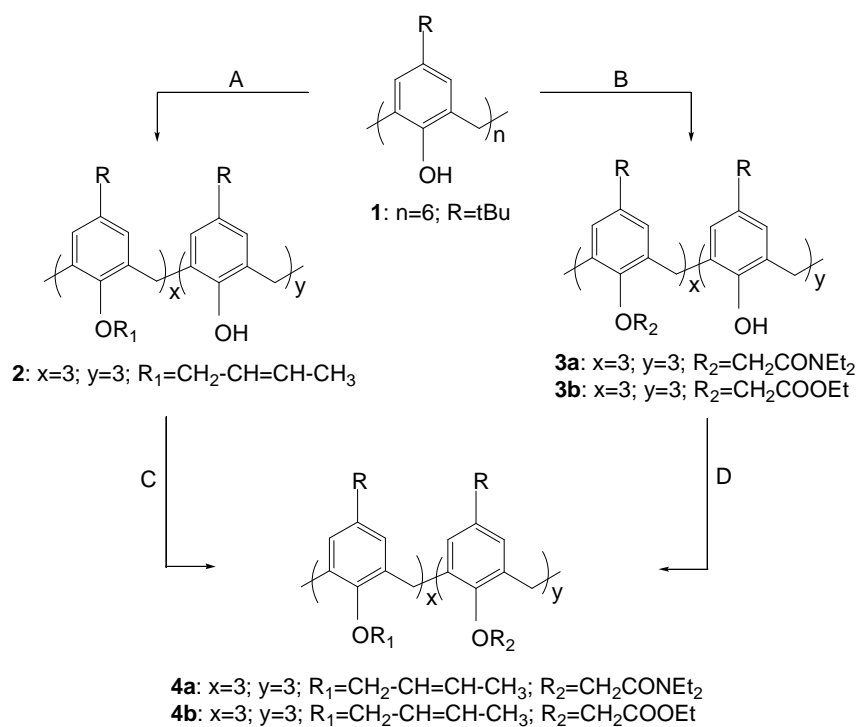
The parent calix[6]arene was treated in the first stage with crotyl bromide in order to obtain calixarene derivative which contains three crotyl groups: 5,11,17,23,29,35-hexa-*t*Butyl-37,38,39-tris[(but-2-enyloxy)-40,41,42-trihydroxy-calix[6] arene (**2**) (scheme 1, pathway A).

In the next stage **2** was treated with α -Chloro-N,N-diethylacetamide or Ethyl bromoacetate (scheme 1, pathway C) in order to obtain a calix[n]arene derivatives: 5,11,17,23,29,35-hexa-*t*Butyl-37,38,39-tris[(N,N-diethylamino-carbonyl)methoxy]-40,41,42-tris-(But-2-enyloxy)-calix[6]arene(**4a**) and 5,11,17,23,29,35 – hexa- *t*Butyl-37,38,39-tris[(carbonyl ethoxy)methoxy]- 40,41,42-tris-(But-2-enyloxy)-calix[6] arene (**4b**), with mixed functional groups at the narrow rim. On the other hand calix[6]arene was treated in the first stage with α -Chloro-N,N-diethylacetamide or Ethyl bromoacetate (scheme 1, pathway B) to obtain calix[6]arene with amide, 5,11,17,23,29,35-hexa-*t*Butyl-37,38,39-tris[(N,N-diethylamino carbonyl) methoxy]-40,41,42-trihydroxy-calix[6] arene (**3a**), or ester functionality, 5,11,17,23,29,35-hexa-*t*Butyl-37,38,39-tris-[(ethoxycarbonyl)metoxy]-40,41,42-trihydroxy-calix[6]arene (**3b**), which reacts in the next stage with crotyl bromide to yield the same calixarene derivatives **4a** and **4b**, respectively.

The narrow rim functionalization is well illustrated by $^1\text{H-NMR}$ spectra which show the expected differences in the chemical shifts, between **1** and **3a**, **3b**. The chemical shift of the proton from the phenolic OH group appears at 10.55 ppm for compound **1** and between 7.09– 7.14 ppm for compounds **3a** and **3b**.

Infrared absorption spectra show that the band corresponding to OH stretching vibration of calixarene **1** appear at 3172 cm^{-1} , while for the intermediates **2**, **3a** and **3b** it is at: $3387(\mathbf{2})$, $3248(\mathbf{3a})$ and $3399\text{ cm}^{-1}(\mathbf{3b})$. In the FTIR spectrum of **3a** and **3b**, the band corresponding to the stretching vibration of carbonyl groups appears at $1644(\mathbf{3a})$ and $1741(\mathbf{3b})\text{ cm}^{-1}$, respectively (Fig. 1).

CALIX[n]ARENE DERIVATIVES WITH BINDING PROPERTIES TOWARD Eu^{3+} METAL CATION



Scheme 1. Two pathways for the synthesis of calixarene compounds **2,3a,3b,4a, 4b**.

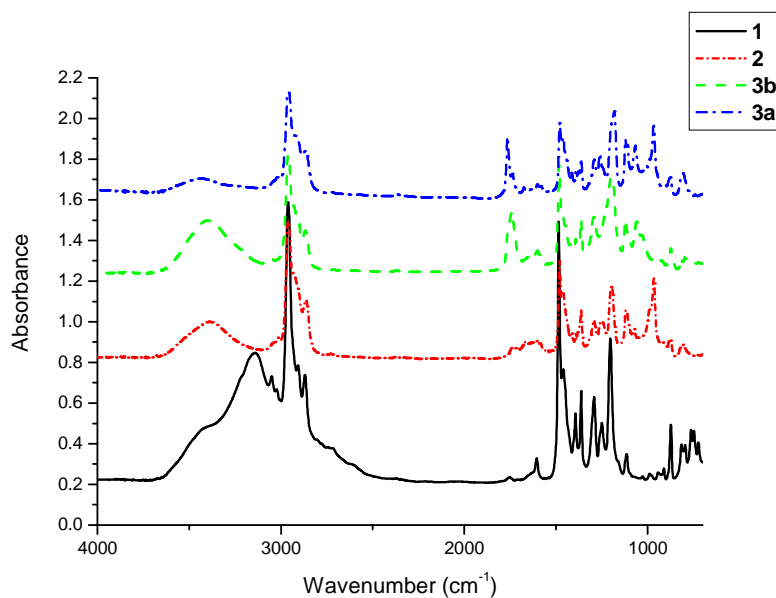


Figure 1. FTIR spectral characterization of compounds **1, 2, 3a** and **3b**.

The UV-Vis spectra show the shift of the two specific absorption bands of the parent calix[n]arene towards shorter wavelengths. For **2**, **3b** and **4b** the specific absorption bands appear at 272, 280 nm; 272, 279 nm and 271, 280 nm respectively in comparison with 284 and ~291 nm in the parent calixarene (Fig. 2).

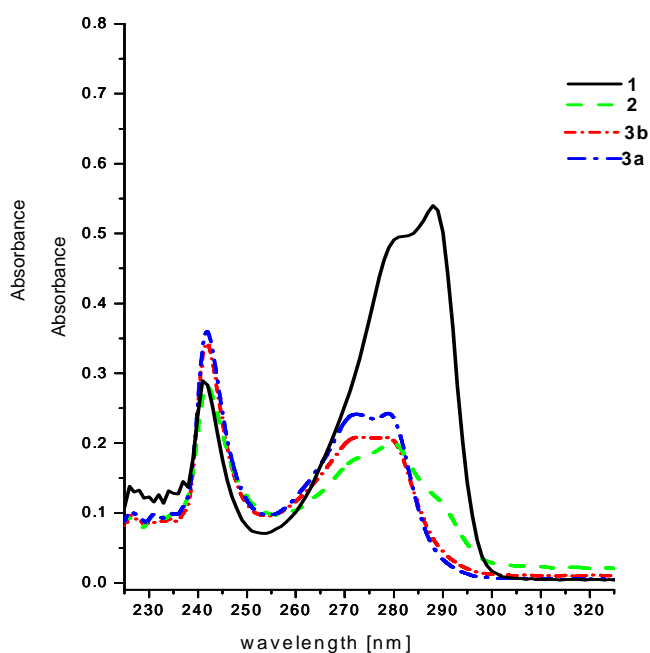


Figure 2. UV-vis absorption spectra of compounds **1,2,3a** and **3b**.

Extraction experiments were performed using 1×10^{-3} mol/l solution of calixarene in chloroform. The calixarene: metal ratio was varied between 2:1 to 1:2 and the pH of the medium was kept constant at 2.8. Extraction yield was determined by comparing the metal content from the aqueous phase before and after extraction. The concentration of the metal was determined with an ICP-OES Spectrometer (Spectroflame).

The ability of calixarene **3a**, **3b**, **4a** and **4b** to extract rare earth ions from the aqueous medium was estimated from the extraction yield values (Table 1).

The extraction yield is influenced by the ratio between calixarene and metallic ions (Cx:Eu). Best results were obtained with **3b** derivative, for Eu^{3+} ions.

Table 1.Extraction yield of Eu³⁺ using calixarene **1**, **2**, **3a-b**, **4a-b**.

Calixarene derivatives	Extraction yield (%)		
	Ratio Cx :Eu 1:1	Ratio Cx :Eu 2:1	Ratio Cx :Eu 1:2
1	23.85	26.14	13.16
2	18.70	42.62	23.79
3a	38.67	13.45	25.01
3b	57.06	58.33	44.59
4a	29.89	16.76	20.28
4b	34.22	55.21	61.13

EXPERIMENTAL PART

The parent *tert*-butyl-calix[6]arene (compound **1**) was prepared and purified by using the Gutsche technique [20].

Calixarene derivatives have been obtained from *tert*-butyl-calix[6]arene and 2-butenyl (crotyl) bromide, α -Chloro-N,N-diethyl acetamide or ethylbromoacetate, in acetonitrile or dimethylformamide-tetrahydrofuran mixture as solvent and K₂CO₃ or NaH as base.

All reactions were performed under nitrogen atmosphere using oven-dried glassware. Reagents were obtained from commercial suppliers and were used without further purification. All solvents were dried over standard drying agents and distilled prior to use. The complete conversion of the parent calix[n]arenes was checked up by thin layer chromatography on Kieselgell 60F₂₅₄ plates with detection by UV or iodine. Melting points (m. p.) were determined with KSP II apparatus in a sealed capillary and are uncorrected values.

¹H-NMR and ¹³C-NMR were recorded on Varian Gemini 320S (300 MHz) spectrometer. Deuterated chloroform was used as solvent and TMS as internal standard. Infrared absorption spectra were recorded on FTIR (JASCO) 610 and UV-VIS spectra on UNICAM UV4 spectrometers.

The main characteristics of the compound **2** were already reported [16] while the compounds **3a**, **3b**, **4a**, **4b** are described below:

*5,11,17,23,29,35-hexa-*t*Butyl-37,38,39-tris[(N,N-diethylaminocarbonyl) methoxy] - 40,41,42-trihydroxy-calix[6] arene (3a).*

M.p. = 272-3°C.

M.W. calculated for C₈₄H₁₁₇N₃O₉ = 1312.82

E.A.(%): Calcd:C = 76.85; H = 8.98; N = 3.20 / Found: C =75.57;H = 8.44; N = 3.03

UV-Vis: [CHCl₃ ; λ_{max} (nm): 281 ; 288.

FTIR : (ν_{max} , KBr , cm⁻¹): $\nu_{C=O}$ =1644 ; ν_{OH} =3248 .

¹H-NMR(δ_{ppm} , CDCl₃): 0.92-0.97 (t, 18H, N-CH₂-CH₃); 1.09 (s, 27H, C(CH₃)₃); 1.26 (s, 27H, C(CH₃)₃); 3.11 – 3.18 (q, 12H, N-CH₂-CH₃); 3.62 (s, 12H, Ar-CH₂-Ar); 4.33 (s, 6H, O-CH₂-CO); 6.72 (s, 6H, ArH); 7.03 (s, 6H, ArH); 7.09 (s, 3H, OH).
¹³C-NMR(δ_{ppm} , CDCl₃): 169.1, 151.8, 144.9, 1414.3, 125.9, 124.2, 69.7, 40.3, 39.8, 32.9, 31.9, 31.4, 30.5, 12.0.

5, 11, 17, 23, 29, 35-hexa-tButyl-37, 38, 39-tris[(ethoxycarbonyl)methoxy]-40, 41, 42-trihydroxy-calix[6] arene (3b).

M.p. = 248-250°C.

M.W. calculated for C₇₈H₁₀₂O₁₂ = 1231,62

E.A.(%): Calcd: C = 76.06; H = 8.35; O = 15.59 / Found: C = 75.90; H = 8.21; O = 15.89

UV-Vis [CHCl₃; λ_{max} (nm): 272 ; 279.

FTIR (ν_{max} , KBr, cm⁻¹): $\nu_{\text{C=O}}$ = 1741 ; ν_{OH} = 3399.

¹H-NMR; (δ_{ppm} , CDCl₃): 0.92 (t, 9H, CH₂-CH₃); 1.10 (s, 27H, C(CH₃)₃); 1.17 (s, 27H, C(CH₃)₃); 3.84 (brs, 12H, Ar-CH₂-Ar); 4.12 (q, 6H, CH₂-CH₃); 4.47 (s, 6H, O-CH₂-CO); 6.91 (s, 6H, ArH); 6.95 (s, 6H, ArH); 7.14 (s, 3H, OH).

¹³C-NMR; (δ_{ppm} , CDCl₃): 169.6; 151.8; 149.3; 147.7; 142.5; 132.9; 125.84; 70.9; 61.4; 34.25; 33.95; 32.55; 29.71; 14.0.

5, 11, 17, 23, 29, 35-hexa-tButyl-37, 38, 39-tris[(N,N-diethylaminocarbonyl) methoxy]- 40, 41, 42-tris-(But-2-enyloxy)-calix[6] arene (4a).

M.W. calculated for: C₉₆H₁₃₅O₉N₃

M.p.: 218-220°C

E.A (%): Calcd. C = 78.18; H = 9.22; N = 2.85 / Found C = 79.39; H = 8.94; N = 2.56

UV-Vis [CHCl₃ ; λ_{max} (nm)/ ϵ (M⁻¹cm⁻¹)] : 272/ ϵ ; 279/ ϵ

FTIR; (ν_{max} , KBr, cm⁻¹): $\nu_{\text{C=O}}$ = 1649; $\nu_{\text{CH=CH}}$ = 966, 3016

¹H-NMR (δ_{ppm} , CDCl₃) : 1.02 [t, 18H, -CH₂-CH₃]; 1.14 [s, 27H, C(CH₃)₃]; 1.18 [s, 27H, C(CH₃)₃]; 1.56 [d, 9H, =CH-CH₃]; 3.32-3.39 [brs, 12H, N-CH₂-CH₃]; 3.87 [brs, 12H, Ar-CH₂-Ar]; 3.99 [d, 6H, O-CH₂-CH=]; 4.42 [s, 6H, O-CH₂-CO-]; 5.45-5.67 [m, 6H, -CH=CH-]; 6.88 [s, 6H, ArH]; 7.08 [s, 6H, ArH]

¹³C-NMR (δ_{ppm} , CDCl₃): 168.2; 152.2; 151.8; 144.9; 141.4; 132.6; 131.7; 126.6; 125.9; 75.7; 69.6; 40.3; 39.7; 31.5; 30.8; 17.7; 12.1.

5, 11, 17, 23, 29, 35 – hexa- tButyl-37, 38, 39-tris[(carbonylethoxy) methoxy] - 40, 41, 42-tris-(But-2-enyloxy)-calix[6] arene (4b).

M.W. calculated for: C₉₀H₁₂₀O₁₂

M.p.: 206-208°C

E.A. (%): Calcd: C = 77,55; H = 8,68; N=13,77/Found :C = 78,18; H = 8,87; N=12,96.

UV-Vis[CHCl₃ ; λ_{max} (nm)/ ϵ (M⁻¹cm⁻¹)] : 271/ ϵ ; 280/ ϵ .

FTIR; (ν_{max} , KBr, cm⁻¹): $\nu_{\text{C=O}}$ = 1763, 1737; $\nu_{\text{CH=CH}}$ = 966.

¹H-NMR: (δ_{ppm} , CDCl₃) : 0.90 [t, 9H, -CH₂-CH₃]; 1.01 [s, 27H, C(CH₃)₃]; 1.19 [s, 27H, C(CH₃)₃]; 1.65 [d, 9H, =CH-CH₃]; 3.51 [brs, 12H, Ar-CH₂-Ar]; 4.13 [q, 6H, O-CH₂-CH₃]; 4.57 [d, 6H, O-CH₂-CH=]; 4.72 [s, 6H, O-CH₂-CO-]; 5.57-5.86 [m, 6H, -CH=CH-]; 7.04 [s, 6H, ArH]; 7.15 [s, 6H, ArH].

¹³C-NMR : (δ_{ppm} , CDCl₃): 169.5; 153.1; 150.8; 149.3; 147.7; 132.8; 126.0; 125.1; 75.7; 70.9; 61.4; 34.2; 33.8; 32.5; 31.2; 29.7; 17.7; 14.1.

CONCLUSIONS

The spectroscopical investigations confirm the formation of calix[6]arene derivatives with three ethylester (**3b**), three N,N-diethylacetamido (**3a**), three crotyl and three N,N-diethylacetamido (**4a**), three crotyl and three ethylester (**4b**) groups. These calixarenes show ability for the extraction of europium ions from slightly acid aqueous phase.

ACKNOWLEDGEMENTS

The financial support of the Romanian Ministry of Education and Research [contract 71-062/2007] is gratefully appreciated.

REFERENCES

1. S. K. Menon, M. Sewani, *Review of Anal.Chem.*, **2006**, 25, 49.
2. J. H. Feng, Y. Yang, X. Xu, G. Baown, *Org.and Biomol.Chem.*, **2006**, 4, 770.
3. P. Jose, S. Menon, *Bioinorganic Chemistry and Applications*, **2007**, 1.
4. M. R. Ganjali, P. Norouzi, *Sensors*, **2006**, 6, 1018.
5. I. Dumazet-Bonnamour, H. Halouani, *C.R.Chimie*, **2005**, 8, 881.
6. A. I. Konovalov, I. S. Antipin, A. R. Mustafina, *Russian Journal of Coordination Chemistry*, **2004**, 30(4), 227.
7. R. Ludwig, N. T. K. Dzung, *Sensors*, **2002**, 2, 397.
8. S. Memon, E. Akceyla, B. Sap, *Journal of Polymers and Environment*, **2003**, 11(2), 67.
9. T. Ursales, N. Popovici, C. Ciocan, I. Silaghi-Dumitrescu, R. Grecu, E. J. Popovici, *Environment and Progress*, **2003**, 533.
10. D. E. Carden, D. Diamond, *Journal of Experimental Botany*, **2001**, 52, 1353.
11. M. Bochenska, M. Hoffmann, U. Lesinska, *Journal of Inclusion Phenomena an Macrocyclic Chemistry*, **2004**, 49, 57.
12. M. I. Ogden, B. W. Skelton, A. H. White, *C.R.Chimie*, **2005**, 8, 181.

ALINA SAPONAR, IOAN SILAGHI-DUMITRESCU, ELISABETH-JEANNE POPOVICI, NICOLAE POPOVICI

13. P. D. Beer, G. D. Brindley, O. D. Fox, *J.Chem.Soc., Dalton Trans.*, **2002**, 3101.
14. J. Y. Kim, Y. H. Kim, J. I. Choe, *Bull.Korean Chem.Soc.*, **2001**, 22(6) 635.
15. C. Ciocan, E.-J. Popovici, C. Dan, M. Vadan, R. Grecu, N. Popovici, *Studia Universitatis Babes-Bolyai, Physica*, **2001**, 451.
16. T. Ursales, I. Silaghi-Dumitrescu, C. Ciocan, N. Palibroda, N. Popovici, E.-J. Popovici, *Rev.Roum.Chim.*, **2004**, 49, 741.
17. T. Ursales, I. Silaghi-Dumitrescu, E. J. Popovici, A. Ursales, N. Popovici, *J. Optoelectron. Adv. Mater.*, **2004**, 6(1), 307.
18. T. Ursales, I. Silaghi-Dumitrescu, E. J. Popovici, A. Ursales, N. Popovici, *Studia Universitatis Babes-Bolyai Physica*, **2003**, 2, 370.
19. A. Saponar, I. Silaghi Dumintrescu, E. J. Popovici, N. Popovici, *Rev.Chim.*, **2007**, 49, 741.
20. C. D. Gutsche, B. Dhawan, M. Leonis, *Org.Synthesis*, **1989**, 68, 238.

In memoriam prof. dr. Ioan A. Silberg

SYNTHESIS AND SPECTROSCOPIC INVESTIGATION OF METAL COMPLEXES WITH AN AZO-DYE AS LIGAND

CARMEN BĂTIU^a, IOAN PANEA^a, MIRELA PELEA^a,
ANCA MARCU^b, LEONTIN DAVID^b

ABSTRACT. The Cu(II), Co(II) and Ni(II) metal complexes derived from 1-(4-hydroxy-6'-methyl-pyrimidin-2'-yl)-3-methyl-4-(4''-nitrophenylazo)-pyrazolin-5-one were synthesized and characterized by elemental analysis, thermogravimetry, as well as by FT-IR, UV-VIS and ESR spectrometry. The results indicate that the organic compound act as a bidentate ligand *via* the nitrogen of azo group and the oxygen bound to the pyrazole ring. All complexes correspond to the molar ratio M : L : H₂O = 1 : 2 : 8. The local symmetry around the metal ions is pseudotetrahedral.

Keywords: azo dyes, metal complexes, thermal behaviour, spectroscopic studies, 5-pyrazolone derivatives

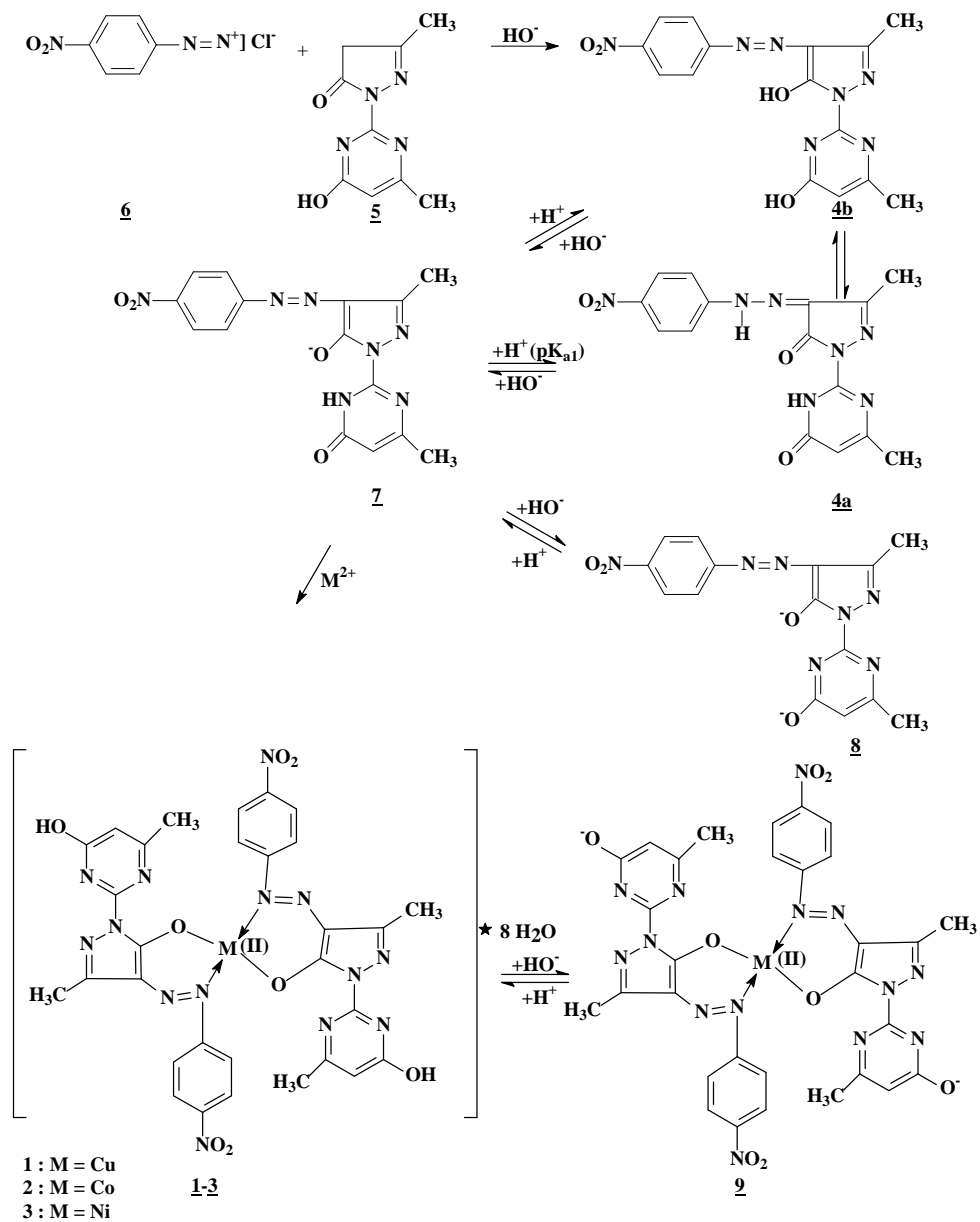
INTRODUCTION

Pyrazolin-5-one azo derivatives and their complexes with several metal ions (Cu²⁺, Co²⁺, Ni²⁺, Cr³⁺, Fe²⁺ etc.) are important pigments for vinyl polymers and synthetic leather or dyes for textile [1 - 4]. The metal complexes of 5-pyrazolone derivatives applied also as analytical reagents for microdetermination of metals [5, 6]. Over the past years the complexes of azo dyes have drawn the attention of many researchers [7 - 10]. Recently, a series of 1-pyrimidinyl analogs of the azocoupling products of 1-phenyl-3-methyl-pyrazolin-5-one has been prepared [11 - 13]. We intend to study the complexation of these new ligands with transition metal ions.

The present paper describes the synthesis and the structural investigation of three new metal complexes (**1** - **3**) obtained by the reaction of 1-(4-hydroxy-6'-methyl-pyrimidin-2'-yl)-3-methyl-4-(4''-nitrophenylazo)-pyrazolin-5-one (**4**) (**H-PNPhP**) with Cu (II), Co (II) and Ni (II) ions (Scheme 1).

^a Department of Organic Chemistry, "Babeș-Bolyai" University, Faculty of Chemistry and Chemical Engineering, Arany Janos 11, 400028 Cluj-Napoca, Romania

^b Department of Biomedical Physics, "Babeș-Bolyai" University, Physics Faculty, Mihail Kogălniceanu 1, 400084 Cluj-Napoca, Romania



Scheme 1

RESULTS AND DISCUSSION

The structure of the ligand (4)

The azocoupling product (**4**) has several azo- and hydrazone-tautomeric forms (e.g. **4a**, **4b**) [11, 13 - 15]. According to our previous spectral studies [13, 15] the ligand (**4**) appears as a hydrazone tautomer (**4a**) in common solvents (e.g. acetic acid, methanol, benzene, chloroform, aqueous or acidulate ethanol) which is also in good agreement with other literature data on the azocoupling products of pyrazolin-5-one derivatives [9, 10, 12, 16 - 19]. In certain solvents, such as alkalized ethanol or DMF the ligand (**4**), is probably deprotonated similar to other pyrazolin-5-one azocoupling products [9, 13, 15, 18 - 20]. The deprotonation of ligand was confirmed by the pH dependence of the UV-VIS absorption spectra of isomolar solutions of (**4**) recorded in aqueous ethanol (1v/1v).

The absorption curves set, corresponding each to a certain pH-range: a) 2.87 - 8.19 (Fig. 1a) and b) 9.50 - 12.80 (Fig. 1b) show the same isosbestic points that indicate an equilibrium [1, 16, 18 - 22]. The absorbance vs. pH at the analytical wavelength for (**4**) (Fig. 2) generates two sigmoidal curves that are characteristic to the acid-base equilibrium [1, 21]. The two sigmoidal curves indicate two acid dissociation steps [20], corresponding to a dibasic acid AH₂, which is compatible with the structure (**4**), which has two mobile acidic hydrogens (Scheme 1).

By derivation of the sigmoidal curves two pKa values are obtained, *i.e.* pKa₁ = 5.84 and pKa₂ = 10.56. The species (**4a**), (**7**), (**8**) involved in the equilibrium are characterized by different absorption bands registered at 412, 442 and 490 nm.

The identification of the forms that are present in the basic medium is important because even these forms (**7** or **8**) will react with the metal ions.

As it is known other pyrazolin-5-one azocoupling products participate by complexation act as a bidentate ligand *via* the nitrogen of the azo group and the oxygen bound to the pyrazole ring [1, 6, 8 - 10]. In the case of the ligand (**4**), this oxygen atom should be corresponding to the form (**7**) or (**8**).

The structure of the metal complexes

The complexation reaction of Cu(II), Co(II) and Ni(II) salts with the ligand solution in each case yields a solid product. Higher melting points of these products as well as their different colours when compared to that of the ligand (**4**), indicate the formation of metal complexes. All complexes are coloured, microcrystalline and stable at room temperature. The complexes are insoluble in water and most usual organic solvents (chloroform, acetone, benzene, alcohol) but soluble in DMF.

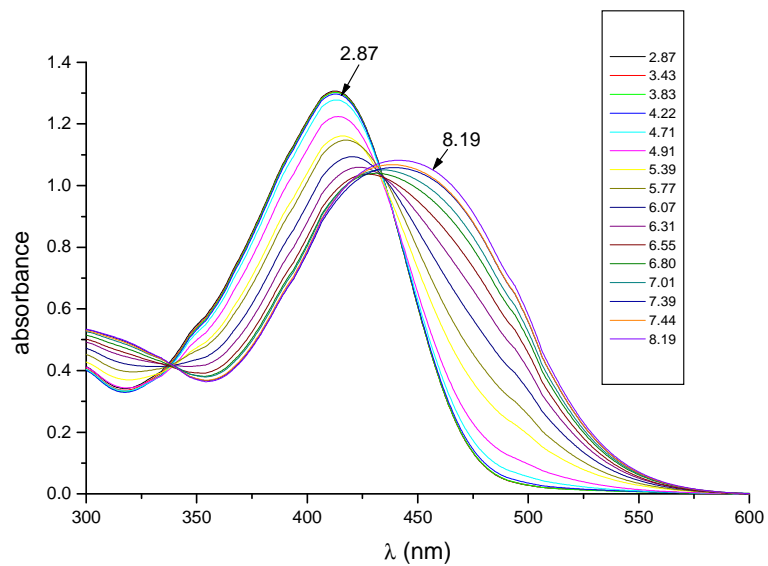


Figure 1a

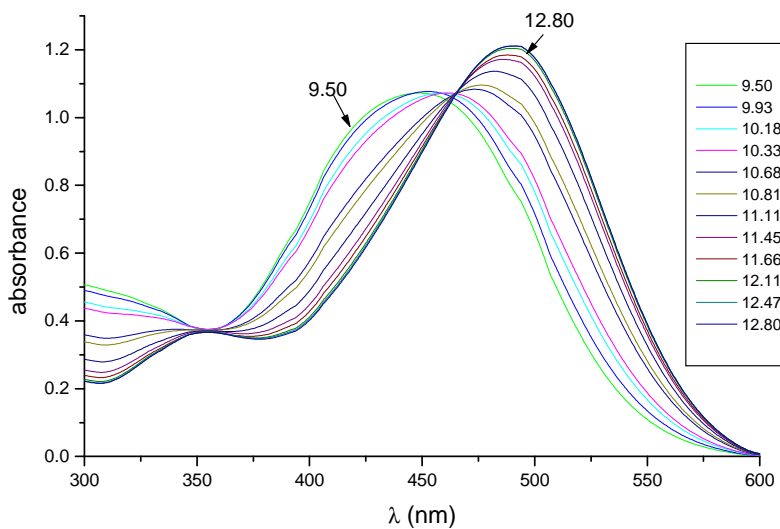


Figure 1b

Figure 1. The pH' dependence of the UV-VIS spectra of the isomolar solutions of (**4**) ($c = 2.25 \times 10^{-5}$ mol/L) in ethanol-water (1v/1v) at ionic strength of 0.01 mol/L KCl at 25°C, in the pH' range 2.87-8.19 (1a), respectively 9.50-12.80 (1b).

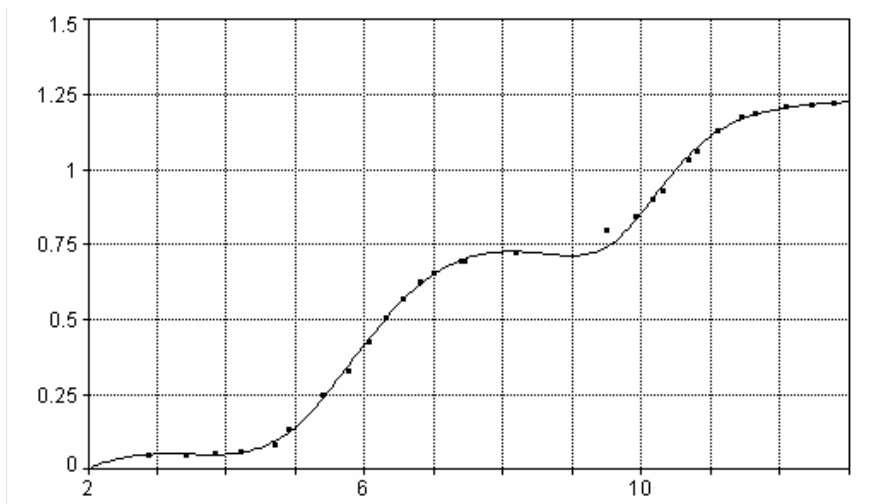


Figure 2. The plot absorbance at 490 nm vs. pH' corresponding to the spectra from Figure1

Some physico-chemical and elemental analysis data of the ligand (**4**) and its metal complexes (**1** - **3**) are given in Table 1 - 3.

The elemental analysis data (Table 1) and thermal analysis data (Table 3) indicate the molar ratio $M : L : H_2O = 1 : 2 : 8$, for each complex.

The UV-VIS spectra in DMF for the complexes (**1** - **3**) (Table 1) indicate a small hypsochromic shift and a low hypochromic effect comparative to the spectrum of the initial ligand (**4**), like the other similar complexes [9]. Since in DMF the UV-VIS spectrum of the ligand (**4**) (Table 1) corresponds to the dianion (**8**) (Fig. 1b) and the spectra of the complexes are only slightly shifted hipsochromically, the structure of the complexes in DMF solution should be (**9**), a situation that is to be expected for the initial structure (**1** - **3**) of the complexes in the presence of the basic impurities from DMF [17].

The structures (**1** - **3**) of the complexes are supported also by the fact that their UV-VIS spectra in ethanol correspond to the UV-VIS spectrum of more (**7**) or less (**4a**) deprotonated ligand (Fig.1a). Such a participation of the monodeprotonated species of pyrazolin-5-one azocoupling products to the complexation of metal ions occurs usually [9].

The IR spectra of the metal complexes (**1** - **3**) (Table 2) comparative to the free ligand supported these structures.

Table 1

Physico-chemical and elemental analysis data of the ligand (**4**)
and metal complexes (**1** - **3**)

Compound	C ₁₅ H ₁₃ N ₇ O ₄ (4)	C ₃₀ H ₄₀ CuN ₁₄ O ₁₆ (1)	C ₃₀ H ₄₀ CoN ₁₄ O ₁₆ (2)	C ₃₀ H ₄₀ NiN ₁₄ O ₁₆ (3)	
Molec. Weight	355.31	916.28	911.64	911.39	
Yield [%]	73.21	64.85	63.67	51.98	
Colour	orange	brown-yellow	brown-red	purple	
Melting point [°C]	310	340	350	380	
Visible absorption spectrum data, in DMF	λ_{\max} (nm)	486	473.5	481.5	
	ϵ	30,800	25,700	13,500	
	A	0.8059	0.6655	0.5632	
Elemental analysis data [%] found. (calcd.)	C	51.12 (50.71)	38.57 (39.32)	39.42 (39.52)	39.14 (39.53)
	H	4.38 (3.69)	4.02 (4.39)	4.15 (4.42)	4.11 (4.42)
	N	27.47 (27.59)	21.04 (21.40)	21.37 (21.51)	21.01 (21.51)

Table 2

IR absorption bands (cm⁻¹) of the ligand (**4**) and its metal complexes (**1** - **3**)

Assignment [cm ⁻¹]	C ₁₅ H ₁₃ N ₇ O ₄ (4)	C ₃₀ H ₄₀ CuN ₁₄ O ₁₆ (1)	C ₃₀ H ₄₀ CoN ₁₄ O ₁₆ (2)	C ₃₀ H ₄₀ NiN ₁₄ O ₁₆ (3)
ν_{OH} , $\nu_{\text{O-H-O}}$	-	2912-3642	3283-3646	3282-3656
ν_{NH}	3309-3633	wide band	wide band	wide band
$\nu_{\text{C=O}^*}$	1696	-	-	-
$\nu_{\text{C=O}^{**}}$	1673	1635	1623	1627
$\nu_{\text{C-NO}_2 \text{ as.}}$	1556	1519	1517	1518
$\nu_{\text{C-NO}_2 \text{ sim}}$	1344	1334	1330	1331
$\nu_{\text{M-N}}$	-	619	598	578
$\nu_{\text{M-O}}$	-	472	473	476

* γ -lactam from the pyrazolin-5-one entity

** γ -lactam from the pyrimidin-2-one entity

The absorption band of the free ligand (**4**) at 1696 cm⁻¹, that may be assigned to the stretching $\nu_{\text{C=O}}$ vibration of γ -lactam type [23] from the pyrazolin-5-one entity, is not registered in the IR spectra of the metal complexes (Table 2). This is caused by the fact that in these complexes the ligand participates as anion (**7**) analogous to other similar ligands [9]. The

anions of the azocoupling products able of azo-hydrazone tautomerism have an azostructure (e.g. **7**) in which the pyrazolin-5-one $>C=O$ group is transformed in $>C-O^-$ group. But in complexes (**1** - **3**) as well as in the ligand (**4**), an other band is present in the range $1620 - 1675\text{ cm}^{-1}$ which may be assigned to a stretching $\nu_{C=O}$ vibration of lactam type, namely a hexaatomic pyrimidin-one lactam [23]. The pyrimidin-2-one lactam form in the compounds (**4**) and (**1** - **3**) is possible on the basis of lactam- lactimic tautomerism of their 4-hydroxy-6- methyl-pyrimid-2-yl entity.

Another proof for the formation of the complexes are the new bands appearing in the range $472 - 476\text{ cm}^{-1}$, which correspond to stretching ν_{M-O} , vibration and in the range $578 - 619\text{ cm}^{-1}$, which could be assigned to stretching ν_{M-N} vibration [6, 9].

Thermal investigation

The thermal behaviours of the ligand (**4**) and its metal complexes (**1** - **3**) are summarized in Table 3.

The thermogravimetric analysis indicated that the ligand (**H-PNPhP**) is anhydrous and the decomposition involved two steps.

In the temperature range $300 - 320^\circ\text{C}$ an endothermic peak at 310°C indicated the melting point of the ligand in good agreement to the literature data [11].

The first decomposition step occurred in the temperature range $320 - 360^\circ\text{C}$ and it has been accompanied by a strong exothermic effect (see the maximum peak at 340°C) with the loss of $\text{C}_6\text{H}_4\text{NO}_2$ rest.

The second step occurred in the temperature range $480 - 600^\circ\text{C}$, with an exo peak at 543°C which indicates the pyrolysis of organic rest.

The recorded mass loss of 65.63% is in good agreement to the calculated data (65.15%).

The aim of the thermal analysis of the metal complexes is to obtain information concerning their thermal stability of these and to decide whether the water molecules are inside or outside the coordination sphere.

The decompositions of each metal complex occur in three steps. The first step is characterized by an endothermic peak at 115°C for the Cu(II) complex, at 130°C for the Co(II) complex and at 125°C for the Ni(II) complex and corresponds to the loss of water molecules (see also the ESR results).

A comparison between the thermal behaviour of the ligand (**H-PNPhP**) and its metal complexes reveals that the melting points are growing up with the complexation. An endo peak in the DTA curves at 340°C for the Cu(II) complex, at 350°C for the Co(II) complex and at 380°C for the Ni(II) complex corresponds to the melting points. This phenomenon proves that the thermal stability is increased by the formation of coordination compounds with M-N and M-O bonds. The second step is accompanied by a strong exothermal effect and corresponds to the loss of 2 mole of $\text{C}_6\text{H}_4\text{NO}_2$ rest of each metal complex.

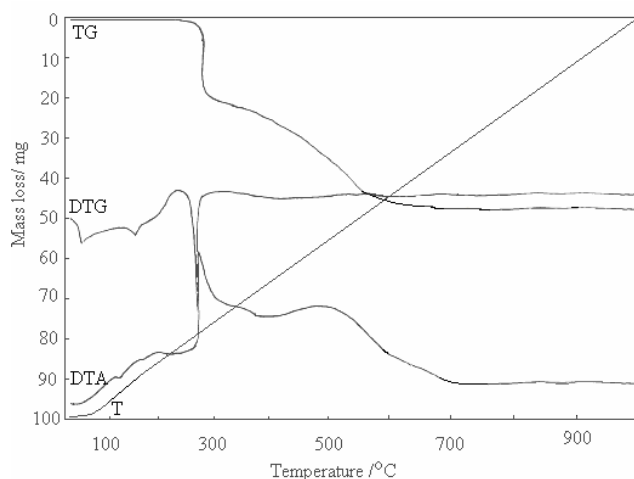
Table 3

Thermogravimetric analysis results of the ligand H-PNPhP (**4**) and its metal complexes (**1** - **3**)

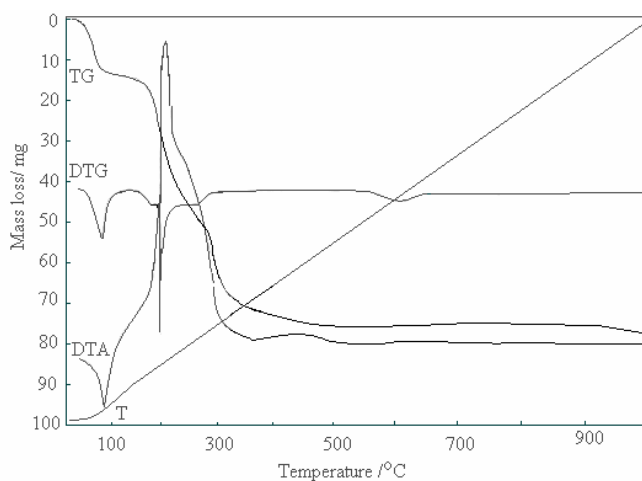
Compound	Temp. range [°C]	DTA peak [°C]		TG weight loss [%]		Assignment
		Endo	Exo	Calcd.	Exp.	
H-PNPhP (4)	300-320	310	-	-	-	melting point - loss of C ₆ H ₄ NO ₂ rest - pyrolysis of organic rest
	320-360	-	340	34.36	35.84	
	480-600	-	543	65.64	64.15	
[Cu(C ₁₅ H ₁₂ N ₇ O ₄) ₂] • 8H ₂ O (1)	80-160	110	-	15.72	15.23	- 8 mole of hydrating water melting point - loss of 2 C ₆ H ₄ NO ₂ rest - pyrolysis of organic rest CuO residue
	320-380	340	-	-	-	
		-	375	31.62	32.38	
	400-460	-	440	34.04	43.28	
		-	-	18.88	18.09	
[Co(C ₁₅ H ₁₂ N ₇ O ₄) ₂] • 8H ₂ O (2)	100-200	130	-	15.80	15.89	- 8 mole of hydrating water melting point - loss of 2 C ₆ H ₄ NO ₂ rest - pyrolysis of organic rest CoO residue
	340-420	350	-	-	-	
		-	380	31.81	31.68	
	420-560	-	425	42.17	41.45	
		-	-	10.22	10.98	
[Ni(C ₁₅ H ₁₂ N ₇ O ₄) ₂] • 8H ₂ O (3)	80-180	125	-	15.80	15.72	- 8 mole of hydrating water melting point - loss of 2 C ₆ H ₄ NO ₂ rest - pyrolysis of organic rest NiO residue
	360-440	380	-	-	-	
			405	31.82	32.35	
	440-580	-	450	39.80	40.18	
		-	-	12.58	11.75	

Above 420°C a broad exothermic peak indicate the last step which correspond to the pyrolysis of the organic rest. The final products of the pyrolysis are metal oxide with the stoichiometric ratio M : O = 1:1. Figure 3 displays the derivatograms of the ligand (H-PNPhP) and its Cu(II) complex (**1**).

SYNTHESIS AND SPECTROSCOPIC INVESTIGATION OF METAL COMPLEXES WITH AN AZO-DYE



a-H-PNPhP(4).



b-[Cu(C₁₅H₁₂N₇O₄)₂]•8H₂O(1)

Figure 3. The simultaneous TG, DTG and DTA curves obtained by derivatograph for a- H-PNPhP (4) (sample mass = 50mg) and b-[Cu(C₁₅H₁₂N₇O₄)₂]•8H₂O(1) (sample mass=100mg)

ESR spectra and magnetic properties

The powder ESR spectrum of [Cu(C₁₅H₁₂N₇O₄)₂]•8H₂O(1), complex at room temperature (Fig. 4) is typical for monomeric species with pseudotetrahedral local symmetry around the metal ion. The principal values of the g tensor ($g_{||} = 2.178$, $g_{\perp} = 2.117$) correspond to a CuN₂O₂

chromophore [24]. The ordering of g values indicates the presence of an unpaired electron in the $d_{x^2-y^2}$ orbital. The calculated $g_{av} = 2.137$ value show a considerable covalent character of the complex [25]. The shape and the g values ($g_{||} = 2.213$, $g_{\perp} = 2.026$) for the Co(II) complex are typical for pseudotetrahedral species.

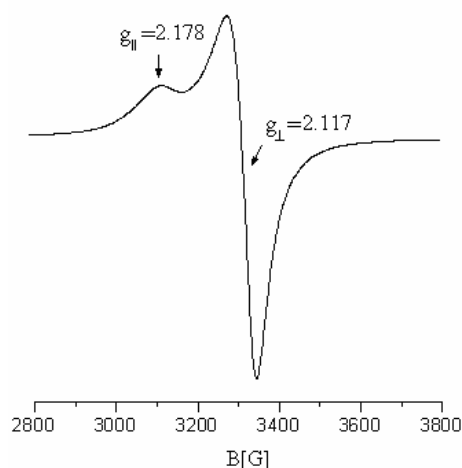


Figure 4. Powder ESR spectrum of $[\text{Cu}(\text{C}_{15}\text{H}_{12}\text{N}_7\text{O}_4)_2] \cdot 8\text{H}_2\text{O}(\mathbf{1})$ complex at room temperature

The magnetic susceptibility measurements indicate a Curie-Weiss behaviour (Fig. 5) with values of magnetic moments specific to monomeric species. The values of magnetic moments were calculated considering also the temperature independent contribution. The magnetic moments ($\mu_{\text{eff}} = 1.91 \mu_B$, $\mu_{\text{eff}} = 5.21 \mu_B$, $\mu_{\text{eff}} = 3.21 \mu_B$ for Cu(II), Co(II) and Ni(II) complexes) confirm the pseudotetrahedral local symmetries around the metallic ions [26].

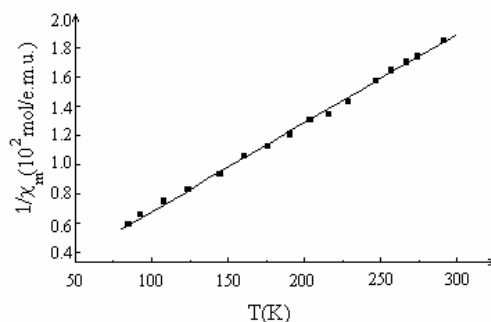


Figure 5. Temperature dependence of $1/\chi_m$ for $[\text{Cu}(\text{C}_{15}\text{H}_{12}\text{N}_7\text{O}_4)_2] \cdot 8\text{H}_2\text{O}(\mathbf{1})$

EXPERIMENTAL PART

Materials and instrumentation

All reagents and chemicals were purchased from commercial sources and used as received. Elemental analyses were carried out at the Vario El III CHNS-analyzer. The electronic absorption spectra were performed on Jasco V-530-UV-VIS spectrophotometer. The IR spectra were recorded in KBr pellets with a FT-IR-615-spectrophotometer. The thermoanalytical curves were recorded on an OD-103 MOM derivatograph. The samples were heated at a constant rate of $5^{\circ}\text{C min}^{-1}$ from 20-1000 $^{\circ}\text{C}$. Al_2O_3 was used as reference material in static air atmosphere. Powder ESR spectra at room temperature were recorded at 9.4 GHz (X band) using standard JEOL-RES-3S equipment. Magnetic susceptibility measurements were made on powdered samples with a Faraday balance.

Synthesis of the metal complexes

The azocoupling product (**4**) was prepared by using a standard procedure from 1-(4-hydroxy-6'-methyl-pyrimidin-2'-yl)-3-methyl-pyrazolin-5-one (**5**) and 4-nitrobenzenediazonium salt (**6**) [11 - 14]. The metal complexes (**1** - **3**) were synthesized by the following procedure: to a suspension of ligand (**4**) (1mmol) in 50 mL methanol was slowly added with stirring a solution of tetra-n-butylammonium hydroxide until the azocoupling product is completely dissolved. To this solution of ligand was added slowly, dropwise, a solution of the metal salt [$\text{CuSO}_4 \cdot 5\text{H}_2\text{O}$, $\text{Co}(\text{NO}_3)_2 \cdot 6\text{H}_2\text{O}$, $\text{Ni}(\text{NO}_3)_2 \cdot 6\text{H}_2\text{O}$] (0.5 mmol) in distilled water. The mixture was stirred for 2h. After standing at room temperature for 16h, the resulted precipitate was vacuum filtrated and washed on the filter with distilled water and methanol, dried in air 48h and kept in dark bottles.

CONCLUSIONS

The ligand (**4**) and its Cu(II), Co(II) and Ni(II) complexes (**1** - **3**) were characterized by elemental analysis, thermal behaviour and spectral studies. The results are in agreement with the corresponding formulae: $\text{C}_{15}\text{H}_{13}\text{N}_7\text{O}_4$ (**4**), $[\text{Cu}(\text{C}_{15}\text{H}_{12}\text{N}_7\text{O}_4)_2] \cdot 8\text{H}_2\text{O}$ (**1**), $[\text{Co}(\text{C}_{15}\text{H}_{12}\text{N}_7\text{O}_4)_2] \cdot 8\text{H}_2\text{O}$ (**2**), respectively $[\text{Ni}(\text{C}_{15}\text{H}_{12}\text{N}_7\text{O}_4)_2] \cdot 8\text{H}_2\text{O}$ (**3**).

The IR and UV-VIS spectra indicated that the organic compound act as a bidentate ligand *via* the nitrogen of the azo group and the oxygen bound to the pyrazole ring.

The greater value of the melting point for complexes, as compared to the free ligand indicates that thermal stability is increased by the formation of complexes with M-N and M-O bonds.

The ESR spectra and magnetic susceptibility measurements confirm the pseudotetrahedral local symmetries around the metal ions.

ACKNOWLEDGEMENT

Financial support from Romanian National University Research Council (CNCSIS), project type A No 1347/2007, gratefully acknowledged.

REFERENCES

1. H. Zollinger, "Colour Chemistry", 2nd Edn. VCH, Basel **1991**, p.110-137, 156-157, 289-290.
2. M. M. Moustafa, R. M. Issa, *Egypt. J. Chem.*, **1999**, *42*, 267.
3. R. R. Rudalal, J. J. Patel, A. G. Mehta, *Orient. J. Chem.*, **1999**, *15*, 559.
4. J. J. Patel, G. H. Bhat, K. R. Desai, *J. Inst. Chem. (India)*, **1999**, *71*, 185.
5. F. A. Adam, M. T. El-Haty, A. H. Amarallah N. A. Abdalla, *Bull. Soc. Chim. Fr.* **1998**, *4*, 605.
6. S. A. Abdel - Latif, H. B. Hassib, *J. Thermal Anal. Cal.*, **2002**, *68*, 983.
7. M. Badea, A. Emandi, D. Marinescu, E. Cristurean, R. Olar, A. Braileanu, P. Budrugeac, E. Segal, *J. Thermal. Anal. Cal.*, **2003**, *72*, 525.
8. M. Badea, R. Olar, E. Cristescu, D. Marinescu, A. Emandi, P. Burdugeac, E. Segal, *J. Thermal Anal. Cal.*, **2004**, *77*, 815.
9. C. Batiu, I. Panea, L. Ghizdavu, L. David, S. Ghizdavu-Pellascio, *J. Thermal. Anal. Cal.*, **2005**, *79*, 129.
10. M. Szymczyk, A. El-Shafei, H.S. Freeman, *Dyes Pigm.* **2007**, *72*, 8.
11. I. Panea, A. Ghirisan, I. Cristea, R. Gropeanu, Rom. Pat.114797 B1, **1999**.
12. I. Panea, A. Ghirisan, I. Cristea, R. Gropeanu, I. A. Silberg, *Het. Commun.* **2001**, *7*, 563.
13. I. Panea, A. Ghirisan, F. Iura, R. Gropeanu, I. A. Silberg, *Studia Univ. „Babes-Bolyai”, Chemia*, **2003**, *48*, 55.
14. I. Baldea, A. Ghirisan, I. Panea, *J. Chem. Soc., Perkin Trans.* **1992**, *2*, 1715.
15. I. Panea, A. Ghirisan, I. Baldea, I. Silaghi-Dumitrescu, L. Craciun, I. A. Silberg, *Studia Univ. „Babes-Bolyai”, Chemia*, **2003**, *48*, 67.
16. F. Karci, N. Ertan, *Dyes Pigm.* **2002**, *55*, 99.
17. I. Panea, M. Pelea, I. A. Silberg, *Dyes Pigm.*, **2006**, *68*, 165.
18. I. Panea, M. Pelea, I. A. Silberg, *Dyes Pigm.*, **2007**, *74*, 113.

SYNTHESIS AND SPECTROSCOPIC INVESTIGATION OF METAL COMPLEXES WITH AN AZO-DYE

19. M. Dakiky I. .Nemcova, *Dyes Pigm.*, **2000**, 44, 181.
20. A. M. Khedr, M. Gaber, R. M. Issa, H. Erten, *Dyes Pigm.*, **2005**, 67, 117.
21. N. M. Rageh, *J. Chem. Eng. Data*, **1998**, 43, 373.
22. N. Ertan, P. Gurkan, *Dyes Pigm.*, **1997**, 33,137.
23. L. J. Bellamy, "The Infrared Spectra of Complex Molecules" Methuen and Co., 2nd Edn, London, **1964**, p. 205-214.
24. F. Mabbs, D. Callison, "Electron Paramagnetic Resonance of d Transition Metal Compounds", Elsevier, Amsterdam, **1992**, p.102.
25. C. Batiu, C. Jelic, N. Leopold, O. Cozar, L. David, *J. Mol. Struct.* **2005**, 744-747, 325.
26. R. L. Carlin, „Magnetochemistry“, Springer Verlag Berlin, **1986**, 64.

In memoriam prof. dr. Ioan A. Silberg

TOWARDS NEW DOUBLE-BONDED ORGANOPHOSPHORUS DERIVATIVES OF C=P=C=P TYPE

GABRIELA NEMEȘ, RALUCA ȘEPTLEAN, PETRONELA M. PETRAR,
LUMINIȚA SILAGHI-DUMITRESCU, IOAN SILAGHI-DUMITRESCU^a

ABSTRACT. New potential precursors for diphosphaallenes with C=P=C=P skeleton have been synthesized. Compounds 2-4 (bearing a 2,4,6-tri-*tert*-butylphenyl group bound to phosphorus) are stabilized by the large steric hindrance which prevents the approach of monomers to form dimers or oligomers.

Keywords: *heteroallenes, diphosphaallenes, organophosphorus compounds*

INTRODUCTION

Sterical protected heterocumulenes [1-5] containing multiple double bonds of the heavier main group elements, such phospho-, or diphosphaallenes [6a, 7] are currently the focus of many research groups. Using bulky substituents like Mes* (2,4,6-tri-*tert*-butylphenyl), C(SiMe₃)₂ or *t*-Bu we have reported some precursors of diphosphaallenes with the C=P=C-P skeleton which are expected to be useful as starting materials for new organophosphorus compounds [6].

Due to the multiple possibilities to coordinate the C=P=C-P unit to an organometallic ML_n fragment, such systems are excellent ligands in coordination compounds with potential catalytic action. Thus, there were obtained complexes with P=C=P units attached to M(CO)_n fragments, M = W, Cr [8-12] or Pd, Cr [12, 13]. Some of these systems have interesting catalytic properties, exhibited for example in the direct conversion of the alcohols in allylic compounds [14, 15].

Herein we report the synthesis of diphosphaallenic systems (Me₃Si)₂C=P(Mes*)=C(Cl)-PCl₂ **2**, (Me₃Si)₂C=P(Mes*)=C(Cl)-PCl(*t*-Bu) **3**, and (Me₃Si)₂C=P(Mes*)=C(Cl)-P(O)Cl₂ **4**, with C=P=C-P skeleton. Due to the polytopal coordination abilities, such ligands might be used in the synthesis of various interesting coordination compounds.

^a *Universitatea Babeș-Bolyai, Facultatea de Chimie și Inginerie Chimică, Str. Kogălniceanu Nr. 1, RO-400084 Cluj-Napoca, Romania, isi@chem.ubbcluj.ro*

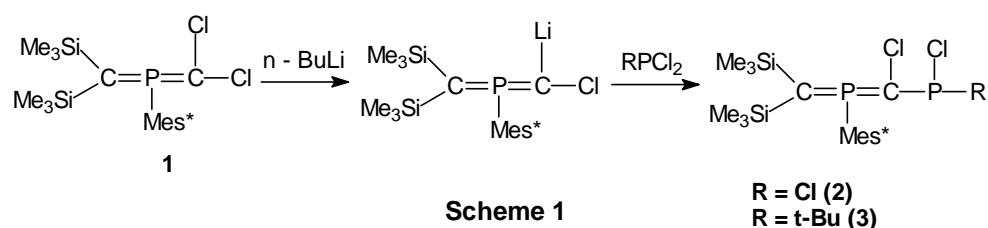
RESULTS AND DISCUSSION

Diphosphaallene derivatives **2-4** have been prepared starting from phosphoallene **1** (Scheme 1) in the presence of butyl lithium and the corresponding dihalophospha derivatives RCl_2 .

Bis(trimethylsilane)phosphorane **1** was obtained with a very good yield (98 %) by resorting to a modified version [16] of Niecke's method.

Diphosphaallenes **2** and **3** were prepared by reaction of **1** with RCl_2 ($\text{R} = \text{Cl}, t\text{-Bu}$). Note however that if $\text{R} = \text{Mes}^*$, due to the high steric demands, the formation of corresponding diphosphaallene has never been observed.

Addition of phosphorus trichloride to the lithium derivative of **1** afforded the expected diphosphaallene $(\text{Me}_3\text{Si})_2\text{C}=\text{P}(\text{Mes}^*)=\text{C}(\text{Cl})-\text{PCl}_2$ **2**, (Scheme 1):



The *Z* and *E* isomers, **2a** and **2b** are formed in a 5 : 1 ratio. Both isomers **2a** and **2b** have been characterized in solution by NMR spectroscopy. The ^{31}P NMR spectra of **2a** show two signals at 165.41 ppm (d) and at 151.75 ppm (d) respectively.

3 is obtained nearly quantitatively from **1**, by the route shown in Scheme 1. $(\text{Me}_3\text{Si})_2\text{C}=\text{P}(\text{Mes}^*)=\text{C}(\text{Cl})-\text{P}(t\text{-Bu})\text{Cl}$ **3** was characterized by NMR spectroscopy and mass spectrometry. The ^{31}P NMR spectrum show two signals for the phosphorus atoms at 166.08 ppm (d) and 112.7 ppm (d) (Figure 1). The high-field shift in the ^{31}P NMR is in the expected range for *t*-Bu group bonded to a $\lambda^3\sigma^2\text{-P}$ atom [6].

Due to the presence of only one chlorine atom in **3** versus two chlorine atoms at $\lambda^3\sigma^2\text{-P}$ phosphorus in **2**, the ^{31}P NMR shift in **3** is shifted by 40 ppm up-field.

In the presence of air, compound **2** is oxidized at the $\lambda^3\sigma^2\text{-P}$ phosphorus atom giving $(\text{Me}_3\text{Si})_2\text{C}=\text{P}(\text{Mes}^*)=\text{C}(\text{Cl})-\text{P}(\text{O})\text{Cl}_2$ **4** (^{31}P NMR: 195.17 ppm (d) and 69.48 ppm (d)) (Scheme 2).

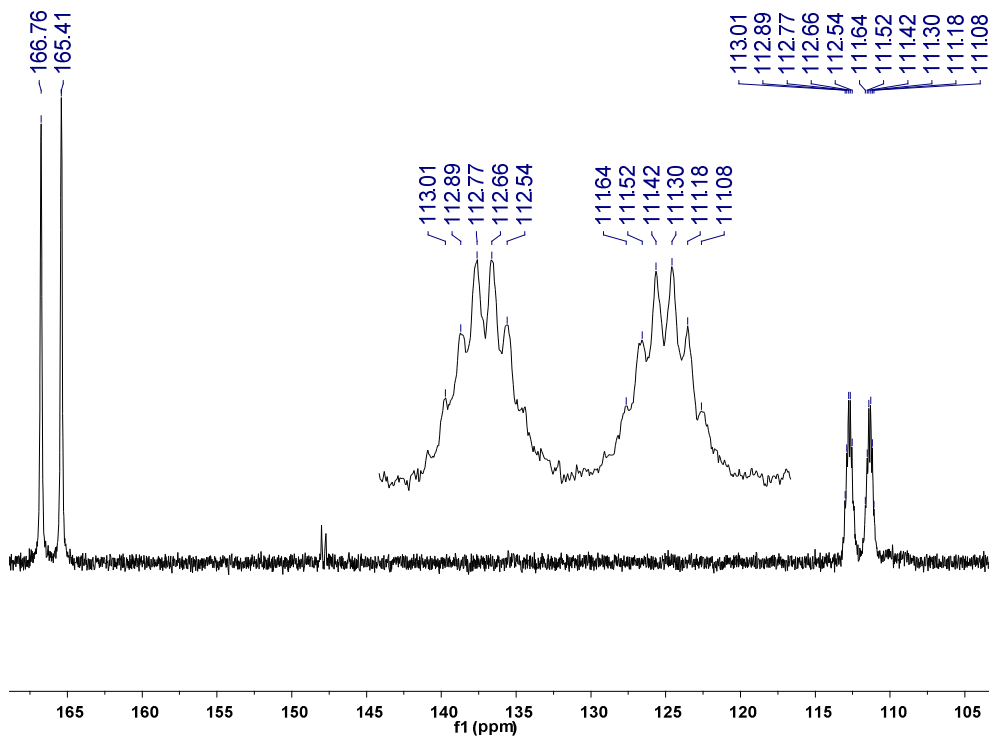
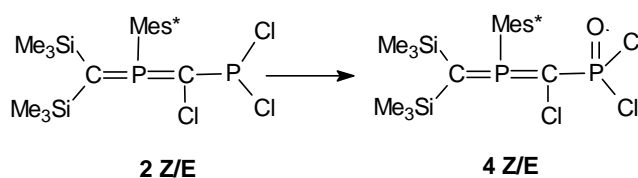


Figure 1. ^{31}P NMR (coupled with hydrogen) spectrum of $(\text{Me}_3\text{Si})_2\text{C}=\text{P}(\text{Mes}^*)=\text{C}(\text{Cl})-\text{P}(\text{t-Bu})\text{Cl}$ **3**



Scheme 2

The *Z* and *E* isomers, **4a** and **4b** are identified in the same ratio like the *Z/E* ratio for **2**.

CONCLUSION

Three new diphosphaallenes have been synthesized and characterized by NMR spectroscopy. Their coordinative properties are under current investigation.

EXPERIMENTAL SECTION

All experiments were carried out in flame-dried glassware under argon atmosphere using high-vacuum line techniques. Solvents were dried and freshly distilled from sodium benzophenone ketyl and carefully deoxygenated on the vacuum line by several freeze-pump-thaw cycles. NMR spectra were recorded in CDCl_3 and C_6D_6 by using a Bruker AC300 spectrometer (^1H : 300 MHz; ^{13}C : 75 MHz, reference TMS; ^{31}P : 121.49 MHz, reference H_3PO_4). Mass spectra were obtained with Hewlett-Packard 5989A spectrometer by EI at 70 eV. BuLi (1.6 M in hexane), PCl_3 and t-BuPCl₂ commercially available (Merck) were used.

Synthesis of $(\text{Me}_3\text{Si})_2\text{C}=\text{P}(\text{Mes}^*)=\text{CCl}_2$ **1** [14]

To a solution of CHCl_3 (1 mL, 1.3 g) in THF (50 mL) cooled at $-90\text{ }^\circ\text{C}$ were added 6.9 mL of a solution of n-BuLi (0.7 g). After 1 h of stirring to $-78\text{ }^\circ\text{C}$, the brown solution of CCl_3Li was frozen at $-120\text{ }^\circ\text{C}$. A solution of $\text{Mes}^*\text{P}=\text{C}(\text{SiMe}_3)_2$ (5.5 g) in THF (50 mL) cooled at $-78\text{ }^\circ\text{C}$ was cannulated to the frozen CCl_3Li . The reaction mixture was allowed to warm at room temperature. After removal of the lithium salts, recrystallization from pentane afforded a white powder of pure **1**, the yield 98 % [14].

Synthesis of $(\text{Me}_3\text{Si})_2\text{C}=\text{P}(\text{Mes}^*)=\text{C}(\text{Cl})-\text{PCl}_2$ **2**

To a solution of **1** (0.75 g) in THF (20 mL) cooled at $-100\text{ }^\circ\text{C}$ were added 1.9 mL of a solution of n-BuLi. After 1 h of stirring at $-78\text{ }^\circ\text{C}$ the brown liquid was cannulated to a solution of trichlorophosphine (0.2 g, 0.13 mL) in THF (40 mL) cooled at $-78\text{ }^\circ\text{C}$. After stirring the mixture at $20\text{ }^\circ\text{C}$ for 2h, LiCl was eliminated by filtration, the solvent was removed in vacuum and the residue dissolved in 15 mL of pentane. The product was unambiguously characterized by NMR spectroscopy but could not be isolated in pure form by crystallization. We obtained the mixture of **2a** and **2b** in 5 : 1 ratio.

NMR ^{31}P **2a**: 165.41 ppm (d, $^2J_{\text{PP}}$: 178.8 Hz, $\lambda^5\sigma^3\text{-P}$), 151.75 ppm (d, $^2J_{\text{PP}}$: 178.5 Hz, $\lambda^3\sigma^2\text{-P}$).

NMR ^{31}P **2b**: 163.88 ppm (d, $^2J_{\text{PP}}$: 179.9 Hz, $\lambda^5\sigma^3\text{-P}$), 150.26 ppm (d, $^2J_{\text{PP}}$: 179.9 Hz, $\lambda^3\sigma^2\text{-P}$).

Oxidation of **2** to $(\text{Me}_3\text{Si})_2\text{C}=\text{P}(\text{Mes}^*)=\text{C}(\text{Cl})-\text{P}(\text{O})\text{Cl}_2$ **4**

In normal condition after 7 hours, compound **1** is oxidized to $(\text{Me}_3\text{Si})_2\text{C}=\text{P}(\text{Mes}^*)=\text{C}(\text{Cl})-\text{P}(\text{O})\text{Cl}_2$ **4**. A mixture of **4a** and **4b** in the 5:1 ratio has been obtained. The reaction product was unambiguously characterized by NMR spectroscopy but could not be isolated in pure form by crystallization.

NMR ^{31}P **4a**: 195.17 ppm (d, $^2J_{\text{PP}}$: 342.6 Hz, $\lambda^5\sigma^3\text{-P}$), 69.48 ppm (d, $^2J_{\text{PP}}$: 342.6 Hz, $\lambda^5\sigma^3\text{-P=O}$).

NMR ^{31}P **4b**: 195.30 ppm (d, $^2J_{\text{PP}}$: 342.6 Hz, $\lambda^5\sigma^3\text{-P}$), 69.61 ppm (d, $^2J_{\text{PP}}$: 342.6 Hz, $\lambda^5\sigma^3\text{-P=O}$).

Synthesis of $(\text{Me}_3\text{Si})_2\text{C}=\text{P}(\text{Mes}^*)=\text{C}(\text{Cl})\text{-PCl}(\text{t-Bu})$ 3

To a solution of **1** (2.1 g, 4.06 mmol) in THF (50 mL) cooled at $-100\text{ }^\circ\text{C}$ were added 1.82 mL of a solution of *t*-BuLi 1.7 M. After 1h of stirring at $-78\text{ }^\circ\text{C}$ the brown solution of $(\text{Me}_3\text{Si})_2\text{C}=\text{P}(\text{Mes}^*)=\text{CClLi}$ was canulated to a solution of dichloro-*tert*-butylphosphine (0.66 g, 4.2 mmol) in THF (50 mL) cooled at $-78\text{ }^\circ\text{C}$. After stirring the mixture at $20\text{ }^\circ\text{C}$ for 10 h, LiCl was eliminated by filtration, the solvent was removed in vacuum and the residue dissolved in 25 mL of pentane. The product was unambiguously characterized by NMR spectroscopy but could not be isolated in pure form by crystallization.

NMR ^{31}P (CDCl_3) 2: 166.08 ppm (d, $^2J_{\text{PP}}$:164.25 Hz, $\lambda^5\sigma^3\text{-P}$), 112 ppm (dm, $^2J_{\text{PP}}$:164.25 Hz, $^3J_{\text{PH}}$: 13.4 Hz, $\lambda^3\sigma^2\text{-P}$).

NMR ^1H (CDCl_3) 2: 7.57 (dd, $J = 4.92, 1.63$ Hz, 1H), 7.51 (dd, $J = 4.70, 1.88$ Hz, 1H), 1.70 (d, $J = 0.55$ Hz, 1H 9H), 1.32 (s, 1H 9H), 1.67 (s, 1H 9H), 1.24 (d, $J = 14.70$ Hz, 1H 9H), 0.39 (s, 1H 9H), -0.16 (s, 1H 9H)

NMR ^{13}C (C_6D_6): 155.41 (d, $J = 7.81$ Hz, 1C, C orto), 154.69 (d, $J = 3.15$ Hz, 1C, C para), 125.47 (d, $J = 13.24$ Hz, 1C, C meta), 121.07 (d, $J = 93.29$ Hz, 1C, C ipso), 90.04 (d, $J = 156.10$ Hz, 1C, $\text{PCCl}_2\text{CP}_2\text{Cl}$), 54.36 (d, $J = 48.74$ Hz, 1C, $\text{PC}(\text{SiMe}_3)_2$), 40.22 (d, $J = 2.81$ Hz, 1C, orto $\text{C}(\text{CH}_3)_3$), 35.23 (d, $J = 0.92$ Hz, 1C, para $\text{C}(\text{CH}_3)_3$), 34.02 (s, 1C, orto CH_3), 30.96 (s, 1C, para CH_3), 4.34 (dd, $J = 44.09, 4.76$ Hz, 1C, $\text{C}(\text{SiMe}_3)_2$).

MS (EI): m/z (%) = 604 (1) $[\text{M}]^+$, 589 (1) $[\text{M} - \text{Me}]^+$, 569 (20) $[\text{M} - \text{Cl}]^+$, 547 (18) $[\text{M} - \text{tBu}]^+$.

ACKNOWLEDGMENT

Drs. Jean Escudie and Henri Ranaivonjatovo from Paul Sabatier University of Toulouse are thanked for their hospitality and useful discussion on this manuscript. We thank the Ministry of Education and Research, Bucharest (CEEX ET-49 project) for partial financial support of this work.

REFERENCES

1. For reviews on this subject see: a) J. Escudié, H. Ranaivonjatovo, L. Rigon, *Chem. Rev.* **2000**, *100*, 3639; b) J. Escudié, H. Ranaivonjatovo, M. Bouslikhane, Y. El Harouch, L. Baiget, G. Cretiu-Nemes, *Russ. Chem. Bull.* **2004**, *53*, 1020, c) J. Escudie, H. Ranaivonjatovo, *Organometallics*; **2007**, *26*(7), 1542.
2. M. Yoshifuji, K. Toyota, K. Shibayama, N. Inamoto, *Tetrahedron Lett.*, **1984**, *25*, 1809.
3. M. Yoshifuji, S. Sasaki, N. Inamoto, *Tetrahedron Lett.*, **1989**, *30*, 839.

G. NEMES, R. ȘEPTLEAN, P. M. PETRAR, L. SILAGHI-DUMITRESCU, I. SILAGHI-DUMITRESCU

4. M. Yoshifuji, K. Toyota, H. Yoshimura, K. Hirotsu, A. Okamoto, *J. Chem. Soc. Chem. Commun.*, **1991**, 124.
5. B. E. Eichler, D. R. Powell, R. West, *Organometallics*, **1998**, *17*, 2147.
6. a) R. Septelean, H. Ranaivonjatovo, G. Nemes, J. Escudié, I. Silaghi-Dumitrescu, H. Gornitzka, L. Silaghi-Dumitrescu, S. Massou, *Eur. J. Inorg. Chem.* **2006**, 4237; b) G. Nemes, I. Silaghi-Dumitrescu, P. M. Petrar, R. Septelean, L. Silaghi-Dumitrescu, *Studia Univ. Babeș-Bolyai, Chemia*, 2007, LII (1), 3.
7. K. Toyota, A. Nakamura, M. Yoshifuji, *Chem. Commun.*, **2002**, 3012.
8. D. Gudat, E. Niecke, W. Malisch, S. Quashie, U. Hofmockel, A. H. Cowley, M. A. Arif, B. Krebs, M. Dartmann, *J. Chem. Soc. Chem. Commun.*, **1985**, 1687.
9. C. A. Akpan, P. B. Hitchcock, J.F. Nixon, M. Yoshifuji, T. Niitsu, N. Inamoto, *J. Organomet. Chem.*, **1988**, *338*, C35.
10. M. Yoshifuji, K. Toyota, T. Niitsu, N. Inamoto, K. Hirotsu, *J. Organomet. Chem.*, **1990**, *389*, C12.
11. S. Ito, H. Liang, M. Yoshifuji, *Chem. Commun.*, **2003**, 398.
12. S. Ito, H. Jin, S. Kimura, M. Yoshifuji, *J. Org. Chem.*, **2005**, *70*(9), 3537.
13. S. Kawasaki, A. Nakamura, K. Toyota, M. Yoshifuji *Organometallics*, **2005**, *24*, 2983.
14. H. Liang, S. Ito, M. Yoshifuji, *Organic Letters*, **2004**, *6*, 425.
15. S. Ito, H. Jin, S. Kimura, M. Yoshifuji, *J. Org. Chem.*, **2005**, *70*, 3537.
16. E. Niecke, P. Becker, M. Nieger, D. Stalke, W.W. Schöeller, *Angew. Chem. Int. Ed.*, **1995**, *34*, 1849.

In memoriam prof. dr. Ioan A. Silberg

TLC SEPARATION OF Th(IV) AND LANTHANIDES(III) ON VARIOUS STATIONARY PHASES USING HDEHDTP AS COMPLEXING AGENT

MARIA - LOREDANA SORAN^{a*}, MARIA CURTUI^b, DIANA GHERMAN^b

ABSTRACT. The separation of thorium(IV) and lanthanides(III) (Ln(III)) using different stationary phases: silica gel, silica gel – zirconium(IV) silicate mixture, silica gel – titanium(IV) silicate mixture, and silica gel impregnated with NH_4NO_3 2.5M has been investigated. The solvent mixtures *o,m,p*-xylene – methyl-ethyl-ketone (MEK) - N,N-dimethylformamide (DMF) (16 + 2 + 1, v/v) and methyl-ethyl-ketone – tetrahydrofuran (THF) (6.8 + 3.2, v/v) containing di(2-ethylhexyl)dithiophosphoric acid (HDEHDTP) 0.04 M as complexing agent were used as mobile phases. The results obtained show that the separation of Th(IV) from Ln(III) and Ln(III) from each other is achieved using silica gel impregnated with NH_4NO_3 2.5 M and MEK – THF (6.8 + 3.2, v/v) – HDEHDTP 0.04 M as mobile phase.

INTRODUCTION

Dialkyldithiophosphoric acids, well known as good complexing agents have been efficiently used for solvent extraction of metal ions [1-7]. Di(2-ethylhexyl) monothiophosphoric, di(2-ethylhexyl)dithiophosphoric and di(2,4,4-trimethylpentyl)dithiophosphinic acids were investigated as selective extractants impregnated on polymer supports [8-10]. The ammonium salt of diethyldithiophosphoric acid was used for preconcentration of heavy metals from water and biological material, using different sorbents [11].

In our earlier paper, we have studied the extraction of U(VI) by different dialkyldithiophosphoric acids (HDADTP) [5-7,12] and the separation of uranium and *d* transition metal dithiophosphates by TLC technique [13]. Later, we extended our investigation on the separation of U(VI), Th(IV), Ln(III) and other elements using dithiophosphoric complexants in solvent extraction and chromatographic systems [14-18].

^a National Institute of Research & Development for Isotopic and Molecular Technology, 71-103 Donath Street, RO-400293 Cluj-Napoca, Romania

* Corresponding author: loredana_soran@yahoo.com

^b Faculty of Chemistry and Chemical Engineering, 11 Arany János, RO-400028, Cluj-Napoca, Romania

In several papers we described the use of dialkyldithiophosphoric acids for separation of metal cations mentioned by thin-layer chromatography on silica gel H [14-18]. In order to improve the separation conditions we investigated the TLC behavior of these cations on various stationary phases [16, 19].

The goal of this work is to obtain information about the separation of thorium(IV) and lanthanides(III) (Ln(III)) on silica gel H, silica gel H impregnated with 2.5M NH_4NO_3 , silica gel H – Zr(IV) silicate and silica gel H – Ti(IV) silicate mixtures, using di(2-ethylhexyl)dithiophosphoric acid (HDEHDTP) in organic mobile phase.

RESULTS AND DISCUSSIONS

TLC separation of Th(IV) and Ln(III): La(III), Ce(III), Pr(III), Sm(III), Gd(III) and Er(III) on silica gel H, silica gel H impregnated with 2.5M NH_4NO_3 , silica gel H – Zr(IV) silicate and silica gel H – Ti(IV) silicate mixtures was studied using HDEHDTP as complexing agent in the mobile phase.

A mixture of organic solvents containing MEK, DMF or THF were used as mobile phase since previous studies have shown that the presence of a polar solvent with electron-donor properties in addition to dialkyldithiophosphoric ligand is crucial for actinides and lanthanides migration [22].

The results obtained using stationary phases mentioned above and *o,m,p*-xylene – MEK – DMF (16 + 2 + 1, v/v) mixture containing 0.4M HDEHDTP as mobile phase are presented in Table 1.

Table 1

R_F values of the studied cations obtained on various stationary phases.
Mobile phase: *o,m,p*-xylene – MEK – DMF (16 + 2 + 1, v/v)
mixture containing 0.4M HDEHDTP

No.	Stationary phase	$R_F \times 100$						
		La(III)	Ce(III)	Pr(III)	Sm(III)	Gd(III)	Er(III)	Th(IV)
1.	Silica gel H	17	23	23	20	8	15	14
2.	Silica gel H - Zr(IV) silicate	18	14	17	18	18	14	9
3.	Silica gel H - Ti(IV) silicate	24	19	20	16	5	14	21

It can be noticed that Th(IV) and the lanthanides migrate on all stationary phases investigated. The R_F values show that on silica gel Th(IV) can be separated from La(III), Ce(III) Pr(III), and Gd(III) and a tendency of separation of Ln(III) from each other excepting for Ce(III) - Pr(III) pair. The separation of Th(IV) from Ln(III) studied is also observed when silica gel H-Zr(III) silicate mixture is used as stationary phase. In this case the pairs La(III)-Ce(III), Ce(III)-Pr(III) and Gd(III)-Er(III) are separated too. The results obtained on silica gel H - Ti(IV) silicate mixture show that Th(IV) can be separated from La(III), Sm(III), Gd(III) and Er(III). The pairs La(III)-Ce(III), Pr(III)-Sm(III), Sm(III)-Gd(III) and Gd(III)-Er(III) can also be separated.

Series of experiments were also carried out on different stationary phases using MEK – THF mixture (6.8:3.2, v/v) containing 0.4M HDEHDTP as mobile phase. Data presented in Figure 1 (curve 1) suggest the possibility of separation on silica gel H of Th(IV) from La(III), Gd(III), Er(III) and tendency of Ln(III) separation from each other excepting for Ce(III) – Pr(III) pair.

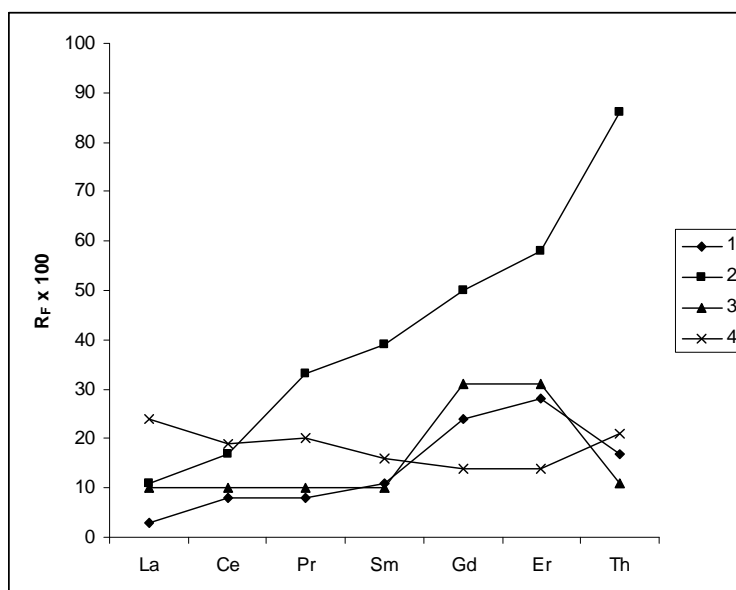


Fig. 1 - Retention factors of metal ions for various stationary phases
Stationary phase: 1 – silica gel H; 2 – silica gel H impregnated with 2.5M NH_4NO_3 ; 3 – silica gel H - Zr(IV) silicate mixture;
 4 – silica gel H - Ti(IV) silicate mixture.
Mobile phase: MEK – THF (6.8 : 3.2, v/v) – 0.4 M HDEHDTP

A similar chromatographic behavior is observed on silica gel H -Zr(IV) silicate mixture as stationary phase (Fig 1, curve 3). In this case, Gd(III) and Er(III) can be separated from La(III), Ce(III), Pr(III), Sm(III) and Th(IV). Clear separation of Th(IV) from Ln(III) occurs on silica gel H impregnated with NH_4NO_3 when using this mobil phase. Ln(III) are also separated from each other (Fig 1, curve 2). Generally, the order of migration of Ln(III) is the order of increasing atomic number Z, on both plain silica gel H and silica gel H impregnated with NH_4NO_3 , effect observed in Ln(III) separation by liquid-liquid extraction.

In order to asses the quality of separation of metal ions investigated on silica gel impregnated with 2,5M NH_4NO_3 the values of resolution factor R_f were calculated according to Ecuation (1) [23, 24]:

$$R_s = \frac{\Delta R_F \sqrt{z_f - z_0}}{2(\sqrt{R_{F1} H_1} + \sqrt{R_{F2} H_2})} \quad (1)$$

where R_{F1} and R_{F2} are retention factors of a neighboring pair of ions; $z_f - z_0$

is the distance between the origin and mobile phase front; $H = \frac{z_f - z_0}{N}$ is

the theoretical plate height; $N = 16 R_F \left(\frac{z_f - z_0}{\delta_x} \right)^2$ is the number of plates;

δ_x is the spot diameter; and z_x is the distance of spot migration.

Data obtained are presented in Figure 2 (for simple and double development). R_s values higher than 1,5 show that very good resolution is obtained on silica gel H impregnated with NH_4NO_3 especially by duple development with MEK-THF mixture containing HDEHDTP as complexing agent. For the pairs Ce(III)-Pr(III) and Er(III)-Th(IV) separation is poorer after double elution but is still suitable for quantitation ($R_s > 1,5$).

Under these conditions separation of more lantanides (La(III), Ce(III), Pr(III), Nd(III), Sm(III), Gd(III), Dy(III), Hb(III), Er(III) and Yb(III)) was attempted. The order of migration folowed that of increasing atomic number, but very close R_F values were obtained for consecutive lantanides. Double development was therefore performed to achieve better separation. The R_F values obtained for double development where used to calculate

$R_M^* = \log \frac{R_F}{1 - R_F}$ [23] where R_F is the retention factor of lanthanide (R_M^* is

a quantity used to understand the correlation between the extraction chromatography and liquid-liquid extraction).

The plots of R_M^* versus atomic number of lantanides a represented in Figure 3. The tetrad – effect very similar to that observed in liquid – liquid extraction is clearly seen after duple elution. It can be noticed that lanthanides a divided in four groups.

TLC SEPARATION OF Th(IV) AND LANTHANIDES(III) ON VARIOUS STATIONARY PHASES ...

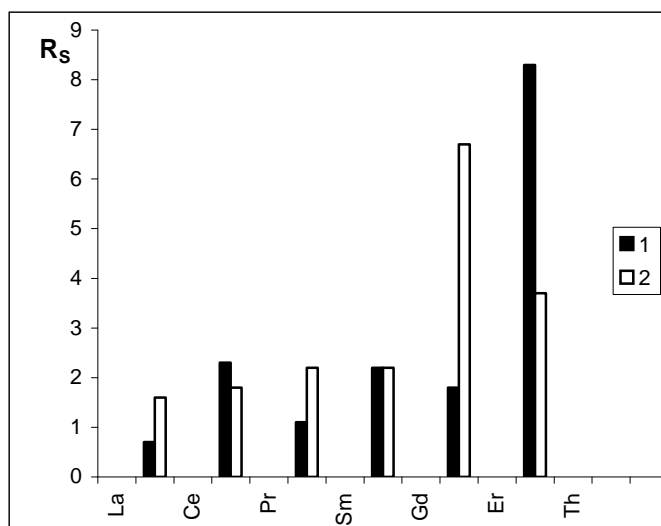


Fig. 2 - Resolution of separation of Th(IV) and Ln(III) on silica gel H impregnated with 2.5M NH_4NO_3 ; Mobile phase: MEK – THF (6.8 : 3.2 , v/v)– 0.4 M HDEHDTP mixture; 1 – simple elution; 2 – double elution.

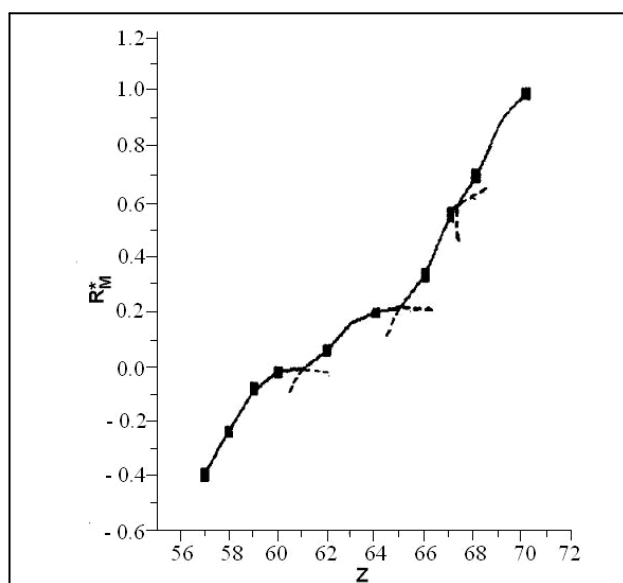


Fig. 3 - Dependence of R_M^* on Z for the investigated lanthanides. Stationary phase: silica gel H impregnated with 2.5 M NH_4NO_3 ; Mobile phase: MEK-THF (6.8 : 3.2, v/v)- 0.4 M HDEHDTP

CONCLUSIONS

It has been found that separation of Th(IV) from Ln(III) and separation of certain lanthanide (III) pairs can be achieved on silica gel H, silica gel H - Zr(IV) silicat and silica gel H - Ti(IV) silicat using *o,m,p*-xylene-MEK-DMF and MEK-THF mixtures containing HDEHDTP as mobile phase. When silica gel H impregnated with NH_4NO_3 is used as stationary phase there is a marked difference between TLC behavior of the metal ion investigated. By use of the binary mobil phas MEK-THF containing HDEHDTP the resolution is much improved and the separation of lanthanides from each other is also achieved. The tetrad – effect is observed in variation of R_m^* versus atomic number of lanthanides.

EXPERIMENTAL PART

Materials

TLC plates coated with silica gel H, silica gel H impregnated with 2.5M NH_4NO_3 , silica gel H – Zr(IV) silicate and silica gel H – Ti(IV) silicate mixtures were prepared in laboratory as described elsewhere [20].

Metal nitrates and Arsenazo III were supplied by Aldrich Chemie (Germany). HDEHDTP was synthesized by published procedure [21] and its purity was higher than 95%. All other reagents were of analytical grade supplied by Chimopar, Bucharest (Romania). Standard solutions of metal ions (5×10^{-3} M) were prepared by dissolving of the metal salts in demineralized water.

Procedure

Silica gel H, silica gel H impregnated with 2.5M NH_4NO_3 , silica gel H – Zr(IV) silicate and silica gel H – Ti(IV) silicate mixtures were tested as stationary phases. Mixtures of *o,m,p*-xylene – methyl-ethyl-ketone (MEK) – dimethylformamide (DMF) and MEK – tetrahydrofurane (THF) were used as mobile phase.

Standard solutions of metal ions were spotted on the chromatographic plates by means of Brand micropipettes. The plates were developed in unsaturated normal chromatographic chambers; the development distance was 10 cm. After development the plates were dried for 15 min in a hood and then, the spots were visualized by spraying with an aqueous solution of Arsenazo III (0.05%). The metal ions were detected as blue-green spots. All separations were performed at room temperature.

The evaluation of chromatograms was performed at 600 nm with a Desaga CD 60 densitometer. The results are means from 3 measurements.

ACKNOWLEDGMENT

This work was supported by the Romanian Ministry of Education and Research under the research program CEEEX project nr. 2995/2005 and CNCSIS project nr.170/2005.

REFERENCES

1. G. Cote and D. Bauer, *Rev. Inorg. Chem.*, **1989**, *10*, 121.
2. J.L. Sabot and D. Bauer, *J. Inorg. Nucl. Chem.*, **1978**, *40*, 1129.
3. R. Fitousi and C. Musikas, *Sep. Sci. Techn.*, **1980**, *15*, 845.
4. I. Haiduc and M. Curtui, *J. Radioanal. Nucl. Chem.*, **1986**, *99*, 257.
5. I. Haiduc, M. Curtui, Iovanca Haiduc and I. Silaghi-Dumitrescu, "Chemical Aspects of Nuclear Methods and Analysis", *Proceedings of the Final Research Co-Ordination Meeting organized by International Atomic Energy Agency*, Hamanatsu Japan, Oct. 2-5, **1984**, IAEA-TECDOC-350, Viena, **1985**, 101.
6. M. Curtui, *J. Radioanal. Nucl. Chem., Letters*, **1994**, *186*, 273.
7. M. Curtui, I. Haiduc and L. Ghizdavu, *J. Radioanal. Nucl. Chem.*, **2001**, *250*, 359.
8. L. Bromberg, *J. Phys. Chem.*, **1996**, *100*, 1767.
9. A. G. Strikovskiy, A. Warshawsky, L. Hankova and K. Jerabek, *Acta Polym.*, **1998**, *49*, 600.
10. A. Warshawsky, A.G. Strikovskiy and J.L. Cortina, *Solvent Extr. Ion Exch.*, **1997**, *15*, 259.
11. S.P. Quináia, J.B.B. da Silva, M.C.E. Rollemberg and A.J. Curtius, *Talanta*, **2001**, *54*, 687.
12. M. Curtui, *Rev. Roum. Chim.*, **1997**, *42*, 621.
13. I. Haiduc and M. Curtui, *Studia Univ. „Babeş-Bolyai”, Chemia*, **1974**, *19*, 71.
14. T. Hodişan, M. Curtui and I. Haiduc, *J. Radioanal. Nucl. Chem.*, **1998**, *238*, 129.
15. T. Hodişan, M. Curtui, S. Cobzac, C. Cimpoiu and I. Haiduc, *J. Radioanal. Nucl. Chem.*, **1998**, *238*, 179.
16. M.L. Soran, C. Măruţoiu, M. Curtui and M. Dascălu, *Chem. Environ. Res.*, **2003**, *12*, 135.
17. M.L. Soran, C. Măruţoiu, M. Curtui, T. Hodişan and R. Oprean, *Acta Universitatis Cibiniensis, Seria F, Chemia*, **2002**, *5*, 69.
18. L. Soran, T. Hodişan, M. Curtui and D. Casoni, *J. Planar Chromatogr.-Mod. TLC*, **2005**, *18*, 164.

19. M.L. Soran, M. Curtui, T. Hodişan, E. Hopîrtean, *Acta Universitatis Cibiniensis, Seria F, Chemia*, **2005**, 8(1), 55.
20. M.L. Soran, *Ph.D. Thesis*: „The use of thiophosphoric acids' derivates as extracting agents in extraction chromatography”, **2005**.
21. K. Sasse, *Organische Phosphor-Verbindungen (Houben-Weyl). Methoden der Organischen Chemie*, Band XII, Teil 2, G. Thieme Verlag, Stuttgart, **1964**.
22. L. Soran and M. Curtui, *J. Planar Chromatogr.-Mod. TLC*, **2007**, 20, 153.
23. F. Geiss, „Fundamentals of Thin Layer Chromatography”, Hüthig, Heidelberg, **1987**.
24. C. Liteanu, S. Gocan, T. Hodişan, H. Naşcu, „Cromatografia de lichide”, Ed. Ştiinţifică, Bucureşti, **1974**; 425.

In memoriam prof. dr. Ioan A. Silberg

SPECTRAL INVESTIGATION OF 3-MERCAPTO-1,2,4-TRIAZOLE LIGANDS

MONICA M. VENTER^a, VALENTIN ZAHARIA^b

ABSTRACT. Preliminary spectral studies on 5-aryl-3-mercapto-1,2,4-triazoles, Ar-C₂H₂N₃S, Ar = C₆H₅- (1), 4-H₃CC₆H₄- (2), 4-ClC₆H₄- (3) and 4-BrC₆H₄- (4) and 5,5'-(1,4-phenylen)-bis(3-mercapto-1,2,4-triazole), 1,4-C₆H₄(C₂H₂N₃S)₂ (5) are discussed. The FT-IR and ¹H NMR spectra of 1-5 are consistent with the structure of triazole rings and aromatic systems. The IR data recorded for 1-5 and Raman data recorded for 5 confirm the occurrence of the thiol tautomeric form of the heterocycle in solid state. The ¹H NMR data are consistent with the presence of the thioamido (thione) form in solution. All spectra suggest a mixture of thione/thiol tautomers in both solid state and solution.

Keywords: mercaptotriazole, FT-IR, FT-Raman, ¹H NMR.

INTRODUCTION

The N and N-S heterocyclic derivatives (i.e. mercapto-thiadiazoles, mercapto-triazoles and -tetrazoles, etc.) remain of great interest in coordination and supramolecular chemistry. The flat, rigid geometry of such heterocycles, along with their increased number of heteroatoms, encourage the association of these molecules into outstanding supramolecular structures. The self-assembly pattern and the resulting architectures depend – among other criteria – on the extension and nature of interacting atoms/groups. More specific, crystallographic evidences proved in several cases that heterocycles containing thioamido groups (HN-C=S) generate multiple N-H...E (E = N, O, S) hydrogen bonding [1-5]. For example, the co-crystallization of 1,3,5-triazine-2,4,6-trithione, C₃N₃S₃H₃ (also known as trimercaptotriazine or trithiocyanuric acid) with melamine, tricyanuric acid, 4,4'-bipyridine, etc. produced supramolecular structures with nanometric cavities and channels.

^a Faculty of Chemistry and Chemical Engineering, "Babeș-Bolyai" University, Arany Janos 11, RO-400028 Cluj-Napoca, Romania. Fax: 0040-264-590818; Tel: 0040-264-593833; E-mail: monica@chem.ubbcluj.ro

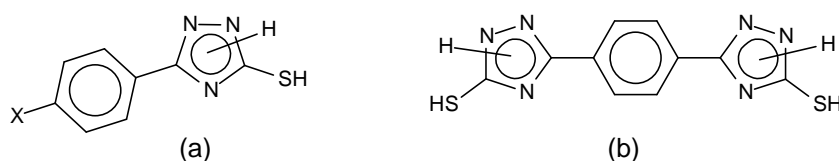
^b Faculty of Pharmacy, "Iuliu Hațieganu" University of Medicine and Pharmacy, Emil Isac 13, RO-400023 Cluj-Napoca, Romania

Many of these compounds have proved excellent zeolitic properties [1-3]. On the other hand, the thione sulfur atoms may involve in intermolecular S...S interactions, which have been found of great importance in the supramolecular construction of molecular electronics [6]. It is the case of dimercapto-thiadiazole, $C_2H_2N_2S_3$ and phenyl-dimercapto-thiadiazole, $C_6H_5-C_2HN_2S_3$ (also known as Bismuthiol I and II, respectively) that revealed short S...S interactions (3.4 – 3.7 Å) in metal complexes [7].

Deprotonation of such heterocycles usually leads to anions in their thiolato tautomeric form. Coordination of the anionic ligand to metal centers through sulfur may generate a large variety of molecular structures, ranging from mono- and dinuclear units [i.e. trithiocyanuric complexes of Na and Cu(I) [4]; organotin(IV) complexes of Bismuthiol II [7], etc.] to infinite 1D or 2D polymers [i.e. organotin(IV) complexes of Bismuthiol II [7], Au(I) complexes of Bismuthiol I, [8,9] etc.].

We have recently initiated the vibrational and crystallographic investigation of a new range of π -excessive heterocyclic systems derived from Bismuthiol I [10-13]. Due to the encouraging results concerning the involvement of the heterocycles in self-assembly and the increased role of heteroatoms in such interactions, we decided to vary the number of nitrogen vs. sulfur atoms. In this respect, we decided to focus on 5-aryl-3-mercapto-1,2,4-triazoles as potential candidates for coordination and supramolecular chemistry, due to the lack of crystallographic evidences for such species [14].

Hence, the aim of this work is the preliminary spectral characterization of 5-aryl-3-mercapto-1,2,4-triazoles, 4- $XC_6H_4-C_2H_2N_3S$, X = H (**1**), CH_3 (**2**), Cl (**3**) and Br (**4**) (Scheme I.a) and 5,5'-(1,4-phenylen)-bis(3-mercapto-1,2,4-triazole), 1,4- $C_6H_4(C_2H_2N_3S)_2$ (**5**) (Scheme I.b). Despite the possibility of several thione (thioamide) and thiol tautomers, the Scheme I illustrates only the thiol form for simplicity.



Scheme I

RESULTS AND DISCUSSION

Five mercaptotriazole derivatives **1** – **5** have been prepared and characterized by vibrational and 1H NMR.

The FT-IR spectra of **1** – **5** were recorded in the 4000 – 400 cm^{-1} spectral range. For the bis-mercaptotriazole (**5**), the Raman spectrum was recorded in the 3500 – 200 cm^{-1} spectral range. The most relevant spectral data are listed in Table 1 and 2.

Table 1

Selected FT-IR data (cm^{-1}) for compounds **1** – **4**.

$\text{C}_2\text{H}_3\text{N}_3\text{S}$ [17]	1	2	3	4	Assignment
		3433 mw	3446 w	3446 mw	v(OH)
3150 w*	3089 sh	3130 sh	3105 sh	3100 sh	v(NH)
3080 w	3060 s	3086 s	3057 s	3055 s	v(CH)
	3003 s	3020 s	3035 s	2989 s	
	2642 m	2692 mw	2665 m	2663 mw	v(SH)
2565 w	2577 m	2594 w	2580 mw	2582 w	
	1593 mw	1618 m	1608 s	1604 s	Ar quadrant stretching
	1582 w	1593 s	1588 m	1581 m	
1559 s	1566 s	1565 s	1562 s	1560 s	v(CN)
1460 vs	1508 vs	1525 vs	1506 vs	1504 vs	v(CN)
	1485 s	1485 s	1484 s	1481 ms	Ar semicircle stretching +
	1453 m	1460 s	1439 m	1439 m	δ (CH) ip
1430 vw	1423 mw		1426 m		v(CN)
	1290 w	1288 w	1294 w	1294 w	δ (CH) ip
1260 s	1225 ms	1234 s	1228 m	1228 m	v(NN)
1187 vs					δ (NH)
		1119 mw	1110 w	1106 w	δ (CH) ip
			1095 s		v(CCl)
944 vs	966 ms	976 m	968 ms	966 m	v(CS)
	918 w	818 m	835 s	833 s	δ (CH) op
	785 ms		786 w	783 w	
	699 s	715 m	727 m	725 ms	Ar op bending by sextants
701 ms	686 s	691 mw	690 w	688 w	δ (CSH) ip
526 w	540 m	538 m	552 w	557 mw	δ (NCS) ip
485 vw	469 vw	474 w	462 w	479 vw	δ (CSH) op

Abbreviations: w – weak, mw – medium weak, m – medium, ms – medium strong, s – strong, vs – very strong, br – broad, sh – shoulder, v - stretching, δ - bending, ip – in plane, op – out of plane, Ar – aromatic ring.

* IR data from reference 18.

The following discussion is based on the comparison between our spectral data recorded for **1** – **5** and the known literature data published for the unsubstituted 3-mercapto-1,2,4-triazole, $\text{C}_2\text{H}_3\text{N}_3\text{S}$ [17,18].

The 4000 – 2000 cm^{-1} spectral range is relevant for the characterization of NH, CH and SH groups. The characteristic stretching modes give rise to a large and complex band in the IR spectra of all compounds. The best

described peaks are assigned to $\nu(\text{CH})$ at $3086 - 3055 \text{ cm}^{-1}$, while the $\nu(\text{NH})$ mode can be hardly distinguished as a shoulder at $3130 - 3089 \text{ cm}^{-1}$. However, the assignment of $\nu(\text{NH})$ at 3150 (IR) [18] and 3156 cm^{-1} (Raman) [17] for 3-mercapto-1,2,4-triazole support our interpretation.

Table 2Selected FT-IR and Raman data (cm^{-1}) for compound **5**.

IR	Raman	Vibrational Assign.
3433 mw		$\nu(\text{OH})$
3103 m	3109 vw, sh	$\nu(\text{NH})$
3068 m	3063 vw	$\nu(\text{CH})$
2997 m	2997 vw	
2683 w		$\nu(\text{SH})$
2596 w	2577 vw	
1595 s	1592 w	Ar quadrant stretching
1527 s	1554 w	$\nu(\text{CN})$
1493 s	1496 s	$\nu(\text{CN})$
1458 m	1473 m	Ar semicircle stretching + $\delta(\text{CH})$ ip
1436 m	1433 w	$\nu(\text{CN})$
1294 w	1300 w	$\delta(\text{CH})$ ip
1236 s	1245 w	$\nu(\text{NN})$
1105 m	1106 vw	$\delta(\text{CH})$ ip
964 ms	967 w	$\nu(\text{CS})$
858 w	863 vw	$\delta(\text{CH})$ op
766 w	749 vw	
706 m		Ar op bending by sextants
667 m	668 vw	$\delta(\text{CSH})$ ip
528 m		$\delta(\text{NCS})$ ip
471 w		$\delta(\text{CSH})$ op

Vibrational investigations on various mercaptans have located the SH stretching in the approx. $2650 - 2500 \text{ cm}^{-1}$ range, as a well defined, medium to weak band [15, 17, 19]. The IR spectra of **1** – **5** reveal distinctive peaks in the mentioned range, which may be assigned to the $\nu_{\text{as}}(\text{SH})$ ($2692 - 2642 \text{ cm}^{-1}$) and $\nu_{\text{s}}(\text{SH})$ ($2596 - 2577 \text{ cm}^{-1}$) modes. In addition, the Raman spectrum of **5** shows a weak but very neat band at 2577 cm^{-1} , which definitely support the previous assignment.

The 2000 – 1000 cm^{-1} spectral range is relevant mainly for the characterization of the heterocyclic skeleton. The most important bands fall in the 1560 – 1527, 1525 – 1493 and 1436 – 1423 cm^{-1} regions for $\nu(\text{CN})$, and 1234 – 1225 cm^{-1} range for $\nu(\text{NN})$. In addition, at least one assignment should be made for the $\delta(\text{NH})$ or $\delta(\text{CNH})$ modes at approx. 1470 – 1420 and/or 1200 cm^{-1} [17, 19]. However, this assignment proved very difficult due to the overlap with other bands.

The 1000 – 400 cm^{-1} spectral range brings new evidences for the identity of the CS group. Thus, the assignment of the band located in the 976 – 964 cm^{-1} region to the $\nu(\text{CS})$ fundamental is in good agreement with the spectral data published for 3-mercapto-1,2,4-triazole in its thiol tautomeric form (944 cm^{-1}) [17-18]. Moreover, this value is significantly lower than that found for thione CS groups in related heterocycles [i.e. thiadiazole-thiones, $\nu(\text{CS})$ approx. 1060 – 1040 cm^{-1}] [10-13]. The presence of the thiol tautomer in solid state is also suggested by the location of the $\delta(\text{CSH})$ bands at 691 – 667 and 479 – 462 cm^{-1} .

The ^1H NMR spectra of compounds **1** – **4** were recorded in ordinary DMSO- d_6 at room temperature and are largely unexceptional as it concerns the characterization of aryl groups (Tab. 3). The spectrum of **5** was of unsatisfactory quality due to its poor solubility. According to literature data, the thioamido (NH) and thiol (SH) protons should fall into the 8-11/13-14 ppm and 2-6 ppm range, respectively [20-22]. The four spectra show small but clear broad singlets at 13.66-13.78 ppm, which may be assigned to thioamido protons. In addition, the spectra reveal singlets located at 3.48-3.61 ppm for each compound. These peaks can be only tentatively assigned to SH protons as long as humidity is present in compounds and/or deuterated solvent.

Table 3

^1H NMR data (δ in ppm, J in Hz) for compounds **1** - **5**.

1	δ 13.71 (s br, 1H, NH), 7.87 (m, 2H, 2- C_6H_5), 7.45 (m, 3H, 3,4- C_6H_5), 3.61 (bs, $\text{H}_2\text{O}/\text{SH}$).
2	δ 13.66 (s br, 1H, NH), 7.78 (d, 2H, 2- C_6H_4 , ^3J 8.1), 7.32 (d, 2H, 3- C_6H_4 , ^3J 8.4), 3.48 (s, $\text{H}_2\text{O}/\text{SH}$), 2.35 (s, 3H, CH_3).
3	δ 13.77 (s br, 1H, NH), 7.90 (d, 2H, 2- C_6H_4 , ^3J 8.7), 7.58 (d, 2H, 3- C_6H_4 , ^3J 8.5), 3.51 (bs, $\text{H}_2\text{O}/\text{SH}$).
4	δ 13.78 (s br, 1H, NH), 7.83 (d, 2H, 2- C_6H_4 , ^3J 8.7), 7.73 (d, 2H, 3- C_6H_4 , ^3J 8.5), 3.48 (bs, $\text{H}_2\text{O}/\text{SH}$).

CONCLUSIONS

The preliminary spectral investigation of **1** – **5** brings evidences for the identity of heterocyclic and aryl fragments. The FT-IR and Raman spectra strongly suggest the presence of the thiol tautomers in solid state and suspect, with rather poor arguments, the presence of the thione (thioamide) forms. Alternatively, the ^1H NMR spectra of **1** – **4** suggest the presence of the thioamide forms in solution and only suspect the thiol tautomers. Further Raman measurements, as well as complete ^1H and ^{13}C NMR investigations in dry deuterated solvent will be performed in order to elucidate the present ambiguities.

EXPERIMENTAL PART

FT-Raman spectra on solid samples were recorded using a Bruker FT-IR Equinox 55 Spectrometer equipped with an integrated FRA 106 S Raman module. The excitation of the Raman spectra was performed using the 1064 nm line from a Nd:YAG laser with an output power of 250 mW. An InGaAs detector operating at room temperature was used. FT-IR spectra were recorded on KBr pellets, using a FT-IR JASCO 600 Spectrometer. The spectral resolutions were 2 cm^{-1} . Room-temperature ^1H NMR spectra were recorded in ordinary DMSO- d_6 on a BRUKER AVANCE 300 instrument operating at 300.11 MHz. The chemical shifts are reported in ppm relative to the residual peak of the deuterated solvent (ref. DMSO: ^1H 2.49 ppm).

The starting materials were purchased from commercial sources as analytical pure reagents and were used with no further purification. Compounds **1** – **5** were prepared following a literature protocol [15,16]. The thiosemicarbazide was reacted with acyl chloride in 2N NaOH solution and the resulting acyl-thiosemicarbazide was isolated in HCl medium, filtered and recrystallized from ethanol. The intermediate was re-dissolved in 2N NaOH solution and refluxed for approx. 1.5 hours. After filtering and diluting the reaction mixture, the mercapto-triazoles were precipitated with aqueous HCl, filtered and recrystallized from ethanol (**1**, **3**, **4**), water (**2**) or ethanol/dmfa (**5**). In all cases, the products were isolated as white microcrystalline solids. MP ($^{\circ}\text{C}$): 262-4 (**1**), 267-8 (**2**), 296-8 (**3**), 294-5 (**4**) and >300 (**5**).

ACKNOWLEDGEMENTS

M.M.V. thanks The National University Research Council Romania for financial support during the course of this work (grant CNCSIS-A 14/1449/2007). The authors also thank Dr. Simona Cinta Pinzaru (Babes-Bolyai University, Dept. of Physics) for facilitating Raman measurements.

REFERENCES

1. V. R. Pedireddi, S. Chatterjee, A. Ranganathan, C. N. R. Rao, *J. Am. Chem. Soc.*, **1997**, *119*, 10867.
2. A. Ranganathan, V. R. Pedireddi, S. Chatterjee, C. N. R. Rao, *J. Mater. Chem.*, **1999**, *9*, 2407.
3. A. Ranganathan, V. R. Pedireddi, C. N. R. Rao, *J. Am. Chem. Soc.*, **1999**, *121*, 1752.
M. F. Mahon, K. C. Molloy, M. M. Venter, I. Haiduc, *Inorg. Chim. Acta.*, **2003**, *348*, 75.
4. K. Henke, D. A. Atwood, *Inorg. Chem.*, **1998**, *37*, 224.
5. D. W. Bruce, D. O'Hare (eds.), "Inorganic Materials", John Wiley & Sons, New York, 1999.
6. V. Bercean, C. Crainic, I. Haiduc, M. F. Mahon, K. C. Molloy, M. M. Venter, P. J. Wilson, *J. Chem. Soc., Dalton Trans*, **2002**, 1036.
7. J.D.E.T. Wilton-Ely, A. Schier, H. Schmidbauer, *Organomet*, **2001**, *20(10)*, 1895.
8. J.D.E.T. Wilton-Ely, A. Schier, M.W. Mitzel, H. Schmidbauer, *Inorg. Chem*, **2001**, *40*, 6266.
9. M.M. Venter, S. Cîntă-Pînzaru, I. Haiduc, V. Bercean, *Studia Univ. Babeş-Bolyai, Physica*, **2004**, *XLIX(3)*, 285.
10. M.M. Venter, V. Chiş, S. Cîntă Pînzaru, V.N. Bercean, M. Ilici, I. Haiduc, *Studia Univ. Babeş-Bolyai, Chemia*, **2006**, *LI(2)*, 65.
11. M.M. Venter, A. Pascui, V.N. Bercean, S. Cîntă Pînzaru, *Studia Univ. Babeş-Bolyai, Chemia*, **2007**, *LII(1)*, 55.
12. M.M. Venter, V.N. Bercean, M. Ilici, S. Cîntă Pînzaru, *Rev. Roum. Chim.*, **2007**, *52(1-2)*, 75.
*** The Cambridge Structural Database System (CSDS), The Cambridge Crystallographic Data Center, 12 Union Road, Cambridge, CB2 1EZ, UK; 2007 upgrades.
13. V. Zaharia, L. Vlase, N. Palibroda, *Farmacia*, **2001**, *XLIX(4)*, 54.
14. C. Ainsworth, *J. Am. Chem. Soc.*, **1956**, *78*, 1973.
15. V. Krishnakumar, R. John Xavier, *Spectrochim. Acta. Part A*, **2004**, *60*, 709.
16. A. Elhajji, N. Oujija, M. Saidi Idrissi, C. Carrigou-Lagrange, *Spectrochim. Acta. Part A*, **1997**, *53*, 699.
17. H.G.M. Edwards, A.F. Johnson, E.E. Lawson, *J. Mol. Struct.*, **1995**, *351*, 63.
18. K. Zamani, K. Faghihi, M.R. Sangi, J. Zolgharnein, *Turk. J. Chem.*, **2003**, *27*, 119.
19. H. Tannai, K. Tsuge, Y. Sasaki, O. Hatozaki, N. Oyama, *Dalton Trans.*, **2003**, 2353.
20. P. Ortega-Luoni, L. Vera, C. Astudillo, M. Guzmán, P. Ortega-López, *J. Chil. Chem. Soc.*, **2007**, *53(1)*, 1120.

In memoriam prof. dr. Ioan A. Silberg

SYNTHESIS AND CHARACTERIZATION OF SOME MIXED LIGAND ZINC(II) COMPLEXES OF THEOPHYLLINE

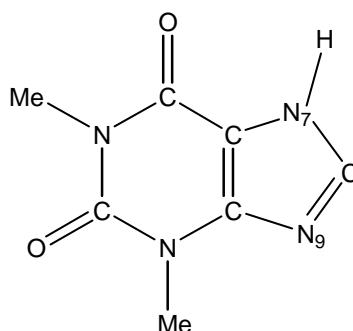
BELA MIHALY, EDIT FORIZS^a, IOAN SILAGHI-DUMITRESCU

ABSTRACT. The synthesis, spectral and thermal properties of four mixed ligand complexes of Zn(II) with deprotonated theophylline (th) are reported: [Zn(th)₂(ba)₂].2H₂O (1), [Zn(th)₂(dmen)].H₂O (2), [Zn(th)₂(ea)₂].H₂O (3) and [Zn(th)₂(pa)₂].H₂O (4) (ba = benzylamine; dmen = N,N-dimethyldiaminoethane; ea = 2-aminoethanol; pa = 3-aminopropanol). The FTIR spectra of complexes indicate that theophylline acts as a monodentate ligand and coordinates *via* the N(7) nitrogen atom.

Keywords: 2-aminoethanol, 3-aminopropanol, benzylamine, N,N-dimethyldiaminoethane, theophylline, mixed ligand complexes

INTRODUCTION

Transition metal complexes of theophylline (Scheme 1) are of considerable interest because they may serve as model compounds for the interaction between metal ions and oxopurine bases of nucleic acids. According to previous studies, theophylline coordinates as a monodentate ligand in neutral media *via* N(9), while in basic media it coordinates *via* N(7) [1–5].



Scheme 1

^a Faculty of Chemistry and Chemical Engineering, Babeș-Bolyai University, RO-400028 Cluj-Napoca, Romania; E-mail: eforizs@chem.ubbcluj.ro

In some cases theophylline acts as a bidentate ligand, forming N(7)/O(6) chelates [6, 7]. In our research on coordination compounds with theophylline and various amines, we have reported the synthesis and characterization of some new mixed ligand complexes of Cu(II), Co(II) and Ni(II) containing the theophyllinato anion and 2-aminoethanol or benzylamine as co-ligands [8–11]. Here we report the synthesis of four new systems, corresponding to the general formula: $[\text{Zn}(\text{th})_2\text{L}_n] \cdot x\text{H}_2\text{O}$, where L: benzylamine (ba) ($n=2$, $x=2$), N,N-dimethyldiaminoethane (dmen) ($n=1$, $x=1$), 2-aminoethanol (ea) ($n=2$, $x=1$), 3-aminopropanol (pa) ($n=2$, $x=1$). The complexes were investigated and characterized by FTIR spectroscopy and thermoanalysis.

EXPERIMENTAL PART

The Zn(II)-complexes were prepared in alkaline aqueous solution as previously reported [2, 8]. FTIR spectra were recorded on a Jasco FTIR 600 spectrophotometer in the $4000\text{--}400\text{ cm}^{-1}$ range, using KBr pellets. Thermal decomposition was investigated with a 103 MOM Radelkis Derivatograph, by using sample of $100 \pm 2\text{ mg}$ and $\alpha\text{-Al}_2\text{O}_3$ as reference (for complexes **1** and **4**) and with an Universal V2.3C TA Instruments, by using sample of $10\text{--}12\text{ mg}$ (for complex **3**), respectively, at a heating rate of $10^\circ\text{C min}^{-1}$. The composition of complexes was determined by elemental analysis (C, H, N).

Synthesis of $[\text{Zn}(\text{th})_2(\text{ba})_2] \cdot 2\text{H}_2\text{O}$ (1). To a suspension of theophylline (0.4 g, 2.02 mmol) in water (15 cm^3), benzylamine (0.5 cm^3) was added. The resulted clear solution was mixed with a second solution of $\text{ZnAc}_2 \cdot 2\text{H}_2\text{O}$ (0.2195 g, 1 mmol) in a benzylamine–water mixture (1 cm^3 of benzylamine in 5 cm^3 of water). The reaction mixture was heated at 50°C for 30 min, under stirring and stored at room temperature over night. The resulted white polycrystalline powder was collected by filtration, washed with aqueous benzylamine (5%) and dried. M.W.: 673.69, Yield: 81.8%, M.P.: $>320^\circ\text{C}$ (dec.).

Complexes **2–4**, *i.e.* $[\text{Zn}(\text{th})_2(\text{dmen})] \cdot \text{H}_2\text{O}$ (**2**), $[\text{Zn}(\text{th})_2(\text{ea})_2] \cdot \text{H}_2\text{O}$ (**3**), $[\text{Zn}(\text{th})_2(\text{pa})_2] \cdot \text{H}_2\text{O}$ (**4**), were prepared by the described procedure, using the appropriate amine or aminoalcohol. Complexes **3** and **4** precipitated after two weeks as crystalline powder.

The main data of complexes **2–4** are presented in Table 1.

Table 1.

Analytical data of complexes 2–4

Complexes	M.W.	M.P. (°C)	Yield [%]	Elemental analysis [%] Found (calc.)		
				C	H	N
[Zn(th) ₂ (dmen)]·H ₂ O ZnC ₁₈ H ₂₈ N ₁₀ O ₅ 2	529.87	295– 325 (dec.)	80	42.05 (40.80)	4.65 (5.33)	26.83 (26.43)
[Zn(th) ₂ (ea) ₂]·H ₂ O ZnC ₁₈ H ₃₀ N ₁₀ O ₇ 3	563.88	278	70	37.65 (38.34)	5.59 (5.36)	24.57 (24.84)
[Zn(th) ₂ (pa) ₂]·H ₂ O ZnC ₂₀ H ₃₄ N ₁₀ O ₇ 4	591.94	258– 259 (dec.)	68	40.85 (40.58)	5.70 (5.79)	23.46 (23.66)

RESULTS AND DISCUSSION

FTIR spectra

The characteristic vibration bands of the ligands and complexes with their assignments are given in Table 2.

Table 2.FTIR vibrations (cm⁻¹) of the ligands and complexes 1–4

Ligand/complex	$\nu(\text{OH})$	$\nu(\text{NH})$	$\nu(\text{C=O})$	$\nu(\text{C=N})$
Theophylline (th)	–	3120m	1714s 1667s	1566s
Ethanolamine (ea)	3642s	3331m 3286m	–	–
Propanolamine (pa)	3636s	3351m 3286m	–	–
[Zn(th) ₂ (ba) ₂]·2H ₂ O 1	3420b	3256m	1687s 1645s	1530s
[Zn(th) ₂ (dmen)]·H ₂ O 2	3529m 3446b	3329m	1693s 1645s	1531m
[Zn(th) ₂ (ea) ₂]·H ₂ O 3	3421b	3291m	1695s 1638s	1530s
[Zn(th) ₂ (pa) ₂]·H ₂ O 4	3446b	3286m	1694s 1640s	1530s

Abbreviations: b - broad, m - medium, s – strong

FTIR spectra of the complexes exhibit obvious differences to the spectrum of theophylline. The two strong bands in the IR spectrum of theophylline, which are assigned to the stretching vibration of the carbonyl groups, are shifted after coordination toward lower wavenumbers, due to the deprotonation of theophylline and the participation of C(6)=O and C(2)=O groups to intra- or intermolecular hydrogen bonds [8–10]. In complexes, the C=N ring vibrations of theophylline are shifted toward lower values, suggesting that the ligand coordinates *via* the imidazole nitrogen atoms. The carbonyl C(2)=O stretching vibration at 1645 cm^{-1} suggests that the carbonyl group does not interact with the water molecules of the framework [9].

There are significant changes in the bands assigned to N–H vibrations, as a consequence of the deprotonation of theophylline at N(7) atom and coordination of the amine type ligands. In the spectra of complexes with a primary amine ligand the symmetric and antisymmetric stretching vibrations of the coordinated NH_2 groups can be assigned in the $3329\text{--}3256\text{ cm}^{-1}$ region. In spectrum of **2**, the symmetric and antisymmetric vibrations are overlapped and the symmetric vibration is reduced to a shoulder, recorded at 3309 cm^{-1} . The ν_{CH} vibrations of benzylamine are observed at 2954 cm^{-1} for the aliphatic CH_2 and at $3027\text{--}3066\text{ cm}^{-1}$ for the aromatic CH. The ν_{CH} vibrations of coordinated N,N-dimethyldiaminoethane are recorded as a broad band centered at 2953 cm^{-1} . The corresponding aliphatic CH_2 vibrations of alcoholamine are registered at 2962 cm^{-1} for complex **3** and at 2953 cm^{-1} for complex **4**.

The strong broad bands of complexes **3** and **4**, recorded at $3600\text{--}3400\text{ cm}^{-1}$, may be assigned to different hydrogen bonds [11–14]. The water content of complexes with aminoalcohols was also confirmed by thermogravimetry.

The FTIR spectra of complexes **1–4** suggest that theophylline acts as a monodentate ligand and coordinates the metal ion *via* the N(7) atom.

Thermal analysis

The investigated complexes undergo a gradual decomposition during heating in flowing air atmosphere. The thermogravimetric curves of complexes with benzylamine (**1**) and of complexes with bidentate ligands (**2–4**) are very different.

The thermogravimetric curve of complex **1** indicates a stepwise decomposition. In the first step, two molecules of water are eliminated in the temperature range of $100\text{--}140^\circ\text{C}$ (experimental weight loss 7%, calculated 5.3%), suggesting that both molecules are bonded similarly. The next step, which occurs in the temperature range $240\text{--}350^\circ\text{C}$, corresponds to the elimination of two molecules of benzylamine, such as in the case of the related Cu(II) complex [10]. Above 350°C , the thermal decomposition is

similar to that of $[\text{Zn}(\text{th})_2(\text{NH}_3)_2]$ [15], with the release and pyrolysis of two theophyllinato moieties. The DTG curve shows that the two theophylline molecules are eliminated in the range of 350–420°C and 420–540°C, respectively. The last two decomposition steps are exothermic, showing maxima at 560 and 660°C, while the final decomposition product is ZnO (exp. solid residue 13%; calc. 12%).

The water molecule of complex **3** is eliminated at 85°C (exp. weight loss 4%, calc. 3.1%) and demonstrates that the respective water is not involved in coordination. Above 200°C, two ethanolamine molecules are evolved in two separate steps, recorded in the range 215–250°C (exp. weight loss 11 %, calc. 10.8 %) and 285–310°C, respectively. The high decomposition temperatures suggest a bidentate binding mode of ethanolamine [6, 7]. Further weight loss corresponds to the release and pyrolysis of theophyllinato moieties. The final decomposition product is ZnO (exp. solid residue 14%, calc. 14.4%), in good agreement with the results of Zelenák for similar complexes [15].

The same decomposition pattern was observed for complex **4**.

CONCLUSIONS

FTIR spectra and thermal data of complexes **1** and **2** suggest a tetrahedral, while in the case of **3** and **4** an octahedral coordination of the metal ions with bidentate bonding of aminoalcohol ligands. The theophylline coordinates *via* the N(7) nitrogen.

ACKNOWLEDGEMENTS. The authors thank Mr. János Madarász for his kind help in thermal investigation of complex **3**.

REFERENCES

1. N. S. Begum, H. Manohar, *Polyhedron*, **1994**, *13*, 307.
2. W. J. Birdsall, M. S. Zitzman, *J. Inorg. Nucl. Chem.*, **1979**, *41*, 116.
3. W. J. Birdsall, *Inorg. Chim. Acta*, **1985**, *99*, 59.
4. P. Umaphathy, R. A. Shaikh, *J. Indian Chem. Soc.*, **1985**, *62*, 103.
5. J. Madarász, P. Bombicz, M. Czugler, G. Pokol, *Polyhedron*, **2000**, *19*, 457.
6. E. Colacio, J. Suarez-Varela, J. M. Dominguez-Vera, J. C. Avila-Roson, M. A. Hidalgo, D. Martin-Ramos, *Inorg. Chim. Acta*, **1992**, *202*, 219.

7. D. Cozak, A. Mardhy, M. J. Olivier, A. L. Beauchamp, *Inorg. Chem.*, **1986**, 25, 2600.
8. P. Bombicz, J. Madarász, E. Forizs, I. Foch, *Polyhedron*, **1997**, 16, 3601.
9. S. Gál, J. Madarász, E. Forizs, I. Labádi, V. Izvekov, G. Pokol, *J. Therm. Anal. Cal.*, **1998**, 53, 343.
10. P. Bombicz, J. Madarász, E. Forizs, M. Czugler, G. Pokol, S. Gál, A. Kálmán, *Z. Kristallogr.*, **2000**, 215, 317.
11. E. Forizs, L. David, O. Cozar, V. Chiş, G. Damian, J. Csibi, *J. Mol. Struct.*, **1999**, 482–483, 143.
12. M. B. Cingi, A. M. M. Lanfredi, A. Tiripicchio, M. T. Camellini, *Transition Met. Chem.*, **1979**, 4, 221.
13. R. Norris, S. E. Taylor, E. Buncel, F. Belanger-Gariepy, A. L. Beauchamp, *Inorg. Chim. Acta*, **1984**, 92, 271.
14. K. Nakamoto, "*Infrared Spectra of Inorganic and Coordination Compounds*", 2nd ed., Wiley-Interscience, New York, **1970**.
15. V. Zelenák, K. Györyová, E. Andogová, *Thermochimica Acta*, **2000**, 354, 81.

In memoriam prof. dr. Ioan A. Silberg

SYNTHESIS AND CHARACTERIZATION OF A NEW BISMUTHO(III)POLYOXOMETALATE WITH MIXED ADDENDA

**OANA BABAN^a, DAN RUSU^b, ADRIAN PATRUT^a,
CORA CRACIUN^c, MARIANA RUSU^{a*}**

ABSTRACT. A new bismutho(III)polyoxometalate cluster with mixed addenda, which corresponds to the formula $K_8[Bi^{III}_2W_{20}V^{IV}_2O_{70}(OH)_2(H_2O)_4] \cdot 23H_2O$, was synthesized. The cluster was investigated by FT-IR, UV-Vis-NIR and EPR spectroscopy. The FT-IR spectrum exhibits vibrations, which indicates the presence of Bi heteroatoms and of W and V addenda. The UV spectrum contains charge-transfer bands, which are specific to the polyoxometalate building. The Vis-NIR spectrum shows two heteronuclear intervalence charge-transfer bands 608 and 806 nm, due to the presence of V^{4+} metal centers. The EPR spectrum indicates non-interacting V^{4+} metal centers.

KEYWORDS: *polyoxometalate, metal cluster, FT-IR spectroscopy, UV-Vis-NIR spectroscopy; EPR spectroscopy.*

INTRODUCTION

Polyoxometalates, also called metal-oxygen clusters, are the most important representatives of the inorganic molecular nanoclusters. The continuous diversification of polyoxometalates through the synthesis of new substances, with interesting electronic structures, unexpected topologies, various electron-transfer processes and remarkable magnetic-exchange interactions, has triggered numerous applications, especially in catalysis, analysis, biochemistry, medicine and materials science [1-7].

^a "Babes-Bolyai" University, Faculty of Chemistry and Chemical Engineering, 11 Arany Janos Str., 400028 Cluj-Napoca, Romania

^b "Iuliu Hatieganu" University, Faculty of Pharmacy, 13 Iuliu Hatieganu Str., 400023 Cluj-Napoca, Romania

^c "Babes-Bolyai" University, Faculty of Physics, 1 Kogalniceanu Str., 400084 Cluj-Napoca, Romania

* Corresponding author: mrusu@chem.ubbcluj.ro

Polyoxometalates are polyoxoanions of the early transition elements, especially Mo, W and V, made up by linked MO_n units. The M metal centers, which may belong to one or several atomic species, are called addenda. In a simplified classification, polyoxometalates are divided into isopolyoxometalates and heteropolyoxometalates. For isopolyoxometalates one or more atomic species act as addenda, while in the case of heteropolyoxometalates, beside the addenda, there are also one or several atomic species playing the role of X heteroatom(s) [8, 9].

Heteropolyoxometalates in which the X heteroatom has an unshared electron pair are of particular importance, showing special structural characteristics and specific properties. Due to the stereochemical activity of the lone pair, the primary group adopts an unusual XO_3 trigonal pyramid shape. The role of the X heteroatom with an unshared electron pair is usually played by subvalent group 15 elements, *i.e.*, As (III), Sb (III) or Bi (III).

A very interesting heteropolyoxometalate series of this type contains 22 addenda metal centers. It consists of two trivalent $B\beta$ - XW_9O_{33} units ($X = Sb^{3+}, Bi^{3+}$), which are connected to each other by two WO_2 and by two additional *fac*- $WO_2(OH)$ or $M(H_2O)_3$ connector groups. Several such polyoxometalates with the general formula $[X_2W_{22}O_{74}(OH)_2]^{12-}$ and $[X_2W_{20}M^{(n+)}_2O_{70}(H_2O)_6]^{(14-2n)-}$ ($M = Fe^{3+}, Co^{2+}, Ni^{2+}, Ni^{2+}, Mn^{2+}$) have been reported [10-17]. The general structure of the respective polyoxometalates with mixed addenda is displayed in Fig. 1.

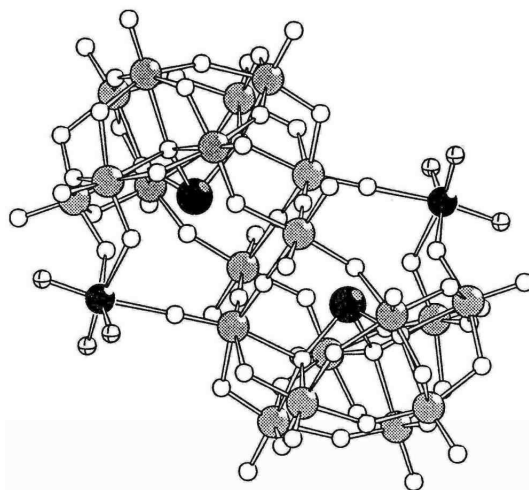
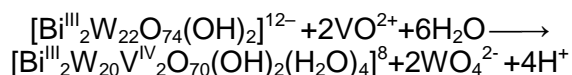


Figure 1. Ball-and-stick representation of the mixed addenda $[X_2W_{20}M^{(n+)}_2O_{70}(H_2O)_6]^{(14-2n)-}$ polyoxometalate structure (X large dark spheres, W large gray spheres, M medium-sized dark spheres, O small white spheres, H_2O small white spheres with crossing lines).

In this paper we describe the synthesis of (the potassium salt of) a new bismutho(III)heteropolyoxometalate with mixed addenda of this series, which corresponds to the formula $K_8[Bi^{III}_2W_{20}V^{IV}_2O_{70}(OH)_2(H_2O)_4] \cdot 23H_2O$. The substance is abbreviated as $K_8[Bi^{III}W_{20}V^{IV}_2]$ for the neutral salt and $[Bi^{III}W_{20}V^{IV}_2]^{8-}$ for the anion, respectively. The new cluster was investigated by vibrational (FT-IR), electronic (UV-Vis-NIR) and EPR spectroscopy.

RESULTS AND DISCUSSION

The new bismutho(III)heteropolyoxometalate with mixed addenda was prepared according to the following formal reaction of metal center/addenda substitution:



The elemental analysis is consistent with the proposed formula for the synthesized substance, *i.e.*, $K_8[Bi^{III}_2W_{20}V^{IV}_2O_{70}(OH)_2(H_2O)_4] \cdot 23H_2O$.

FT-IR spectra. The FT-IR spectra of $K_8[Bi_2W_{20}V_2]$ polyoxometalate with mixed addenda and of the parent $Na_{12}[Bi_2W_{22}]$ polyoxometalate with unique addenda are displayed in Fig. 2. The main vibration bands and their assignment are listed in Table 1.

The FT-IR spectra of $K_8[Bi_2W_{20}V_2]$ and $Na_{12}[Bi_2W_{22}]$ are quite similar, suggesting that the two polyoxometalates belong to the same series.

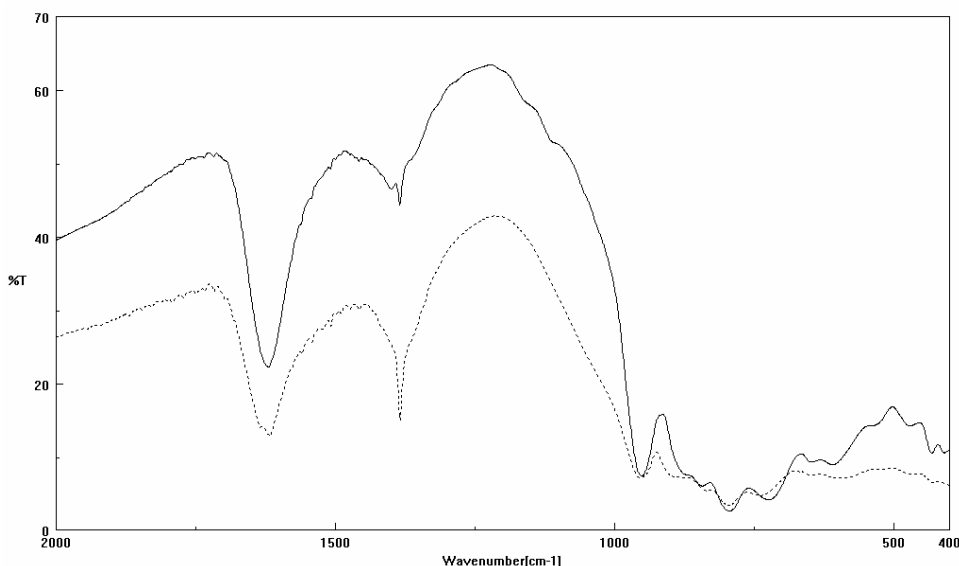


Figure 2. FT-IR spectra of $K_8[Bi_2W_{20}V_2]$ (solid line) and $Na_{12}[Bi_2W_{22}]$ (dashed line).

The stretching vibration of the terminal $W=O_t$ bonds is recorded at about 950 cm^{-1} for both polyoxometalates. This indicates that terminal oxygen atoms are not involved in the coordination of V^{4+} metal centers.

The main stretching vibration of the $Bi-O_i$ bonds is recorded at ca. 840 cm^{-1} for the two substances. This shows that also internal oxygens are not involved in the coordination of V^{4+} .

The vibrations of tricentric $W-O_c-W$ bonds of the corner sharing WO_6 octahedra are recorded at $835, 796$ and 738 cm^{-1} for Bi_2W_{22} and $842, 794$ and 724 cm^{-1} for $Bi_2W_{20}V_2$, respectively. The three peaks demonstrates the non-equivalence of $W-O_c-W$ bonds, when linking octahedra from equatorial and polar regions of the BiW_9 trilacunary fragments [18].

The vibration bands of tricentric $W-O_e-W$ bonds of the edge-sharing WO_6 octahedra are also splitted, being revealed at 648 and 593 cm^{-1} for Bi_2W_{22} and 647 and 609 cm^{-1} for $Bi_2W_{20}V_2$, respectively. The splitting evinces the presence of two non-equivalent bonds of this type in the oxo-cage [19, 20].

As expected, the $Bi_2W_{20}V_2$ spectrum shows additional peaks, due to the new metal centers/addenda. These maxima are recorded at 1158 and 1105 cm^{-1} and can be attributed to the stretching vibration $\nu_{as}V-O$, which is also splitted.

Table 1.
Main vibrations of the FT-IR spectra of $K_8[Bi_2W_{20}V_2]$
and $Na_{12}[Bi_2W_{22}O_{74}]$.

Vibration	$\nu\text{ (cm}^{-1}\text{)}$	
	$Na_{12}[Bi_2W_{22}]$	$K_8[Bi_2W_{20}V_2]$
$\nu_{as}V-O$	-	1158 1105
$\nu_sW=O_t$	953	951
$\nu_{as}Bi-O_i+$ $\nu_{as}W-O_c-W$	835	842
$\nu_{as}W-O_c-W$	796 738	794 724
$\nu_{as}W-O_e-W$	648 593	647 609

UV spectra. The UV spectra of $Bi_2W_{20}V_2$ and Bi_2W_{22} polyoxometalates (Fig. 3) exhibit the two charge-transfer bands, characteristic to the polyoxometalate structure [21, 22]. The ν_2 band ($\sim 50,000\text{ cm}^{-1}$), due to $d\pi-p\pi$ transitions of the $M=O_t$ bonds, is recorded at identical frequencies ($195\text{ nm}/51,165\text{ cm}^{-1}$) in both spectra, which indicates that the terminal O_t atoms are not involved in the coordination of the V^{4+} metal centers. The ν_1 band ($\sim 40,000\text{ cm}^{-1}$), due to $d\pi-p\pi-d\pi$ transitions from the tricentric $M-O_{c,e}-M$ bonds, is also recorded practically at same frequencies in both spectra ($254\text{ nm}/39,370\text{ cm}^{-1}$ for $Bi_2W_{20}V_2$ vs. $255\text{ nm}/39,215\text{ cm}^{-1}$ for Bi_2W_{22}).

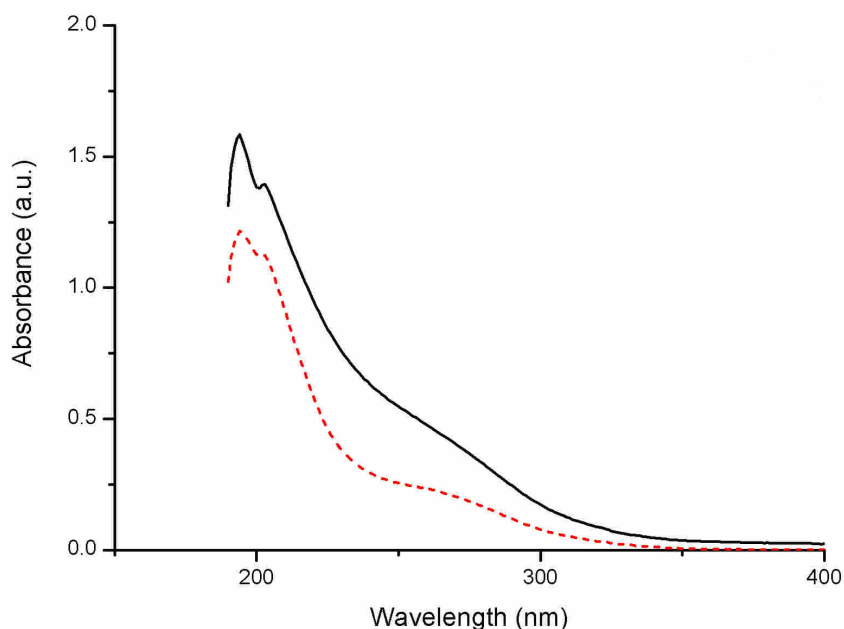


Figure 3. UV absorption spectra of $\text{Bi}_2\text{W}_{20}\text{V}_2$ (solid line) and Bi_2W_{22} (dashed line) in aqueous solution ($c = 5 \cdot 10^{-5} \text{ mol dm}^{-3}$).

The higher intensity of $\text{Bi}_2\text{W}_{20}\text{V}_2$ bands, when compared to Bi_2W_{22} , indicates a higher distortion and decrease in symmetry, due to the presence of two different types of metal centers/addenda.

Vis-NIR spectrum. In polyoxometalates with one or several reduced addenda, new intervalence charge-transfer (IVCT) bands arise in the visible and NIR. In most cases, three IVCT bands are observed, marked by A, B and C [23].

For $\text{Sb}_2\text{W}_{20}\text{V}^{\text{IV}}_2$ polyoxometalate, the reduced addendum is the V^{4+} metal center, which determines the presence of heteronuclear IVCT $\text{V}^{\text{IV}}-\text{W}^{\text{VI}}$ (more precisely, $\text{V}^{\text{IV}}-\text{O}-\text{W}^{\text{VI}}$) bands. The recorded spectrum (Fig. 4) exhibits a strong absorption over the entire visible range, which extends in NIR and accounts for the brown color of the substance, in both solid state and solution.

The A IVCT band, located in NIR at 806 nm ($12,410 \text{ cm}^{-1}$), as well as the B IVCT band, recorded at 628 nm ($15,915 \text{ cm}^{-1}$), are each reduced to a shoulder. The two bands are related to the ${}^2\text{B}_2(\text{d}_{xy}) \rightarrow {}^2\text{B}_1(\text{d}_x^2 - \text{d}_y^2)$ (for A) and ${}^2\text{B}_2(\text{d}_{xy}) \rightarrow {}^2\text{E}(\text{d}_{xz, yz})$ (for B) transitions in the Ballhausen and Gray molecular orbital theory for V^{4+} in a C_{4v} local symmetry [24]. On the other hand, the broad C IVCT band is not recorded.

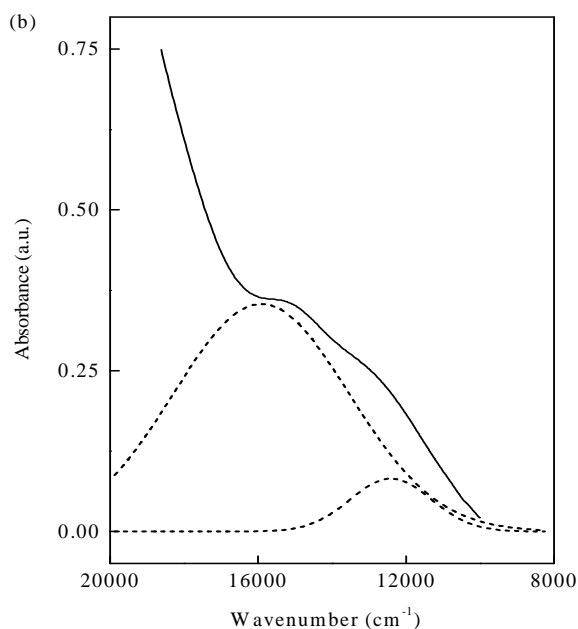


Figure 4. Vis-NIR absorption spectrum of $\text{Bi}_2\text{W}_{20}\text{V}_2^{\text{IV}}$ in aqueous solution ($c = 10^{-4} \text{ mol dm}^{-3}$). The Gaussian components are shown with dashed lines.

EPR Spectrum. Powder EPR spectrum of $\text{K}_8[\text{Bi}_2\text{W}_{20}\text{V}_2^{\text{IV}}]$, recorded at room temperature in the X band contains 8 components, both in the perpendicular and in the parallel bands, due to the hyperfine coupling of the spin of one unpaired electron with the nuclear spin of the ^{51}V isotope ($I = 7/2$) (Fig. 5). The spectrum can be described by an axial spin Hamiltonian, characteristic for the $S = 1/2$ system with C_{4v} local symmetry [25, 26]:

$$H = \mu_B [g_{\parallel} B_z S_z + g_{\perp} (B_x S_x + B_y S_y)] + A_{\parallel} S_z I_z + A_{\perp} (S_x I_x + S_y I_y) \quad (1),$$

where g_{\parallel} , g_{\perp} and A_{\parallel} , A_{\perp} are the axial principal values of the \mathbf{g} and hyperfine tensors, μ_B is the Bohr magneton, B_x , B_y , B_z are the components of the applied magnetic field in direction of the principal \mathbf{g} axes, S_x , S_y , S_z and I_x , I_y , I_z are the components of the electronic and nuclear spin angular momentum operators. This behavior suggests the equivalence of the two paramagnetic V^{4+} ions in the investigated substance.

Parameters were estimated by using a DPPH standard as g-marker ($g = 2.0037$), $g_{\parallel} = 1.908$, $g_{\perp} = 1.974$, $A_{\parallel} = 202.1 \text{ G}$, $A_{\perp} = 71.6 \text{ G}$ for $\text{K}_8[\text{Bi}_2^{\text{III}}\text{W}_{20}\text{V}_2^{\text{IV}}]$. The simulated EPR spectrum indicates no V-V coupling.

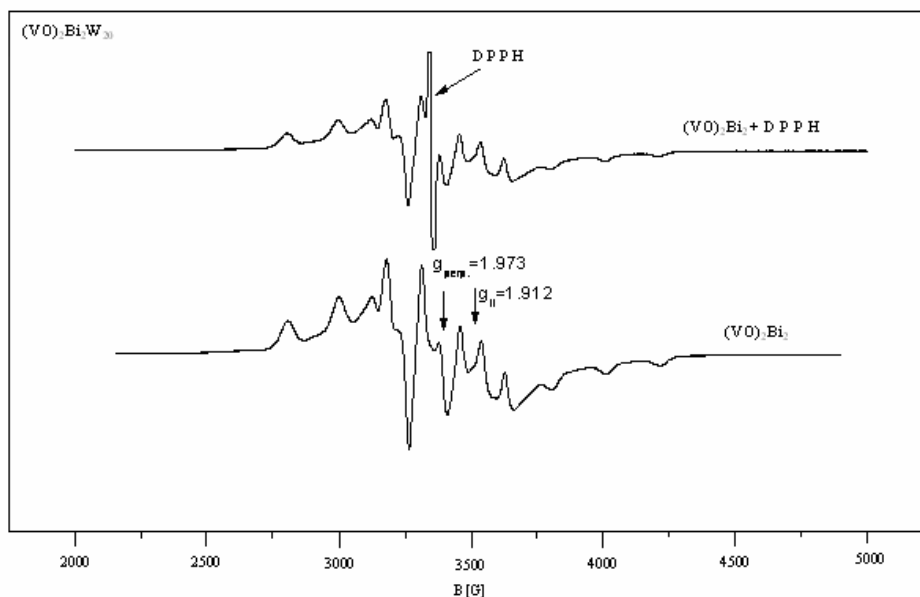


Figure 5. Simulated powder EPR spectrum of $K_8[Bi_2W_{20}V^{IV}_2]$.

EXPERIMENTAL SECTION

Synthesis. An amount of 6.76 g (1 mmol) $Na_{12}[Bi_2W_{22}O_{74}(OH)_2] \cdot 44H_2O$, prepared according to the procedure described in the literature [13], was dissolved in 100 mL AcONa/AcOH acetate buffer (pH 4) and heated at 70°C. Then, 0.50 g (2.5 mmol) $VOSO_4 \cdot 2H_2O$ were added slowly and under continuous stirring to the solution. The mixture was heated again for 1 h, at 70°C, after which 0.90 g (12 mmol) of finely ground KCl were added. The brown solution was purified by filtration and stored at room temperature. Brown-gray microcrystals of $K_8[Bi^{III}_2W_{20}V^{IV}_2O_{70}(OH)_2(H_2O)_4] \cdot 23H_2O$ precipitated after 3-4 days. The crystals were filtered off, washed with distilled water and dried. Eventually, they were recrystallized twice from hot distilled water. Yield: 4.95 g (0.885 mmol; 88.5 % based on W).

Analysis. The synthesized substance was characterized by elemental and thermogravimetric analysis, as follows:

K was determined by FEP with an Eppendorf flame photometer.

Bi, W and V were determined by OES-ICP with a Bird 2070 spectrophotometer.

Water content was determined by dehydration at 350 °C.

Results (wt %): found (calculated for $K_8[Bi^{III}_2W_{20}V^{IV}_2O_{70}(OH)_2(H_2O)_4] \cdot 23H_2O$; M = 6149.81) K 5.05 (5.09); Bi 6.91 (6.80); W 59.02 (59.79); V 1.61 (1.66); H_2O 7.95 (7.91).

Investigation. FT-IR spectra were recorded in the 4000-400 cm^{-1} range by means of a Jasco FT/IR 610 spectrophotometer, using KBr pellets.

Electronic spectra in aqueous solution were acquired in the 190-1300 nm range on an ATI Unicam-UV-Visible spectrophotometer, by means of a Vision Software V 3.20.

EPR spectra were obtained at room temperature and 9.6 GHz (X-band), with a Bruker ESP 380 spectrometer.

CONCLUSION

The paper reports the synthesis and investigation of a new polyoxometalate cluster, with the formula $K_8[Bi^{III}_2W_{20}V^{IV}_2O_{70}(OH)_2(H_2O)_4] \cdot 23H_2O$. The substance is the neutral salt of a heteropolyoxometalate, which contains two Bi^{3+} heteroatoms with an unshared electron pair and mixed addenda, namely W^{6+} and V^{4+} .

The main vibration of the FT-IR spectrum, $\nu_{as}Bi-O$, registered at 835 cm^{-1} , reveals the presence of Bi as a heteroatom. The $\nu_{as}V-O$ vibration, recorded at 1158 and 1105 cm^{-1} , indicates the presence of the V^{4+} metal centers/addenda.

The UV spectrum exhibits two charge-transfer (CT) bands, recorded at 195 and 254 nm, specific to the polyoxometalate edifice.

The Vis-NIR spectrum contains two heteronuclear intervalence charge-transfer (IVCT) bands, owing to the presence of the V^{4+} metal centers, as reduced addenda. The $V^{IV}-W^{VI}$ IVCT bands are registered at 608 and 806 nm.

The EPR spectrum suggests the presence of non-interacting V^{4+} metal centers.

REFERENCES

1. M.T. Pope, A. Müller, *Angew. Chem. Int. Ed. Engl.* **1991**, 30, 34.
2. M.T. Pope, A. Müller, in *Polyoxometalates: From Platonic Solids to Anti-Retroviral Activity* (eds. M.T. Pope, A. Müller), Kluwer, Dordrecht, Boston, London, **1994**, 1.
3. M.T. Pope, A. Müller, in *Polyoxometalate Chemistry: From Topology via Self-Assembly to Applications* (eds. M.T. Pope, A. Müller), Kluwer, Dordrecht, Boston, London, **2001**, 3.
4. A. Müller, M. Luban, M. Schröder, R. Modler, P. Kögerler, M. Axenovich, M. Schmack, J. Canfield, S. Bud'ko, N. Harrison, *ChemPhysChem.*, **2001**, 2, 517.

5. T. Yamase, M.T. Pope, in *Polyoxometalate Chemistry for Nano-Composite Design* (eds. T. Yamase, M.T. Pope), Kluwer, New York, Boston, Dordrecht, London, Moscow, **2002**, 1.
6. A. Müller, *Science*, **2003**, *300*, 749.
7. A. Müller, S. Roy, *Eur. J. Inorg. Chem.*, **2005**, 3561.
8. M.T. Pope, *Heteropoly and Isopoly Oxometalates*, Springer, Berlin, Heidelberg, New York, Tokyo, **1983**, 3.
9. L.C.W. Baker, D.C. Glick, *Chem. Rev.*, **1998**, *98*, 3.
10. B. Krebs, R. Klein, in *Polyoxometalates: From Platonic Solids to Anti-Retroviral Activity* (eds. M.T.Pope, A. Müller), Kluwer, Dordrecht, Boston, London, **1994**, 41.
11. M. Bösing, I. Loose, H. Pohlmann, B. Krebs, *Chem. Eur. J.*, **1997**, *3*, 1232.
12. D. Rodewald, Y. Jeannin, *C. R. Acad. Sci. Paris, Ser. II c*, **1998**, *1*, 175.
13. M. Bösing, A. Nöh, I. Loose, B. Krebs, *J. Am. Chem. Soc.*, **1998**, *120*, 7252.
14. I. Loose, E. Droste, M. Bösing, H. Pohlmann, M.H. Dickman, C. Rosu, M.T. Pope, B. Krebs, *Inorg. Chem.*, **1999**, *38*, 2688.
15. D. Drewes, E.M. Limanski, M. Piepenbrink, B. Krebs, *Z. Anorg. Allg. Chem.*, **2004**, *630*, 58.
16. Y. Jeannin, *C. R. (Chimie)*, **2004**, *7*, 1235.
17. D. Laurencin, R. Villanneau, P. Herson, R. Thouvenot, Y. Jeannin, A. Proust, *Chem. Commun.*, **2005**, 5524.
18. R.Thouvenot, M. Fournier, R.Franck, C. Rocchiccioli-Deltcheff, *Inorg. Chem.*, **1984**, *23*, 598.
19. C. Rocchiccioli-Deltcheff, R. Thouvenot, R. Frank, *Spectrochim. Acta A*, **1976**, *32*, 587.
20. C. Rocchiccioli-Deltcheff, R. Thouvenot, R., *C. R. Acad. Paris, Ser. C*, **1974**, *278*, 857.
21. S. Hyunsoo, M.T. Pope, *Inorg. Chem.*, **1972**, *11*, 1441.
22. X. Zhang, G. Chen, D.C. Duncan, R.J. Lachicotte, C.L.Hill, *Inorg. Chem.*, **1997**, *36*, 4381.
23. M. T. Pope, *Heteropoly and Isopoly Oxometalates*, Springer, Berlin, Heidelberg, New York, Tokyo, **1983**, 109.
24. A.B.P. Lever, *Inorganic Electronic Spectroscopy*, 2nd ed., Elsevier, New York, **1984**, 385.
25. C.W. Lee, H. So, *Bull. Korean Chem. Soc.*, **1986**, *7*, 318.
26. J. Park, H. So, *Bull. Korean Chem. Soc.*, **1994**, *15*, 752.

In memoriam prof. dr. Ioan A. Silberg

AN ALTERNATIVE MECHANISM FOR CATALASE ACTIVITY

RADU SILAGHI-DUMITRESCU^a

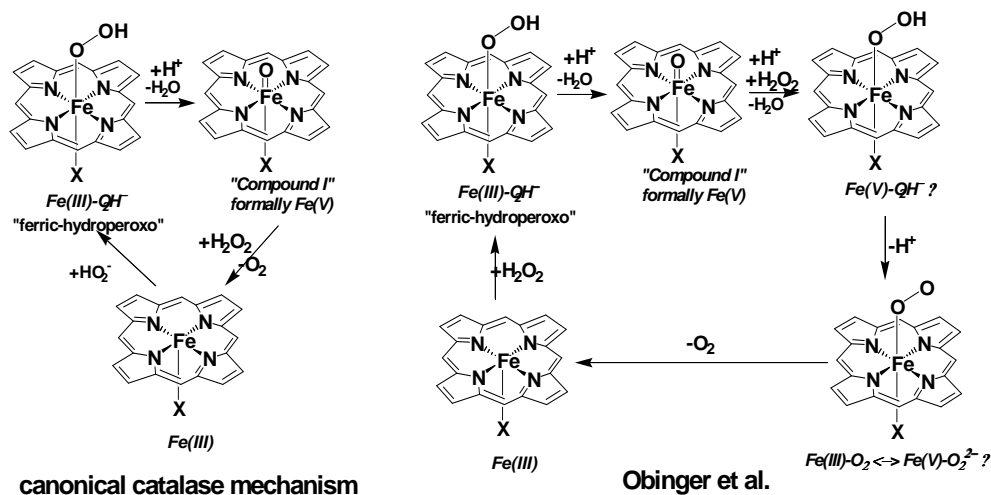
ABSTRACT. The ferric heme active sites of enzymes such as catalases and peroxidases react with hydrogen peroxide to generate a “high-valent” (formally, Fe(V)) species, known as Compound I. In peroxidases, Compound I generally decays back to the ferric state by abstracting electrons from various organic substrates or redox proteins. In catalases, the electrons required for Compound I reduction are supplied by a second H₂O₂ molecule. It has long been implied that the reaction between Compound I and H₂O₂ in catalase implies either outer-sphere electron transfer and/or hydrogen/proton abstraction mechanisms. Recent DFT calculations have confirmed that such mechanisms may be viable. However, a recent experimental investigation by Obinger and co-workers now prompts us to investigate an alternative mechanism, whereby the oxygen atom in Compound I is substituted by a second peroxide molecule, generating a formally Fe(V)-peroxo adduct which by electromerism would convert to Fe(III) and liberate the final product, O₂. Reported here are DFT calculations illustrating the theoretical viability of this newly proposed catalase mechanism.

INTRODUCTION

The ferric heme active site of enzymes such as catalases and peroxidases react with hydrogen peroxide to generate a “high-valent” (formally, Fe(V)) species, known as Compound I.[1,2] In peroxidases, Compound I generally decays back to the ferric state by abstracting electrons from various organic substrates or redox proteins.[3] In catalases, the electrons required for Compound I reduction are supplied by a second H₂O₂ molecule, which is in turn oxidized to molecular dioxygen, such that the overall reaction catalyzed is: $2 \text{H}_2\text{O}_2 \rightarrow 2\text{H}_2\text{O} + \text{O}_2$. [4,5] Experimental evidence for the mechanism of Compound I + H₂O₂ reaction has not been available. It has for a long time been implied that the reaction between Compound I and H₂O₂ in catalase implies either outer-sphere electron transfer and/or hydrogen/proton abstraction mechanisms. Recent DFT calculations have confirmed that such mechanisms may be viable.[6,7] However, a recent experimental investigation by Obinger and co-workers[8] has suggested an alternative mechanism (cf. Scheme 1), whereby the oxygen atom in Compound I is substituted by the second peroxide molecule, generating a formally Fe(V)-peroxo adduct which by electromerism would

^a Department of Chemistry, “Babeș-Bolyai” University, Cluj-Napoca RO-400028, Romania

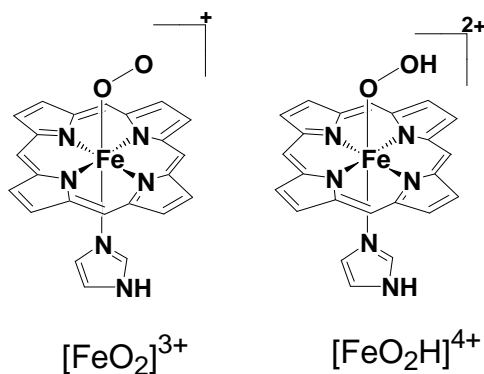
convert to Fe(III) and liberate the final product, O₂. Here we report DFT calculations illustrating the theoretical viability of the newly proposed catalase mechanism.



Scheme 1

RESULTS AND DISCUSSION

The models that we have investigated, shown in Scheme 2, would result following binding of hydroperoxide to Compound I by displacing the "oxo" atom. The nomenclature used in Scheme 2 and throughout the remainder of this discussion stems from the fact that these models can be *formally* described as containing an (Fe(V)-(hydro)peroxo moiety. Calculated geometrical and electronic parameters are shown in Table 1.



Scheme 2

Table 1.
Calculated bond lengths (Å), partial atomic charges and spin densities (the latter shown in italics) for putative catalase catalytic intermediates.

Model	O-O	Fe-O	Fe-N	Fe	O1 ^a	O2 ^b	O ₂ (H) ^c	His ^d	P ^e
S=1/2 [FeO ₂] ³⁺	1.23	3.00	2.14	0.66 <i>2.57</i>	-0.01 <i>0.97</i>	0.01 <i>1.00</i>	0.00 <i>1.97</i>	0.23 <i>0.10</i>	0.11 <i>0.36</i>
S=5/2 [FeO ₂] ³⁺	1.23	3.00	2.14	0.66 <i>2.57</i>	-0.01 <i>0.97</i>	0.01 <i>1.00</i>	0.00 <i>1.97</i>	0.23 <i>0.10</i>	0.11 <i>0.36</i>
S=3/2 [FeOOH] ⁴⁺	1.41	1.85	2.03	<i>0.57</i> <i>1.25</i>	<i>-0.17</i> <i>0.34</i>	<i>-0.17</i> <i>0.19</i>	0.02 <i>0.53</i>	<i>0.39</i> <i>-0.02</i>	<i>1.01</i> <i>-0.76</i>

^airon-bound oxygen atom. ^bnon iron-bound oxygen atom. ^csum over the OO(H) ligand. ^dsum over the imidazole axial ligand. ^esum over the porphyrin ligand

The OOH ligand in the protonated model features significant spin density and is essentially electrically neutral – thus being best described as superoxide. The spin density on iron is distinctly larger than 1, and thus consistent with an S=1 Fe(IV) centre. Likewise, there appears to be ~ 1 spin on the porphyrin. The model is thus best described as containing an Fe(IV) bound to superoxide and to a porphyrin cation radical. The S=3/2 state of the [Fe-O-OH]⁴⁺ model was lower in energy by ~20 kcal/mol compared to its cognate S=1/2 and S=5/2, which nevertheless featured essentially identical electronic and structural parameters and are therefore not further discussed.

For the non-protonated model, the S=1/2 and S=5/2 states were essentially degenerate, with the S=5/2 state slightly lower in energy (~5 kcal/mol). This is in sharp contrast with “ferrous-dioxygen” heme complexes, where theory and experiment agree that the low-spin state is distinctly favoured.[9,10] Remarkably, for S=5/2 [Fe-O₂]³⁺ the Fe-O bond is already broken (i.e., 3 Å), and the O₂ ligand is well described as molecular oxygen, with 2 unpaired electrons and essentially no overall electrical charge. Dissociation of O₂ leaves behind an Fe(III) centre and thus completes the catalase catalytic cycle, cf. Scheme 1. The energy difference between [Fe-O-OH]⁴⁺ and [Fe-O₂]³⁺ defines the (gas-phase) proton affinity of the latter. This value, at 163 kcal/mol, is lower than the proton affinities of water, hydroxide, or imidazole (171, 411, and 232 kcal/mol, respectively), calculated under the same conditions. This indeed suggests that, should the [Fe-O-OH]⁴⁺ species ever form, either solvent or an active site histidine side-chain might in principle serve as electron acceptors, removing a proton from [Fe-O-OH]⁴⁺ and forming [Fe-O₂]³⁺, which, as shown above, is best described as Fe(III) + “free” molecular oxygen. An [Fe-O-OH]⁴⁺ species has recently been observed experimentally in a non-heme iron complex.[8] The present data confirms that such a species would be competent in completing the newly proposed catalase catalytic mechanism, cf. Scheme 1.

CONCLUSIONS

An alternative mechanism is proposed for catalases, whereby the oxygen atom in Compound I is substituted by a second peroxide molecule, generating a formally Fe(V)-peroxo adduct which by electromerism would convert to Fe(III) and liberate the final product, O₂. DFT data supporting the viability of this newly proposed catalase mechanism have been presented.

MATERIALS/METHODS

Geometries were optimized at the DFT level in the *Spartan* software package. The BP86 functional, which uses the gradient corrected exchange functional proposed by Becke (1988) [11] and the correlation functional by Perdew (1986), [12] and the DN** numerical basis set (comparable in size to 6-31G**) were used as implemented in *Spartan*. For the SCF calculations, a fine grid was used and the convergence criteria were set to 10⁻⁶ (for the root-mean square of electron density) and 10⁻⁸ (energy), respectively. For geometry optimization, convergence criteria were set to 0.001 au (maximum gradient criterion) and 0.0003 (maximum displacement criterion). Charges and spin densities were derived from Mulliken population analyses after DFT geometry optimization.

REFERENCES

1. R. Silaghi-Dumitrescu, *J. Biol. Inorg. Chem.*, **2004**, 9, 471.
2. R. Silaghi-Dumitrescu and I. Silaghi-Dumitrescu, *Rev. Roum. Chim.*, **2004**, 3-4, 257.
3. H. B. Dunford, "Peroxidases in Chemistry and Biology" (J. Everse, K. E. Everse, and M. B. Grisham eds.), CRC Press, Boca Raton 1991, vol. II., p. 2-17.
4. D. Metodiewa and H. B. Dunford, *Int. J. Radiat. Biol.*, **1992**, 62, 543.
5. P. Gouet, H. M. Jouve, P. A. Williams, I. Andersson, P. Andreoletti, L. Nussaume and J. Hajdu, *Nat. Struct. Biol.*, **1996**, 3, 951.
6. X. Wang, S. Li and Y. Jiang, *Inorg. Chem.*, **2004**, 43, 6479.
7. F. Buda, B. Ensing, M. C. M. Gribnau and E. J. Baerends, *Chem. Eur. J.*, **2003**, 9, 3436.
8. C. Jakopitsch, A. Wanasinghe, W. Jantschko, P. G. Furtmueller and C. Obinger, *J. Biol. Chem.*, **2005**, 280, 9037.
9. P. Rydberg, E. Sigfridsson and U. Ryde, *J. Biol. Inorg. Chem.*, **2004**, 9, 203.
10. K. P. Jensen, B. O. Roos and U. Ryde, *J. Inorg. Biochem.*, **2005**, 99, 45, Erratum on page 978.
11. A. D. Becke, *Phys. Rev.*, **1988**, 3098.
12. J. P. Perdew, *Phys. Rev.*, **1986**, B33, 8822.

In memoriam prof. dr. Ioan A. Silberg

SPECTROPHOTOMETRIC STUDIES OF DIAZEPAM - β -CYCLODEXTRIN COMPLEX FORMATION

IRINA KACSO^a, IOAN BRATU^{a*}, ANDREEA FARCAS^b, MARIUS BOJITA^b

ABSTRACT. Solid state interactions between a bioactive substance-Diazepam and β -cyclodextrin (β -CD) - the so called inclusion compounds (obtained by different preparation methods: kneading, co-precipitation and freeze-drying) were investigated. The obtained compounds were investigated by FTIR spectroscopy to evidence their formation. The results revealed that the solid state inclusion compound, such as Diazepam/ β -cyclodextrin has a good stability. The stoichiometry of the inclusion complexes of diazepam with β -CD is 1:1 was investigated in solution. The association constant of the complex was determined by UV spectrophotometry. The encapsulation might improve Diazepam stability and bioavailability of the drug.

Keywords: FTIR, UV-Vis, stoichiometry, association constant, inclusion compound, β -cyclodextrin

INTRODUCTION

An antidepressant bioactive substance, diazepam (DZP)(7-Chloro-1,3-dihydro-1-methyl-5-phenyl-2H-1,4-benzodiazepin-2-one,) (Fig. 1), is used in the treatment of severe anxiety disorders, as a hypnotic in the short-term management of insomnia, as a sedative and premedicant, as an anticonvulsant, and in the management of alcohol withdrawal syndrome.

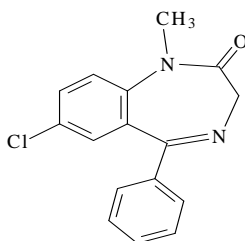


Fig. 1. Diazepam molecule

^a National Institute for R&D of Isotopic and Molecular Technology, P.O. Box 700, RO-400293 Cluj-Napoca, Romania

* Corresponding author: email: ibratu@itim-cj.ro

^b University of Medicine and Pharmacy "Iuliu Hatieganu", Cluj-Napoca, Romania

In order to improve the solubility in water and the bioavailability this compound is encapsulated in cyclodextrins. Cyclodextrins (CDs) - cyclic oligosaccharides, are natural products obtained by enzymatic reaction of starch. Upon the addition of the CGT-ase enzyme to an aqueous solution of starch, every sixth or seventh of the eight α -1, 4-glycosilic linkages is split, reacting with their own non-reducing end. It results a six-, seven- or eight-membered macro-ring. These cyclic maltodextrins are called α -, β -, and γ -cyclodextrins [1]. The aim of the paper was to prepare and to evidence by different spectrophotometric methods some inclusion compounds of diazepam with β -CD.

Two methods, FTIR and UV spectroscopy [2, 3] were employed to confirm inclusion compound formation.

Materials and methods

The inclusion compound was obtained by different methods: physical mixture (*pm*), kneading (*kn*) - grounded the amounts of diazepam and β -cyclodextrin in an agate mortar for 60 min, using ethanol 33% as the wetting agent and the paste thus obtained was dried at 38°C; co precipitation (*co*) - mixing the amounts of diazepam and β -cyclodextrin (15mM alcoholic solution 3:1 v/v) in 1:1 molar ratio, stirring for 48 hours at 40°C succeeded by evaporation and drying at room temperature; freeze-drying (*fd*) - the amounts of diazepam solved in β -cyclodextrin saturated alcoholic solution in molar ratio 1:1, the product was frozen and dried by immersion in freezer-drier (Alpha 1-2 LD plus) for over 24 hrs.

FTIR spectra were obtained with a JASCO 6100 FTIR spectrometer in the 4000 to 400 cm^{-1} with a resolution of 2 cm^{-1} , using the KBr pellet technique.

UV-Vis absorption spectra were recorded on a V-550 JASCO UV/Vis spectrometer equipped with quartz cells having 1.0 cm optical path length.

RESULTS AND DISCUSSION

Inclusion compound of DZP with β -CD

FTIR spectroscopy

FTIR spectrum of the 1:1 physical mixture (*pm*), see Fig. 2, contains the absorption bands of each component so no inclusion compound was obtained in this case.

In the 4000 to 2000 cm^{-1} spectral region the O-H stretching vibration are located at 3400 cm^{-1} for *pm* and 3384 cm^{-1} for β -CD whereas for *kn* this band is shifted to 3401 cm^{-1} and to 3390 cm^{-1} for *fd* products. One concludes that the hydrogen bonds are implied severely in the inclusion compound formation. In the 1800 to 1550 cm^{-1} spectral region, see Fig. 3, one identify the carbonyl group vibration (located at 1686 cm^{-1}) for pure DZP and *pm* system.

SPECTROPHOTOMETRIC STUDIES OF DIAZEPAM - β -CYCLODEXTRIN COMPLEX FORMATION

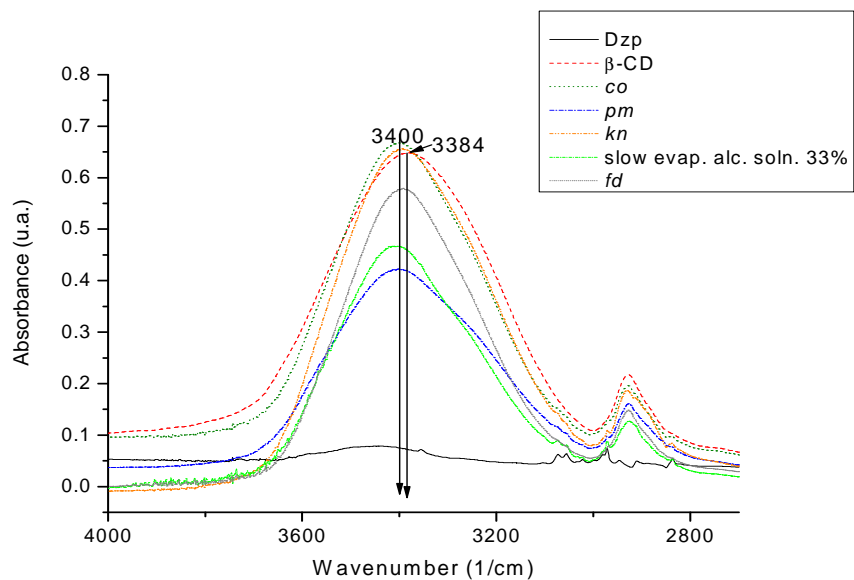


Fig. 2. FTIR spectra of Diazepam and its inclusion compounds obtained by different methods, 4000-2700 cm^{-1} spectral region

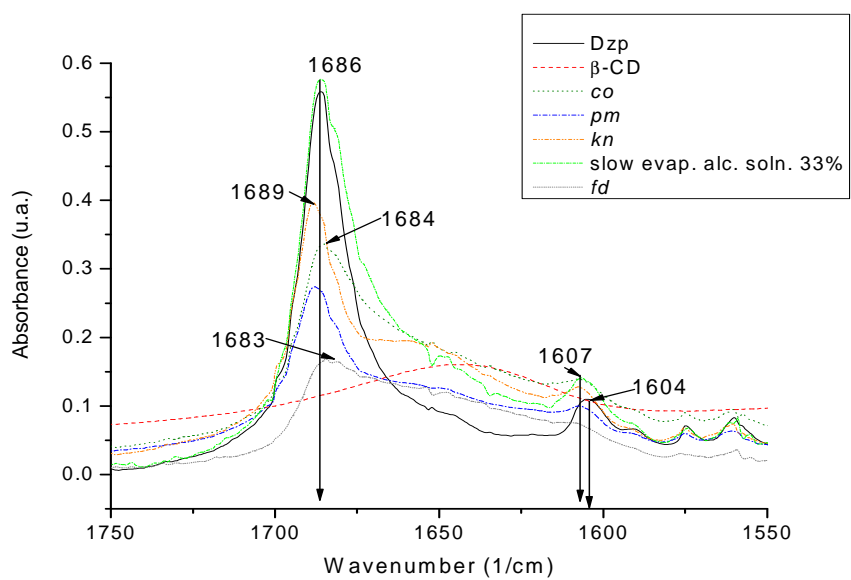


Fig. 3. FTIR spectra of Diazepam and its inclusion compounds obtained by different methods, 1750-1550 cm^{-1} spectral region

UV-Vis spectroscopy

The investigated solutions of DZP at constant concentration 2.5×10^{-5} M and β -CD at increasing concentrations (1; 1.5; 2; 2.5; 3; 4; 5; 6; 7; 8) $\times 10^{-3}$ M have been prepared. The obtained solutions were mixed for 6 hours at 30°C and then left for 24 hours for equilibration. This procedure was replicated in order to obtain two or more absorbance values for each of the β -CD concentration studied. The absorption spectra of the inclusion complex were showed in Fig.4.

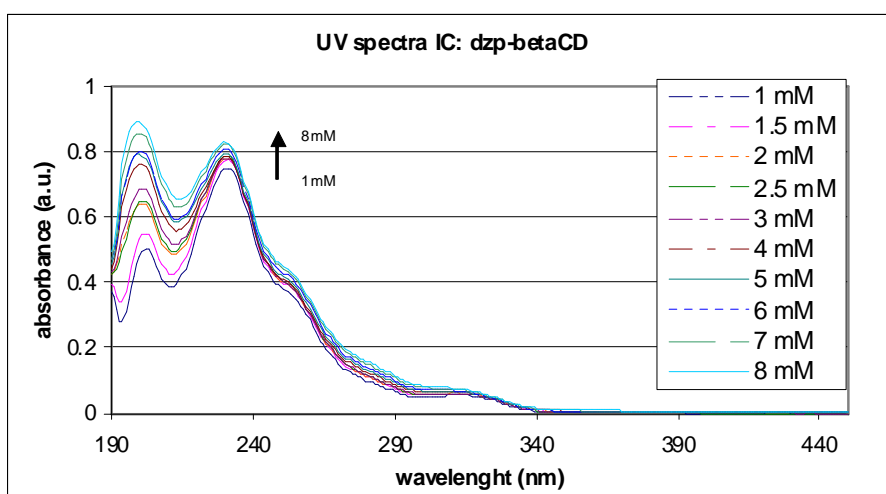


Fig. 4. UV-Vis absorption spectra of 0.025 mM diazepam at different concentration of β -CD: 1, 1.5, 2, 2.5, 3, 4, 5, 6, 7, 8 mM in alcoholic solution (3:1 v/v)

The stoichiometric ratio of inclusion complex of host (β -CD) – guest (DZP) should theoretically be 1:1, according to their chemical reaction equation (1) [4]. A linear relationship should be obtained between $1/dA$ and $1/[\beta CD]$ based on the Benesi-Hildebrand equation [5] (2):



$$\frac{1}{A} = \frac{1}{\epsilon[G]_0 K[CD]} + \frac{1}{\epsilon[G]_0} \quad (2)$$

where A is the absorbance of the DZP solution at each β -CD concentration; $[G]_0$ the initial concentration of DZP; K the apparent formation constant; $[CD]$ the concentration of β -CD and ϵ is the molar absorptivity. From the changes in the absorbance, an apparent formation constant value for the

inclusion complex can be determined. The result is shown in Fig. 5, a good linear relationship obtained proved that stoichiometric ratio of inclusion complex of host (β -CD) – guest (DZP) was 1:1. Fig. 6 presents the Scott plot, used as well as the Benesi-Hildebrand plot for the stability (association) constant determination.

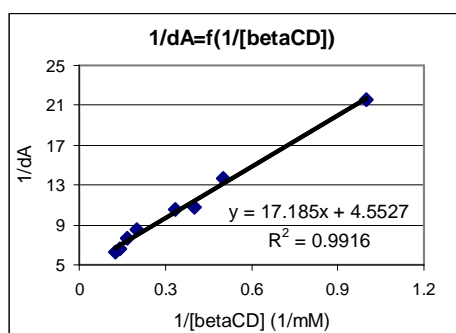


Fig. 5. Benesi-Hildebrand plots for the DZP- β CD systems

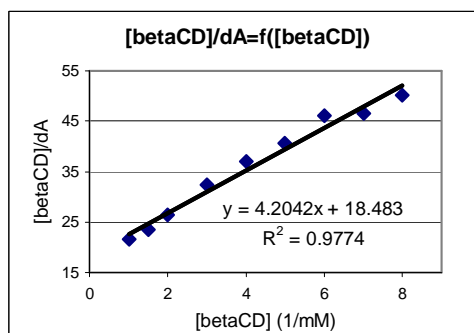


Fig.6. Scott plots for the DZP- β CD systems

The values of the association constants calculated by the two methods [5, 6] (Table 1) differ from each other no more than by their errors. This fact suggests a satisfactory level of correlation between the obtained results.

Table 1.

Association constants for complexation of DZP with β -CD

Method of binding constant calculation	$K_a(\text{DZP}-\beta\text{CD}) \text{ M}^{-1}$	Correlation coefficient, R^2
Benesi-Hildebrand	264	0.9916
Scott	227	0.9774

CONCLUSIONS

The inclusion compounds of DZP with β -CD were obtained and evidenced by FTIR spectroscopy. The 1:1 stoichiometry and the stability constants of approx. 264 M^{-1} and 227 M^{-1} were determined for aqueous solutions with UV-vis spectroscopy by using Benesi-Hildebrand and Scott methods, respectively. These association constant values show that the encapsulation might improve Diazepam stability and bioavailability of the drug.

ACKNOWLEDGMENTS

The FTIR and UV-Vis measurements were supported by the CEEEX no7 / 2005 VIASAN project.

REFERENCES

1. J. Szejtli, *Chem. Rev.* **1998**, 98,1743.
2. M.A. Vandelli, G. Salvioli, A. Mucci, R. Panini, L. Malmusi, F. Forni, *J Pharm. Sci.* **2000**, 90(8),1186.
3. H.J. Schneider, A. Yatsimirsky, Principles and Methods in Supramolecular Chemistry, John Wiley & Sons, New York, **1999**, 137.
4. H. Y. Wang, J. Han, X.G. Feng, Spectroscopic study orange G - β -cyclodextrin complex and its analytical application, *Spectrochimica Acta Part A: Molecular and Biomolecular Spectroscopy*, **2007**, 66, 578.
5. H.A. Benesi, J.H. Hildebrand, *J. Am. Chem. Soc.*, **1949**, 71, 2703.
6. R.L. Scott, *Rev. Trav. Chim.*, **1956**, 75, 787.

In memoriam prof. dr. Ioan A. Silberg

SUPRAMOLECULAR ORGANIZATION AND NANO STRUCTURATION OF COLLAGEN AND ANTI CANCER DRUGS

GHEORGHE TOMOAIA^a, VASILICA-DANIELA POP-TOADER^b,
AURORA MOCANU^b, OSSY HOROVITZ^b, DOREL-LIVIU BOBOS^b,
MARIA TOMOAIA-COTISEL^b

ABSTRACT. Several mixed biosystems comprising a fibrous protein, namely type 1 collagen (COL), which co-assemble with an anti-cancer drug, such as fluorouracil (FLU), doxorubicin (DOX) or lipoic acid (LA), to form ordered films on glass substrate, were visualized by atomic force microscopy (AFM). The obtained nanostructures show different morphology and stability of mixed assemblies made of COL:FLU, COL:DOX and COL:LA. The anti-cancer drugs appear to lead to supramolecular collagen structures with a remarkable level of nanoscale order on glass, which mimics natural protein assemblies. The obtained patterns, especially for COL:FLU biosystem, reflect a high level of internal order within the ordered molecules network. In these cases, the external order reflects high internal organization within these highly evolved systems. Using anti-cancer drugs to self assemble with collagen molecules we have more control over the collagen assembly process. This ability of anti-cancer drugs to control COL assembly brings further utility to the system as it allows additional compounds to be added to self assembly mixtures. In turn, it allows morphology and function of protein to be engineered. Due to current attention given to the design and production of novel bio-inspired materials for applications in nanoscience and nanobiotechnology our findings could offer a strong promise for nanoscale engineering of self-assembling systems. Direct incorporation of small molecules into the collagen assemblies represents a step toward rational design of nanostructured materials for potential applications in industry, medicine and synthetic biology, drug delivery systems and nanobiotechnology.

Keywords: *type I collagen; doxorubicin; 5-fluorouracil; lipoic acid; nanostructure; AFM.*

^a *Iuliu Hațieganu University of Medicine and Pharmacy, Department of Orthopedic Surgery and Traumatology, 47 Mosoiu Str., 400132 Cluj-Napoca, Romania*

^b *Babeș-Bolyai University of Cluj-Napoca, Faculty of Chemistry and Chemical Engineering, 11 Arany J. Str., 400028 Cluj-Napoca, Romania,
e-mail: horovitz@chem.ubbcluj.ro, mcotisel@yahoo.com*

INTRODUCTION

The organization of proteins at surfaces is of increasing importance [1-16] in a wide range of applications, including implant biocompatibility, cell adhesion and growth [5, 6], and biomaterials design [4, 5]. Such applications require a controlled morphology of the self-assembled dried layers of biomolecules at different surfaces, as in the case of biosensor devices, for which the distribution of proteins can influence the signal transduction [11] and the cellular response [11, 13]. Several factors drive the nano scale organization of protein layers, such as distribution of charged groups in the protein interfacial layer, the characteristics of the substrate surface, the structural rearrangements in the protein molecules [17, 18] and the spatial organization at the supramolecular scale [4, 7]. Among the various investigated parameters, the influence of the protein nature and of the solid substrate has received a considerable attention [1, 2, 4, 7-14].

In particular, type I collagen is the major fibrillar protein in the extracellular matrix and in connective tissues [7]. It is a protein of molecular mass about 300 Kg/mol, length about 300 nm, diameter around 1.5 nm, abundant in bone, cartilages, ligaments, tendons and skin [8]. Structurally, it consists of three chains, twisted to form a semi-rigid helical structure, the so called collagen monomer. Non-helical parts (telopeptides) are found at the extremities of each monomer. It contains regions which are specifically recognized by cell-surface receptors, being therefore involved in biorecognition processes.

Chemically, each chain is constructed from repeated amino acid sequences glycine-X-Y, where X and Y positions may be occupied by any amino acid; frequently proline is in X position and hydroxyproline in Y position. A characteristic of type I collagen is that, among the three polypeptide chains, two (α_1) are identical and one (α_2) is different. For instance, in calf skin collagen, the α_1 chains are made of 1056 amino acids residues each and the α_2 chain of 1038 residues [7]. Telopeptides participation seems to be catalytic rather than constitutive and they facilitate the appropriate packing into fibers.

By the assembly of collagen monomers, characteristic band patterns with a periodicity of 67 nm (D banding pattern) along the fibril length are formed. Further linear (end to end) and lateral association (entwining of the structures) gives rise to microfibrils which can further assembly into large fibrillar structures and finally into fibers [19].

Collagen presents different morphologies according to the sample history. For example, homogeneous layers of collagen molecules are observed after adsorption or layer by layer deposition on solid substrates from diluted acidic collagen aqueous solutions. In contrast, fibrillar or fiber structures

were obtained at high concentrations [19]. It was also indicated that the morphology of collagen films can be changed upon drying process [12] depending on the solid substrate characteristics, like roughness, hydrophilicity or the charge surface.

The collagen supramolecular assembly plays an important role in mechanical reinforcement of tissues, and in proliferation, migration, and signal transduction of adjacent cells. Since only the fibril surface is available for cell-collagen interactions, it is crucial to understand the physical and biochemical properties of the fibril surface. However, the surface structure of collagen fibrils and its implications in cellular interactions have not yet been fully understood, primarily due to technical limitations in analyzing in situ the collagen fibril surface at high resolution.

During the last decade, it is recognized that atomic force microscopy (AFM) observations [1, 8, 12, 13, 16, 19] allow a better understanding of biomolecule layer organization. The atomic force microscope has received considerable attention due to its potential to analyze in situ a broad range of biological objects. It can be also expected that the AFM serves to gain deeper insight into the surface properties of collagen auto-associative properties.

In this study, we explore how the anti-cancer drugs influence the formation of supramolecular organization and nano structuration of collagen adsorbed on glass surface using AFM. The preliminary AFM analysis of the following systems consisting of collagen (type I, COL) and anti-cancer drugs (fluorouracil: FLU, doxorubicin: DOX or lipoic acid: LA) indicates the presence of specific molecular interactions with the development of supramolecular associations. Thus, it is of great interest to deeply investigate the molecular and colloidal self association of collagen from aqueous solutions within these systems containing anti-cancer compounds.

As an effect of self association of pure compounds (FLU, DOX, and LA), as well as of their supramolecular associations with collagen, the multifunctional bionanostructures are formed by molecular or colloidal self-assembly on glass solid surfaces by adsorption from aqueous solutions on glass surface. The nanostructures obtained on glass were studied by AFM, in order to determine what kind of structures are formed in vitro under various conditions in the presence of anti-cancer drugs.

AFM imaging offers the advantage of giving both topographic and phase images, as well as the surface roughness of the nanostructured mixed films obtained. In the following we will give an account of a systematic study using atomic force microscopy for collagen and anti-cancer drugs.

By the use of AFM images, structure changes from a pure component to another are visualized (topographic images), and at the same time the structural characteristics of their supramolecular associates are shown.

Simultaneously, the phase images reveal the viscoelastic properties of the obtained bionanostructures and help to identify supramolecular self-aggregates, which could modify the physical and chemical properties of biomolecules, with important biological and medical effects.

The structure of collagen films is not yet well known. Here, we use AFM investigations for evidencing the 2- and 3-dimensional organization of collagen molecules in the presence of anti-cancer drugs. Collagen films might be used to cover the implants in nanomedicine, due to their biocompatibility with natural bone structures. Further, the collagen films mixed with anti-cancer drugs could be new drug delivery systems for the treatment of bone cancer.

EXPERIMENTAL PART

A strategy in three stages was followed:

- first: the use of collagen solutions presenting different states of aggregation; collagen solutions were prepared at different pH values
- second: solutions were aged for varying periods of time; the aggregation of collagen in solution was monitored by using UV-Vis spectrophotometry
- third: collagen solutions with different states of aggregation were used for: a) adsorption/deposition on hydrophilic glass substrates; b) the supramolecular organization of the obtained adsorbed collagen layers was investigated using a combination of self-assembly layers and atomic force microscopy (AFM).

Type I collagen (COL, from bovine Achilles tendon) was purchased from Sigma-Aldrich Chemical, Co., St. Louis, MO. Collagen was dissolved in 0.167 M acetic acid solution at 4 °C and an acidic aqueous dispersion of collagen concentration of 0.5 mg/ml was obtained (pH ≈ 3). After sonication for 30 min, the collagen dispersion was filtered through a 0.45 µm Millipore filter, to remove pre-aggregated collagen oligomers.

From this initial collagen solution, two series of stock collagen solutions were prepared, namely one in the absence and the other in the presence of an anti-cancer drug. The stock collagen solution was obtained starting from the initial collagen solution mixed at 37 °C with an equal volume of 0.3 M NaCl solution. Similarly, the stock mixed collagen solutions containing an anti-cancer drug were prepared, but in this case, the aqueous saline solution contained also 0.1 mM anti-cancer drug.

The used anti-cancer drugs are doxorubicin hydrochloride (DOX, of purity >98% by TLC), 5-fluorouracil (FLU, minimum 99% by TLC) and lipoic acid, all purchased from Sigma- Aldrich Inc., St. Louis, MO. The aqueous solutions of DOX (in 0.3 M NaCl) and FLU (in ethanol:water, 1:1 v/v, containing 0.3 M NaCl), of the initial concentration in anti-cancer drug about 0.1 mM, were obtained. A 0.1 mM solution of lipoic acid in ethanol was prepared. Ethanol was pro analysis purchased from Merck. Ultra pure

deionized water was used (pH 5.6) in all experiments. In the resulted final suspensions of collagen or of collagen and anti-cancer drugs, the collagen concentration of about 250 $\mu\text{g}/\text{ml}$ was obtained.

The final collagen suspensions both in the absence and in the presence of anti-cancer drugs were allowed to stand at 37 °C, for 48 h, 3 days or even 5 days, to let the association of collagen monomers in solution and probably the formation of collagen supramolecular assembly.

The final suspensions of collagen were further used to prepare thin films deposited or adsorbed on glass surface at room temperature. By using the above experimental strategy, the aggregation of collagen was induced by increasing the ionic strength and the temperature of the initial cold collagen solution, in substantial agreement with findings on type I collagen, from calf skin [8, 12, 13].

The used hydrophilic substrates are glass plates (2.5 x 2.5 cm^2). The glass plates, optically polished, were sequentially cleaned with sulfochromic mixture and washed with methanol and water, before deposition of collagen layers with or without anti-cancer drugs.

Then, at room temperature, the final collagen dispersion (about 2 ml) both in the absence and in the presence of anti-cancer drugs, was delivered onto the horizontal glass substrate. After the solvent evaporation the collagen, as well as the collagen with anti-cancer drug, are adsorbed and self assembled on substrate surface.

Two series of samples were prepared starting from final stock collagen solutions, namely in the absence and in the presence of anti-cancer drugs. For all samples the adsorption time lasted 30 min at room temperature, or otherwise specifically mentioned. Then, gentle water rinsing was performed on slightly tilted substrates, with said adsorbed layers on them, in order to eliminate the salt and other solution ingredients. The resulted samples were dried slowly in air for AFM examination.

Atomic force microscopy (AFM) investigations were executed on collagen samples, without and with anti-cancer drugs, using a commercial AFM JEOL 4210 equipped with a 10 x 10 (x-y) μm scanner, operating in tapping (noted *ac*) mode. Standard cantilevers, non-contact conical shaped of silicon nitride, coated with aluminium were used. The tip was on a cantilever with a resonant frequency in the range of 200 - 330 kHz and with a spring constant between 17.5 and 50 N/m.

AFM observations were repeated on different areas from 20 x 20 μm^2 to 0.5 x 0.5 μm^2 of the same collagen sample. The images were obtained from at least ten macroscopically separated areas on each sample. All images were processed using the standard procedures for AFM. All AFM experiments were carried out under ambient laboratory conditions (about 20 °C) as previously reported [1, 2].

RESULTS AND DISCUSSION

Self assemblies of collagen

In Figs. 1-4 are given AFM images for the *pure COL film* deposited on glass from the 0.5 mg/ml aqueous solution, for a scanned area $1 \times 1 \mu\text{m}^2$ (Figs. 1, 3, 4) and $500 \times 500 \text{ nm}^2$ (Fig. 2).

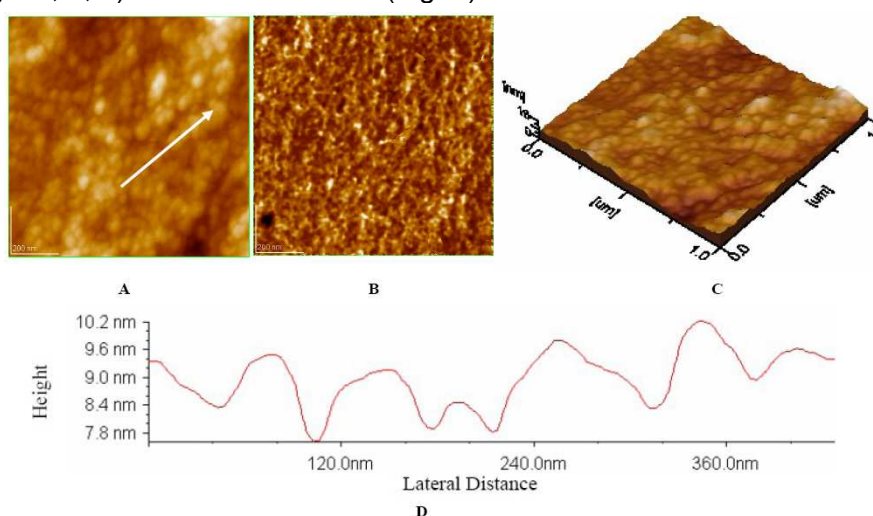


Fig. 1. Collagen film on glass, zone 1. A) 2D – topography B) phase image C) 3D-topography, D) profile of the cross section along the arrow in Fig. 1A. Scanned area: $1 \mu\text{m} \times 1 \mu\text{m}$.

The topographic images of the nanostructured pure COL film, present the self-organization of the COL molecules as rows, linear or curved (Figs. 1A, 2A, 3A), or assembled in star-shaped configurations (Fig. 4A). The organization of COL molecules is observed in the phase images, namely in linear rows (Figs. 1B, 2B), in round forms or circles (Fig. 3B), or star-shaped (Fig. 4B). Similar structures are also observed in 3D-topographies (Figs. 1C - 4C).

From the cross-section profiles (Figs. 1D, 3D, 4D) one can identify formations of COL fragments about 60-70 nm in length (Fig. 1D), in good agreement with literature data, where a 67 nm size is reported for the ordered regions, axially repeated on the collagen micro-fibrils [19]. The height of collagen formations in the outermost film is in the range from 1.4 to 1.6 nm (Figs. 1D-4D), in good agreement with the 1.5 nm value reported in literature [7, 8, 19] for the diameter of the collagen molecule (triple helix).

The film roughness (Table 1) estimated from the cross sections profiles (Figs. 1D-4D) presents low values, between 0.4 and 0.6 nm, suggesting a high supramolecular organization in the surface of the COL

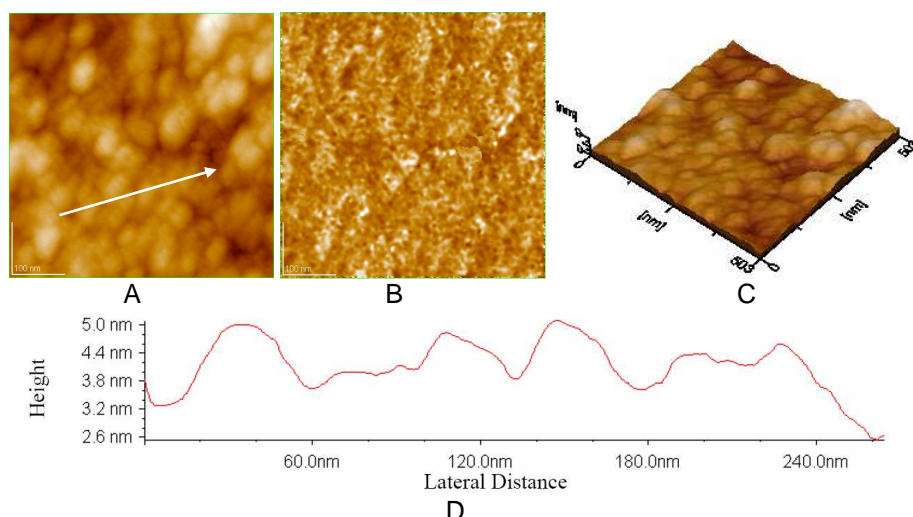


Fig. 2. Collagen film on glass, zone 1: A) 2D – topography B) phase image C) 3D-topography, D) profile of the cross section along the arrow in Fig. 2A. Scanned area: 0.5 μm x 0.5 μm .

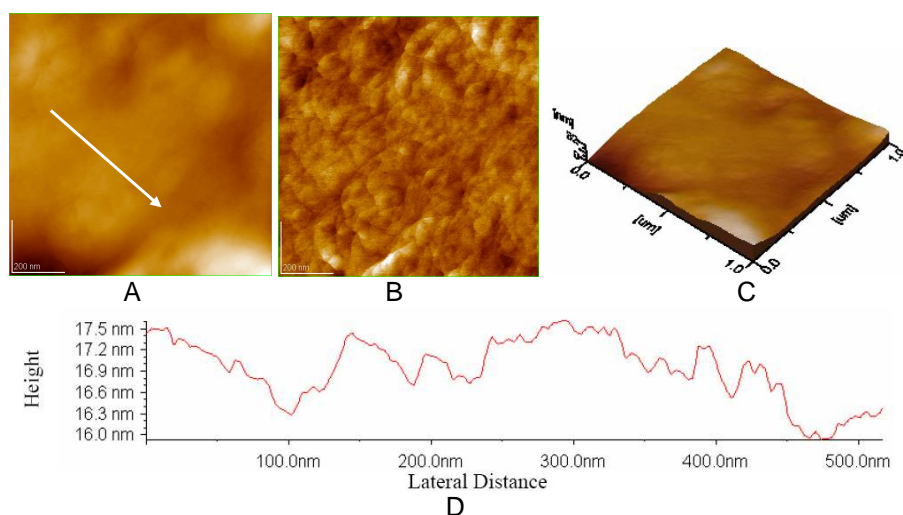


Fig. 3. Collagen film on glass, zone 2: A) 2D – topography B) phase image C) 3D-topography, D) profile of the cross section along the arrow in Fig. 3A. Scanned area: 1 μm x 1 μm .

film deposited on glass. By the examination of the profile in Fig. 3D, large supramolecular associates up to 300 nm are visualized, formations referred as tropocollagen or simply collagen monomer. The collagen fragments are much shorter. The disposition of collagen fragments or collagen monomers can be linear, ramified or curved, even concentric.

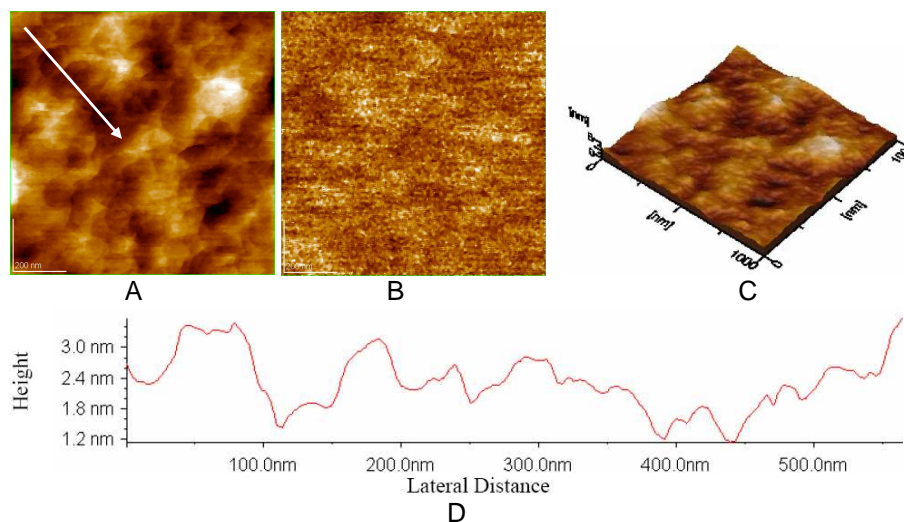


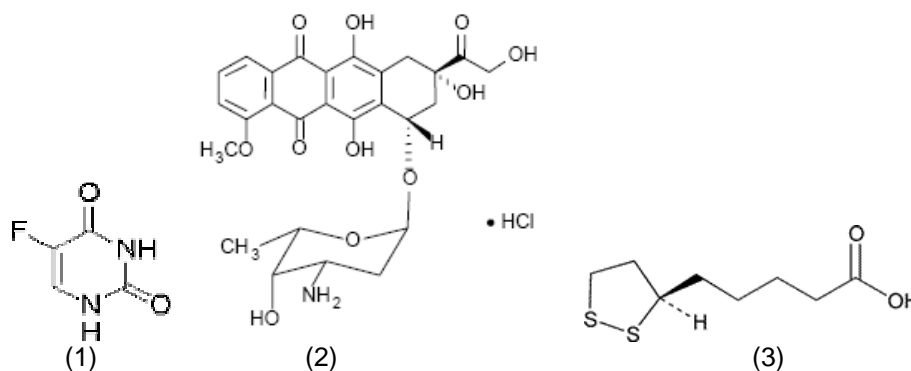
Fig. 4. Collagen film on glass, zone 3: A) 2D – topography B) phase image C) 3D-topography, D) profile of the cross section along the arrow in Fig. 4A. Scanned area: 1 μm x 1 μm .

The collagen fragments or monomers aggregate (associate) in a supramolecular lattice with an ordered zone of about 67 nm, axially repeated to finally form collagen assembly.

This complex morphology suggests that the self-assemblies can order themselves into various arrangements, even in linear or concentric features; they are not always parallel to one another and cannot retain the same neighbours among arrangements.

Self assembly of anticancer drugs

Three anti-cancer drugs are studied and their formulas are given in Scheme A.



Scheme A. Formulas of 5-fluorouracil (FLU, 1), doxorubicin-HCl (DOX, 2) and α -lipoic acid (LA, 3)

AFM images are given for the pure anti cancer drugs as follows: pure fluorouracil (FLU) film (Fig. 5), deposited on glass from a 10^{-4} M solution in ethanol:water, by adsorption, for a scanned area $1 \times 1 \mu\text{m}^2$; AFM images for the doxorubicin, (DOX film) are presented in Fig. 6. Finally, Fig. 7 shows the lipoic acid (LA) film, also deposited on glass from its ethanolic solution.

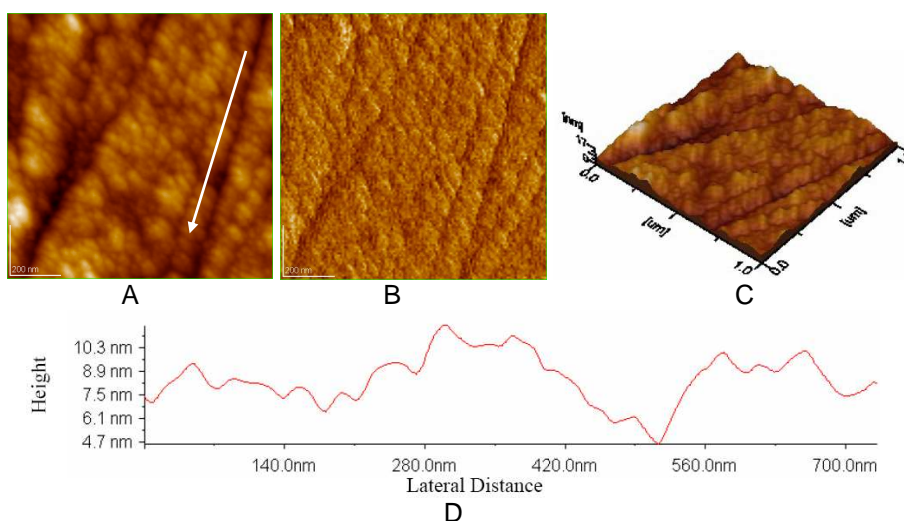


Fig. 5. Fluorouracil film on glass: A) 2D – topography; B) phase image; C) 3D-topography; D) profile of the cross section along the arrow in Fig. 5A. Scanned area: $1 \mu\text{m} \times 1 \mu\text{m}$.

The topographic images corresponding to the nanostructured films of 5-fluorouracil indicate the self aggregation of FLU molecules in self-associations, in long parallel rows, apparently close-packed, as visualized in Fig. 5A. DOX molecules aggregates present a rather round shape, with a slight tendency to row arrangements (Fig. 6A).

As for the lipoic acid (LA) film, it shows an association in large aggregates, arranged in distant rows (Fig. 7A). The phase images (Fig 5B-7B), the 3-dimensional images (Figs. 5C-7C), as well as the cross sections profiles (Figs. 5D-7D) support the arrangements of supramolecular aggregates, as described by the topographic images (Figs. 5C-7C). The roughness of anti-cancer drugs films, as described by the rms values on the film surface (Table 1) is about 2.5 nm (FLU), 3.8 nm (DOX) and 1.4 nm (LA), and on the cross section profile 1.5 nm (FLU), 0.9 nm (DOX) and 0.8 nm (LA). It seems that FLU, DOX and LA films generally present a somewhat higher roughness than collagen films.

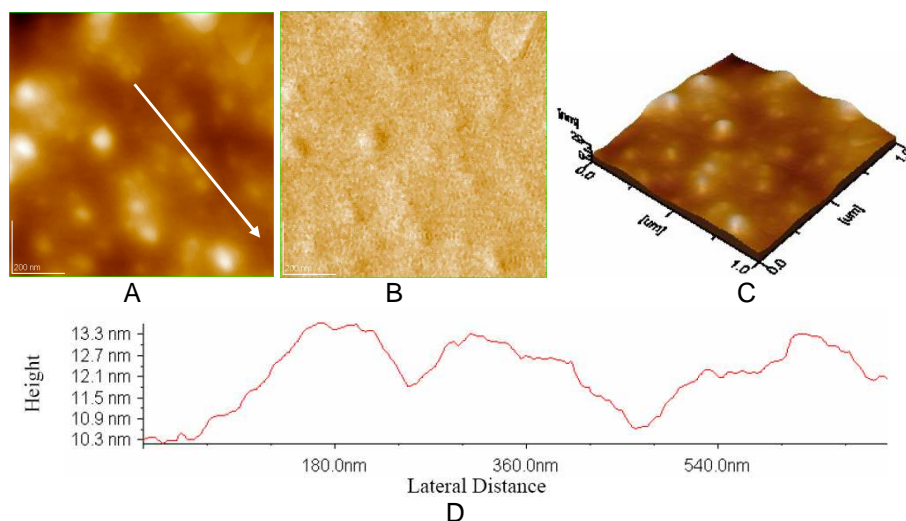


Fig. 6. Doxorubicin film on glass: A) 2D – topography; B) phase image; C) 3D-topography; D) profile of the cross section along the arrow in Fig. 6A. Scanned area: $1\ \mu\text{m} \times 1\ \mu\text{m}$.

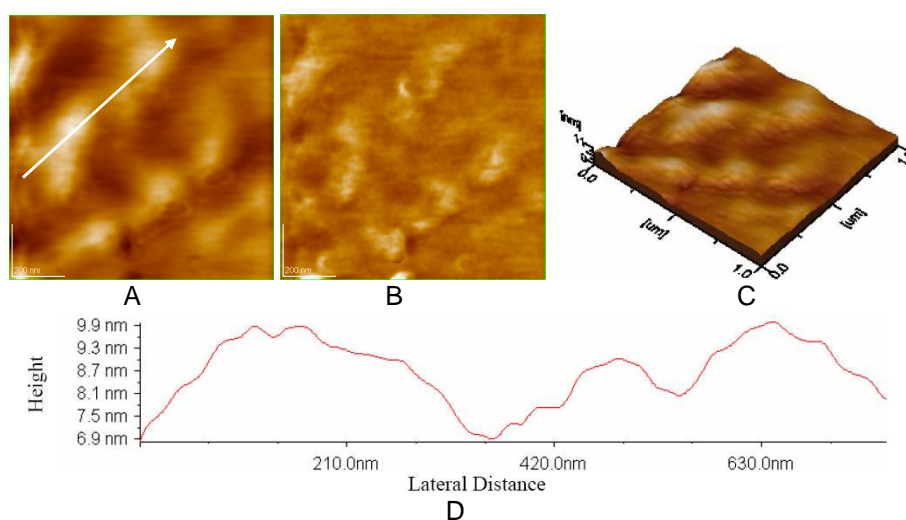


Fig. 7. Lipoic acid film on glass: A) 2D – topography; B) phase image; C) 3D-topography; D) profile of the cross section along the arrow in Fig. 7A. Scanned area: $1\ \mu\text{m} \times 1\ \mu\text{m}$.

Nanostructured organization of collagen and anti cancer drugs

In Fig. 8 AFM, images are given for the *mixed COL + FLU film*, deposited on glass from the liquid mixture, (see the experimental part), for a scanned area of $1 \times 1 \mu\text{m}^2$. Similarly, in Fig. 9, AFM images for the *COL + DOX film*, deposited on glass from the mixture of solutions are given, while Fig. 10 presents the *COL + LA film*, also deposited on glass from their mixed solution.

Fig. 8 (A, C) allows us to state that mixed COL+FLU films present an advanced fibril structure long over $1 \mu\text{m}$ and with a width over $0.5 \mu\text{m}$, while the height fluctuates between 1.5 and 3.5 nm.

From Fig. 9 (A, C) it is evident that mixed COL+DOX films show a different structure than the pure DOX film (Fig. 6) or the pure COL film (Fig. 1-4). In these figures we observe the presence of domains formed by high, rounded supramolecular associations, showing an apparent hexagonal packing. These domains are about $0.3 \mu\text{m}$ long and present a nanostructure, consisting of spherules about 60-70 nm in diameter. Between the domains there are bondings through these isolated spherules.

The phase image in Fig. 9B indicates a rather uniform film, compact and with a good adherence to the glass support.

The mixed COL+LA film in Fig. 10 (A, B, C) presents a homogeneous structure, quite different from that of the COL+FLU film (Fig. 8) and the COL+DOX film (Fig. 9). The LA molecule includes a ring, containing two sulphur atoms and a hydrocarbon chain, presenting a carboxyl group (see formula). The completely different structure built up by

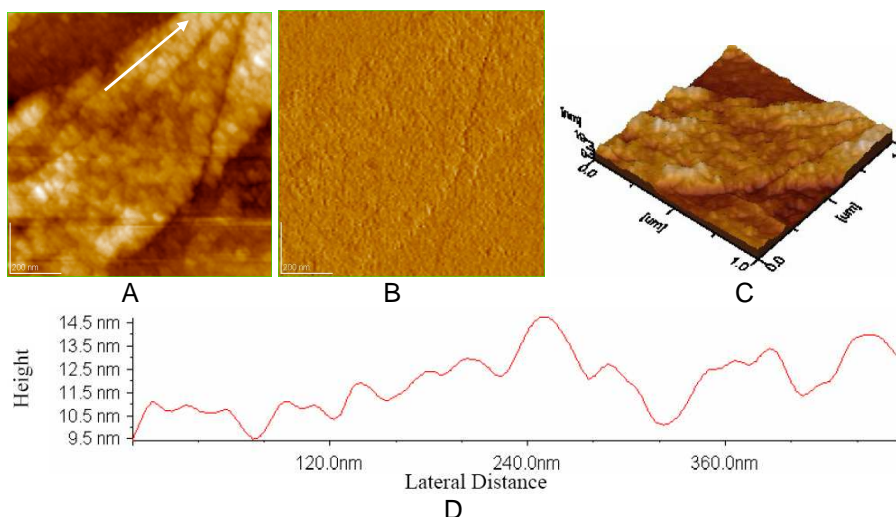


Fig. 8. Collagen with 5-fluorouracil film on glass: A) 2D – topography; B) phase image; C) 3D-topography; D) profile of the cross section along the arrow in Fig. 8A. Scanned area: $1 \mu\text{m} \times 1 \mu\text{m}$.

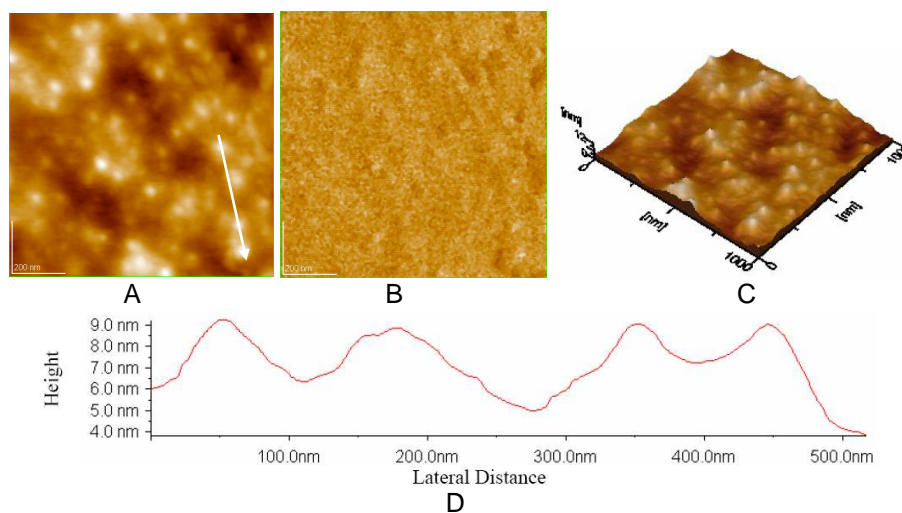


Fig. 9. Collagen with doxorubicin film on glass: A) 2D – topography; B) phase image; C) 3D-topography; D) profile of the cross section along the arrow in Fig. 9A. Scanned area: 1 μm x 1 μm .

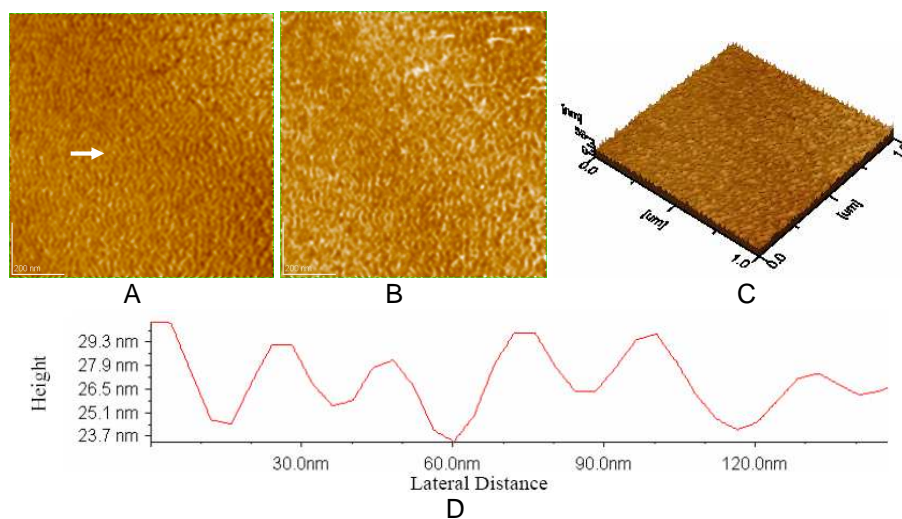


Fig. 10. Collagen with lipoic acid film on glass: A) 2D – topography; B) phase image; C) 3D-topography; D) profile of the cross section along the arrow in Fig. 10A. Scanned area: 1 μm x 1 μm .

Table 1.

RMS values for collagen and collagen mixtures with anti cancer drugs, from AFM cross sections on glass, as a measure for surface roughness of the films

Fig.	Sample	Support	RMS area, nm	RMS profile, nm
1	Collagen 1/1 μm , zone 1	glass	1.8	0.6
2	Collagen 0.5/0.5 μm , zone 1	glass	1.3	0.6
3	Collagen 1/1 μm , zone2	glass	1.0	0.4
4	Collagen 1/1 μm , zone 3	glass	1.1	0.5
5	5-Fluorouracil 1/1 μm	glass	2.5	1.5
6	Doxorubicin 1/1 μm	glass	3.8	0.9
7	Lipoic acid 1/1 μm	glass	1.4	0.8
8	Collagen + 5-Fluorouracil, 1/1 μm	glass	3.4	1.2
9	Collagen +Doxorubicin,1/1 μm	glass	1.9	1.4
10	Collagen + Lipoic acid, 1/1 μm	glass	3.3	1.7

LA with COL in comparison to COL+FLU or COL+DOX could be caused by the specific interaction between LA and COL, leading to the LA spreading on the COL surface, filling out the gaps between the COL fragments and building on oriented LA film on the COL surface. An arrangement of this kind could explain the greater thickness of the mixed COL+AL film against the COL+FLU or COL+DOX films. But this assumption will be verified, in future studies, by building a system containing a COL layer with a superposed LA layer. From the cross section profile (Fig. 10 D), domains are evidenced of about 35-40 nm width and about 3.5 - 4.2 nm high. We also suggest that in the COL+FLU and COL+DOX systems there are specific lateral interactions between components.

Thus, the supramolecular organization of collagen molecules in presence of anti-cancer drugs molecules shows that the anti-cancer drug is strongly bound to collagen fragments. We suggest that the binding between collagen and anti-cancer drug takes place through molecular recognition between the least ordered zone of collagen, named telopeptides, and anti-cancer drug leading to more ordered mixed networks.

CONCLUSIONS

The present study confirms the formation of supramolecular associations and their assembly in nanostructured collagen films deposited on glass support, both in pure state and mixed with anti-cancer drugs: FLU, DOX and LA. The specific interactions between the molecules in the oriented films on glass support could be explained by electrostatic interactions coupled

with molecular recognition interfacial phenomena. Evidently, the formation of hydrogen bonds between the anti-cancer drugs and the collagen matrix is also essential for the stability of the mixed networks observed in AFM images.

This investigation is the basis for future investigations on various collagen structures in different conditions, with the aim to find out the formation of self assemblies and how they could be used in nanotechnology and nanomedicine.

ACKNOWLEDGEMENT

This research was financially supported by the project 1621 /2007.

REFERENCES

1. M. Tomoaia-Cotisel, "The nanostructure formation of the globular seed storage protein on different solid surfaces studied by atomic force microscopy", In *Convergence of Micro-Nano-Biotechnologies*, Series in *Micro and Nanoengineering*, Vol. 9, Editors: Maria Zaharescu, Emil Burzo, Lucia Dumitru, Irina Kleps and Dan Dascalu, Romanian Academy Press, **2006**, Bucharest, pp. 147- 161.
2. M. Tomoaia-Cotisel, A. Tomoaia-Cotisel, T. Yupsanis, Gh. Tomoaia, I. Balea, A. Mocanu, Cs. Racz, *Rev. Roum. Chim.*, **2006**, *51*,1181.
3. O. Horovitz, Gh. Tomoaia, A. Mocanu, T. Yupsanis, M. Tomoaia-Cotisel, *Gold Bull.*, **2007**, *40*, 213.
4. J. T. Elliott, J. T. Woodward, A. Umarji, Y. Mei, A. Tona, *Biomaterials*, **2007**, *28*, 576.
5. M. Brama, N. Rhodes, J. Hunt, A. Ricci , R. Teghil, S. Migliaccio, C. Della Rocca, S. Leccisotti, A. Lioi, M. Scandurra, G. De Maria, D. Ferro, F. Pu, G. Panzini, L. Politi, R. Scandurra, *Biomaterials*, **2007**, *28*, 595.
6. S. Rammelt, T. Illert, S. Bierbaum, D. Scharnweber, H. Zwipp, W. Schneiders, **2006**, *27*, 5561.
- 7 E. Gurdak, P. G. Rouxhet, Ch. C. Dupont-Gillain, *Coll. Surf. B: Biointerfaces*, **2006**, *52*, 76.
8. C.C. Dupont-Gillain, I. Jacquemart, P.G. Rouxhet, *Coll. Surf. B: Biointerfaces*, **2005**, *43*, 178.
9. I.J.E. Pamula, V.M. De Cupere, P.G. Rouxhet, C.C. Dupont-Gillain, *J. Coll. Interf. Sci.*, **2004**, *278*, 63.

10. I.J.E. Pamula, V.M. De Cupere, Y. F. Dufrene, P.G. Rouxhet, *J. Coll. Interf. Sci.*, **2004**, 271, 80.
11. F.A. Denis, P. Hanarp, D.S. Sutherland, J. Gold, C. Mustin, P.G. Rouxhet, Y.F. Dufrene, *Langmuir*, **2002**, 18, 819.
12. V.M. De Cupere, P.G. Rouxhet, *Surface Sci.*, **2001**, 491, 395.
13. K. Kato, G. Bar, H.-J. Cantow, *Eur. Phys. J.*, **2001**, E6, 7.
14. R. Usha, R. Maheshwari, A. Dhathathreyan, T. Ramasami, *Coll. Surf. B: Biointerfaces*, **2006**, 48, 101.
15. K. Poole, K. Khairy, J. Friedrichs, C. Franz, D. A. Cisneros, J. Howard, D. Mueller, *J. Mol. Biol.*, **2005**, 349, 380.
16. Y.F. Dufrene, T.G. Marchal, P.G. Rouxhet, *Langmuir*, **1999**, 15, 2871.
17. I. Bratu, M. Tomoaia-Cotisel, G. Damian, A. Mocanu, *J. Optoelectron. Adv. Mat.*, **2007**, 9, 672.
18. M. Tomoaia-Cotisel, A. Mocanu, N. Leopold, M. Vasilescu, V. Chiş, O. Cozar, *J. Optoelectron. Adv. Mat.*, **2007**, 9, 637.
19. Gh. Tomoaia, M. Tomoaia-Cotisel, A. Mocanu, O. Horovitz, L.D. Bobos, M. Crisan, I. Petean, *J. Optoelectron. Adv. Mat.*, **2007**, in press.

In memoriam prof. dr. Ioan A. Silberg

REMOVAL OF NITRODERIVATES FROM SYNTHETIC WASTEWATERS BY ELECTROCHEMICAL REDUCTION

MIHAELA-CLAUDIA TERTIS, MARIA JITARU^a

ABSTRACT. The electrochemical reduction of 4-nitrophenol (4-NP) and 2,6-dinitrophenol (2,6-DNP) in different conditions (0.2N H₂SO₄ and 0.1 M NaCl aqueous solution) were studied in this work. In the case of 4-NP the cathodic materials were nickel and graphite, and the electrochemical reduction processes were performed in two different reactors (two compartment reactor type filter-press, and undivided electrochemical reactor, both with electrolyte recirculation). In the case of 2,6-DNP the cathode was made from graphite using two compartment reactor with electrolyte recirculation. The experimental processes were pursued by different methods: cyclic voltammetry (BAS100), and spectrophotometry in UV-Visible (Unicam Helyos B and DR/2000 HACH); $\lambda_{\max} = 318$ nm for 4-nitrophenol and $\lambda_{\max} = 440$ nm for 2,6-DNP. The experimental determinations demonstrated practically 65-99% removal yield for the both nitro derivatives, depending on the experimental conditions. The best result have been obtained, in the case of 4-NP, in undivided electrochemical reactor with graphite electrode (90% of 4-NP removal), and in the case of 2,6-DNP the final removal was of 99% in two compartment reactor with graphite cathode.

Keywords: 4-nitrophenol; 2,6-nitrophenol; electrochemical reduction; voltammetry.

INTRODUCTION

Phenolic compounds including nitrophenol are widely used in pharmaceutical, petrochemical, and other chemical manufacturing processes. Nitrophenols are considered as hazardous wastes and priority toxic pollutants by the U.S. Environmental Protection Agency [1]. The E.U. adopted Council Directive 67/544/EEC, classifying nitrophenols as toxic and dangerous for the environment. Due to its harmful effects, wastewaters containing phenolic compounds must be treated before being discharged to receiving water bodies. The secondary biological treatment processes are commonly used for domestic and industrial wastewaters, but they cannot treat phenolic

^a Associated Francophone Laboratory, Faculty of Chemistry and Chemical Engineering, Babes-Bolyai University, 11, Arany Janos, 400028, Cluj-Napoca, Romania, mjitaru@chem.ubbcluj.ro

wastewaters at high concentrations successfully. Moreover, widely used organophosphorus pesticides yield nitrophenols as the initial and major degradation product [2]. Therefore, new treatment technologies are still constantly researched and developed. Research efforts include biological degradation, chemical oxidation, solvent extraction, electrochemical treatment, and adsorption [3]. It is therefore important to assess the fate of these compounds in the environment and develop effective methods to remove them from water. The electrochemical treatment of waste water can be an interesting alternative to the chemical treatment for water containing toxic or non-biodegradable compounds.

Nitroaromatic compounds undergo reductive transformation to aromatic amines. The reduction of nitroaromatics occurred through a series of electron-transfer reactions and protonations, with nitroso compounds and hydroxylamines as highly reactive intermediates. In the case of polynitroaromatic compounds, the location of the first nitro group reduced is influenced by regioselectivity [4].

The electrochemical reductions of nitrophenols were studied in aprotic solvents, such as DMF (N,N-dimethylformamide) [5], and DMSO (dimethylsulphoxide) [6, 7], but they have mainly been studied in protic solvents [8]. Even in so-called "aprotic" solvents, the radical anion of 4-NP is unstable, due to the acidic nature of the parent molecule, giving rise to a self protonation reaction, which is a very rapid step [9]. In literature is proposed a reaction mechanism for the reduction of 4-NP in DMSO, which give the nitrosophenol as the final product, which in this environment is thought to undergo further follow-up chemistry to yield 4-aminophenol (a 6 electrons transfer reaction) [6].

The dinitrophenols have been determined by cyclic voltammetry and differential pulse voltammetry on the base of an irreversible reduction peak [11]. The first peak height was correlated with the pulse amplitude (correlation coefficient of 0.997) and there was also an increase of the peak potential with the pulse amplitude [12], in agreement with a practically irreversible behaviour.

The aim of this paper is to reduce the concentration of some nitrophenols like as: 4-nitrophenol (4-NP), 2,6-dinitrophenol (2,6-DNP) from synthetic wastewaters, in the concentration range 10^{-5} - 10^{-2} M, on nickel and graphite cathodes.

RESULTS AND DISCUSSIONS

Voltamperometric behaviour of 4-NP and 2,6-DNP

4-NP (Fig.1.a.) and 2,6-DNP (Fig.1.b.) present classical voltamperometric behavior characteristic for nitro derivatives. Due to the different reactivity of the two nitro groups, in the case of 2,6-DNP, two well separated ($\Delta E = 300$ mV) reduction peaks have been obtained (Fig.1b).

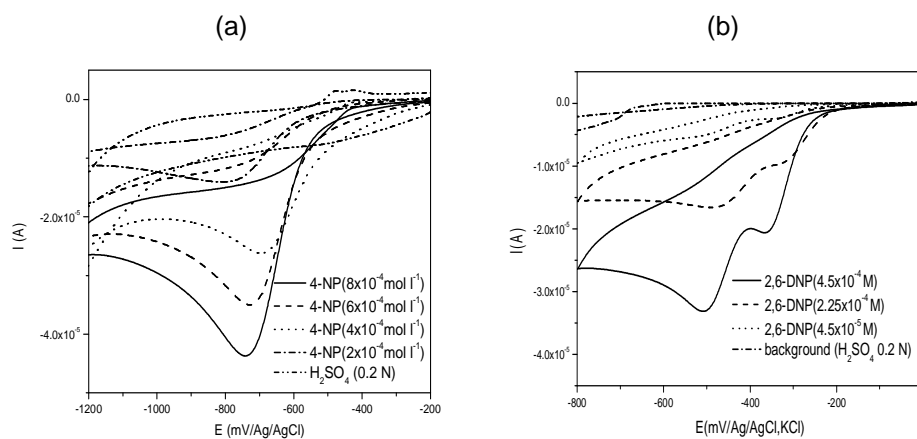
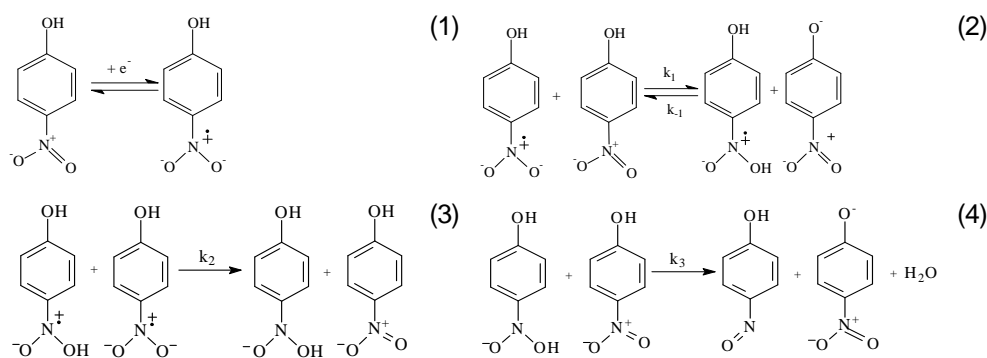


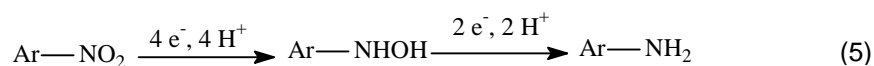
Figure 1. Cyclic voltammograms for: **(a)** 4-NP solutions at different concentrations, in 0.2N H₂SO₄; **(b)** 2,6-DNP solutions at different concentrations, in 0.2N H₂SO₄; WE: GC; RE: Ag/AgCl,KCl; CE: Pt; v : 50mV s⁻¹; s: 10 μA V⁻¹.

The radical anions of nitrophenols are unstable due to a fast self protonation reaction [10]. As it was expected, in protic medium the formation of radical anions during the first monoelectronic charge transfer is not easy to mark out, both for 4-NP and 2,6-DNP.



Scheme 1. Reaction scheme proposed for the reduction of 4-NP [10].

The 4e⁻ reduction of nitro group to the corresponding hydroxylamine, Fig.1, is the representative intermediary step in the electroreduction to amines, reaction 5.



We can see from the examples in figure 2, that the reduction of 4-NP on glassy carbon takes place easier ($E = -0.5 \text{ V/Ag/AgCl,KCl}$) comparing to Ni electrode ($E = -0.88 \text{ V/Ag/AgCl,KCl}$). On Ni the potential is displaced to more negative values, but the involved current is more important, probably because the competitive reduction with electrochemically generated active hydrogen is also possible [13].

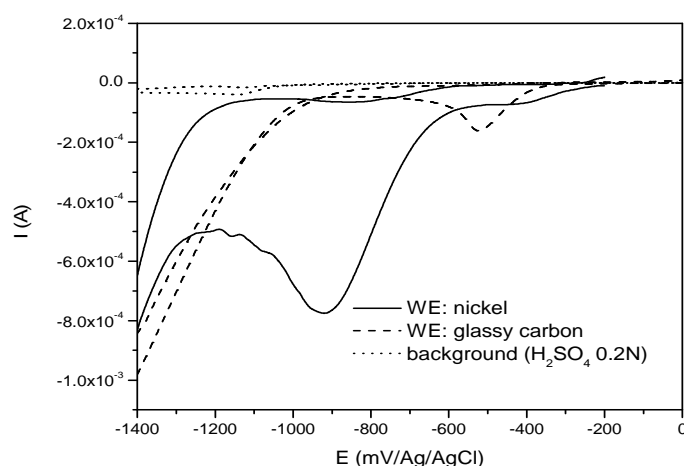


Figure 2. Cyclic voltammograms for a (10^{-2} M) 4-NP solution in $0.2\text{N H}_2\text{SO}_4$ WE: GC and Ni; RE: Ag/AgCl,KCl; CE: Pt; $v : 50\text{mV s}^{-1}$; $s : 100 \mu\text{A V}^{-1}$.

The reduction potential strongly depends on pH, both for 4-NP and 2,6-DNP. The first peak potential, E_{p1} for 2,6-DNP, shows two linear regions with different slopes, corresponding to an acid behavior specific to nitrophenols values ($\text{pK}_a = 4\text{-}5$), figure 3.a.

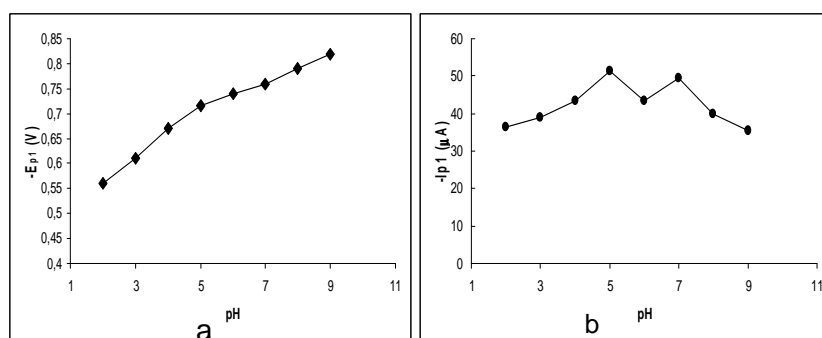


Figure 3. The variation of: **(a)** the first reduction peak potential (E_{p1}); **(b)** current intensity, with the pH, for a $4.5 \times 10^{-4} \text{ M}$ 2,6-DNP solution in Britton-Robinson buffer at different pH values WE: GC; RE: Ag/AgCl,KCl; CE: Pt; $v : 50\text{mV s}^{-1}$; $s : 10 \mu\text{A V}^{-1}$.

The reduction current at $-350\text{mV}/\text{Ag}/\text{AgCl}, \text{KCl}$ corresponding to the first electrochemically active nitro group, reaches the maximum value at $\text{pH} = 5\text{--}7$, figure 3b. The same behaviour is also presented in literature for other dinitrophenols [14].

The variation of the peak intensity with the scan rate was studied. An approximately linear relationship was found between the reduction peak intensity and the square root of the scan rate, both for 4-NP (Fig.4a) and for 2, 6-DNP (Fig.4b). The peak potentials were found to move slightly more negative when the scan rate increased in agreement with the irreversible behavior of these substances.

Electrochemical reduction of 4-nitrophenol in electrochemical two compartment micro flow cel (A)

In figure 5 is presented the variation of the reduction peak current for the electrochemical reduction process for 4-NP solution, in electrochemical two compartment micro flow cell (A).

The reduction peak decreases during the electrochemical reduction of 10^{-3} M 4-NP, with 94% in 90 minutes of galvanostatic electrolyse ($i = 20\text{ mA cm}^{-2}$), (theoretical calculated time is 75 minutes, so it was used 120% of theoretical necessary time); the electrochemical reduction yield is 80%, Fig. 5.

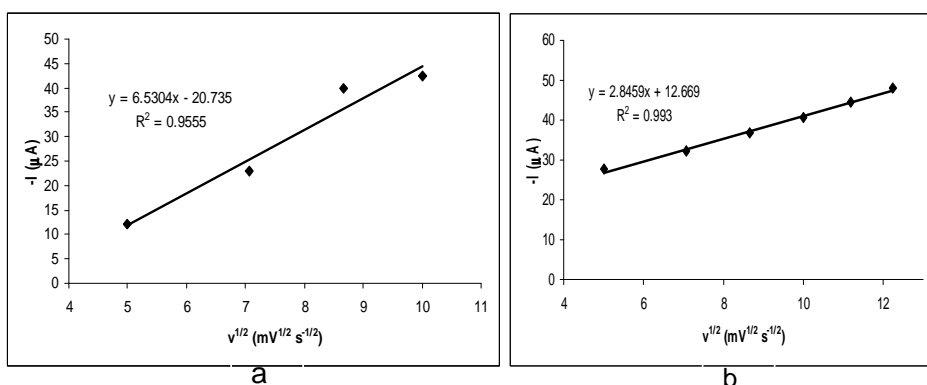


Figure 4. The variation of current with the square root of the scan rate for: **(a)** 10^{-3} M 4-NP and **(b)** $4.5 \times 10^{-4}\text{ M}$ 2, 6-DNP solutions in $0.2\text{N H}_2\text{SO}_4$; WE: GC; RE: $\text{Ag}/\text{AgCl}, \text{KCl}$; CE: Pt; v : 50mV s^{-1} ; s : $10\text{ }\mu\text{A V}^{-1}$.

The removal of 4-NF is quite total after 75 minutes of electrolysis.

During electrolysis the solution becomes shining brown from colourless, probably due to the forming of some colored condensation products. This phenomenon was mentioned in other works [15, 16], and is in good agreement with the characteristic of 4-aminophenol, which was reported to be the most possible intermediate accumulated from the reduction of 4-NP.

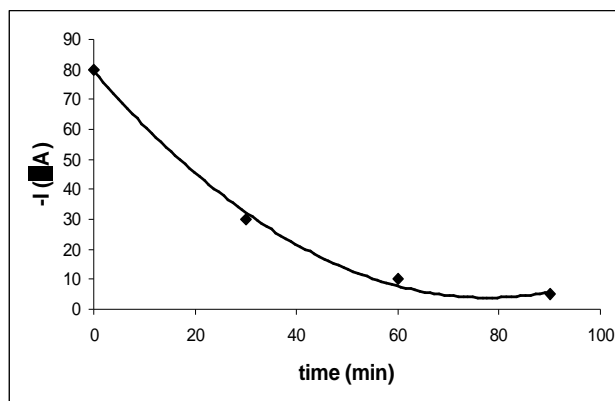


Figure 5. The variation of the reduction peak intensity at -0.9 V/Ag/AgCl,KCl, for 10^{-3} M 4-NP in 0.2 N H_2SO_4 , on Ni (experimental set-up A); $i: 20$ mA cm^{-2} ; WE: nickel; RE: Ag/AgCl,KCl; CE: Pt.

For future experiments it is wanted that the electrochemical reduction obtained products to be identified.

Electrochemical reduction of 4-nitrophenol in electrochemical mono-compartmented reactor with electrolyte recirculation (B)

In figure 6. it can be seen that, in case of electrochemical reduction of 10^{-2} M 4-NP in mono-compartmented reactor (B), the reduction peak intensity, which appears at approximate -0.9 V/Ag/AgCl,KCl, diminishes with approximately 90% comparative tot he initial value in 120 minutes, (theoretical calculated time is 100 minutes), so the electrochemical reduction yield is good enough.

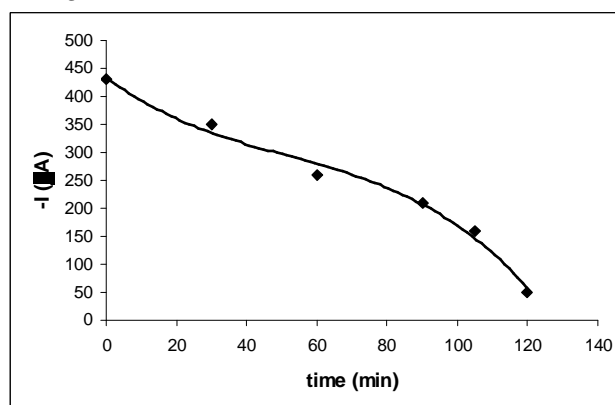


Figure 6. The variation of the reduction peak intensity during electrochemical reduction process for 10^{-2} M 4-NP in 0.2 N H_2SO_4 , on graphite cathode (experimental set-up B); $i: 20$ mA cm^{-2} .

The decrease of the reduction current corresponding to reaction (5) during electrolysis can be used to appreciate the electrochemical removal of 4-NP and 2,6-NP because, for both, quasi-linear variation with the concentration for large concentration range (from 10^{-5} to 10^{-2} M) was found (relations 6 and 7):

$$I_{\text{red}} = 0.5395 \cdot C_{4\text{-NP}}; R^2 = 0.9506 \quad (6)$$

$$I_{\text{red},1} = 0.6448 \cdot C_{2,6\text{-DNP}} + 0.4525; R^2 = 0.9953 \quad (7)$$

The removal on nitrophenols during electroreduction was demonstrated also by spectrophotometric determinations in UV-Visible, as the second method of determination.

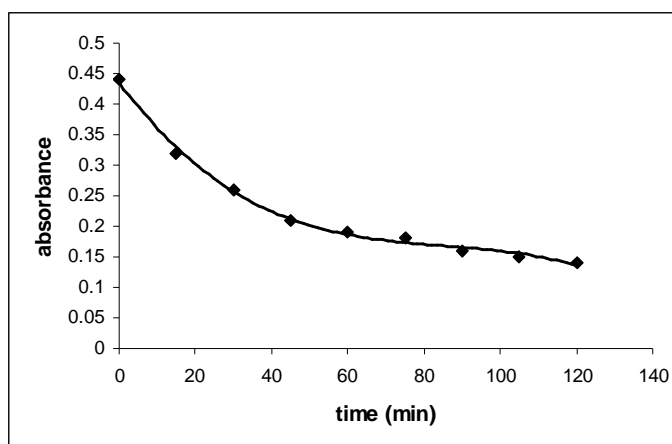


Figure 7. Spectrophotometric control of electrochemical reduction process for 10^{-2} M 4-NP in 0.2 N H_2SO_4 on graphite cathode (B); $\lambda_{\text{max}} = 318$ nm; $\log \epsilon = 3.87$.

The calibration curve for the 4-NP in 0.2N H_2SO_4 is: $A = 0.0923 \cdot C_{4\text{-NP}}$; $R^2 = 0.9839$; where: A is the absorbance of the 4-NP solution; $C_{4\text{-NP}}$ represent the concentration of 4-NP.

In figure7. it can be seen that, in case of electrochemical reduction of 10^{-2} M 4-NP on graphite cathode (experimental set-up B), the absorbance diminishes with approximately 70% comparative tot he initial value in 120 minutes. For the same experimental conditions, using the voltamperometric determination, figure 6, the decrease of the current was about 90%. This difference is probably due to the dyeing of the solution from colourless to brown, during the electrolyse, probably due to the chemical reactions of the electrogenerated species [15,16].

Electrochemical reduction of diluted solution (4.5×10^{-5} M) of 2,6-dinitrophenol

The electrochemical two compartmented reactor (experimental set-up C) has been used. As catholyte it was used 400 ml solution of 4.5×10^{-5} M of 2,6-DNP in aqueous solution of 0.1N NaCl, and as anolyte it was used 300 ml aqueous solution of 0.1N NaCl.

The absorbance of 2,6-DNP solution, figure 8, diminishes with approximately 75% in the first 15 minutes, comparative to the initial value, (theoretical calculated time is 20 minutes) and the discoloration is continuing (99% after 100 minutes).

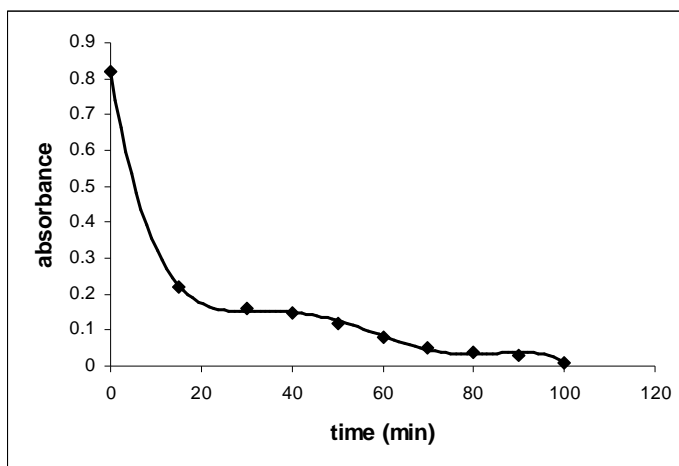


Figure 8. Spectrophotometric control of electrochemical reduction process for 4.5×10^{-5} M 2,6-DNP in (0.1N) NaCl, on graphite cathode (experimental set-up C). $\lambda_{\max} = 440$ nm; $\log \epsilon = 3.58$.

The summarized average results (two determinations for every case) are presented in Table 1.

Table 1.

Synoptic presentation of experimental determinations.

Experimental set-up	Treated nitrophenol	Cathodic material	Initial concentration (mol l^{-1})	Flow rate of recirculation (l min^{-1})	Nitrophenol removal (%)
A	4-NP	nickel	10^{-3}	3.3×10^{-3}	94.2
B	4-NP	graphite	10^{-2}	1.2	90.6
C	2,6-DNP	graphite	4.5×10^{-5}	1.4	99.0
	2,6-DNP	nickel	4.5×10^{-5}	1.4	98.8

CONCLUSIONS

Electrochemical removal of 4-NP and 2,6-DNP have been performed in different reactors, with different hydrodynamic conditions and using different type of electrodic material, with the aim to optimize the process.

The best results (99% removal) have been obtained in diluted solutions (10^{-5} mol l⁻¹). The nature of electrodes seems to be not very important but the high masse transfer (flow rate about 1 l min⁻¹), favorised the nitrophenols removal.

As perspectives, it is envisaged to perform some new electrochemical reduction experiments on 4-NP with the aim to settle the mechanism of electrodic processes, to optimize the experimental conditions for electrochemical reduction of 4-NP, to separate and to determine the products, and to extend the study on others mono and dinitrophenols.

EXPERIMENTAL SECTION

Reagents and solution preparation

4-NP with purity greater than 98% (Merk, Germany), and 2,6-DNP with purity greater than 95% (calculated based on dry substance), moistened with 20% H₂O (ALDRICH, Swizerland) were used to prepare the solutions, with desirable concentration, for the experiments in this study. Distilled water, in the case of 4-NP, and double distilled milliq water, in the case of 2,6-DNP, were used to prepare the aqueous solutions. For electrochemical determinations, the solutions were prepared using Britton – Robinson buffer (1:1:1 mixture of 0.04 M boric acid, phosphoric acid and acetic acid; the pH was adjusted to the right pH with 0.1 M NaOH and 0.2 N H₂SO₄).

Apparatus

The electrochemical experiments were carried out using three different experimental set-up. In the case of 4-NP the experiments were performed in an electrochemical filter press cell commercialised by Electrocell AB (Sweden) as the microflow cell equipped with an DSA-O₂ anode (20 cm² area), an nickel cathode (20 cm² area). Both compartments of the electrochemical cell are separated by a NAFION 350 millipore membrane. The electrochemical cell was inserted into a hydraulic circuit which comprises a GILSON MINIPULS 3 peristaltic pump forcing the circulation of the electrolyte in the compartments of the filter press cell, with flow rates in the range 1×10^{-6} to 3.3×10^{-3} l min⁻¹. The experimental setup (A) comprises two glass tanks containing anolyte and catholyte. The second experimental set-up (B) consist in a mono-compartment electrochemical reactor (with a capacity of 1500 cm³) equipped with a pump, which assure the electrolyte recirculation, with flow rate of 1.2 l min⁻¹, two stainless steel anodes (212.3 cm² area), and an graphite cathode (185.7 cm² area). In the case of 2,6-DNP the experimental set-up (C) consist in a glass

made electrochemical reactor, equipped with an Ti/Pt-Ir anode and a graphite cathode, both of 100 cm², a NAFION 117 millipore membrane, and a WATSON MARLOW Mod.313 F/D peristaltic pump with two heads, operating under conditions of full recycle, with flow rates in the range 0.09 to 1.4 l min⁻¹. In all experiments, the reactors were operated under galvanostatic conditions. Electrolysis efficiency was followed by regularly sampling the electrolyte and analysing the concentration of residual reagents, by voltammetric and spectrophotometric measurements.

Voltammetric measurements were made using a potentiostat-galvanostat system – BAS 100B (Bioanalytical Systems, USA) with the specific software BAS 100W and a classic three electrode electrochemical cell. The electrochemical cell is comprised of a cell bottom of 20 mL capacity and a plastic cell top. The experimental design consist of a platinum plate auxiliary electrode, an Ag/AgCl,KCl reference electrode; the working electrodes were glassy carbon and nickel (2 mm diameter), inserted through the cell top into the cell.

Spectrophotometric determinations were made using a Unicam Helyos B spectrophotometer with the specific software VISION 32, and a quartz vat of 2 ml, with optical route of 1 cm, and a Direct Reading Spectrophotometer type DR/2000 HACH with a glass vat of 25 ml, and with optical route of 2 cm.

The pH measurements for the solutions were made with a pH-meter Basic 20 from Crison.

REFERENCES

1. 4-nitrophenol, Health and Environmental Effects Profile No. 135, U.S. Environmental Protection Agency (EPA), U.S. Government Printing Office, Washington, DC, **1980**.
2. M. Castillo, R. Dominguez, M.F. Alpendurada, D. Barceló, *Analytica Chimica Acta*, **1997**, 353, 133.
3. J-M. Chern, Y-W. Chien, *Water Researche*, **2002**, 36, 647.
4. S.E. Barrows, C.J. Cramer, D.G. Truhlar M.S. Elovitz, E.J. Weber, *Environmental Science and Technology*, **1996**, 30, 3028.
5. C.L. Forryan, N.S. Lawrence, N.V. Rees, R.G. Compton, *Journal of Electroanalytical Chemistry*, **2004**, 561, 53.
6. C. Amatore, G. Copobianco, G. Farnia, G. Sandona, J.M. saveant, M.G. Severin, *Journal of American Chemical Society*, **1985**, 107, 1815.
7. G. Farnia, R. Da Silva, E. Vianello, *Journal of Electroanalytical Chemistry*, **1974**, 57, 191.
8. A.M Heras Caballero, J.L. Avila Manzano, L.C. Delgado, F.G. Blanco, *Afinidad*, **1986**, 43, 76.
9. R. Saraswathi, R. Narayan, *Journal Electrochemical Society, India*, **1990**, 39, 129.

10. D.S. Silvester, A.J. Wain, L. Aldous, C. Hardacre, R.G. Compton, *Journal of Electroanalytical Chemistry*, **2006**, 596, 131.
11. M.M. Cordero-Rando, I. Naranjo-Rodriguez, J.L. Hidalgo de Cisneros, *Analytica Chimica Acta*, **1998**, 370, 231.
12. C. Fernandez, E. Chico, P. Yanez-Sedeno, J.M. Pingarron, L.M. Polo, *Analyst*, **1992**, 117, 1919.
13. M. Noel, P. N. Anantharaman, H. V. K. Udupa, *Journal of Applied Electrochemistry*, **1982**, 12(3), 291.
14. J.D. Voorhies, R.N. Adams, *Analytical Chemistry*, **1958**, 30, 346.
15. S. Yuan, M. Tian, Y. Cui, L. Lin, X. Lu, *Journal of Hazardous Materials B*, **2006**, 137, 573.
16. N. Pradhan, A. Pal, T. Pal, *Colloid and Surfaces A*, **2002**, 247.

In memoriam prof. dr. Ioan A. Silberg

KINETIC STUDY OF CALCINATION FOR PRECIPITATE CALCIUM CARBONATE

SIMION DRĂGAN^a, ADINA GHIRIȘAN

ABSTRACT: In this paper, the calcination reaction of precipitate calcium carbonate (PCC) was investigated, using thermogravimetric analysis technique. All experiments were performed in isothermal conditions, within a temperature range of 1073-1223 K, with main diameters of granules between 0.063 mm and 0.45 mm. Two models were applied to the experimental results and it was found that the Avraami-Erofeev-Kolmogorov is the best model which has fitted the experimental data.

The equation of mathematical model is $\eta_D = 1 - e^{-k(T) \cdot \tau^{n(T)}}$ where $\ln k(T) = 5.674 - \frac{68226.3}{R \cdot T}$ and $n(T) = 0.0034 \cdot T - 2.4803$.

INTRODUCTION

Thermal decomposition of limestone has been the subject of many studies over the years due to its importance in the cement industry and in the flue gas desulphurization processes [1, 2]. For the reactive dry adsorption of sulfur dioxide from flue gases, the most used adsorbents are different assortments of natural and synthetic calcium carbonate: limestone, dolomite, lime, dolomitic lime and precipitate calcium carbonate. Under identical experimental conditions, the reactivity of these adsorbents is significantly influenced by their chemical structure and composition [3]. The optimal temperature for the dry injection of the adsorbent is a function of its origin, particle size and reaction type. Experimental determinations are always necessary in order to establish the optimal work conditions.

The mechanisms and the rate expression for the calcination reactions were analyzed extensively by many investigators and several models, such as shrinking core model, homogeneous reaction model, and structural models, which include grain models proposed for gas-solid reaction, were tested [4].

^a Babeș-Bolyai University, Faculty of Chemistry and Chemical Engineering, Arany Janos 11, 400028 Cluj-Napoca

Since the microstructure of the solid adsorbent has an important influence over its reactivity, a kinetic study of precipitate calcium carbonate (PCC) decomposition will be presented in this paper. The decomposition process was realized at temperatures between 1073 -1223 K and atmospheric pressure. Evolution of the decomposition degree during the heating and calcination intervals of the (PCC) sample for three granulometric classes was established.

RESULTS AND DISCUSSION

Evolution of the PCC decomposition for all grain sizes was followed by means of decomposition degree η_D . On the basis of the material balance, the decomposition degree η_D can be described by equation (1):

$$\eta_D = \frac{m_S^0 - m_S}{m_S^0 \cdot \bar{x}_{PC}^0} = \frac{1}{\bar{x}_{PC}^0} \left(1 - \frac{m_S}{m_S^0} \right) \quad (1)$$

where: m_S^0, m_S – initial and at a given moment sample mass [mg];

\bar{x}_{PC}^0 – mass fraction of the calcination losses (0,41427) determined as arithmetical average of four values obtained for four PCC samples subjected to calcination at 1323 K for two hours.

The obtained results are presented in figures 2, 3 and 4.

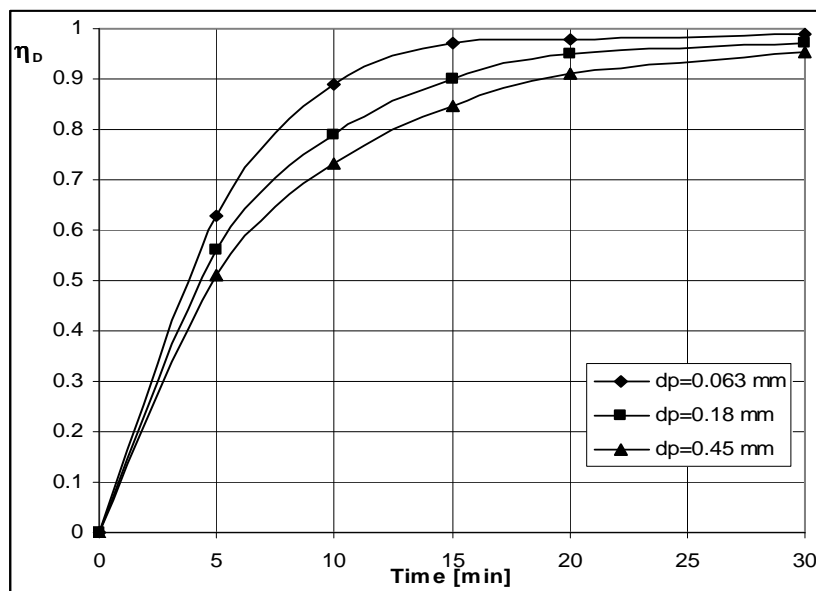


Fig. 2. Particles sizes influence over the decomposition degree of PCC CaCO_3 at $T_c=1173$ K.

KINETIC STUDY OF CALCINATION FOR PRECIPITATE CALCIUM CARBONATE

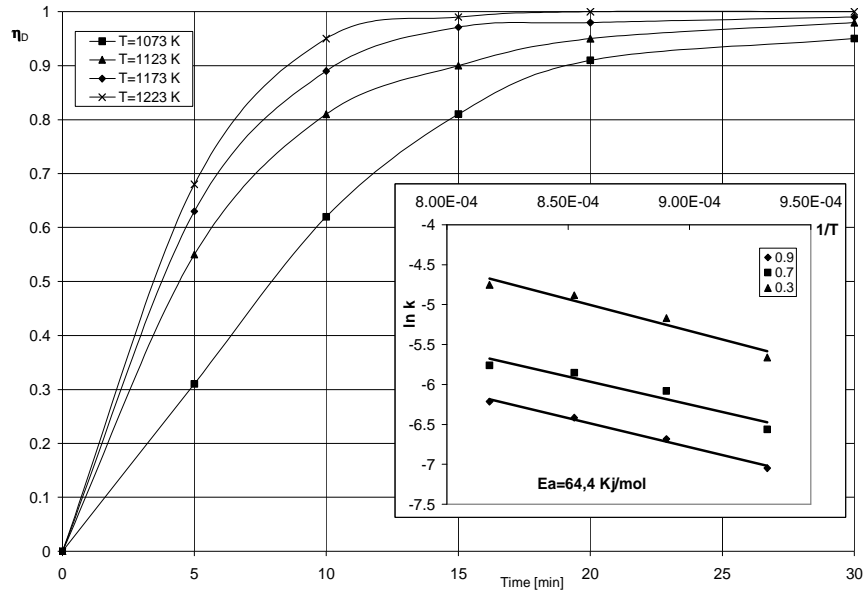


Fig. 3. Temperature influence over the decomposition degree of PCC granules with $d_p=0.063\text{mm}$.

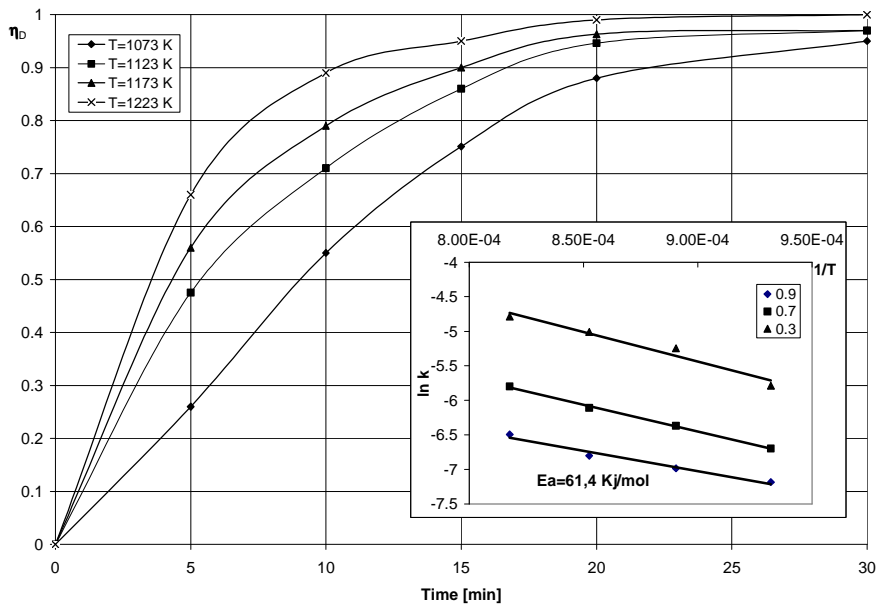


Fig. 4. Temperature influence over the decomposition degree of PCC granules with $d_p=0.18\text{mm}$.

The kinetic curves η_D - τ , plotted in figure 2 have shown a small influence of the grain size on the decomposition degree. The difference which appears between the studied samples was attributed to the different thermal conductivity of the granules layer in the nacelle. In all cases the decarbonation degree reached was higher than 0.95 at 30 minutes.

The results presented in figures 3 and 4 have shown significant influence on the decomposition degree for low temperature and large granule size. With an increase in temperature, the decomposition degree increases also, reaching values higher than 0.95.

The kinetic curves plotted in $\ln \tau^{-1}-1/T$ coordinates, figures 3 and 4 as picture in picture, led to linear Arrhenius dependences at different decomposition degrees for granules with $dp=0.063$ mm and $dp=0.180$ mm. The apparent activation energies evaluated from the slopes are between 61.4 and 64.4 kJ/mol, and indicate that decomposition of precipitate calcium carbonate is generally kinetically controlled.

Model of the real decomposition process. In order to establish the appropriate model which describes better the PCC decomposition process we used the unreacted shrinking core model and Avraami-Erofeev-Kolmogorov equation [5].

By processing experimental data obtained for granules with 0.063 mm in diameter, within the same experimental set, in specific coordinates for unreacted shrinking core model : $F(\eta_D)-\tau$ were $F(\eta_D)=1-(1-\eta_D)^{1/3}$ and in specific coordinate $\ln[-\ln(1-\eta_D)]-\ln \tau$ for Avraami-Erofeev-Kolmogorov (AEK) model $\eta_D = 1 - e^{-k(T) \cdot \tau^{n(T)}}$, we obtained the dependencies presented in figures 5 and 6.

In the figure 5 it is easy to see that the graphic dependences are not linear. This means that the transformation model was not validated by the experimental data, which demonstrates that the macrokinetic model, unreacted shrinking core, do not describes the process in the entire variation range of the decarbonation degree.

KINETIC STUDY OF CALCINATION FOR PRECIPITATE CALCIUM CARBONATE

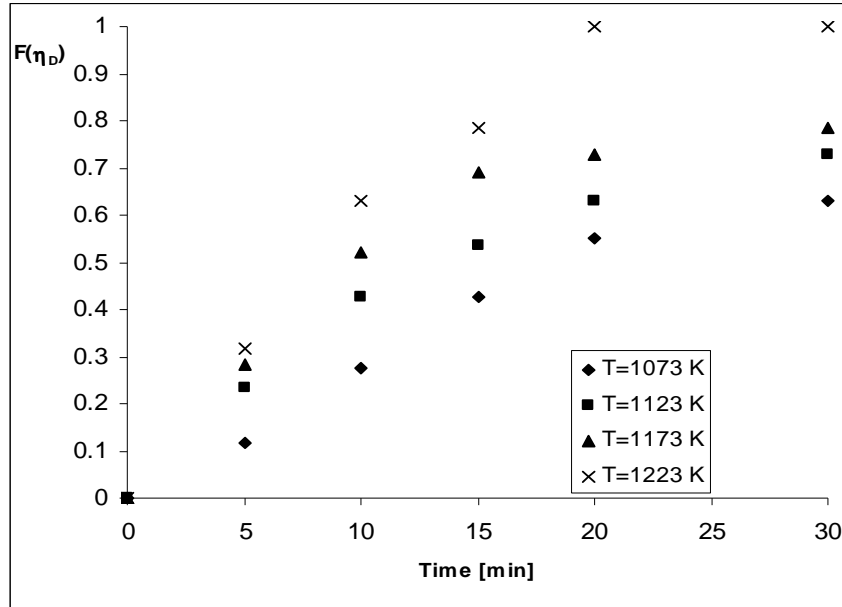


Fig. 5. $F(\eta_D)$ -time dependence for the unreacted shrinking core model for granules with $d_p = 0.063$ mm.

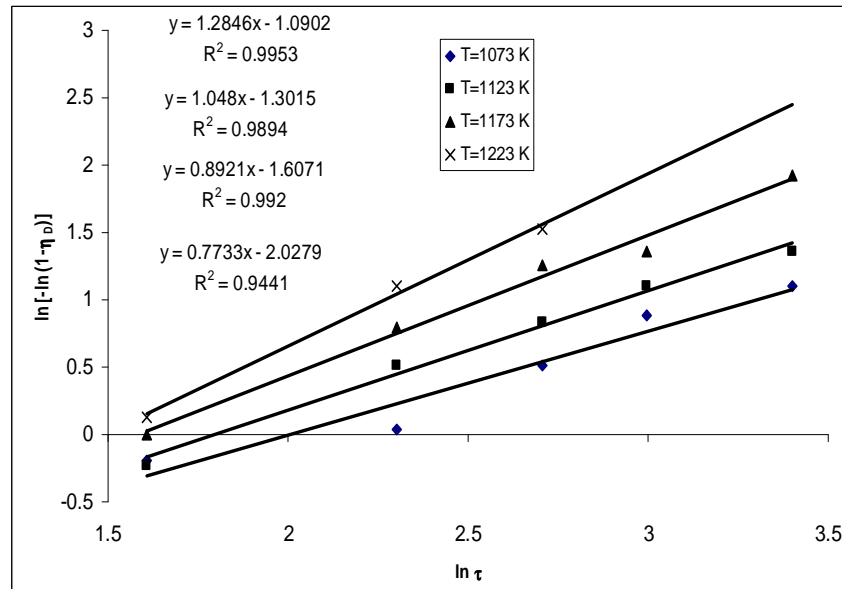


Fig. 6. $\ln[-\ln(1-\eta_D)]$ - $\ln \tau$ dependence for the PCC granules with $d_p = 0.063$ mm at different temperatures (AEK model equation).

Using graphical method to process the experimental results (η_D - τ), the dependence of the process rate constant $k(T)$ and of the kinetic order on temperature $n(T)$ with the temperature was established, figure 7 and figure 8:

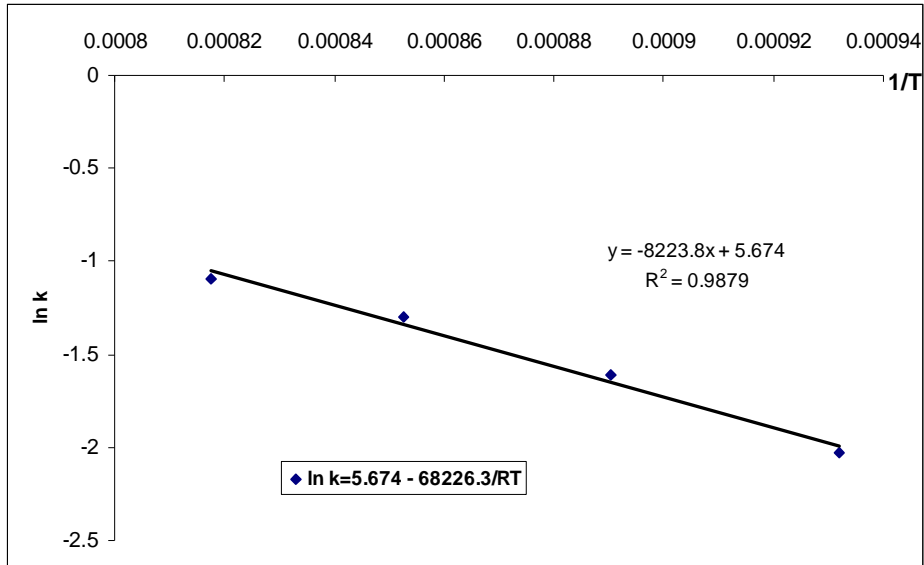


Fig. 7. $\ln k$ versus $1/T$ variation for PCC granules with $d_p=0.063$ mm.

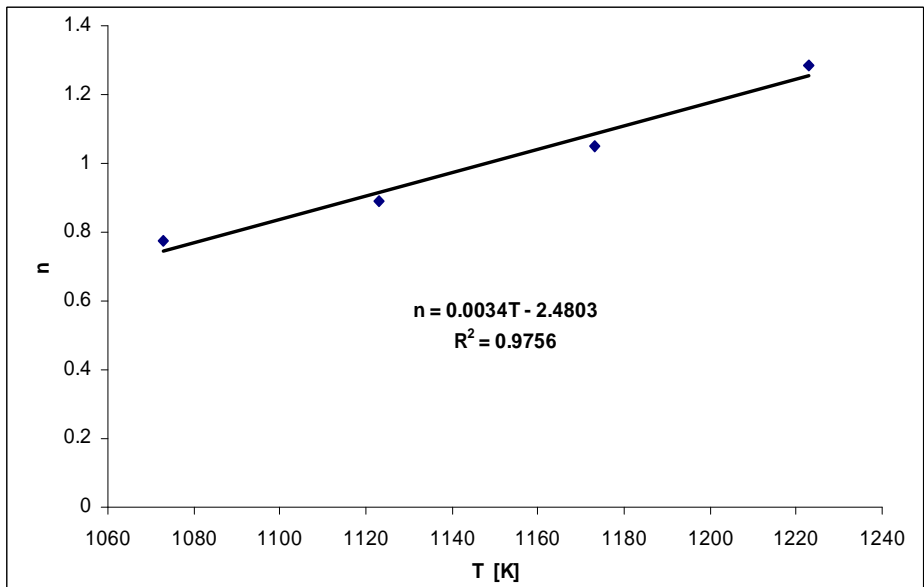


Fig. 8. n versus T dependence for PCC granules with $d_p=0.063$ mm.

For the decomposition of PCC granules having 0.063 mm in diameter, the mathematical equation model (2) was obtained:

$$\eta_D = 1 - e^{-k(T)\tau^{n(T)}} \quad (2)$$

where : $\ln k(T) = 5.674 - 68226.3/RT$ and $n(T) = 0.0034 T - 2.4803$

In figure 9 is presented the validation of the model with experimental data.

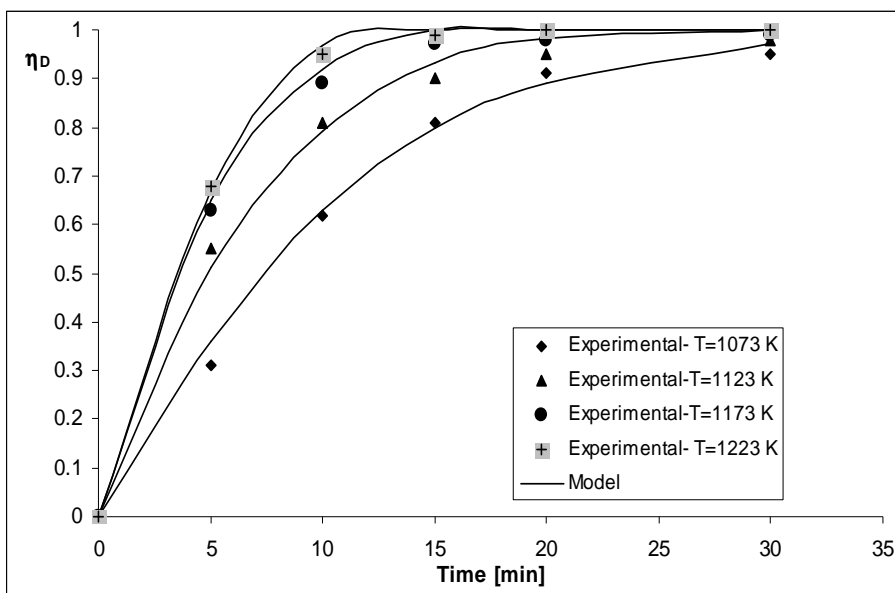


Fig. 9. AEK model validation.

The results given in figure 9 have shown that Avraami-Erofeev-Kolmogorov model describes the decomposition of precipitate CaCO_3 granules with $d_p=0.063$ mm in good agreement with experimental data. Standard deviation was in all cases less than 10%.

CONCLUSIONS

1. The results obtained have indicated that the effect of temperature in the case of PCC calcination is more significant than the grain size.
2. Apparent activation energy obtained, over 61.4 kJ/mol suggested that the global process of decomposition is kinetically controlled.
3. The results obtained during the calcinations process of PCC showed that the unreacted core model is not valid for the entire domain of the decarbonation degree values.

4. The equation of Avraami-Erofeev-Kolmogorov model can describe the real process of PCC decomposition with good precision; the standard deviations were less than 10%.

EXPERIMENTAL

In order to elucidate the effect of the temperature and grain size on the rate of the decomposition process, the isothermal gravimetric method was employed. The experiments were carried out on an experimental installation presented in figure 1.

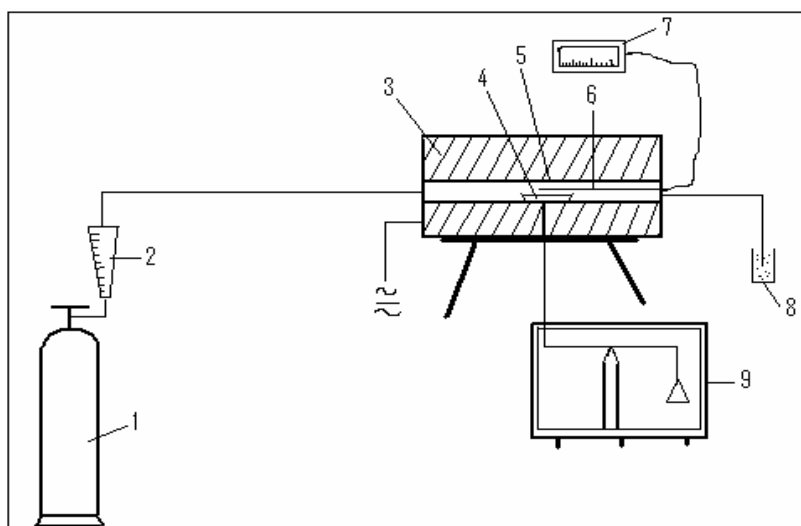


Fig. 1. Experimental set-up for PCC calcination
1-Gas cylinder with N_2 ; 2- Gas flow meter; 3- Electric Furnace; 4- Nacelle with solid sample; 5-Tubular reactor; 6- Thermocouple; 7- Temperature controller; 8- Absorbing vessel for gas ; 9- Thermo balance

This installation contains a hand-made thermo balance, having a 30 mm diameter tubular reactor placed in a tubular electric furnace, with possibilities to operate in temperature range of 373-1473 K. The solid reactant placed in thin layer on a ceramic nacelle, was introduced in the tubular reactor and the experiments were carried out isothermally within the temperature range of 1073-1223 K. We used samples of 0.4-0.5g (PCC) with main diameter of 0.063 mm, 0.18 mm and 0.45 mm. The granulometric classes of the particles in the considered samples were obtained by sizing of precipitate calcium carbonate with a Retzsch set of sieves, mesh between 0-1000 μm .

To evaluate the decomposition process in the time the variation of sample mass was determined every five minute.

REFERENCES

1. T.R. Rao, *Can. J. Chem. Eng.*, **1993**, 71, 481-484.
M.S. Murthy, B.R. Harish, K.S. Rajandam, K.Y.A.P. Kumar, *Chem. Eng. Sci.* **1996**, 51, 623.
2. S. Drăgan, M. Drăgan, *Stud. Univ. "Babes-Bolyai", Chemia* **2005**, 50 (1), 89.
3. I. Ar, G. Doğu, *Chem. Eng. J.* **2001**, 83, 131.
4. Al. Szép, Gh. Mihăilă, A.M. Busuioc, *Analele Științifice ale Universității „AL. I. Cuza” Iași, Seria Chimie, Tomul IX*, **2001**, 197.

In memoriam prof. dr. Ioan A. Silberg

ADHESIVE INFLUENCE MODELING ON DOUBLE-LAP JOINTS ASSEMBLIES

OVIDIU NEMEȘ^a

ABSTRACT. The paper presents a numerical analysis of metal-composites plane assemblies joined with adhesive. After the CAD model, constraints and applied load definition, we made a stress field analysis.

The aim of this work is to validate an analytical model, based on an energy method, developed by the author. Thus the analytical model makes it possible to determine the rigidity of the assembly and to obtain a simple formulation very rapidly which gives the total behavior of the assembly.

Keywords: *Stress Analysis, Adhesives, Numerical modeling*

INTRODUCTION

The adhesive bonded joints assembling method distributes the stresses over the whole joining surface and removes the stress concentrations to the boundary of holes generated by bolting or riveting assemblies. The mechanical performance of an adhesive bonded joint is related to the distribution of the stresses in the adhesive layer. Consequently it is essential to know this distribution, which, because of its complexity, makes prediction of fractures difficult.

From the first works of Volkersen [1] when only a distribution of the shear stress in the adhesive joint was taken into account to the more recent studies by finite elements, many formulations have made it possible to define the stress field in such assemblies better and better.

Following Goland and Reissner [2], Volkersen [3] introduced into his new analysis the normal stress "stress of shearing" (peeling stress) which is variable in the thickness of the adhesive layer. This assumption enabled him to build a stress field observing the boundary conditions of the assembly. However, due to the complexity and difficulty of its implementation, this analytical formulation is not easily applicable.

^a *Technical University of Cluj-Napoca, 105 Bd-ul Muncii, Cluj-Napoca, Romania*

Gilibert and Rigolot [4, 5] propose, based on the method of the asymptotic developments connected in the vicinity of the ends, an analytical formulation of the stress field over the entire covering length. If this formulation constitutes a clear improvement of the modeling of the field of the constraints on the level of the ends and represents experimental reality better, it is however not valid near the free edges.

Adams and Peppiatt [6], in their finite element analysis, circumvented this difficulty by studying a joint modified by the addition of a regularizing part. However even this study is not satisfactory on the level of the ends.

Tsai and Oplinger [7] develop the existing traditional solutions by the inclusion of shearing strains, neglected until there. The solutions obtained ensure a better forecast of the distribution and intensity of the shear stress.

Mortensen and Thomsen [8, 9] developed the approach for the analysis and the design of the adhesive bonded joints. They held into account the influence of the interface effects between the adherents and they modeled the adhesive layer by assimilating it to a spring.

Nemes [10, 11] use a technique based on the minimization of the potential energy. The first stage consists in building a statically acceptable stress field, i.e. verifying the boundary conditions and the equilibrium equations. Then, the potential energy generated by such a stress field is calculated. In the third stage, the potential energy is minimized in order to determine the stress distributions. As we have just seen, the analytical formulations and the finite element analysis provide a stress field satisfying for the median part of the joints. On the other hand, these two approaches provide results that do not satisfy the boundary conditions imposed at the ends of covering. The majority of the degradation phenomena are observed in the vicinity of joints end (non-linear behavior, damage, cracking, even fracture). The analytical study that follows gives a first solution of the stress field respecting the whole of these conditions.

RESULTS AND DISCUSSION

NUMERICAL MODELING BY FINITE ELEMENTS

1. Meshing and boundary conditions

The objective of this study is to compare our analytical models of the adhesive-bonded joints with models made of finite elements.

For the numerical analysis by finite elements of the adhesive-bonded joints, we used the computer code SAMCEF from SAMTECH®.

The diagram of the C.A.D., basis of the finite element model, is presented in figure 1. The diagram also describes the boundary conditions and the applied load.

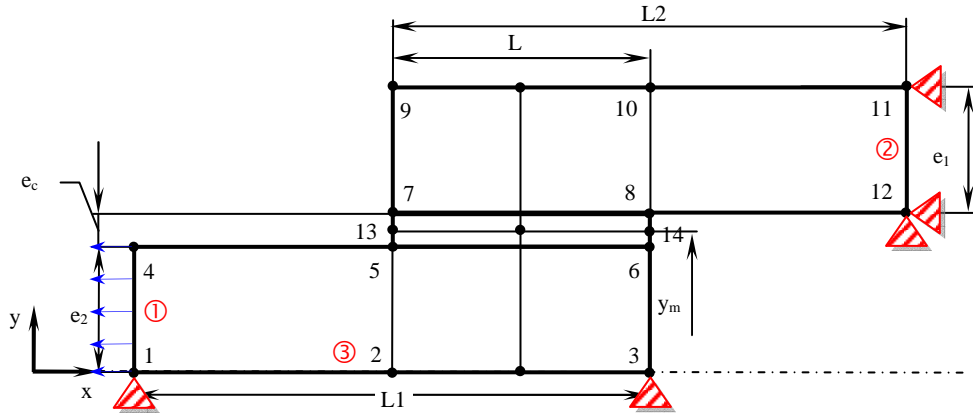


Figure 1. CAD diagram of a double-lap adhesive-bonded joint.

The double-lap assembly is modeled by 2D quadrangles of degree 2 and interface finite elements ($x \rightarrow z$, $y \rightarrow r$, $z \rightarrow \theta$). The displacements along x and y on face ② of the upper substrate and those along y on face ① of the lower substrate are blocked. The load is applied as a pressure on face ① (Figure 1).

Figure 2 shows an example of the grid used in this study where all the finite elements are quadrangles. We imposed ten finite elements in the to the adhesive layer.

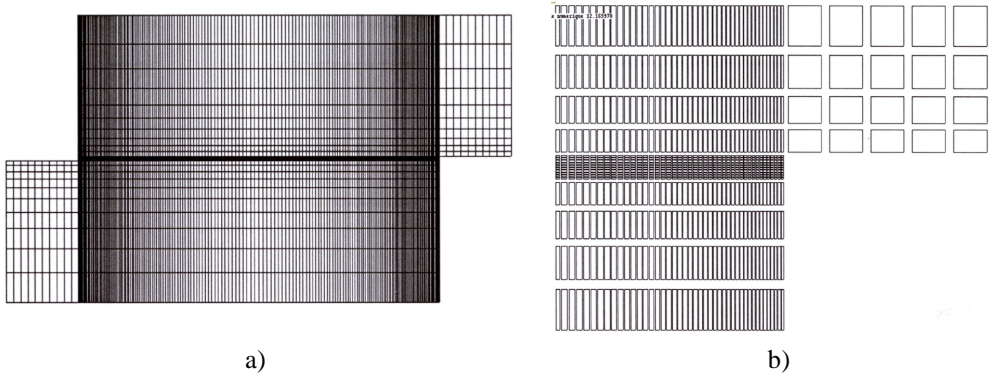


Figure 2. Numerical modeling of a double-lap bonded joint with quadrangles elements: a) assembly; b) detail.

Figure 3 shows an example of the grid used in this study where all the finite elements which mesh the adhesive are interface type. We imposed 1 finite element row in the adhesive layer.

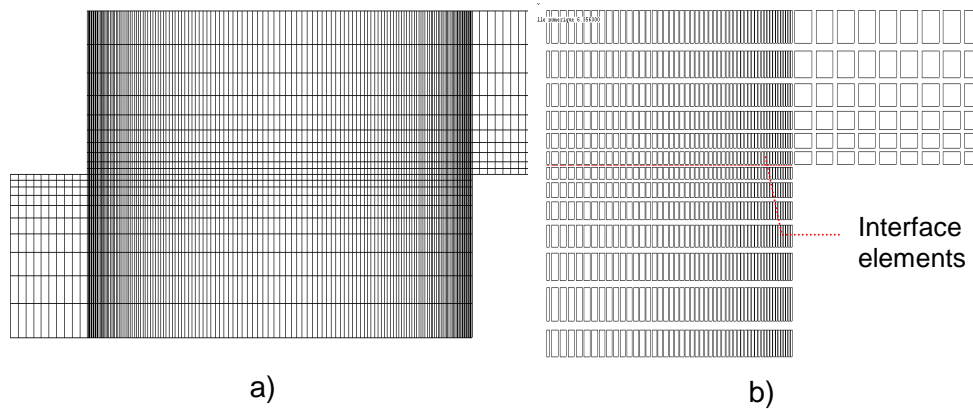


Figure 3. Numerical modeling of a double-lap bonded joint with interface elements: a) assembly; b) detail.

2. Load transfer

To compare the analytical model with the finite elements model we determine the load transfer in the middle of the bonded substrates, Figure 4.

We can note some differences in the variation of the load given by the ideal model in the case of a metal-composite assembly (Adherent 1 – Aluminium AU 2024 T3, Adhesive – Araldite AV119, Adherent 2 – Glass fiber $\pm 45^\circ$), (Figure 4), while it still has a similar evolution.

The point of equivalence in stress in the two substrates is shifted (according to the length of the joint) from approximately 1 % in the finite element analysis. It should be noted that the position of this point varies according to the characteristics of the substrates: it is centered compared to the length of the joint for substrates of equivalent total rigidities, and shifts on both sides as a function of the ratio of the rigidities of the bonded substrates.

3. Stress distributions

The stresses in the adhesive are very important to predict the failure moment. For that it is primordial to have their distributions.

Figure 5 shows the stress distributions in the assembly in the form of cartography.

We can observe that the distribution curves had the same shape like the curves obtained by the analytical model [11], and so the model is validated.

ADHESIVE INFLUENCE MODELING ON DOUBLE-LAP JOINTS ASSEMBLIES

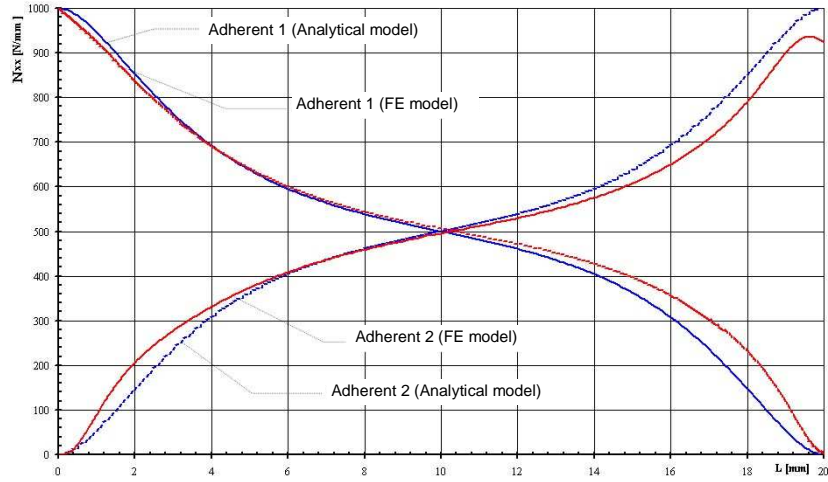


Figure 4. Load transfer in an AU 2024 T3-AV 119-VE $\pm 45^\circ$ assembly.

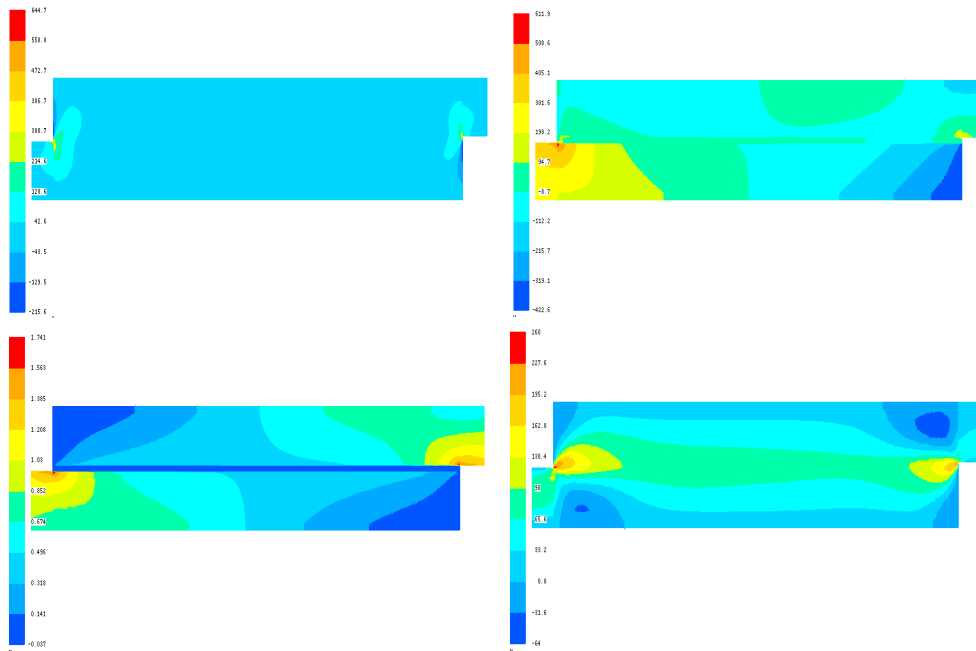


Figure 5. Stress distribution in double-lap bonded joint

CONCLUSION

Adhesive joining is a simple method of assembly. Its interest lies in the fact that it minimizes the machining of the parts to be assembled. The performance of the adhesive bonded joints depends on the performance of the adhesive. The latest generations of adhesives, delivered in the form of film, make it possible to minimize the number of operations to make the join and greatly increase the mechanical resistance. However, the design engineer must have at his disposal methods and/or reliable computer codes for pre-dimensioning with known margins.

The objectives of our studies were to entirely develop analytical models for dimensioning adhesive-bonded joints.

The basis of our analytical model was the analysis of the stresses applied to an elementary volume of the assembly under consideration, observing the boundary conditions, the geometry and materials of the assembly. The application of an energy method made it possible to obtain the stress distribution in any point of the structure [11]. The behavior law enabled us to obtain the deformations then, by integration, the displacements. The problem for stress, deformation and displacements was thus entirely defined.

The validation of the analytical model is presented by comparison with finite elements models. For the assembly, the total force-displacement behavior is well defined. Thus, the analytical model makes it possible to determine the rigidity of the assembly and to obtain a simple formulation very quickly, which gives the total behavior of the assembly.

The comparison was also carried out for the stress distribution in the substrates and the adhesive joint. We showed that the transfer of force by joining was well determined by the model. The distribution of stress in the adhesive remained very close to the solution given by finite elements.

The analytical model underestimated the stresses in the adhesive leading to an over-estimate of the forces at rupture. However, this model is reliable and allows fast analysis of this type of assembly.

ACKNOWLEDGMENT

The Ministry of Education and Research, Bucharest (ID-1100, PN II project) is thanked for financial support of this work.

REFERENCES

1. O. Volkersen, *Die Luftfahrtforschung*, **1938**, 15, 41.
2. M. Goland, N.Y. Buffalo, E. Reissner, *Journal of Applied Mechanics*, **1944**, 66, A17.
3. O. Volkersen, *Recherche Construction métallique*, **1965**, 4, 3.
4. Y. Gilibert, A. Rigolot, *Matériaux et Constructions*, **1985**, 18, 363.
5. Y. Gilibert, *Matériaux et techniques*, **1991**, 5.
6. R.D. Adams, N.A. Peppiat, *Journal of Strain Analysis*, **1974**, 9, 185.
7. M.Y. Tsai, D.W. Oplinger, J. Morton, *International Journal of Solid Structures*, **1998**, 35, 1163.
8. F. Mortensen, O.T. Thomsen, *Composite Structures*, **2002**, 56, 165.
9. F. Mortensen, O.T. Thomsen, *Composite Science and Technology*, **2002**, 62, 1011.
10. O. Nemeş, *Contribution à l'étude des assemblages collés cylindriques et plans*, PhD. Thesis, INSA Toulouse, France, **2004**.
11. O. Nemeş, F. Lachaud, A. Mojtabi, V. Soporan, O. Tătaru, *Studia Universitatis Babeş-Bolyai, Seria Chimia*, **2006**, LI, 2, 201.